PROCEEDINGS

OF THE

AMERICAN SOCIETY OF CIVIL ENGINEERS

VOL. 73 OCTOBER, 1947 No. 8

TECHNICAL PAPERS

AND

DISCUSSIONS

Published monthly, except July and August, at Prince and Lemon Streets, Lancaster, Pa., by the American Society of Civil Engineers. Editorial and General Offices at 33 West Thirty-ninth Street, New York 18, N. Y. Reprints from this publication may be made on condition that the full title of paper, name of author, page reference, and date of publication by the Society are given.

Entered as Second-Class Matter, September 23, 1937, at the Post Office at Lancaster, Pa., under the Act of March 3, 1879. Acceptance for mailing at special rate of postage provided for in Section 1103, Act of October 3, 1917, authorized on July 5, 1918.

Subscription (if entered before January 1) $8.00 per annum Price $1.00 per copy

Copyright, 1947, *by the* AMERICAN SOCIETY OF CIVIL ENGINEERS

Printed in the United States of America

	Published	Discussion closes
Machis, Alfred. Experimental Observations on Grouting Sands and Gravels	Nov., 1946	
Discussion in Feb., Mar., June, 1947		Closed*
Symposium: Cleaning and Grouting of Limestone Foundations, Tennessee Valley Authority	Dec., 1946	
Discussion in Mar., May, June, 1947		Closed*
Matthes, Gerard A. Mississippi River Cutoffs	Jan., 1947	
Discussion in Mar., June, Sept., 1947		Closed*
Tan, Ek-Khoo. Stability of Soil Slopes	Jan., 1947	
Discussion in May, June, Sept., 1947		Closed*
Muldrow, W. C. Forecasting Productivity of Irrigable Lands	Feb., 1947	
Discussion in May, June, Oct., 1947		Nov. 1, 1947
Freudenthal, Alfred M. Reflections on Standard Specifications for Structural Design	Feb., 1947	
Discussion in June, 1947		Nov. 1, 1947
Blaisdell, Fred W. Development and Hydraulic Design, Saint Anthony Falls Stilling Basin	Feb., 1947	
Discussion in Sept., 1947		Nov. 1, 1947
DuVal, Miles P. The Marine Operating Problems, Panama Canal, and the Solution	Feb., 1947	
Discussion in Apr., 1947		Uncertain
Claybourn, J. G. Sea Level Plan for Panama Canal	Feb., 1947	
Discussion in Apr., 1947		Uncertain
Hrennikoff, Alexander. Theory of Inelastic Bending with Reference to Moment Design	Mar., 1947	
Discussion in June, Oct., 1947		Dec. 1, 1947
Hsu Shih-Chang. Beam Deflections by Second and Third Moments	Mar., 1947	
Discussion in Sept., 1947		Dec. 1, 1947
Ryder, Frederick L. A Rational Explanation of Column Behavior	Mar., 1947	
Discussion in May, June, Sept., Oct., 1947		Dec. 1, 1947
Rathbun, J. Charles, and Cunningham, C. W. Continuous Frame Analysis by Elastic Support Action	Apr., 1947	
Discussion in Sept., 1947		Dec. 1, 1947
Hickox, G. H., Peterka, A. J., and Elder, R. A. Friction Coefficients in a Large Tunnel	Apr., 1947	
Discussion in June, Sept., Oct., 1947		Dec. 1, 1947
Sturm, R. G. Stability of Thin Cylindrical Shells in Torsion	Apr., 1947	
Discussion in Oct., 1947		Dec. 1, 1947
Report: Water Supply Engineering: Report of the Committee of the Sanitary Engineering Division for the Two Years Ending December 31, 1946	Apr., 1947	
Committee of the San Francisco (Calif.) Section, ASCE, on Timber Test Program. Tests of Timber Structures from Golden Gate International Exposition	May, 1947	
Discussion in Oct., 1947		Dec. 1, 1947
Westergaard, H. M. New Formulas for Stresses in Concrete Pavements of Airfields	May, 1947	Dec. 1, 1947
Bergendoff, R. N., and Sorkin, Josef. Mississippi River Bridge at Dubuque, Iowa	June, 1947	
Discussion in Sept., Oct., 1947		Jan. 1, 1948
Casagrande, Arthur. Classification and Identification of Soils	June, 1947	
Discussion in Sept., Oct., 1947		Jan. 1, 1948
Barron, Reginald A. Consolidation of Fine-Grained Soils by Drain Wells	June, 1947	Jan. 1, 1948
Kazmann, Raphael G. River Infiltration as a Source of Ground Water Supply	June, 1947	Jan. 1, 1948
Spangler, M. G. Underground Conduits—An Appraisal of Modern Research	June, 1947	Jan. 1, 1948
Jens, Stifel W. Drainage of Airport Surfaces—Some Basic Design Considerations	Sept., 1947	Feb. 1, 1948
Peterson, Dean F., Jr. Influence Lines for Continuous Structures by Geometrical Computations	Sept., 1947	Feb. 1, 1948
Boissonnault, Frank L. Estimating Data for Reservoir Gates	Sept., 1947	Feb. 1, 1948
Coddington, E. F., and Marshall, O. C. J. Least Squares Adjustment of Triangulation Net Between Geodetic Stations	Sept., 1947	Feb. 1, 1948
Kellogg, F. H. Investigation of Drainage Rates Affecting Stability of Earth Dams	Sept., 1947	Feb. 1, 1948

NOTE.—The closing dates herein published are final except when names of prospective discussers are registered for special extension of time.

* Publication of closing discussion pending.

CONTENTS FOR OCTOBER, 1947

PAPERS

PAGE

Thin-Shelled Domes Loaded Eccentrically.
By Walter C. Voss, Dean Peabody, Jr., Howard R. Staley, and Albert G. H. Dietz . 1173

Subsidence of the Terminal Island-Long Beach Area, California.
By Frederic R. Harris and Eugene H. Harlow 1197

Variation of Coefficients of Simultaneous Linear Equations.
By Bernard L. Weiner 1219

Application of Geology to Tunneling Problems.
By Ernest E. Wahlstrom 1245

The General Principles of Highway Transition Curve Design.
By John Joseph Leeming 1257

Analysis of Stepped-Column Mill Bents.
By Daniel S. Ling 1271

DISCUSSIONS

Theory of Inelastic Bending with Reference to Limit Design.
By Michael R. Horne 1293

Stability of Thin Cylindrical Shells in Torsion.
By S. B. Batdorf and Manuel Stein 1302

Forecasting Productivity of Irrigable Lands.
By M. R. Lewis 1305

Friction Coefficients in a Large Tunnel.
By G. S. Tapley 1307

Classification and Identification of Soils.
By James H. Stratton, and Donald J. Belcher 1310

Mississippi River Bridge at Dubuque, Iowa.
By A. Floris, and T. H. Rust 1319

CONTENTS FOR OCTOBER, 1947 (*Continued*)

PAGE

A Rational Explanation of Column Behavior.
By Ernest L. Robinson 1322

Tests of Timber Structures from Golden Gate International Exposition.
By James H. Carr, Jr., Howard J. Hansen, and E. G. Stern 1323

A list of "Current Papers and Discussions" may be found on the page preceding the table of contents

The Society is not responsible for any statement made or opinion expressed in its publications

HINTS TO AUTHORS

Those who are planning papers for submission to PROCEEDINGS *will expedite Committee action measurably by first studying the standard instructions as to style, content, and format. For reprints, address the Manager, Technica Publications, 33 W. 39th St., New York 18, N. Y.*

AMERICAN SOCIETY OF CIVIL ENGINEERS

Founded November 5, 1852

PAPERS

THIN-SHELLED DOMES LOADED ECCENTRICALLY

BY WALTER C. VOSS,[1] ASSOC. M. ASCE, DEAN PEABODY, JR.,[2] M. ASCE, AND HOWARD R. STALEY[3] AND ALBERT G. H. DIETZ,[4] ASSOC. MEMBERS, ASCE

SYNOPSIS

A shallow thin-shelled model dome of plaster of Paris was subjected to a concentrated load successively placed between the springing and the crown. Strains were measured at near-by and distant stations on the upper surface. Compression and transverse tests of the plaster gave data concerning moduli of elasticity and Poisson's ratio whereby stresses were computed from the recorded strains. Sand loads were distributed uniformly over an eighth segment and over a quarter segment to study the transition from a concentrated load to a uniformly distributed load over the entire surface.

A mathematical analysis was made to determine the stresses caused by a concentrated load applied at the crown of a shallow thin-shelled spherical dome. Stresses of any magnitude are essentially local ones, so this analysis applies approximately to an eccentric load applied at some distance from the springing or any hole in the dome. As far as the test of one model dome can authorize, this series of tests seems to justify the use of the mathematical analysis to compute maximum stresses in a shallow dome.

INTRODUCTION

The absence of information on the effects of eccentric concentrated loads on thin-shelled domes with small rise prompted these tests. Domes of this type were already in existence and were being built without accurate data in regard to the stresses carried by load concentrations.

NOTE.—Written comments are invited for immediate publication; to insure publication the last discussion should be submitted by March 1, 1948.

[1] Head, Dept. of Bldg. Eng. and Constr., Mass. Inst. Tech., and Consultant, Cambridge, Mass.

[2] Associate Prof., Dept. of Bldg. Eng. and Constr., Mass. Inst. Tech., Cambridge, Mass.

[3] Asst. Prof., Dept. of Bldg. Eng. and Constr., Mass. Inst. Tech., Cambridge, Mass.

[4] Asst. Prof., Dept. of Bldg. Eng. and Constr., Mass. Inst. Tech., Cambridge, Mass.

To check laboratory and theoretical studies against loading data from actual structures, it was decided to build a plaster model of a large dome, actually erected, to a scale of one to eight. The base of the spherical dome was 8 ft in diameter; its rise was 1 ft ($\frac{1}{8}$ *d*); and the thickness of the shell was 0.25 in. The radius of the sphere was 8.5 ft.

This exploratory test was made in 1941, before the mathematical analysis had been initiated; and it was not considered wise at that time to assume that an eccentric concentrated load would produce measurable strains only in the surface close to the area of load application. Consequently, sixty-four gage stations were located on the dome surface with two wires connected to each station. The assumption was made that the axes of principal strains for highly strained stations would be at, or near, the meridional and circumferential axes of the dome. A mathematical analysis by Eric Reissner[5] confirms this assumption (see Appendix I) and indicates that any divergence in test data would probably be slight. It would be necessary to add sixty-four more wired connections to obtain a third strain at each station to complete a rosette.

The inner form of the dome was not dropped far enough to permit strain readings on the under surface. An attempt was made to read deflections to 0.001 in. with a transit, but no deflections of this magnitude were recorded. If subsequent tests are made, it is desirable that the number of stations be reduced so that three strains at each station may be taken to complete a rosette, that stations be located on both the upper and lower surfaces near the area of load application, and that accurate measurement of deflections be attempted near the load application.

Strains were measured in the meridional and circumferential directions at each station. After the completion of the concentrated load tests, the distributed sand load tests were made, the sand load remaining several days on the dome while the time effect on the strains was measured. Finally, the dome was tested to failure by a concentrated load applied about three tenths of the meridian length from the springing.

Notation.—The letter symbols used in this paper are defined as they occur, and are assembled for convenience of reference in Appendix II.

PART I. EXPERIMENTAL DETERMINATION OF STRAINS

General

Objective.—The objective of these tests was to study the effect of concentrated loads on a spherical dome. Test data on models or full-sized domes are lacking for such loads, especially for loads that are not applied at the central axis. As nearly as can be determined, theoretical analyses were not in existence prior to the work done by Mr. Reissner.[5] Test data for eccentric loadings will be valuable for establishing the extent of the surface strained and the comparative magnitude of these strains, and for a comparison with the mathematical analysis.

Eccentric distributed loading is desirable to supply the transition from an eccentric concentrated load to a symmetrical uniformly distributed load.

[5] "Stresses and Small Displacements of Shallow Spherical Shells," by Eric Reissner, *Journal of Mathematics and Physics*, February, 1946, p. 80.

Construction of the Model.—A rigid wooden ring was mounted in a frame in an even plane. A recess left on the top inner part of this ring acted as a support and also took the reaction of the model when loaded. The bottom of this recess acted as a guide for the templet during the operation of fabricating the base mold on which the dome shell was cast. The top of the recess was used as a guide for forming the dome shell. The base mold and dome shell were formed by rotating a metal templet about a central shaft. The shell was cast with the usual heavier ring, or haunch. Before testing, the base mold was lowered by jacks.

Strain Gages.—Electrical resistance wire gages of the type developed by Professors A. C. Ruge, Assoc. M. ASCE, and A. V. deForest of the Massachusetts Institute of Technology at Cambridge were adopted as best meeting the requirement for precision over a short gage length. Gages were placed at the sixty-four stations shown in Fig. 1. At each station, strains were measured in the circumferential and meridional directions. The 128 gages were connected to a central selector panel which allowed any one gage to be read at will. For the initial tests, the gages were straight wires, approximately 3 in. long, and were cemented to the surface, as shown in Fig. 2. Subsequently, hairpin gages were used at, or near, the loaded stations. These hairpin gages measured the strain for a 1.5-in. length. In the autumn of 1940 the shorter gages, now in use, were not on sale.

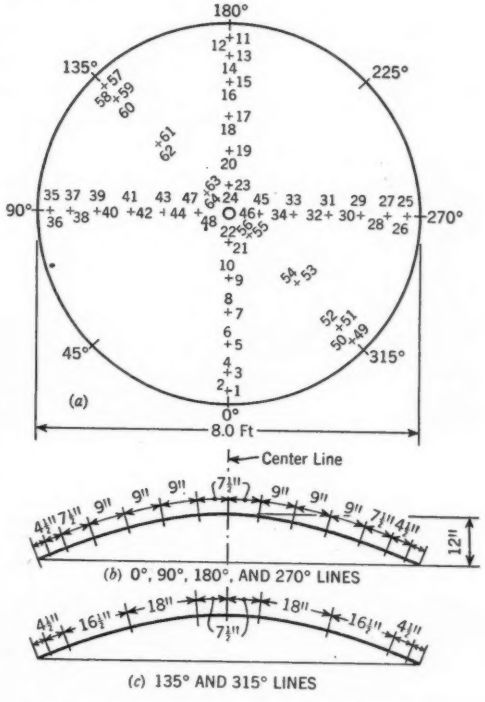

FIG. 1.—LOCATION OF STRAIN GAGE STATIONS ON THE DOME

LOADING PROCEDURE

Concentrated Loads.—For most of these tests a concentrated load of 40 lb was used. Lead blocks, 4 in. square, rested on four soft rubber pads, each $\frac{1}{8}$ in. thick and $1\frac{1}{4}$ in. square. The pads were separated by $\frac{1}{2}$-in. clearance, so that it was 3 in. out-to-out for the pads, whereas the actual loaded area was 6.25 sq in. The loads were applied on the 0° meridian or at other points between the 45° and 315° meridians.

The test to failure was made by applying a concentrated load at Station 5,6 on the 0° meridian (see Fig. 1). In this case, a lever system was employed which consisted of an arm swinging about a pivot through the center of the

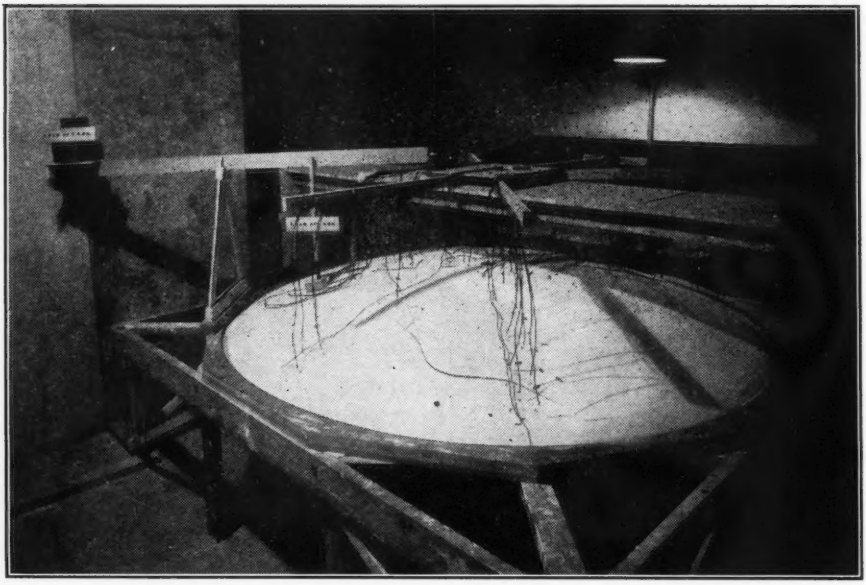

FIG. 2.—TEST TO FAILURE

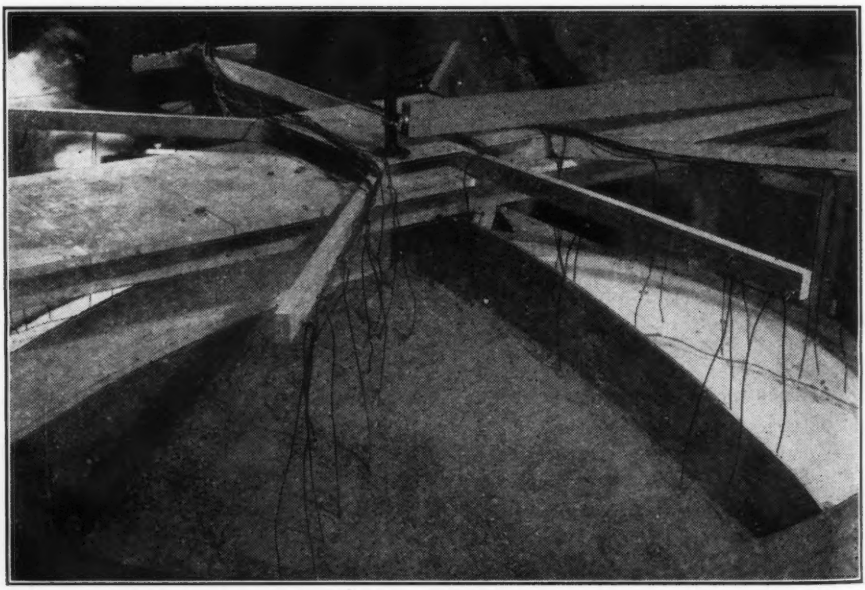

FIG. 3.—DISTRIBUTED LOAD OVER ONE QUARTER OF THE SURFACE

dome. This arm had a load platform at the far end, and rested on a leg bearing on a shoe placed on the rubber pads (Fig. 2).

Sand Loads.—A form of plywood and sheet metal rested on the dome shell and confined the sand to a definite area (Fig. 3). Dry sand was spread uniformly over the segment until the desired weight was obtained.

Poisson's Ratio and the Modulus of Elasticity

Compression tests were made on plaster cylinders, 2 in. in diameter and 4 in. high. Gages similar to those used on the dome were installed to give longitudinal and circumferential strains. From the data, the modulus of elasticity and Poisson's ratio were computed.

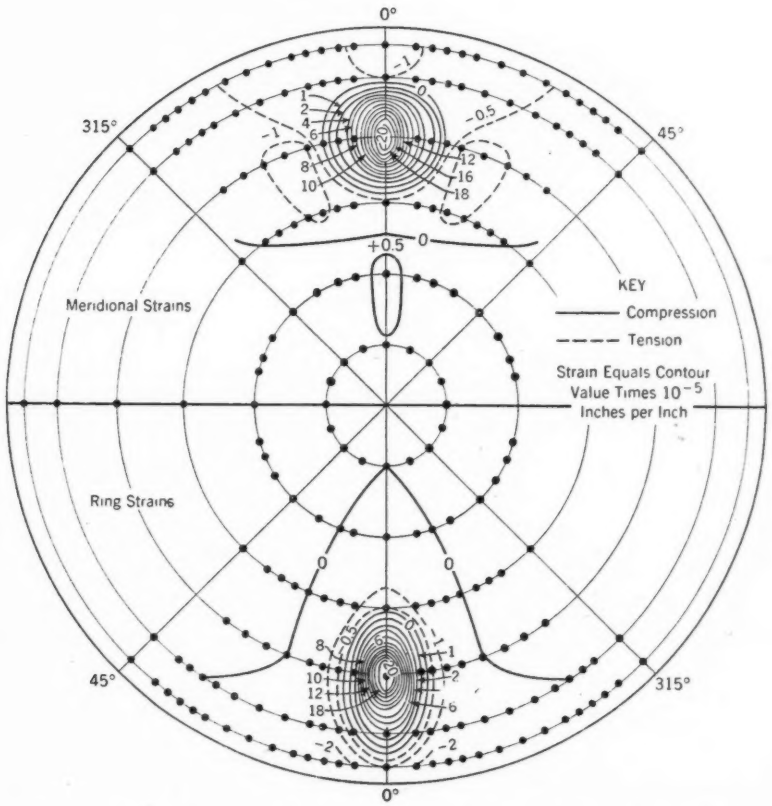

Fig. 4.—Strain Contours for a Concentrated Load of 40 Lb at Station 5,6

Transverse tests were also made on small pieces of the broken dome. Assuming uniformly varying stresses and strains, fiber stresses and the modulus of rupture were computed, as well as the modulus of elasticity. For each specimen a plot of the load-strain data can be represented by two straight lines at slightly different slopes. However, the comparison of moduli of elasticity with

the compression moduli (presented subsequently in Table 7) has been made as the stress varies by tenths of the ultimate.

Experimental Data and Results

The complete report on which this paper is based (including Mr. Reissner's complete mathematical treatment, which is reported briefly in Appendix I) can be consulted at Engineering Societies Library[5a] as well as at the library of Massachusetts Institute of Technology.

Concentrated Loads.—The strains measured for a given position of the concentrated load were assembled in tables such as Tables 1(*a*) and 1(*b*). These strain data were plotted to show the variation along a meridian and along circumferences. The contour plots in Fig. 4 show equal compression strain by full lines, and equal tension by dashed lines. Table 2 gives the data for the test to failure by a concentrated load at Station 5,6, and Fig. 2 shows the type of failure.

TABLE 1.—Strains Resulting from 40-Lb Loads Applied on
(The Number Times 10^{-5} is the Strain in Inches Per Inch.

Station No.[a]	(*a*) Strains at Various Stations														
	Distance (in Inches) of Load (in														
	0	4	4	4	4	6	6	8	8	10	10	13	13	16	16
	(1)	(2)	(3)	(4)	(5)	(6)	(7)	(8)	(9)	(10)	(11)	(12)	(13)	(14)	(15)
Load[b]	40	55	40[c]	40	40	40	40	40	40	40	40	40	40	40	40
Cols. average	....	....	....	....	....	....	....	....	....	....	....	....	....	....	....
1.....	− 1.0	− 3.35	−2.44	....	....	....	....	....	....	....	....	....	....	....	....
2.....	− 1.5	− 1.4	−1.0	....	....	....	....	....	....	....	....	....	....	....	....
3.....	+ 2.94	− 1.0	−0.75	−0.5	−0.5	−1.25	−1.25	−1.0	−1.0	−1.0	....	−0.5	....	−0.5	....
4.....	− 1.0	− 0.75	−0.55	−0.25	−0.5	−0.75	−0.75	−0.75	−0.75	−0.75	....	−0.6	....	−0.3	....
5.....	+21.65	+ 1.95	+1.42	+1.25	+1.96	−0.75	−0.6	−1.0	−0.75	−0.5	0	0	....	+0.5	....
6.....	+20.69	+10.06	+7.33	+6.60	+6.79	+2.93	+2.35	+0.4	0	−1.0	−1.0	−1.1	−1.15	−0.95	−1.0
7.....	− 0.5	− 1.15	−0.85	−1.0	−1.25	−1.0	−1.25	−1.0	−1.0	−0.5	....	0	....	+0.5	....
8.....	− 0.75	− 1.35	−1.0	−1.0	−0.8	−0.5	−1.0	−0.5	−0.75	−1.0	....	−1.0	....	−0.75	....

[a] See also Stations Nos. 9 to 62, inclusive, in the continuation of Table 1. [b] Load, in pounds. [c] Values in the 26-in. distance, on the 315° line and on the 45° line, were identical. The average strain in Col. 30 is the aver-

PART II. DISCUSSION OF RESULTS

Concentrated Loads

Strains.—The strains were measured on the upper surface of the dome for various concentrated loads applied at a gage station, or applied at measured distances on a circumference through the gage station. Thus, it was possible to record, with a minimum of stations, the strains at definite distances from the loading point. For certain loadings several tests were made on the same circumference. In these cases the readings have been averaged. Most of the loads were constant at 40 lb, but in certain cases loads of 20 lb, 55.0 lb, 55.1 lb,

[5a] 29 West 39th St., New York, N. Y.

and 56.1 lb were used. The corresponding strain data were revised to a common base load of 40 lb, assuming strains to vary directly with the low loads used.

It was not feasible to locate gage points on the under surface of the dome because the form was dropped only a few inches and only the gage stations near the outer haunch could have been reached.

The averaged strain data are also shown on the contour plots, using contour lines to connect points of the same strain value. These contours (see Fig. 4) were located by scaling the plotted strain values. Of necessity many of these contour lines were sketched in to connect rather widely dispersed points of equal strain. However, close to the loaded areas, they are accurate.

THE CIRCUMFERENCE AT THE LEVEL OF STATION 5,6 IN FIG. 1
Elongation Is Negative and Shortening Is Positive)

					(*b*) AVERAGE STRAINS FOR STATIONS LOADED SIMILARLY									
Pounds) from Station 5, 6:														Station No.
19 (16)	19 (17)	22 (18)	22 (19)	26[d] (20)	0 (21)	4 (22)	6 (23)	8 (24)	10 (25)	13 (26)	16 (27)	19 (28)	22 (29)	26[d] (30)	
40	40	40	40	40	40 Col. 1	40 Cols. 3, 4, and 5	40 Cols. 6 and 7	40 Cols. 8 and 9	40 Cols. 10 and 11	40 Cols. 12 and 13	40 Cols. 14 and 15	40 Cols. 16 and 17	40 Cols. 18 and 19	40 Col. 20	Load
....	....	....	....	....	− 0.1	−2.44	....	....	....	....	....	....	....	....	1
....	....	....	....	....	− 1.5	−1.0	....	....	....	....	....	....	....	....	2
....	....	....	....	....	+ 2.94	−0.58	−1.25	−1.00	−1.00	−0.5	−0.5	....	....	....	3
....	....	....	....	....	− 1.0	−0.43	−0.75	−0.75	−0.75	−0.6	−0.3	....	....	....	4
+0.5	....	+0.5	....	....	+21.65	+1.54	−0.68	−0.88	−0.25	0	+0.5	+0.5	+0.5	....	5
−0.75	−0.75	−0.45	−0.4	−0.3	+20.69	+6.91	+2.64	+0.2	−1.0	−1.13	−0.98	−0.75	−0.43	−0.3	6
....	....	....	....	....	− 0.5	−1.03	−1.13	−1.0	−0.5	0	+0.5	....	....	....	7
....	....	....	....	....	− 0.75	−0.93	−0.75	−0.63	−1.0	−1.0	−0.75	....	....	....	8

Col. 3 are the strain readings in Col. 2 revised to a common base corresponding to a 40-lb load. [d] The strains at age of the two.

The common characteristic of these plots is the large compressive strain immediately under the loaded area in both meridional and circumferential directions. The strains decrease rapidly outside the loaded area; farther away small tensile strains usually occur, often followed by equally small compressive strains. The deformations suggest those observed if one presses a finger against the surface of an inflated toy balloon. Except for the area close to the loaded point, the magnitude of the strains is very small. Near the loaded area, the meridional contours are approximately circular whereas the circumferential contours are elliptical. The reader should note that "meridional" and "circumferential" refer to the central dome axis and not to an axis through the center of the load.

The strains are comparatively small for a load applied at Station 1,2 near the outer ring, or haunch (see Fig. 5). The stiffer haunch influences the strain distribution. As the position of application of the 40-lb load is moved up the meridian toward the crown of the dome, the strains increase to a maximum at

Station 21,22, which was the station nearest to the hole at the crown, the increase being about 40% more than the maxima at Station 3,4. The numerical values of the maximum strains in the meridional and circumferential directions at the same station are approximately equal.

Stresses.—The stress-strain plots of the compression and transverse tests indicate that the plaster behaves as an elastic material for stresses of less than 700 lb per sq in. To convert strain data to stresses, average values of the modulus of elasticity E (1,770,000 lb per sq in.) and of Poisson's ratio μ (0.20) are used. Knowing the meridional strain ϵ_m and the circumferential strain ϵ_c, under the load, the corresponding stresses σ_m and σ_c can be computed by the elastic relations:

$$\sigma_m = \frac{E}{1-\mu^2}(\epsilon_m + \mu\,\epsilon_c) = 1{,}844{,}000\,(\epsilon_m + 0.2\,\epsilon_c) \ldots\ldots\ldots (1a)$$

and

$$\sigma_c = \frac{E}{1-\mu^2}(\epsilon_c + \mu\,\epsilon_m) = 1{,}844{,}000\,(\epsilon_c + 0.2\,\epsilon_m) \ldots\ldots\ldots (1b)$$

TABLE 1.—(*Continued*)

Station No.	(a).—(*Continued*)			(b).—(*Continued*)	
	Distances.—(*Continued*):				
	0 (1)	4 (2)	4 (3)	0 (21)	4 (22)
Load[b]	40	55	40[c]	40	40
Cols. averaged	....	....	....	Col. 1	Cols. 3, 4, and 5
9	−1.75	−1.75	−1.27	−1.75	−1.27
10	+0.75	+0.6	+0.45	+0.75	+0.45
11	....	0	0	....	0
12	....	+0.25	+0.2	....	+0.3
13	....	0	0	....	0
14	....	+0.4	+0.3	....	+0.3
15	....	−0.25	−0.2	....	−0.2
16	....	0	0	....	0
17	....	−0.5	−0.35	....	−0.35
18	....	0	0	....	0
19	....	−0.75	−0.55	....	−0.55
20	....	−0.15	−0.1	....	−0.1
21	0	−0.5	−0.35	0	−0.35
22	+0.25	0	0	+0.25	0
23	....	−0.4	−0.3	....	−0.3
24	....	−0.25	−0.2	....	−0.2
41	....	−0.75	−0.55	....	−0.55
42	....	−0.75	−0.55	....	−0.55
49	....	−0.75	−0.55	....	−0.55
50	....	−1.25	−0.9	....	−0.9
51	....	−1.0	−0.75	....	−0.75
52	....	+0.5	+0.35	....	+0.35
53	....	+0.5	+0.35	....	+0.35
54	....	−0.5	−0.35	....	−0.35
55	....	−0.5	−0.35	....	−0.35
56	....	−0.75	−0.55	....	−0.55
61	....	−0.75	−0.55	....	−0.55
62	....	−0.25	−0.2	....	−0.2

[b] Load, in pounds. [c] Values in Col. 3 are the strain readings in Col. 2 revised to a common base corresponding to a 40-lb load.

Using the averaged maximum strains under the load, the maximum stresses for a 40-lb load applied at the successive gage stations are given in Table 3. These maximum stresses increase as the load is applied nearer the crown of the dome. At any given station, the maximum meridional and circumferential stresses may be regarded as equal. The computed stresses at Station 21,22 are about 16% of the compressive strength of the plaster cylinders tested in compression (3,850 lb per sq in.).

Stress Comparison with the Mathematical Analysis.—Equations for the normal stress in a thin shell of a shallow dome, due to a concentrated load applied over a small circular area at the crown, are presented in Appendix I. The assumption is made that the load is applied relatively distant from any boundary or hole in the shell. Eqs. 6 in Appendix I give the values of the

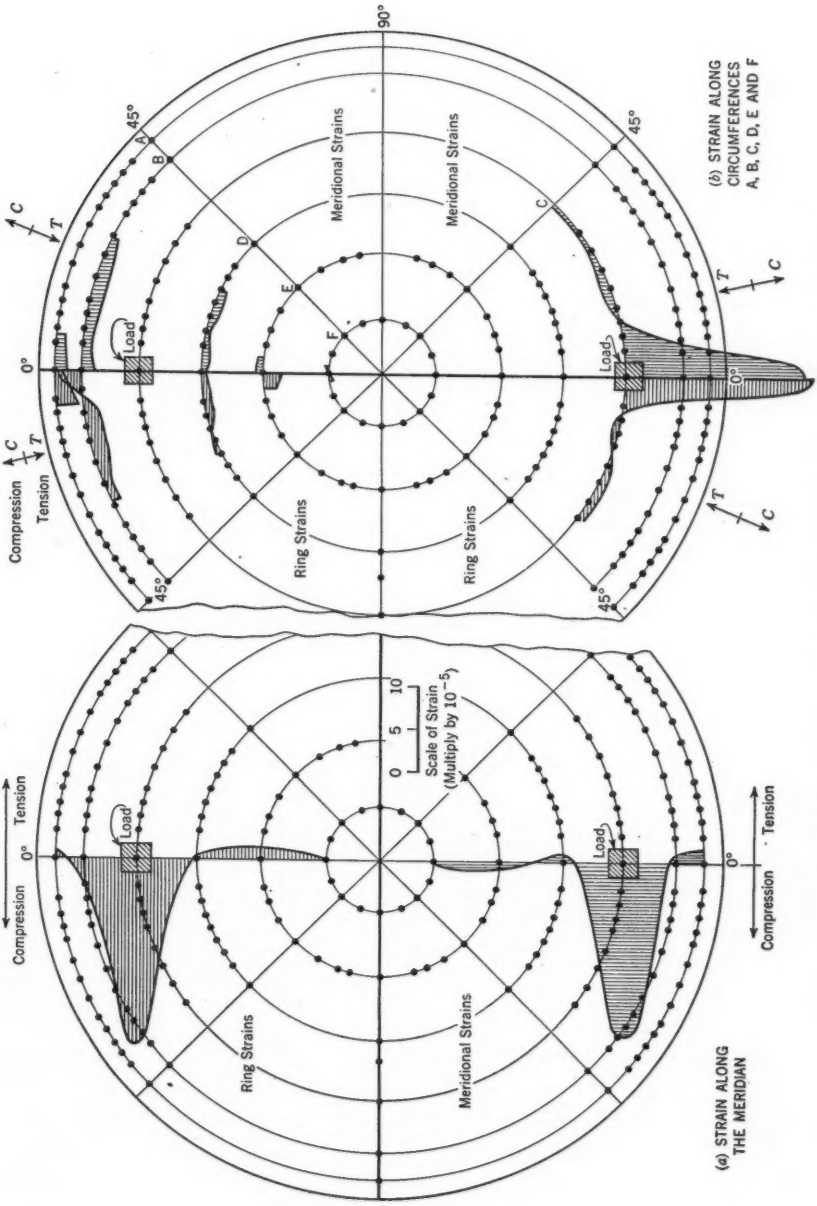

FIG. 5.—ANALYSIS OF STRAIN VARIATION FOR A CONCENTRATED LOAD OF 40 LB AT STATION 5.6

normal stresses in the meridional and circumferential directions at the upper and lower surfaces of the shell due to direct stress and bending. The equations are then applied to a structure with the dimensions of the test dome. The theoretical analysis is compared with test results in Appendix I (see heading, "Illustrative Example"), where the loaded circular area is assumed to be 6.25 sq in. It is believed that these results are comparable because the actual

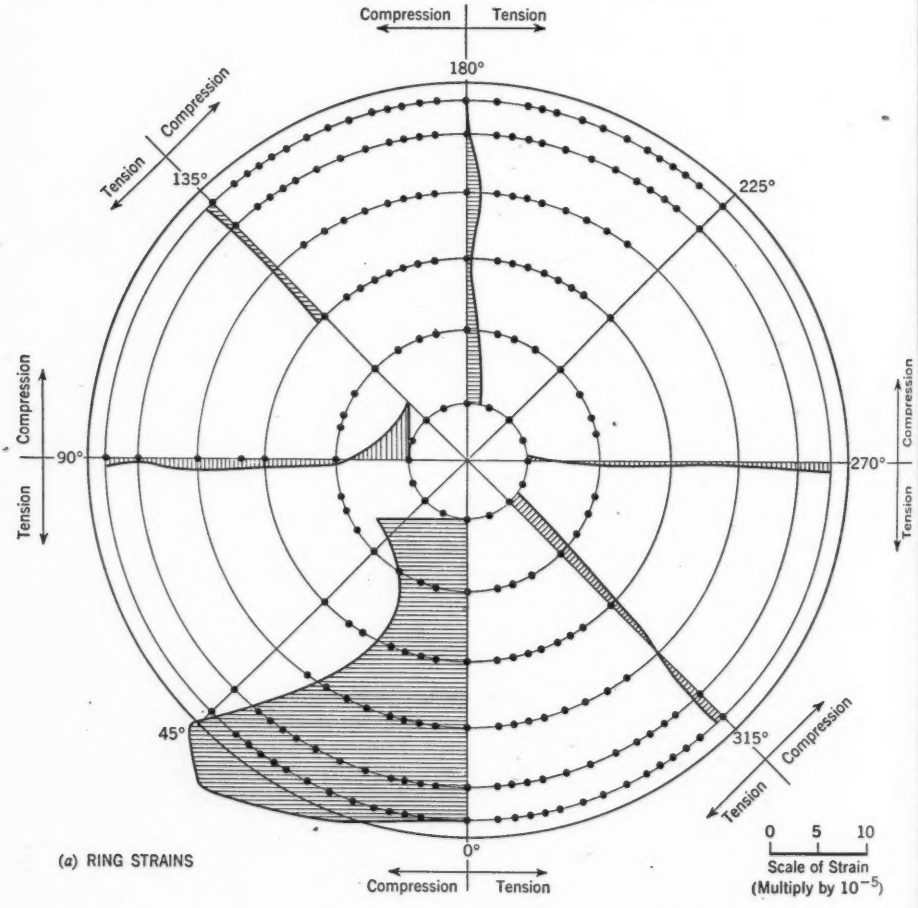

FIG. 6.—STRAIN VARIATION ALONG THE MERIDIANS FOR A SAND LOAD

loaded area during the tests was through four thin rubber pads, each 1.25 in. square. Therefore, the actual loaded test area was 6.25 sq in. Using the numerical results thus determined, the normal stresses, direct and bending, at the upper surface equal:

$$\sigma_m = \frac{P}{\pi \xi_c^2 h^2}[\sqrt{3(1-\mu^2)}(1-C_1) + 3(1+\mu)C_2] \ldots\ldots\ldots (2a)$$

and

$$\sigma_c = \frac{P}{\pi \xi_c^2 h^2}[\sqrt{3(1-\mu^2)}(1-C_1) + 3(1+\mu)C_2] \quad \ldots\ldots\ldots (2b)$$

in which $\xi_c = 0.5146$, $C_1 = 0.9050$, and $C_2 = 0.1728$. By computation:

$$\sigma_m = \sigma_c = (0.1938 + 0.7477)\frac{P}{h^2} = \frac{(0.9415)P}{(0.25)^2} \quad \ldots\ldots\ldots\ldots (3)$$

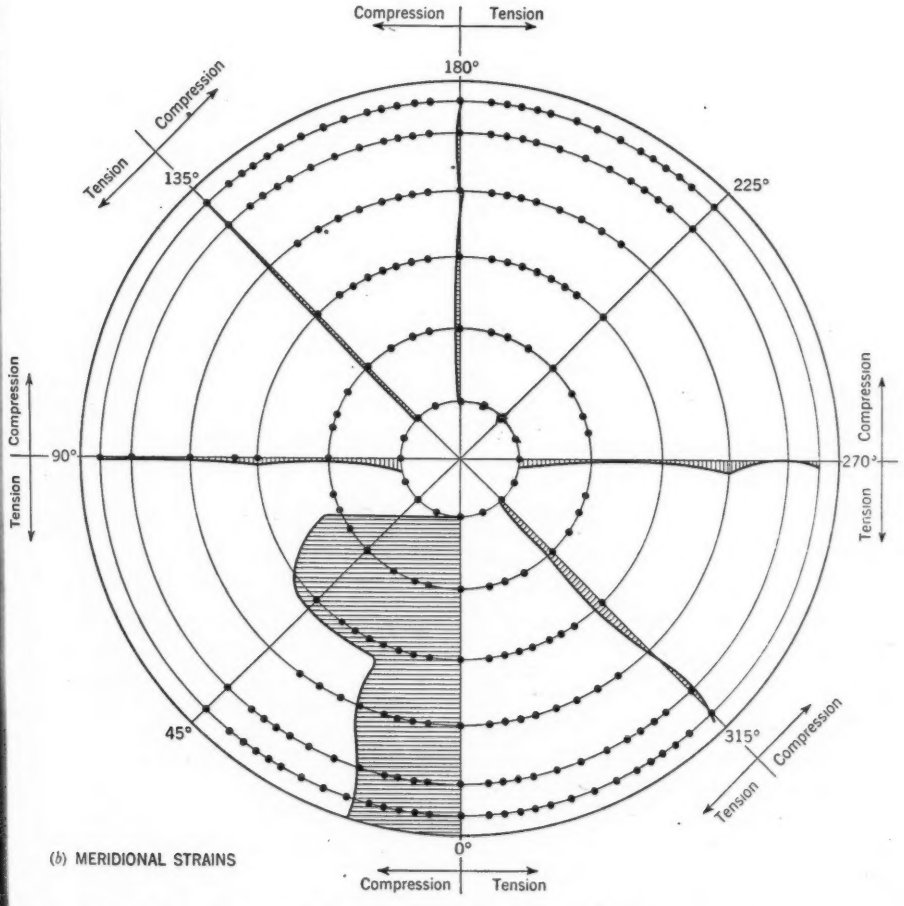

(*b*) MERIDIONAL STRAINS

OF 267 LB ON AN EIGHTH SEGMENT CENTERED ABOUT THE 0° MERIDIAN

If $P = 40$ lb, $\sigma_m = \sigma_c = 124 + 479 = 603$ lb per sq in. (compression). This value is close to the average of the test stresses at Station 21,22. The stresses on the upper surface are larger than the resultant stresses on the under surface. It appears that the theoretical analysis approximates closely the maximum stresses given by the test data, even though Station 21,22 is about 6.5 in. from the edge of a hole, approximately 2 in. in diameter, at the crown of the test dome. The results from only one test dome are not conclusive, but they

establish the possibility that the theoretical analysis may be used with safety to design shallow domes subjected to a concentrated load.

If Fig. 6(*a*) is examined, it will be noted that the curves of stress variation are similar to the plots of strain variation from the test data. Measuring along the meridian the theoretical stresses should equal zero about 4.95 in. out from the center of the loaded area, for meridional stresses, and about 7.15 in. out, for circumferential stresses. The strain data of the tests indicate that zero stresses occur, in general, about 8 in. out for both stresses. The difference between the theoretical circular area and the actual four squares probably explains the nonconformance. In either case, the compressive stresses on the upper surface have reduced to zero at a distance beyond the loaded boundary of about twice the diameter, or width, of the loaded area.

TABLE 2.—TEST TO FAILURE, WITH A CONCENTRATED LOAD ON A 3-IN. SQUARE, APPLIED BY LEVER SYSTEM AT STATION 5,6

(The Number Times 10^{-5} Is the Strain in Inches per Inch. Elongation Is Negative and Shortening Is Positive)

Line No. (1)	Load (lb) (2)	Station 5 (3)	Station 6 (4)
1	37.6	+ 3.9	+ 4.4
2	66.6	+ 15.6	+ 17.5
3	96.5	+ 28.35	+ 31.0
4	124.7	+ 41.0	+ 45.8
5	153.0	+ 56.5	+ 59.2
6	181.7	+ 73.9	+ 79.4
7	211	+ 90.8	+ 95.8
8	280	+110.0	+118.6
9	37.6[a]	+ 11.2	+ 12.6
10	178.3	+ 76.1	+ 84.2
11	236	+108.9	+117.0
12	264.5	+127.1	+137.9
13	293	+160.3	+165.5
14	322[b]	....	....

[a] Load release. [b] Load at failure.

Test to Failure.—The test to failure was made by applying a concentrated load at Station 5,6 (Fig. 1). The load-strain data are recorded in Table 2. These data, with moduli of elasticity and values of Poisson's ratio estimated from the plaster cylinder and transverse tests, were used to compute stresses. The results are given in Table 4.

This test was made several weeks after the concentrated load test of 40 lb at Station 5,6; and the strains due to the load of 37.6 lb, even for the reloading (see Table 4(*b*)), are about half those recorded earlier at Station 5,6. It would appear that the strains for the lower loads are smaller than would be expected from the previous tests. During the period of testing, the plaster had dried thoroughly. However, with the greatest load applied (293 lb), the computed stresses approach the compressive strength of the moist cylinders, giving about 94% of the cylinder strength for a load that was 91% of the load at failure.

TABLE 3.—MAXIMUM COMPRESSIVE STRESSES (IN POUNDS PER SQUARE INCH) CREATED BY A 40-LB LOAD

Station (Fig. 1)	σ_m (1)	σ_θ (2)
1,2	164	167
3,4	437	436
5,6	462	476
7,8	471	453
9,10	545[a]	545[a]
21,22	596	631

[a] Strains assumed to be equal in meridional and circumferential directions.

The stresses computed by the mathematical analysis in Appendix I approximated the stresses obtained from the measured strains only for the load applied at Station 21,22. For the 40-lb load applied at Station 5,6, the average

stress from the strain data was 469 lb per sq in., or 77.8% of the theoretical stress of 603 lb per sq in. Using this percentage reduction of the theoretical stress applied to the second loading, a comparison is afforded by Table 4(*b*) of the stresses from strain data (Col. 6) and the corrected theoretical stresses.

TABLE 4.—MAXIMUM COMPRESSIVE STRESSES AT THE UPPER SURFACE

Load (lb)	E (number times 10^6)[a]	Poisson's ratio μ	Maximum Compressive Stress (Pounds Per Square Inch)				Percentage of cylinder strength[c]	Load (percentage of ultimate)[d]
			Meridional, σ_m	Circumferential, σ_c	Average			
					Strain data	Formula[b]		
(1)	(2)	(3)	(4)	(5)	(6)	(7)	(8)	(9)
				(*a*) Initial Loading				
37.6.....	1.77	0.20	96	88	92	....	2.4	11.7
66.6.....	1.77	0.20	380	352	366	....	9.5	20.7
96.5.....	1.77	0.20	676	636	656	....	17.1	30.0
124.7.....	1.77	0.20	995	925	960	....	25.0	38.7
153.0.....	1.77	0.20	1,300	1,260	1,280	....	33.3	47.5
181.7.....	1.76	0.21	1,746	1,670	1,708	....	44.3	56.4
211	1.76	0.23	2,164	2,096	2,130	....	55.3	65.5
280	1.69	0.24	2,600	2,484	2,542	....	66.1	87.0
				(*b*) Load Released and Reloaded				
37.6.....	1.77	0.20	274	254	264	441	6.9	11.7
178.3.....	1.76	0.22	1,858	1,740	1,799	2,090	46.8	55.5
236	1.71	0.23	2,564	2,450	2,507	2,770	65.2	73.3
264.5.....	1.67	0.25	3,020	2,880	2,950	3,100	76.6	82.3
293	1.65	0.26	3,662	3,598	3,630	3,440	94.3	91.0

[a] Pounds per square inch. [b] By Eq. 4 (see text). [c] Col. 6 $\times \frac{1}{3,850}$. [d] Col. 1 $\times \frac{1}{322}$.

The values in Col. 7 were computed by the formula:

$$\sigma = 0.778 \frac{0.9415}{0.25^2} P \ldots\ldots\ldots\ldots\ldots\ldots\ldots (4a)$$

The theoretical stress of 441 lb per sq in. for a load of 37.6 lb is the value that would be expected from the strain data of the initial tests at Station 5,6. As the dome approached failure this same ratio (0.778) of test data to theoretical analysis was approached for the strain data of Table 2. The dome failed close to the load predicted by stress computations for the upper surface.

However, the computed stresses for the lower surface are tensile and

$$\sigma_m = \sigma_c = (0.7477 - 0.1938) \frac{P}{h^2} \ldots\ldots\ldots\ldots\ldots\ldots (4b)$$

For a load of $P = 293$ lb, this tensile stress equals $\sigma_m = \sigma_c = 0.778 \times 0.5539 \times 16 \times 293 = 2{,}020$ lb per sq in., as compared with the compressive value of 3,440 lb per sq in. on the upper surface (Col. 7, Table 4(*b*)). The transverse tests of Table 5 indicate a modulus of rupture for the plaster of about 750 lb

per sq in., the failure being tensile. It would seem that the effect of shrinkage and plastic flow is such that the computed tensile stresses on the under surface are not realized. Until greater experience is gained, the high computed tensile stresses are an added incentive to use conservative allowable stresses and to

TABLE 5.—TRANSVERSE TESTS OF BEAMS CUT FROM DOME FRAGMENTS

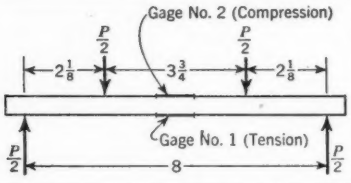

Specimen number	Widths	Depths
1	1.98	0.306
2	2.00	0.295
3	2.02	0.256

(*a*) PHYSICAL DATA, IN INCHES (AGE OF SPECIMENS, SIXTY DAYS)

Specimen No.	Gage No.	Load *P*, in Pounds								
		0	2.205	4.410	6.615	8.820	11.025	15.435	19.845	22.050
(*b*) STRAIN, IN INCHES PER INCH, IS THE NUMBER MULTIPLIED BY 10^{-5}										
1	1	0	−4.78	−9.88	−14.74	−19.90	−25.08	−35.80	−46.5	−53.3
1	2	0	+4.74	+9.61	+14.29	+18.88	+33.88	+33.40	+43.5	+48.6
2	1	0	−5.07	−10.27	−15.51	−20.75	−26.46	−37.20	−49.5	....[a]
2	2	0	+5.03	+10.32	+15.35	+20.60	+25.77	+36.25	+45.3	....[a]
3	1	0	−6.15	−12.42	−18.70	−24.94	−30.94	−45.20	....[b]	....
3	2	0	+6.06	+12.25	+18.16	+24.07	+30.40	+42.85	....[b]	....
(*c*) FIBER STRESS, IN POUNDS PER SQUARE INCH, ASSUMING THAT STRESS AND STRAIN AT A SECTION VARY UNIFORMLY										
1	....	0	75.8	151.5	227.5	300	379.5	530.5	682	758
2	....	0	80.8	161.9	242.9	320	404.0	566.0	728	....
3	....	0	106.2	212.5	318.8	425	531.0	744.0	....	....
(*d*) MODULUS OF ELASTICITY, IN POUNDS PER SQUARE INCH (USING AVERAGE STRAINS), IS THE NUMBER MULTIPLIED BY 10^6										
1	....	....	1.59	1.56	1.56	1.55	1.55	1.535	1.515	1.485
2	....	....	1.60	1.57	1.57	1.55	1.55	1.54	1.535	....
3	....	....	1.74	1.72	1.73	1.735	1.73	1.69	....	....

[a] Specimen 2 broke at a load of 22.05 lb. [b] Specimen 3 broke at a load of 17.64 lb.

disregard such stress reduction factors for position of the load as the value 0.778 used in Eq. 4*a*. Tests to observe variations in modulus of elasticity are presented in Table 6.

Continued Loading.—A time-load test was made with 40 lb applied at Station 7,8 for 5 days. During this interval the compressive strains directly under the loaded area gave increased values. The strains at the other stations tended to become tensile, this effect being most marked from 1 day to 5 days. Between the initial and the 24-hour readings, the maximum increase in compressive strain occurred at Station 7,8, followed by a slight steady decrease for

the next 4 days. From 0 days to 1 day a few of the other stations also showed an increase of compressive strain which was overcome by the decrease for the next 4 days.

Summary.—Concentrated loads about one eighth of the ultimate load were applied at stations on a meridian varying in position from close to the outer haunch to close to the central hole. In every test the greatest stresses occur at the upper surface of the shell directly under the load, and they increase as the load is moved toward the crown. The stresses for a load close to the crown check closely those obtained by mathematical analysis (see Appendix I). The compressive stresses on particles in the upper surface decrease rapidly as the distance increases away from the loaded area. The stresses located twice the width of the loaded area from the loaded boundary have ceased to be compressive. Beyond this perimeter all stresses are comparatively small in magnitude. A concentrated load has only a local effect as far as stress intensities are concerned.

TABLE 6.—SUMMARY OF AVERAGE TESTS FOR MODULUS OF ELASTICITY IN POUNDS PER SQUARE INCH (NUMBER TIMES 10^6)

Stress[a] (%)	Transverse tests	Compression Tests	
		Secant	Tangent
10.....	1.64	1.77	1.77
20.....	1.62	1.78	1.79
30.....	1.62	1.78	1.72
40.....	1.61	1.76	1.65
50.....	1.61	1.76	1.59
60.....	1.60	1.71	1.59
70.....	1.60	1.69	1.59
80.....	1.59	....	....
90.....	1.58	....	....

[a] Percentage of the ultimate strength.

If a concentrated load remains in place for several days, the strains increase about 15% under the load during the first day. Thereafter, there is a slow decrease; at 5 days the strains are about 5% greater than the initial readings. Elsewhere in the dome the strains showed small elongations due to plastic flow.

DISTRIBUTED LOADS

Eighth Segment Loaded.—The sand load of 267 lb on an eighth segment corresponds to an intensity of 40 lb per sq ft, or 0.278 lb per sq in., as compared with the concentrated load of 40 lb on 6.25 sq in. or 6.4 lb per sq in. Table 7 gives strain data at the time of load application for continued loading to 1.7 days. Fig. 6 shows the plotted strain data at the time of load application. The sand load was centered on the 0° meridian, and all other recorded stations were outside the loaded area. The initial circumferential strains (Fig. 6(*a*)) were relatively large along the 0° meridian with maximum values at Stations 3 and 5 of about the magnitude of those recorded for the concentrated load of 40 lb at Station 21,22. Elsewhere in the dome the circumferential strains were of small tensile magnitudes, except for the innermost Station 47 on the 90° meridian and three stations on the 315° meridian. The meridional strains (Fig. 6(*b*)) were also compressive on the 0° meridian, but the maximum values occurred nearer the crown of the dome at Stations 10 and 22. Elsewhere the strains were very low tensile values. Using these strain data, with a modulus of elasticity of 1.77×10^6 lb per sq in., and a Poisson ratio $\mu = 0.20$, the computed stresses along the 0° meridian are given in Table 8(*a*).

None of these stresses, caused by a load of 267 lb, exceed those obtained

TABLE 7.—STRAINS RESULTING FROM SAND LOADS CENTERED ON THE 0° RADIUS, INCLUDING THE EFFECT OF CONTINUOUS LOADING

(The Number Times 10^{-5} Is the Strain in Inches Per Inch. Elongation Is Negative and Shortening Is Positive)

Station No. (Fig. 1)	(*a*) 267 Lb on an Eighth Segment			(*b*) 534 Lb on a Quarter Segment				
	Duration of Loading, in Days:							
	0 (1)	0.85 (2)	1.7 (3)	0 (4)	0.8 (5)	1.8 (6)	2.8 (7)	4.8 (8)
1	+13.2	+ 4.75	+ 0.8	+ 5.4	−1.0	+0.05	+1.2	−0.55
2	+11.8	+ 7.3	+ 2.65	− 0.1	−295	−1.05	+0.2	−0.95
3	+28.2	+14.4	+ 6.75	+ 0.95	+0.7	+2.3	+4.0	+3.1
4	+10.9	+11.75	+ 7.35	+ 1.9	+2.1	+3.0	+4.7	+4.7
5	+29.15	+ 7.6	+ 4.4	+ 0.4	+1.4	+2.8	+3.9	+3.1
6	+11.1	+ 8.0	+ 5.4	− 2.75	−0.1	+1.3	+2.2	+1.45
7	+11.85	+ 6.6	+ 4.85	+ 2.85	+1.25	+2.6	+4.1	+2.8
8	+ 8.8	+ 7.5	+ 7.0	+ 2.9	−1.3	+0.75	+1.6	+2.1
9	+ 6.9	+ 5.35	+ 4.25	+ 0.8	−2.1	+0.15	+2.3	−1.9
10	+17.1	+ 9.1	+10.6	+ 4.9	+1.05	+3.1	+4.45	+4.5
11	− 0.1	− 0.1	+ 0.95	+ 0.25	−2.4	−1.45	−1.1	−0.9
12	− 0.25	− 1.2	− 0.8	+ 0.75	−2.35	−3.15	−3.2	−0.55
13	− 0.4	− 1.0	− 0.5	+ 0.2	−2.25	−2.05	−1.5	−0.45
14	+ 0.2	− 0.55	− 0.85	+ 1.05	−1.0	−1.8	−1.35	+0.6
15	− 1.55	− 2.45	+ 0.4	+ 1.55	−1.15	−0.45	−2.95	−0.2
16	− 0.05	− 0.8	+ 0.15	+ 1.05	−0.85	−1.15	−0.9	+0.5
17	− 0.3	− 0.9	+ 0.4	− 0.75	−2.4	−2.0	−1.4	−0.25
18	+ 0.15	− 0.25	+ 1.0	+ 1.0	−0.6	−0.45	+0.05	+3.0
19	− 1.25	− 1.7	0	− 1.0	−2.45	−1.95	−2.05	−1.15
20	+ 0.3	0	+ 0.95	+ 1.6	+0.05	−0.15	+0.05	+1.25
21	+ 9.25	+ 6.4	+ 4.8	− 0.7	+0.2	+2.6	+4.8	+3.8
22	+14.3	+ 5.5	+ 6.0	+ 0.65	+0.3	+2.8	+4.35	+3.35
23	− 1.5	− 1.7	− 0.35	− 1.5	−3.25	−3.3	−3.0	−2.0
24	+ 0.2	+ 0.25	+ 1.2	+ 0.5	−0.75	−1.25	−1.1	+0.55
25	− 0.9	− 1.65	− 1.1	− 1.4	−1.7	−1.1	−1.9	−0.9
26	− 0.5	− 1.25	+ 1.5	− 1.35	−3.1	−4.2	−4.45	−0.15
27	− 0.65	− 0.8	− 0.8	− 1.3	−3.0	−4.0	−3.2	−0.7
28	+ 0.2	− 0.25	+ 1.15	− 0.35	−1.0	−2.05	−1.0	+1.85
29	− 0.25	− 1.05	+ 0.15	− 0.4	−2.35	−2.85	−2.3	−0.25
30	− 1.2	− 1.05	− 0.3	+ 0.85	−1.0	−1.9	−1.5	+1.05
31	− 0.1	− 1.8	+ 1.0	0	−2.1	−2.7	−2.65	−0.4
32	− 0.15	− 0.6	− 0.15	0	−1.6	−2.0	−1.65	+0.5
33	− 0.1	− 0.8	− 0.3	0	−1.8	−2.2	−1.85	−0.25
34	− 0.1	− 0.45	+ 0.05	− 0.4	−1.75	−2.2	−1.9	−0.35
35	− 0.9	− 1.1	− 1.0	+ 0.15	−2.0	−1.5	−1.2	−0.75
36	− 0.2	− 1.25	− 1.4	+ 0.6	−2.15	−3.65	−3.75	−0.1
37	− 0.25	− 0.8	− 2.15	+ 0.65	−2.15	−2.6	−3.1	−0.3
38	− 0.25	− 0.9	− 2.2	+ 1.5	−1.05	−2.2	−2.55	+0.7
39	− 0.9	− 0.85	0	+ 3.4	−2.25	−1.9	−1.25	−0.1
40	− 0.4	− 0.1	+ 0.45	0	−0.85	−0.95	−0.25	+1.05
41	− 0.7	− 0.85	− 0.3	− 0.2	−2.3	−2.45	−2.35	−0.1
42	− 0.7	− 0.95	+ 0.85	0	−1.5	−1.5	−1.6	+0.35
43	− 0.3	− 0.7	+ 0.55	0	−1.65	−1.5	−1.35	+0.2
44	− 0.35	− 0.5	+ 0.65	− 1.0	−1.75	−1.75	−1.4	0
45	+ 0.4	0	+ 0.3	+ 1.75	−0.65	−0.65	+0.1	+2.0
46	− 0.65	− 1.75	− 1.5	− 1.0	−3.5	−3.6	−3.75	−1.45
47	+ 5.8	+ 0.5	+ 1.35	+ 1.45	0	−0.95	−0.75	+0.2
48	− 1.05	− 1.45	− 0.6	− 0.7	−2.8	−3.9	−4.15	−2.95
49	− 0.85	− 1.25	− 0.6	− 5.75	−4.5	−1.6	0	−1.1
50	− 0.1	− 1.45	− 1.0	− 1.5	−3.6	−2.55	−0.85	−0.45
51	− 0.6	− 1.35	+ 0.2	− 2.95	−1.6	+0.7	+1.15	+0.5
52	+ 0.55	− 0.25	0	+ 3.8	+1.1	+1.35	+2.9	+4.4
53	+ 0.95	+ 0.15	+ 0.6	− 2.0	−1.1	+0.65	+1.9	+1.55
54	− 1.0	− 2.3	− 1.4	+ 2.94	−1.6	−0.9	+0.15	+0.9
55	+ 1.5	+ 0.75	+ 1.32	0	+0.6	+2.85	+4.8	+5.4
56	− 0.15	− 0.85	− 1.25	+11.95	−2.95	−1.2	−0.4	+0.8
57	− 0.7	− 0.9	− 0.75	− 0.65	−2.05	−2.1	−1.75	−0.3
58	0	− 1.2	− 0.45	0	−2.6	−4.8	−3.7	0
59	− 0.5	− 1.3	− 0.4	− 0.65	−2.45	−2.95	−2.5	−0.4
60	− 0.1	− 0.55	+ 0.35	0	−1.45	−2.55	−1.75	+1.05
61	− 0.65	− 0.85	+ 0.15	− 1.0	−1.9	−2.05	−1.95	−0.25
62	− 0.3	− 0.45	+ 0.65	+ 0.4	−0.9	−1.45	−1.1	+1.25
63	....	....	....	....	....	....	....	....
64	− 0.15	+ 0.2	+ 1.0	− 0.4	−1.05	−1.6	−1.45	+0.1

by the concentrated load of 40 lb at Station 21,22. If the meridional stress, σ_m, at each station is plotted according to its position on the meridian, the individual values do not deviate greatly from their average. This is not true for the circumferential stresses, σ_c, which greatly exceed their average from a location close to Station 1,2 (and the haunch) to a position about halfway up the meridian; beyond this point the circumferential stresses are much lower than their average.

TABLE 8.—COMPARISON OF STRESSES ALONG THE 0° MERIDIAN (POUNDS PER SQUARE INCH) FOR A DISTRIBUTED SAND LOAD OF 267 LB ON A GIVEN SEGMENT

(Compression Is Positive)

Station (see Fig. 1)	(*a*) EIGHTH SEGMENT		(*b*) QUARTER SEGMENT	
	σ_m	σ_c	σ_m	σ_c
(1)	(2)	(3)	(4)	(5)
1,2	267	287	18	99
3,4	305	560	39	25
5,6	312	579	−3	−49
7,8	206	252	64	63
9,10	341	191	93	33
21,22	298	224	9	−11
Average....	(288)	(349)	....	....

Continued loading for 0.85 day gives a marked decrease in compressive strains along the central 0° meridian. The amount of depression had decreased but the general shape was unchanged, since the stations of greater strain had proportionately greater reductions. Elsewhere in the dome there was an increase in tensile strains, with the changes again proportional to the magnitude of the initial strain. It appears that the depression under the load was reduced, whereas elsewhere the dome shell bulged outward.

In the interval from 0.85 to 1.7 days there was further readjustment. The circumferential compressive strains on the 0° meridian again decreased roughly in proportion to the strain value, whereas the meridional strains increased at Stations 10 and 22 with a considerable decrease at Stations 2 and 4 near the haunch. Elsewhere in the dome, outside the loaded area, the change in strain was largely a reduction of tensile strain, so that about half of the final strains were compressive. It appears that the depression under the load was again reduced; elsewhere the previous bulge was also decreased.

The total effect of continued loading from 0 to 1.7 days was to reduce the compressive strains under the load on the 0° meridian. The circumferential strains were reduced from 38% to 94%; and the meridional, from 20% to 68%. The greater strains had the greater percentage reduction so that the strains at 1.7 days tended to approach a common value more closely. The stations outside the loaded area, for the most part, had net shortenings so that compressive strains were increased and tensile strains were reduced. Of the twenty-five circumferential stations outside the loaded area, twenty one recorded small initial tensile strains of less than 1.55×10^{-5} upon application of the load. The other four were close to the hole at the crown of the dome. At the end of 1.7 days eleven had tensile, twelve compressive, and two zero strains, compared with the unloaded dome. Similarly, for the twenty-six meridional stations outside the loaded area, the initial strains were: Nineteen tensile, six compressive, and one zero. Four of the compressive strains were on the 180° meridian, the other two were near the haunch. At the end of 1.7 days these twenty-six stations divided into twelve with tensile, thirteen with compressive, and one with zero, strains.

The effect of plastic flow on this plaster dome appears to be a readjustment by which the strains on the upper surface under the loaded area are markedly reduced, with a tendency to approach more uniform values. Stations outside the loaded area show an increase in tension from 0 day to 0.85 day and then a greater decrease, so that the general net result is a decrease in the original tensile values. However, stations on the circumference including Station 3,4 have final stresses indicating that the restraint of the near-by haunch causes bending.

The foregoing statement covers the observed readings on the upper surface. A complete knowledge of the effect of plastic flow cannot be obtained unless data in regard to the strains on the under surface and the change of deflection are also known. The area under the load is in bending as well as direct stress and the plastic readjustment is complex. It is possible that the dome is no longer a perfect spheroid elsewhere, and has been displaced horizontally as well as vertically.

Quarter Segment Loaded.—The load of 534 lb also corresponded to an intensity of 40 lb per sq ft, or 0.278 lb per sq in. The sand load centered on the 0° meridian, and its boundaries were the 45° and 315° meridians. Compared with eighth-segment loading, the initial strains were much reduced. Using a modulus of elasticity of 1.77×10^6 lb per sq in. and a Poisson ratio of 0.2, the computed stresses along the 0° meridian are given in Table 8(*b*).

At the boundary on the 315° meridian the circumferential strains on the top surface were tensile and the meridional strains were compressive. Outside the loaded area the strains were all of small magnitude, whereas their reversals suggested wave action in the shell.

This sand load remained in place for 5 days. Strain readings to measure plastic flow were taken at approximately 1, 2, 3, and 5 days. The readings varied considerably from day to day with many reversals of strain from compression to tension and vice versa. Many readings were as small as the probable error of reading. On the center line of the loaded area (0° meridian), the circumferential strains indicated that proximity to the haunch affected Station 1 and the hole at the crown may have affected Stations 9 and 21. The haunch apparently affected the meridional strains as far out as Station 6. Neglecting the readings at Station 1,2, at the end of 2.8 days the average circumferential strain was $+ 3.8 \times 10^{-5}$ and the individual values were fairly uniform; at 4.8 days the average strain was $+ 2.2 \times 10^{-5}$, but the values at Stations 9 and 21 departed considerably from this average. Similarly, the meridional strains averaged $+ 3.5 \times 10^{-5}$ at 2.8 days and $+ 3.2 \times 10^{-5}$ at 4.8 days.

At the boundary of the sand load on the 315° meridian, the circumferential strain curve preserved its general shape as time passed but steadily shifted to the compression side, so that initial strains that were wholly tensile by 2.8 days became wholly compressive. The 4.8-day readings were slightly lower. The meridional strains were wholly compressive for the initial readings (except for those at Station 50) with the greatest strain recorded for all stations at Station 56 near the crown (11.95×10^{-5}). There was a marked shift at 0.8 days so that all strains were tensile, except those at Station 52 near the haunch.

Thereafter the general pattern was preserved but the shift was toward small compressive strains.

The general effect of plastic flow on the upper surface of the shell along the center line meridian of the loaded area was to produce fairly uniform compressive strains which oscillate above and below $+ 3 \times 10^{-5}$ between 1.8 days and 4.8 days, except for the station close to the haunch. These strains were usually greater than the initial strains. At the boundary of the sand load (315° meridian) the strains reversed, the circumferential strain becoming compressive, whereas the meridional strain became tensile at 0.8 day, and then the strains slowly returned to low compressive values.

Outside the loaded area the initial strains had low values, some compressive, some tensile. From 0.8 day to 2.8 days they all shifted toward greater tensile values, remaining fairly constant during this time interval. At 4.8 days the strains all tended to approach zero strain: Seventeen with final compressive values (maximum $= + 3.0 \times 10^{-5}$), twenty four with final tensile values (maximum $= - 2.95 \times 10^{-5}$), and two with zero strain.

Uniform Load on Entire Dome Surface.—The tendency for the stresses to decrease as a larger area is loaded is reasonable. If the same sand load of 40 lb per sq ft is assumed to be spread over the entire surface, the circumferential and meridional stresses can be computed, assuming the shell to be a membrane.[6] In the part of the shell close to the haunch, the circumferential stress equals 40 lb per sq in.; and the meridional stress, 60 lb per sq in. No allowance was made for bending stresses caused by the proximity to the larger and more rigid haunch; but a load four times that on the quarter segment produced direct stresses of the general magnitude of those computed in Table 8(*b*) for the quarter segment.

General Summary

The distributed load tests were made to clarify the transition from an eccentric concentrated load to a uniformly distributed load. They emphasize the fact that progressive concentration causes increasingly larger strains under the loaded area.

The discussion of concentrated loads is based on a load of 40 lb bearing on an area of 6.25 sq in. The distributed loads were $6\frac{2}{3} \times 40$ on an eighth segment and $13\frac{1}{3} \times 40$ on a quarter segment. The maximum stresses for the eighth-segment loading were comparable to those obtained for the concentrated load in the position producing the greatest recorded strains. The maximum stresses for a quarter-segment loading were about a sixth as much. The part of the dome well outside the loaded area had negligible stresses.

The readjustments due to plastic flow tended to reduce the strains in the upper surface of the loaded area. Elsewhere, the strains tended to become tensile in the first day of quiescent loading. Thereafter the strains outside the loaded area tended to approach zero. During these adjustments the restraining effect of the haunch was noticed at near-by stations.

[6] "Analytic Solution of Masonry Domes," by David C. Coyle, *Transactions*, ASCE, Vol. 88, 1925, p. 102.

ACKNOWLEDGMENT

This investigation was planned and executed for the Preload Company. The test was made on a plaster model to a reduced scale of a large dome designed and erected by this company.

APPENDIX I. MATHEMATICAL ANALYSIS

By Eric Reissner

To facilitate the analysis of the test data of the model dome, theoretical equations were derived[5] for the direct stresses and bending stresses as components of the total normal stress in a shallow spherical dome treated as a thin shell. The equations apply to a total load P distributed uniformly over a circular area with its center at the apex of the dome. Let "ber," "bei," "ker," and "kei" be used to designate tabular functions. Also let $\xi_v = x/l$ and $\xi_c = r_c/l$ denote a dimensionless variable and a dimensionless constant, respectively (see Fig. 7). For small values of ξ_v:

$$\text{ber } \xi_v \approx 1 - \frac{\xi_v^4}{64} \quad \ldots\ldots (5a)$$

$$\text{bei } \xi_v \approx \frac{\xi_v^2}{4} - \frac{\xi_v^6}{64 \times 36} \quad \ldots\ldots (5b)$$

$$\text{ker } \xi_v \approx -\log_e \xi_v + 0.1159 + \frac{\pi}{16}\xi_v^2 \quad \ldots\ldots (5c)$$

and

$$\text{kei } \xi_v \approx -\frac{\xi_v^2}{4}\log_e \xi_v - \frac{\pi}{4} + (0.1159 + 1)\frac{\xi_v^2}{4} \quad \ldots\ldots (5d)$$

Equations for maximum stresses, σ, are: Direct—

$$\sigma_m(0) = \sigma_c(0) = \frac{P}{h^2}\frac{\sqrt{3(1-\mu^2)}}{\pi\,\xi_c^2}(1 - C_1) \quad \ldots\ldots (6a)$$

and bending—

$$\sigma_m(0) = \sigma_c(0) = \pm\frac{P}{h^2}\frac{3(1+\mu)}{\pi\,\xi_c^2}C_2 \quad \ldots\ldots (6b)$$

TABLE 9.—FORMULAS FOR THE DETERMINATION OF ARBITRARY DESIGN CONSTANTS

C_1	C_2	D_2	D_4	Value
ber ξ_c	bei ξ_c	−ker ξ_c	−kei ξ_c	1
−bei ξ_c	ber ξ_c	kei ξ_c	−ker ξ_c	0
ber′ ξ_c	bei′ ξ_c	−ker′ ξ_c	−kei′ ξ_c	0
−bei′ ξ_c	ber′ ξ_c	kei′ ξ_c	−ker′ ξ_c	0

in which subscript m denotes "meridional"; and subscript c denotes "circumferential." To use Eqs. 5 and 6, the following data must be known: The concentrated load P; the radius r_s of the spherical dome shell; the thickness h of the shell; the radius r_c of the circular loaded area, equal to the actual loaded area; and Poisson's ratio μ. For concrete $\mu = 0.20$ is a reasonable value. The arbitrary constants C_1 and C_2 in Eqs. 6 are determined by solving the equations in Table 9.

The procedure consists in first determining the values of the arbitrary constant $\xi_c = r_c/l$, the length parameter l being defined as:

$$l = \frac{\sqrt{h\,r_s}}{\sqrt[4]{12(1-\mu^2)}} \qquad (7)$$

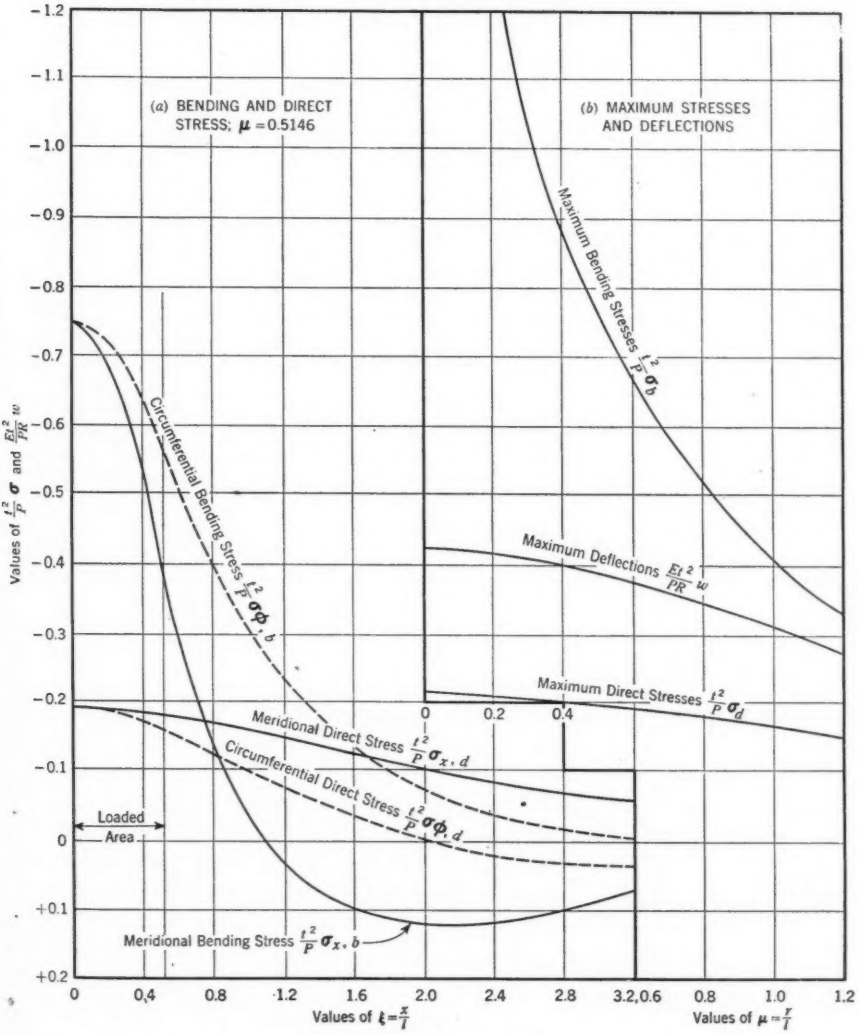
(a) BENDING AND DIRECT STRESS; $\mu = 0.5146$
(b) MAXIMUM STRESSES AND DEFLECTIONS
Values of $\frac{t^2}{P}\sigma$ and $\frac{Et^2}{PR}w$
Maximum Bending Stresses $\frac{t^2}{P}\sigma_b$
Maximum Deflections $\frac{Et^2}{PR}w$
Maximum Direct Stresses $\frac{t^2}{P}\sigma_d$
Circumferential Bending Stress $\frac{t^2}{P}\sigma_{\phi,b}$
Meridional Direct Stress $\frac{t^2}{P}\sigma_{x,d}$
Circumferential Direct Stress $\frac{t^2}{P}\sigma_{\phi,d}$
Meridional Bending Stress $\frac{t^2}{P}\sigma_{x,b}$
Loaded Area
Values of $\xi = \frac{x}{l}$
Values of $\mu = \frac{r}{l}$

FIG. 7.—DESIGN VALUES OF DIMENSIONLESS FACTORS ξ_v AND ξ_s

With this value of ξ_c enter Fig. 7(*a*) and read the maximum bending stress σ_b and the maximum direct stress σ_d. Fig. 7(*a*) is not applicable for $\xi_c < 0.2$ or $\xi_c > 1.3$; but Eqs. 5 can be solved directly or by interpolation in Table 10.

Illustrative Example.—A numerical example was solved and discussed in detail in the original analytical report.[5] For this study the dimensions of the model were used—namely: $r_s = 102$ in.; $h = 0.25$ in.; and $\mu = 0.20$. By Eq. 7, then, $l = 2.7410$; and $\xi_v = x/l = 0.3648\,x$. The load was assumed to

TABLE 10.—VALUES OF FUNCTIONS OCCURRING IN THE SOLUTION OF THE EQUATIONS OF THE FLAT SPHERICAL DOME PROBLEM

x	ber x	bei x	ker x	kei x	$\frac{\text{ber}' x}{x}$	$\frac{\text{bei}' x}{x}$	$\frac{\text{ker}' x}{x}$	$\frac{\text{kei}' x}{x}$
0	1.0000	0	$+\infty$	−0.7854	0	0.5000	$-\infty$	$+\infty$
0.2	1.0000	0.01000	1.7331	−0.7581	−0.00250	0.5000	−24.615	1.1146
0.4	0.9996	0.04000	1.0626	−0.7038	−0.01000	0.4999	−5.8802	0.7738
0.6	0.9980	0.8998	0.6931	−0.6374	−0.02250	0.4997	−2.4276	0.5803
0.8	0.9936	0.1599	0.4529	−0.5664	−0.3999	0.4989	−1.2342	0.4488
1.0	0.9844	0.2496	0.2867	−0.4950	−0.06245	0.4974	−0.6946	0.3524
1.5	0.9211	0.5576	0.05294	−0.3314	−0.1400	0.4368	−0.1961	0.1971
2.0	0.7517	0.9723	−0.04164	−0.2024	−0.2465	0.4585	−0.05330	0.1099
3.0	−0.2214	1.9376	−0.06703	−0.05115	−0.5233	0.2935	+0.00716	0.03068
5.0	−6.2301	0.1160	−0.01148	+0.01118	−0.7691	−0.8708	0.00344	−0.00016

act on three different areas—$\pi\, r_c^2 = 1.5625$ sq in., 6.25 sq in., and 16 sq in. The case in which the loaded circular area equals 6.25 sq in. approaches closely the test case of 6.25 sq in. composed of four squares with outer boundaries of 3 in. in each direction. For this case: $\xi_c = 0.5146$; $C_1 = 0.9050$; and $C_2 = 0.1728$. The maximum combined stress at the upper surface of the shell equals:

$$\sigma_m = \sigma_{m,d} + \sigma_{m,b} \quad \ldots\ldots\ldots\ldots\ldots\ldots\ldots\ldots\ldots\ldots (8a)$$

and

$$\sigma_c = \sigma_{c,d} + \sigma_{c,b} \quad \ldots\ldots\ldots\ldots\ldots\ldots\ldots\ldots\ldots\ldots (8b)$$

These maximum stresses are equal for the meridional and circumferential directions. Fig. 7 shows, not only the maximum stresses, but the variation of stress over, and beyond, the loaded area as the loaded area is increased in size.

Table 10 gives the values of the functions used in the equations of Table 9 to obtain the constants C_1 and C_2. These stress equations are derived for a concentrated load on a circular area at the crown of the dome. The fact that the loaded area is not circular can be neglected, provided the area is small compared to the total dome surface. The equations can also be applied approximately, if the load is not at the crown, so long as the loaded area is not near the springing, a hole, or other discontinuity. These results are approximate because an eccentrically applied gravity load is not normal to the surface loaded.

APPENDIX II. NOTATION

The following letter symbols, adopted for use in the paper, and in its discussion, conform essentially to American Standard Letter Symbols for Mechanics (ASA—Z10.3—1942), prepared by a Committee of the American

Standards Association, with Society participation, and approved by the Association in 1942:

C = an arbitrary constant; formulas for the determination of C_1, C_2, D_2, and D_4 are listed in Table 9;
c = subscript denoting "circumferential";
D = an arbitrary constant, such as D_2 and D_4 in Table 9;
d = diameter;
E = modulus of elasticity;
h = thickness of shell;
l = a length parameter defined by Eq. 7;
m = subscript denoting "meridional";
P = a concentrated point load, or the resultant of a distributed load assumed to be acting at the centroid of pressure;
r = radius, with subscript c to denote radius of area of concentrated loading, with subscript s to denote radius of spherical shell;
x = perpendicular distance from the axis of symmetry of a spherical shell;
ϵ = strain, with subscripts m and c to denote "meridional" and "circumferential," respectively;
μ = Poisson's ratio;
ξ = dimensionless quantity, with subscripts c and v to denote a "dimensionless constant" and "dimensionless variable," respectively; and
σ = unit stress, with subscripts b and d to denote "bending" and "direct" stress, respectively, and subscripts m and c to denote "meridional" and "circumferential," respectively.

The various tabular functions "ber," "bei," "ker," and "kei" are defined by Eqs. 5. These operators primed denote first differentials.

AMERICAN SOCIETY OF CIVIL ENGINEERS

Founded November 5, 1852

PAPERS

SUBSIDENCE OF THE TERMINAL ISLAND-LONG BEACH AREA, CALIFORNIA

BY FREDERIC R. HARRIS,[1] M. ASCE, AND EUGENE H. HARLOW,[2] ASSOC. M. ASCE

SYNOPSIS

By early 1945 the subsidence taking place in and around Terminal Island, Long Beach, Calif., had reached a maximum of more than 4 ft and the rate was approaching 1 ft per yr. Therefore, to protect existing structures and to evaluate the risks in future engineering enterprises in the area, it became imperative to determine the answers to three questions:

(1) What is the cause of the subsidence?

(2) Can its future progress be predicted?

(3) What effect will it have on civil engineering works?

This paper presents answers to these questions. It now appears certain that by far the predominant influence is the effect of pumping oil from the Wilmington oil field, which coincides in location and extent with the subsiding area. Extensive data were gathered to determine the factors producing oil field settlements, and laboratory tests were performed on samples of shales from different depths to determine the relative compressibilities. Calculated theoretical subsidence was compared with observed subsidence, a correction factor was computed, and theory was then extended into a prediction as to the future course of the settlement. From these studies it is concluded that the maximum rate of settlement has probably been reached and that henceforth the rate will gradually diminish until eventually, in perhaps ten or fifteen years, the maximum subsidence will reach about 9 ft.

Elevations of waterfront structures, gravity flow pipe lines, etc., may have to be adjusted accordingly. Since differentials will be gradual, only very long or rigid structures will be subjected to warping or cracking.

NOTE.—Written comments are invited for immediate publication; to insure publication the last discussion should be submitted by March 1, 1948.

[1] Rear Admiral, CEC, U.S.N. (*Retired*); Cons. Engr., New York, N. Y.

[2] Foundation Engr., Frederic R. Harris, Inc., New York, N. Y.

Nature of Observed Subsidence

Occurrences of differential movements in the Los Angeles-Long Beach harbor areas of California have long been recognized (1)(2)(3)(4).[3] However, comparison of records of tide gages maintained at several points in the Los Angeles and Long Beach Harbor areas for many years with observations at La

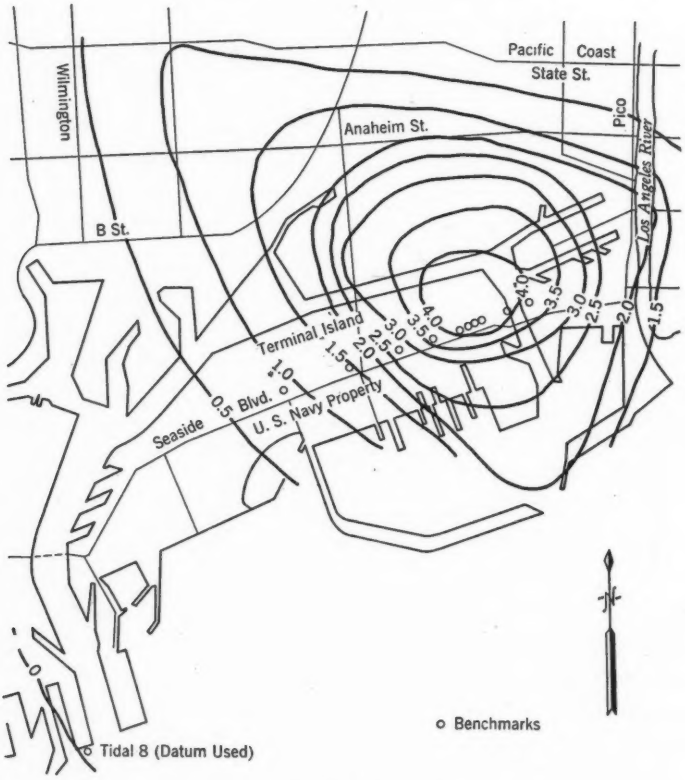

Fig. 1.—Contours of Subsidence—1945

Jolla and San Francisco show that the gage at berth 60, municipal pier No. 1, Los Angeles harbor, referred to as "tidal 8," has not changed in elevation since 1931 by more than about 0.1 ft.

Subsidence at various bench marks in the affected area during different periods was determined, in general, by subtraction of corresponding elevations. Those for 1933 were taken as representing zero subsidence, because study of the Long Beach outer harbor tide gage record, as well as of frequent levelings by the Southern California Edison Company, reveals the 1933 leveling to be the most recent extensive survey prior to the beginning of the rate of subsidence prevailing in 1945 and 1946.

[3] Numerals in parentheses .thus: (1), refer to corresponding items in the Bibliography (see Appendix).

Fig. 1 shows contours of the subsidence that occurred from 1933 to 1945. Profiles taken on several dates along a representative line through the area are given in Fig. 2. Fig. 3 shows the increase of subsidence at certain bench marks plotted against time.

Geology of the Region

The geologic history of the region has been amply described in previous reports and papers (5)(6). Generally, all the sediments in the upper 7,000 ft are poorly consolidated "shales" and sands of Miocene, Pliocene, Pleistocene, and recent origin. The Miocene and lower Pliocene strata are warped into a gentle anticline with its axis in a northwest-southeast direction, forming an elongated dome whose highest parts are close to the east end of Terminal Island. These strata are all highly faulted, and form the structure of the Wilmington oil field, at present one of the largest producing fields in California. The faults have been traced upward to an unconformity at the base of the Upper Pliocene, or Pico, formation, about 2,000 ft below the surface, but not above this point Varying thicknesses of beds in the underlying Repetto formation indicate that the motion along these faults was still occurring until late Pliocene times, but did not continue into later periods. The upper 1,800 ft of sediments generally contain more or less fresh water in the voids, and have been the source of fresh water supply to residents of the basin for many years.

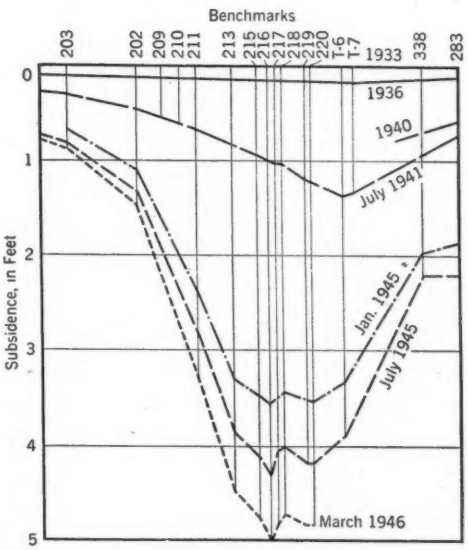

Fig. 2.—Subsidence Along Seaside Boulevard

Factors Contributing to the Subsidence

At least five major sources of settlement operating in this area have contributed to the observed subsidence in varying degree. They are: (*a*) Changes in the land surface from filling and dredging; (*b*) pumping of water for industrial and domestic uses; (*c*) pumping of water during dewatering of the site of dry dock No. 1, United States naval drydocks; (*d*) pumping of oil from five major oil zones in the Wilmington oil field; and (*e*) tectonic forces. Any study of this problem resolves itself finally into an opinion based on factual observation and accepted principles of statics and mechanics, concerning the relative importance of these possible sources. Therefore, each of them is discussed.

Filling and Dredging Operations.—Development of the Los Angeles and Long Beach harbor areas has been in progress since about 1900. At that time,

Terminal Island, then called Rattlesnake Island, was a low sand spit. It has been gradually enlarged by dredged fill to several times its initial size, and was eventually built up to about El. +13. However, as far as is known, no fill materials have been brought by man into this area from any distance. Consequently, no part of the over-all subsidence of the area can be attributed to an increase in the total weight of overburden, except for the accretion that has taken place from natural causes.

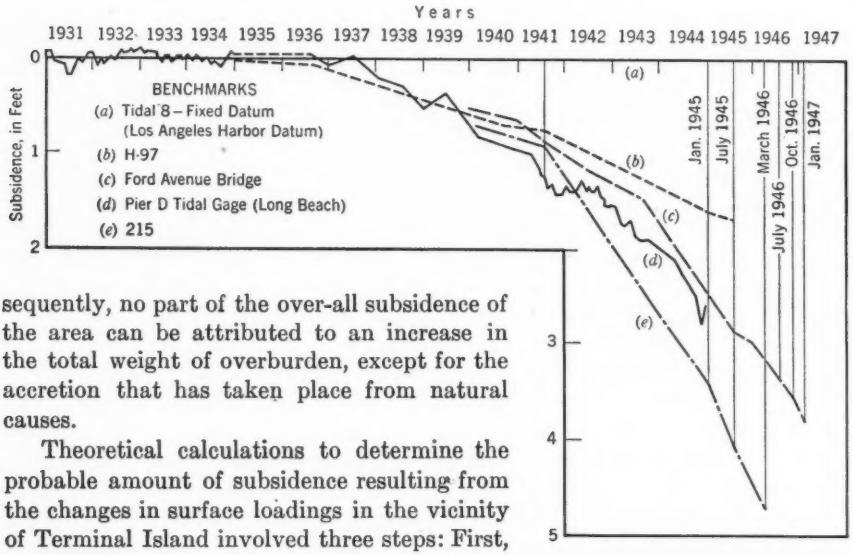

FIG. 3.—SUBSIDENCE OF TYPICAL BENCH MARKS IN PERIOD 1931–1947

Theoretical calculations to determine the probable amount of subsidence resulting from the changes in surface loadings in the vicinity of Terminal Island involved three steps: First, the determination of the change in weight of surface deposits over different parts of the area, and the time sequence of these changes; second, the total consolidation of underlying compressible strata that should ultimately occur; and, third, the influence of time effects during the consolidation, which reflect the proportion of the settlement that would cause observed movement of surface bench marks. From a study of many consolidation tests on clays and loams by several investigators (7)(8), it was concluded that, of the total subsidence measured, perhaps in the strip along the seaward side of Terminal Island, about 0.2 ft could be attributed to surface loading.

General Effect of Pumping Liquids.—If the ground-water table is lowered, all the sediments between the initial and final ground-water surfaces will experience a loss of buoyancy, and will rest more heavily on the underlying soil skeleton, which will eventually compress. The compression may not occur suddenly, since reduction in volume requires the escape of excess water in the voids. According to the theory of consolidation advanced by Karl Terzaghi, M. ASCE, the time required varies as the square of the thickness of the stratum undergoing compression. Since the more compressible strata are generally the fine-grained silts and clays, which may exist in layers between more pervious sand beds, time is needed for such a volume change before a static equilibrium is reestablished.

If two or more pervious beds are separated by continuous impervious clay strata, the water pressures in the voids of the lower bed may not conform to the

ground-water table in the upper bed (9). Also, if the water pressure in the lower or confined aquifer is reduced, the pressure and level of the water in the surface aquifer will not be affected (see Fig. 4). However, the lower aquifer will undergo compression throughout its thickness.

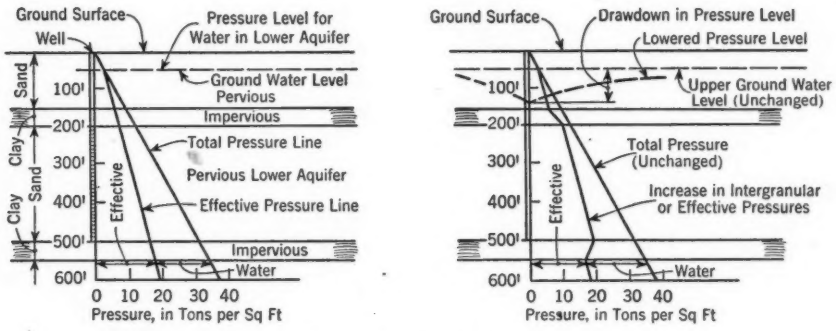

FIG. 4.—PRESSURES IN SOILS
(*a*) Before Pumping
(*b*) During Pumping from Lower Aquifer

From the foregoing, it is seen that there are two distinct effects that may result from the pumping of a liquid from the ground:

1. Loss of buoyancy of the soil particles. This occurs if the ground-water surface is lowered, causing compression of all underlying strata.
2. Increased intergranular pressures in a pervious zone confined between impervious layers. This occurs if the liquid pressure in the confined zone is reduced, and results in compression of the confined zone and of adjacent parts of the "aquicludes" (impervious layers) at top and bottom.

The same general principles apply to the effect of pumping any liquid—whether water or oil.

Water Pumping for Industrial and Domestic Uses.—Fresh water in the Long Beach-Wilmington coastal plain is obtained from two water-bearing zones. The upper or Gaspar zone occurs in the surface deposits of recent age and consists of from 100 ft to 200 ft of alluvial deposits of sand and gravel interbedded with silt and clay. It includes both surface waters and confined waters. The lower or Silverado zone is a confined aquifer of Pleistocene deposits of sand and gravel with intervening layers of silt and clay. The zone varies from 150 ft to 500 ft in thickness. It varies in depth, being from 200 ft to 900 ft below the land surface in the Wilmington section.

The Newport-Inglewood fault forms a partial barrier to the flow of underground water. The area to the northeast of the fault was originally highly artesian, deriving pressure from water entering the pervious strata in the foothills of the mountains which surround the basin. The area to the southwest of the fault was probably only slightly artesian originally. Water-bearing zones in this area are replenished mainly by underflow across the Newport-Inglewood

fault, through imperfections in the fault barrier. As a result, the effect on lowering the ground-water levels by pumping is much more noticeable in the coastal area south of the fault than in the areas to the north.

Development of ground water in the Los Angeles coastal plain began about 1870 (10). Records show that wells drawing from the Gaspar and Silverado zones had static water levels from 10 ft to 30 ft above sea level in 1903, gradually dropping to about sea level in the Gaspar zone and to as much as from 60 ft to 70 ft below sea level in the Silverado zone (11).

Changes in elevation of the ground surface caused by pumping water from the lower strata are almost certainly part of the reason for early survey difficulties. The influence is probably still contributing, but to a moderate extent, with the fraction of total subsidence resulting from this source amounting to inches, not feet. The center of the depression would be expected to lie some distance north of Terminal Island.

Dewatering of the Site of Dry Dock No. 1.—Pumping water from surface and confined pervious strata during the construction of dry dock No. 1 drew down the pressure levels in these beds from sea level to about El. −75, based on mean lower low water datum. The pumping covered a period from June, 1941, to April, 1942. Maximum drawdown in water levels did not occur until some weeks after pumping was begun. After pumping was stopped, readings on near-by wells indicated that the pressure levels rapidly rose to their initial elevations, close to mean sea level.

Water levels in wells in the upper aquifers were affected varying amounts as far north as 2 miles. Local subsidence was observed in the affected area, varying with the drawdown in pressure level, roughly in inverse proportion to the distance from the dock site. The Southern California Edison Company, whose Long Beach steam station is about 2,000 ft northeast of the dock, installed fifteen observation wells, some 35 ft deep and some 150 ft deep, to measure the reduction in water pressure level in the two principal pervious strata of the local part of the aquifer (7). Observations were also made of the motion of bench marks around the plant.

Within a radius of 2,000 ft of the dock site the ground settled as much as 0.45 ft around the casings of many oil wells. In most instances, the construction of the derrick foundations permitted the ground and concrete base slabs to settle around the casings without appreciable damage to either casings or concrete. There were a few occurrences of cracked base slabs, and damage was reported to at least one well casing. Differential movement between the ground surface and the casings was observed only during the period of pumping at the dock site. Prior to and since that time, the oil well casings have apparently behaved as if they were part of the ground surface.

To estimate how much of the total subsidence was caused by dewatering the dock site, the theoretical consolidation resulting from the effect of the observed drawdown of liquid pressure levels was computed.

From a study of the stratification and drawdown records, it appears that the substrata affected by the pumping consist of sands and gravels of the Gaspar aquifer, extending in depth from about El. −70 to about El. −270. The silty clay materials bounding, and within, the aquifer were assumed to have a coeffi-

cient of compressibility (C_c) of 0.144. Calculated contours of equal subsidence resulting from this pumping appear consistent with the measurements of motion around well casings. When pumping was stopped, in the spring of 1942, water levels rose to their previous values, and the consolidation ceased. In fact, a slight rebound, or increase in volume of the consolidated strata, occurred. Therefore, this settlement is considered to represent merely an incident in the general subsidence phenomenon in the area, and its effect was felt solely in the period from June, 1941, to April, 1942.

Pumping from the Wilmington Oil Field.—The mechanics of liquid flow during production from an oil well are generally the same as those for pumping water from a confined aquifer. The oil sands forming the equivalent of the aquifer are bounded top and bottom by impervious layers of "shale," or silt and clay compacted by the weight of the overburden. The oil in the sand voids is initially subjected to pressures which depend mainly on the depth of the strata below sea level. As oil is withdrawn from the well, there is a pressure reduction, which produces a gradient toward the well from all sides. This gradient depends on the rate of pumping, the permeability of the sand, and the extent and uniformity of the stratum as it affects the resistance to liquid replacement of the oil withdrawn. In oil wells the flow is complicated somewhat by the presence of large amounts of gas, either free or dissolved in the oil, and by the presence of at least two liquids, oil and water, with different physical properties (12).

As with pumping water from a confined aquifer, reduction in the liquid pressure in the oil sands produces a compensating increase in the intergranular or effective pressures in the soil structure within the stratum affected. Compression of the oil zones results. The amount of compression is influenced by the amount of decrease in liquid pressure and by compressibility of the materials within and bordering the affected zone, at top and bottom.

Compression of oil zones has frequently resulted in subsidence of the ground surface above ((5)(13)(14)(15) and unpublished reports). It is significant that, in the Los Angeles basin, noticeable subsidences have been recorded by first order leveling in the areas of a number of oil fields. Among these are the Wilmington, Signal Hill, Santa Fe Springs, Playa del Rey, Inglewood, and Huntington Beach fields. However, first order levels have not been run across many fields sufficiently often to detect possible subsidence. The relation between the amount of the unchecked compression of the oil zones and the corresponding surface subsidence depends on the structural strength of the sediments in between. It is quite common for extensive oil fields to experience no noticeable surface subsidence. On the other hand, subsidence of large areas from any cause is seldom noticed in inland areas. Along the seashore, the relatively constant sea level provides an automatic reminder whenever subsidence of appreciable amount occurs.

The Wilmington oil field was discovered in 1932, but little attention was paid to it until the last half of 1936, when a carefully cored and tested well revealed the presence of four major oil zones. The drilling boom started in the Los Angeles harbor area thereafter, spreading to the Long Beach harbor area in 1937 (6)(16)(17). Maximum production of 100,000 bbl of oil per day was

reached in February, 1938, dropping gradually to about 82,000 bbl per day in 1940, and then rising again to around 100,000 bbl per day by 1944. The field's oil production rate in 1945–1946 is the highest in California by a wide margin. This time sequence agrees generally with the occurrence of most of the subsidence, as is apparent from a comparison between Fig. 3 and Fig. 6. The anticlinal structure of the oil field shows a remarkable correlation with the contours of equal settlement.

To ascertain the importance of oil pumpage from the Wilmington oil field in producing settlement, quantitative studies were made in 1945 based on actual measurements of the several factors governing consolidation of sediments in the oil zones. These factors consist primarily of the stratification of the sands and shales, the compressibilities of the sands and shales, and the reduction in liquid pressure of the oil and water in the voids after different periods of time.

Stratification was determined from oil well electric logs and coring records. Fairly detailed information is available and has been plotted on contour maps and profiles by the oil companies and by various other agencies interested in the field. The general structural characteristics are shown in Fig. 5. There are five major zones: Tar, Ranger, Upper Terminal, Lower Terminal, and Ford, in that order, varying in depth from about 2,200 ft at the top of the Tar zone to about 4,700 ft at the top of the Ford zone. The basement complex of igneous rock, a schist, is encountered at about 6,500 ft below mean sea level. Each zone varies in thickness to some extent; but except for faulting the differences in

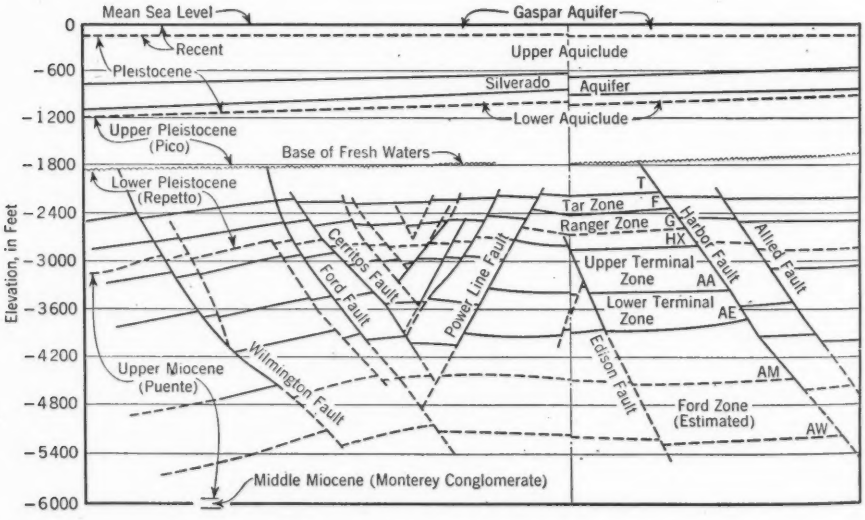

FIG. 5.—SECTION THROUGH WILMINGTON OIL FIELD

stratification between one point and another are remarkably small. The faulting, however, represents the most serious complication. A series of faults extending in a roughly north-south direction divide (see Fig. 5) the field into five major fault blocks, which are themselves broken by innumerable smaller faults,

so that most cross sections of the field do not attempt to trace all details of the complex pattern. The locations of faults are determined mostly by inductive reasoning, through study of the oil well electric logs (18).

Fluid pressures in oil wells constitute one of the most important subjects for study by oil producing companies. Measurements of flowing and shutoff pres-

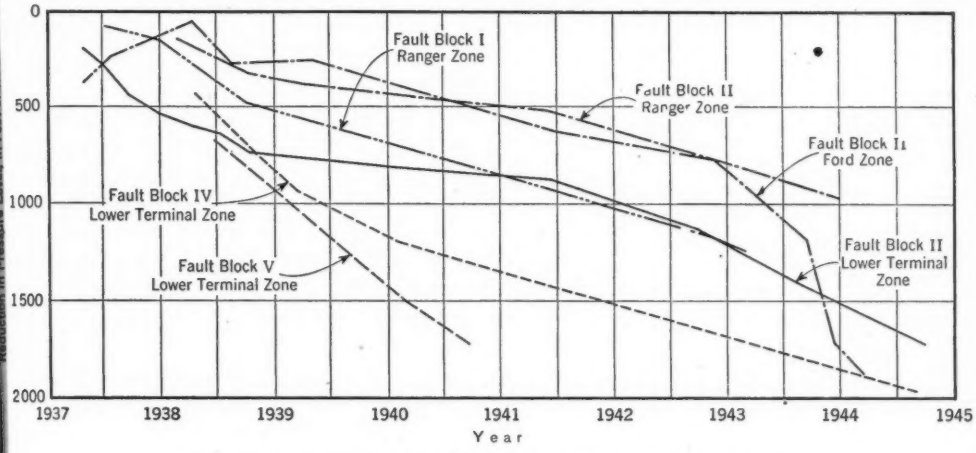

FIG. 6.—REDUCTION IN OIL ZONE PRESSURE LEVELS FOR TYPICAL WELLS

sures are made to determine the productivity of the well, which enables estimates to be made of future production, and also data to be obtained for use in operation to insure maximum total production from the field. The usual custom is to shut off the well for 24 hours or longer before taking the measurements, to allow time for the pressure to build up close to the maximum. A pressure recording instrument is lowered into the well, and readings are taken at intervals so that a pressure-depth curve can be plotted.

Initial pressures in the field, as determined from a large number of initial measurements on early wells, were approximately the same as if the underground liquids were composed of salt water with the surface at mean sea level. Continued pumping has generally caused a steady reduction in the pressures. If pressure at any depth is reduced to terms of pressure level, or the level at which a column of salt water would stand in static equilibrium in a tube whose lower open end is inserted in one of the confined sands of an oil zone, then it may be stated that the pumping has caused a gradual reduction in the pressure level below the initial mean sea level elevation. Typical curves showing pressure levels at various times for different wells are shown in Fig. 6. Pressure levels in the various zones are not the same, because of the impervious shales separating them. It has also been observed that the pressure levels on opposite sides of a fault are likely to differ, the displacement along the fault plane apparently having caused a breakdown of the normal sand structure and the formation of relatively impervious materials, which act as a barrier to the flow of liquids.

Pressure relations in the oil zones are complicated to some extent by the presence of gas. Initially, gas in the Wilmington field is believed to have ex-

isted in a near saturated solution, without any appreciable free gas cap. However, as pumping continued, pressure reduction has caused the formation of some free gas, which may have accumulated in gas caps at the crest of the structure and along faults in some zones. The near saturated condition of the original oil is indicated by the fact that wells originally "came in" as gushers, the gases rapidly expanding out of the solution in the casings, carrying the oil upward in the typical gas lift action. Gas production from the field is still fairly high. The free gas affects intergranular pressures generally by causing a smaller pressure increase than would have occurred had the gas been absent, since the liquid pressure is reduced. Development of a gas cap increases the unit weight of the sand within the depth of the cap, because of the change from submerged to dry weight; but, since the gas is confined beneath an impervious dome of shale, the buoyancy of the liquid volume displaced by gas of very small unit weight produces lower effective pressures in the strata below the shale. Unless the gas cap is quite thick, its presence has a relatively small effect on intergranular pressures. Since the scanty information available for the Wilmington field indicated no large volume of free gas, its effect on consolidation was disregarded in these subsidence studies.

A great many pressure measurements were made in the first five years of development of the Wilmington oil field, particularly by the large property owners. There are many smaller operators, particularly in the northwest part of the field, known as the "Townlot Area," who have made practically no pressure measurements in that section, although there has been considerable pumping since early in the field's history. Also, pressure measurements by the large operators were less frequent after the beginning of World War II. Since insufficient measurements were available for 1945, data were also included for measurements made in 1943 and 1944, which were given the same weight as the 1945 measurements, in preparing pressure contour maps for areas and zones where the later data were not available. Thus, discrepancies were introduced between calculated and observed subsidence for 1945, as will be noted hereafter.

Compressibility of sedimentary materials at the pressures existing in oil zones several thousand feet below the surface is a matter about which little information is available (19)(20)(21). To obtain data more applicable to this problem, it was decided to perform tests on actual samples of materials taken from oil wells in the Wilmington field. For several reasons, shale cores only were selected for testing. In the first place, shales, the product of silts and clays, composed of fine-grained particles, were expected to be much more compressible than sands. Previous tests had demonstrated fairly conclusively that sands, and particularly sandstones, show extremely small volume change when subjected to very high pressures. Secondly, relatively undisturbed shale cores, suitable for testing, could be obtained with much less difficulty than sands, because of their cohesive quality. Most of the sands from the Wilmington field are quite friable, and break up easily.

It was also felt that, rather than adopt triaxial tests, the procedure would more nearly duplicate the consolidation process in nature if the applied load were confined to the vertical direction, at the same time preventing lateral volume change, as is essentially the usual practice for standard consolidation

tests on silts and clays. In most consolidation phenomena, where the load is applied to a relatively wide area in proportion to the thickness of the compressing stratum, the volume change is predominantly vertical. This condition can be approximated in the laboratory by subjecting a sample to increased vertical pressure, at the same time restraining it against lateral expansion.

Available samples consisted of cores drilled from various oil wells. Most of these cores were several years old, having been obtained during the period when the oil companies were exploring the field. In a few instances, fresh cores were obtained from wells where drilling was currently in progress. The cores varied in size from $1\frac{1}{4}$ in. to 5 in. in diameter.

Equipment used in performing the tests was designed to accommodate two sets of samples simultaneously. The apparatus, which is pictured both in assembly and in detail in Fig. 7, employs a manually-operated screw-driven jack

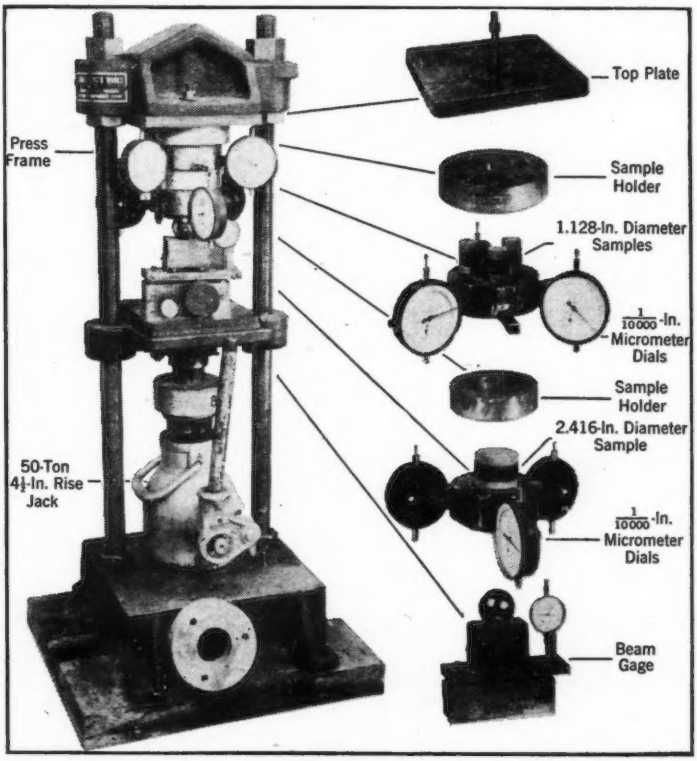

FIG. 7.—ASSEMBLY AND DETAIL OF CORE TESTING APPARATUS

for applying the load, and a beam gage for measuring the load. Porous stones, placed on both ends of each 1-in.-thick sample, enabled application to, and drainage of water from, the samples. Two sets of three equally spaced 1/10,000-in. micrometer dials were used to measure the compression of the samples. In determining the reduction in thickness of each sample from the

average of the dial readings, it was necessary to measure the deflections occurring in the porous stones and to make appropriate adjustments.

Samples to be tested were first placed in a saturated atmosphere to reestablish in them, as nearly as practicable, a saturated condition. They were then accurately trimmed in a lathe—all weathered or damaged parts being removed in the process—to fit the internal diameters of the sample holders, and the ends were faced to provide samples of the desired thickness. After machining, the samples were kept in a saturated atmosphere until ready to be placed in the testing apparatus.

Immediately after application of a small initial load, screws holding the sample holders in position during the setting-up process were released, and water was applied to the top and bottom of the samples through the porous stones, which were kept constantly wet throughout the remainder of the test. Load was applied in a series of increments, with each increment being twice its predecessor, except that two or more additional increments were superimposed on the basic series of increments in the vicinity of the preconsolidation load. On removal of the samples from the testing apparatus, the moisture content, dry

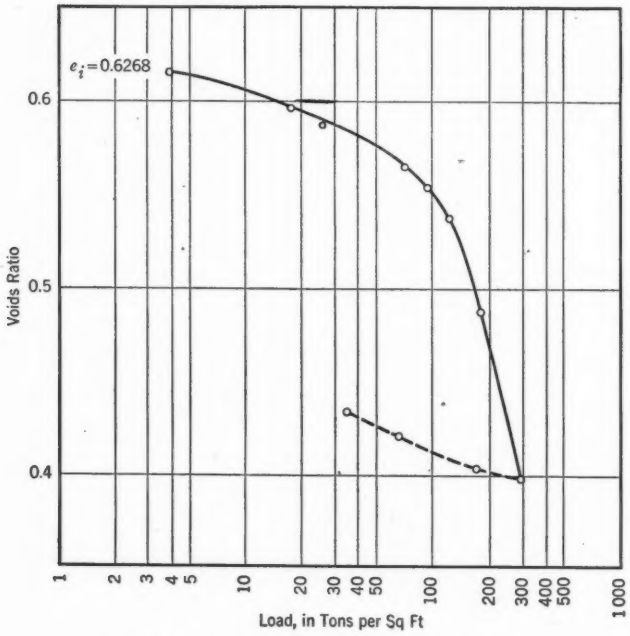

FIG. 8.—TYPICAL CONSOLIDATION TEST OF SHALE

density, and the specific gravity of the soil grains were determined for each sample. A typical curve of pressure versus voids ratio data obtained from the shale consolidation tests is shown in Fig. 8, for a 2.416-in. diameter sample. Typical compression-time curves are shown in Fig. 9. Each point in Fig. 9 represents the average of a set of three dial readings, expressed in terms of the

percentage of the total deflection observed at the end of the first 1,440 min during which a particular load was applied.

For the highest pressure to which two of the samples were subjected, it was observed that some of the material was squeezed by plastic flow into the space

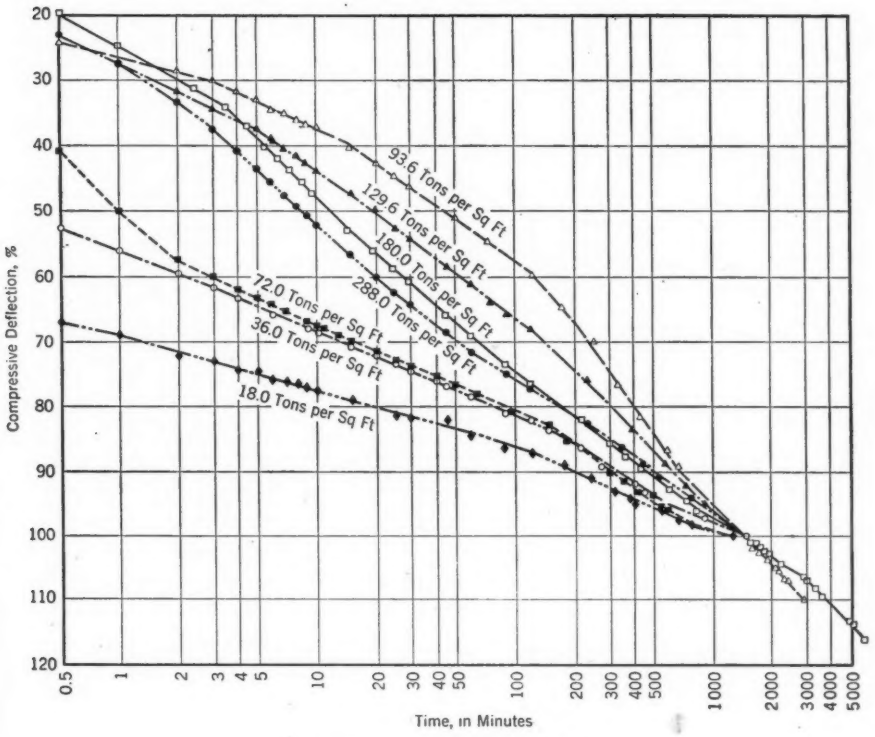

FIG. 9.—CONSOLIDATION TESTS OF SHALES

between the porous stones and the sample ring. In these instances, in arriving at the straight-line approximation, a correction was made to the voids ratio for the last point on the curve in proportion to the amount of material displaced. This plastic flow probably would have been avoided if the diameter of the porous stones could have been made closer to that of the cylindrical openings in the testing rings. No other evidences of plastic flow were observed.

For comparative purposes, the compressibility of each sample can be defined in terms of a coefficient (C_c) determined by the slope of the assumed initial compression curve, or the change in voids ratio for a tenfold increase in pressure. The initial compression curves were assumed to be tangent to the steepest sections of the test curves, and to represent an approximation to the probable compression curves of the shales in their original condition in the ground. If these compression coefficients are plotted against depth, a definite variation is seen to exist (Fig. 10). The inference is that the shales encountered near the contact between the Lower Pliocene and the Upper Miocene deposits, represented by the

Tar, Ranger, and Upper Terminal zones, are more compressible than are materials at greater or lesser depths, under the same conditions of loading.

To compute theoretical consolidation accurately, it would be necessary to know in minute detail the variation in compressibility of all strata encountered by a vertical section through the oil zones. Such information cannot feasibly be obtained. It is certain that the compressibility varies rapidly stratum by stratum, and even foot by foot, ranging from the high values in the more uniformly fine-grained shales, to the relative incompressibility of the cemented sands, which probably have properties close to those of concrete. However, even with the most conservative assumptions, it is clear that compression of the oil zone sediments can easily account for all the observed subsidence. If the total thickness of each zone is assumed to have the same compressibility as the tested shale samples from the zone, then rough computations show a reduction in thickness of the oil zones amounting to more than ten times the observed settlement, based on the pressure data of 1945, for a point near the center of the subsiding area. Data similarly derived for other points indicate that the distribution of the consolidation corresponds closely to the distribution of the observed settlement.

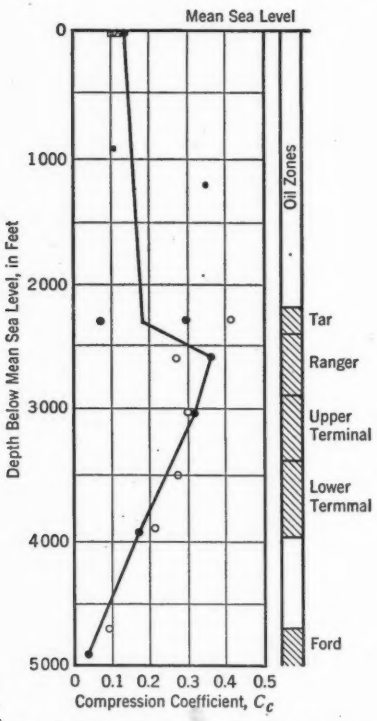

FIG. 10.—COMPRESSIBILITY OF WILMINGTON OIL SHALES IN RELATION TO DEPTH

An estimate of the future course of the subsidence was made, based on the following procedure: Ultimate drawdown of pressure levels in each oil zone was estimated, and a correction factor to be applied to the total thickness of the oil zones was computed. This factor was determined by deducting from the observed subsidence of a point near the center of the depression the computed settlement from water and dock site pumping, as of 1945. The difference was assumed to represent the effect of oil pumping to that time. A constant percentage of the thickness of each zone was chosen so as to make the calculated consolidation at that particular point equal to this difference. Using this factor, the same for all zones over the entire area of the field, together with the average compressibility coefficients, different for each zone, and the total thickness of the zones, which varied over the area of the field, consolidation was computed at some two hundred points. These computations were made using the pressure data of 1945 and also using estimated pressures that may occur in the future. Theoretical subsidence from oil pumping, in 1945, is shown by the contours of Fig. 11.

The many factors that influence the theoretical subsidence computed in this manner perhaps warrant some discussion. In the first place, the consolidation computed for the oil zones was assumed to produce an equal surface subsidence, except for smoothing out local irregularities. This assumption neglects the effect of possible lateral stress changes, which probably may result from the structural strength of the deep beds. The domed structure of these beds itself may result in a certain amount of arching action, which tends to transfer laterally the vertical loads applied near the center of the field, relieving the centrally located shales of some of the increased pressure they would otherwise experience. This action may reduce not only the local irregularities, caused by local variation in drawdown of the liquid level, but also the total surface subsidence at the center of the depression, spreading it over a wider area. However, the same errors from this source exist in the calculated 1945 consolidation as in the calculated ultimate consolidation. Since the predictions for the future are derived from the difference, the net error should be relatively small. This factor may partly explain the lack of agreement in detail between the contours for calculated oil zone consolidation (Fig. 11) and the contours of observed sub-

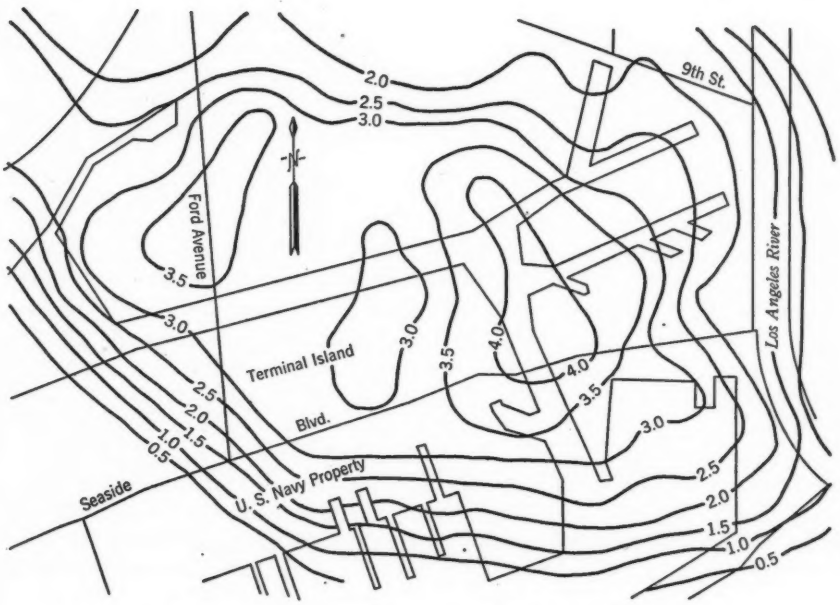

FIG. 11.—CALCULATED CONSOLIDATION OF OIL ZONES—1945

sidence (Fig. 1), neglecting the relatively small and uniform consolidation from water pumping.

The estimates of future drawdown in each of the oil zones probably constitute the greatest single source of error in the estimate of future subsidence. They were obtained in a purely arbitrary manner, but were based to some extent on past experience and on certain limiting factors.

Leading petroleum engineers and geologists familiar with the Wilmington field agree that eventually, as a result of pumping, oil zone pressures will be greatly reduced. In some oil fields, as oil is withdrawn, edge waters encroaching from the sides of the structure replace it freely enough to prevent extreme pressure reductions in the oil. In such cases, the oil reservoirs may be completely depleted with only moderate reduction of the oil pressure level—the rate of oil removal governing to a large degree the amount of pressure reduction. In the Wilmington field, however, it appears that reasonable pumping rates cannot be maintained without gradual reduction in the liquid pressures, since experience shows that edge-water replacement is not sufficiently rapid. This may be caused by low permeabilities in the oil bearing strata, by fault barriers, or by confinement of these strata within relatively impervious layers.

With these factors in mind, it was concluded that ultimate liquid pressures may very likely be reduced to about 200 lb per sq in.—equivalent to about 400 ft of water head at the top of each zone. The distribution of this drawdown over the area of the field is an uncertain matter, but it appeared that the report prepared in 1941 by the Wilmington Field Engineering Committee contained sufficient data for reasonable approximations. Maps prepared by this committee showed in outline the proved limits of each zone in the field, and it is assumed in general that these limits enclose the area where the most severe pressure reduction will occur.

The manner of tapering off the assumed drawdown at the edges of the field was determined by judgment alone. The nature of the gradient from the large drawdown within the field to sea level at some distance from it is not known. Pressure measurements within the field show that fairly steep gradients can exist, particularly in the less pervious sediments of the Ford zone. Across faults there is also quite commonly a very steep gradient. At the edges of the field, there are very few measurements of pressure, yet it seems certain that the pressure gradients must extend for a considerable distance into the surrounding edge waters, as otherwise no inward flow of edge water would occur.

The prediction, which involves the difference between estimated ultimate and measured 1945 pressure levels, also suffers from certain inaccuracies in the "1945" values, which include some data actually obtained in 1943 and 1944.

It should be mentioned that the observed 1945 subsidence is based on the measurement of relatively few points, scattered in rather irregular fashion over a large area. There are a number of regions where no observations at all were made. For this reason, it is quite possible that the actual subsidence may not have been quite as regular in outline as the smooth contours of Fig. 1 would imply.

Compressibility of the oil zone sediments should not change appreciably with time, in the relatively brief geologic interval of this subsidence. Therefore, if the true average compressibility were known for all zones at a given point, and the increase in drawdown after 1945 were the same for all zones, future consolidation could be predicted quite accurately. However, pressure reductions to be expected in the future vary in the different zones. For example, in fault block III, near the center of the depression, a much larger proportion of the ultimate pressure reduction has already taken place in the Upper Ter-

minal and Lower Terminal zones than has occurred in the Tar, Ranger, and Ford zones. Thus, the proportion of the total consolidation caused in each of the zones, for a given increment of pressure reduction, becomes important. This proportion depends on the total thickness of compressing materials in each zone and on the average compressibilities of those materials.

Thicknesses of each of the zones were determined principally from the contour maps prepared by the Wilmington Field Engineering Committee. These maps showed the variation in elevation of the top of each zone. The thicknesses of the Tar, Ranger, and Upper Terminal zones were taken as the differences between the elevation of the top of the zone and the elevation of the top of the next zone below. The Lower Terminal zone has not generally been productive as deep as the top of the Ford zone, and has not been pumped for this full thickness. The Lower Terminal zone was therefore taken to have an average thickness of 500 ft, based on cross sections prepared by the committee and others and on various electric logs. Similarly, the thickness of the Ford zone was taken as 750 ft. The proportion of each zone composed of shale layers varies over a considerable range, but averages about 50%.

Calculated consolidation, both for 1945 and for the future, was obtained for each zone by multiplying the full thickness of the zone by a correction factor of 8% to adjust the calculated change in thickness, for a point at the center of the depression, with the observed subsidence as of 1945. The surprisingly low ratio between observed and calculated unadjusted settlement may be explained by the facts that: (*a*) Total thickness of oil zones was used in the calculation; and (*b*) each zone was assumed to have the compressibility of the average of the tested shale samples. Thus, the presence of sands of low compressibility is disregarded as are the relatively incompressible sediments composed of shales mixed with sands, which affect the average greatly. The presence of many water-bearing strata that may not be greatly affected by pumping is also neglected, since well casings are not perforated in water zones. Also, as previously mentioned, the tested samples were chosen for their suitability for machining, were very fine-grained, and therefore were more compressible than the majority of shales examined at the oil companies' storage racks.

This method leaves much to be desired, when compared with the degree of accuracy usually sought in consolidation studies. However, it is believed to be sufficiently accurate for the purpose required, because most errors inherent in the theoretical approach are canceled by the adjustment to an already sizable consolidation, representing a major part of the possible total, which has been actually measured.

In all the calculations of oil zone consolidation, it was assumed that the time lag between the imposition of load, through reduction of the pressure level, and the corresponding decrease in voids ratio of the compressible shales has been relatively small. Inspection of the time-compression curves obtained in the laboratory tests (Fig. 9) shows that a majority of the curves do not have the same shape as typical time curves explained by the Terzaghi theory of consolidation (22).

In general, the shape of the time curves resembles the results of certain soil tests in which, because of the character and thickness of the sample, the so-

called "secondary" time effects have practically concealed the "primary" effects, or those resulting from squeezing out water. In such cases, instead of the typical reversed S-shape on the semilogarithmic plot, the time curve may be straight, or even slightly concave upward.

The time required for primary consolidation is assumed to vary as the square of the thickness of the compressing layer. The time required for secondary consolidation is more or less an unknown factor, but it is generally held to be independent of the thickness of the layer. In other words, secondary consolidation may occur in nature, in a layer many feet thick, at the same rate as it occurs in the thin laboratory sample.

Those test curves that do display some similarity to the theoretical time curve indicate that for pertinent load increments 90% consolidation takes place in less than 400 min. On this basis, if the average thickness of individual shale laminations, between sand streaks, is assumed to be 2 ft, then 90% consolidation in the oil field would require about 290 days.

For the compression of oil shales considered in this study, many unknown factors influence the time rate. Even the average thickness of the compressible layers is complicated to evaluate, since there are many layers of varying thickness in each of the oil zones. Consequently, no attempt was made to calculate how many of the time effects result from primary compression, inasmuch as the laboratory curves show this influence to be minor compared to that of the secondary or plastic characteristics. The time required for these latter effects is a matter of days, instead of months or years, and it was neglected in computing theoretical consolidation at any particular time. Since the loads themselves are applied gradually, over a period of years, the error introduced by this procedure is probably not very large.

Influence of Tectonic Forces.—It is well known that, in the coastal area of California, motions of the earth's crust are constantly in progress. No attempt will be made to describe the many faults in the subsiding area and around it, or to describe the seismic history of the region (5)(13). It is obvious that in an area interlaced with active faults, where minor quakes are registered almost continuously at the near-by Pasadena Seismological Laboratory, movements along fault zones are more or less likely to occur as the result of slow relative motion of adjacent land masses.

As far as is known, there is no reliable method of estimating or timing the probable occurrence of movements resulting from tectonic forces. However, as far as evidence derived from observations at oil wells is concerned, it appears likely that movement along the many faults in the oil field area ceased in Pliocene times. During these movements, the oil field was generally lifted upward, with downward "cave-ins" of some of the central blocks in the field. A general upward movement of this section of the coast is evident also from the terraced contours of the San Pedro hills around Point Fermin. Geologically, this gradual uplift may still be in progress.

The area that might be affected by tectonic forces is likewise indeterminate. The Newport-Inglewood fault, which is the major known active fault zone passing through the Los Angeles coastal basin, lies some 4 or 5 miles northeast of the center of the subsiding area. Although it might appear that the subsiding

area, which coincides with the Wilmington oil field, is a very highly faulted one, compared with other areas, it should be remembered that knowledge of the subsurface details in this area is highly developed from observations made at many hundreds of oil wells. There is no assurance that many other similarly faulted areas of the Pliocene and Miocene sediments do not lie undetected merely for lack of exploration.

In weighing the probability of tectonic forces causing a major part of the subsidence, several factors must be considered along with the known possibility of such movements in this region. One such factor is the lack of any marked increase in seismic activity in recent years in the Long Beach area. Since the rate of subsidence there has increased to a degree unprecedented in California history, if tectonic forces and movements of underlying rock masses were largely responsible, the area might properly be expected to develop a nest of shocks, as the earth stresses produced during such severe strains readjusted themselves. However, although innumerable shocks have occurred in Southern California, no such nest of shocks has been observed at Long Beach.

Another such factor is the absence of damage to oil well casings in the Wilmington field. If there had been any appreciable motion along the faults traversed by the wells, pinching and shearing off of the casings or puncturing of cement plugs should have taken place; and it seems highly improbable that all the relative motion along these inclined faults could have occurred at depths below the oil wells, without producing considerable displacements in the upper sediments. In this connection, experiences at Dominguez Hills in 1941 indicate that motions along faults of as little as a fraction of an inch were sufficient to collapse oil well casings passing through the faults (23). In many cases, motions of more than a foot were observed, shearing off casings completely—yet this condition occurred at an oil field where surface subsidence, if it took place at all, was so small as to go unnoticed. It is considered, therefore, that, although slow tectonic movements have occurred in the area in question, and probably are occurring at present, these movements are very gradual, possibly on the order of 0.04 ft per yr or less, vertically. They may be either upward or downward; and available facts are insufficient to determine which, or to establish the rate, concealed as it is beneath the very much more rapid subsidence phenomenon centered over the oil field.

Conclusion

Estimated ultimate subsidence, after 1933, from oil and water pumping is shown by Fig. 12, in which some of the irregularities in contours derived on a mathematical basis have been smoothed out, on the assumption that arching and other effects will in nature reduce abrupt changes and transitions in the over-all pattern. This contour map, by no means considered infallible, can serve as a guide for future construction in this area. The most vital conclusion brought out by the contours is that in all probability there will be no large-scale inundation of the easterly end of Terminal Island. Wherever present freeboards above extreme high tide level exceed 5 ft, the chances are that there will be no overtopping of the ground surface.

Nevertheless the possibility of differential movement should be considered

in the design of any large structures to be built in the subsiding area. In general, since the depression in the ground surface covers a very wide area, with flat side slopes, the amount of differential motion to be anticipated in the length of most buildings will be very small. If the buildings are sufficiently flexible

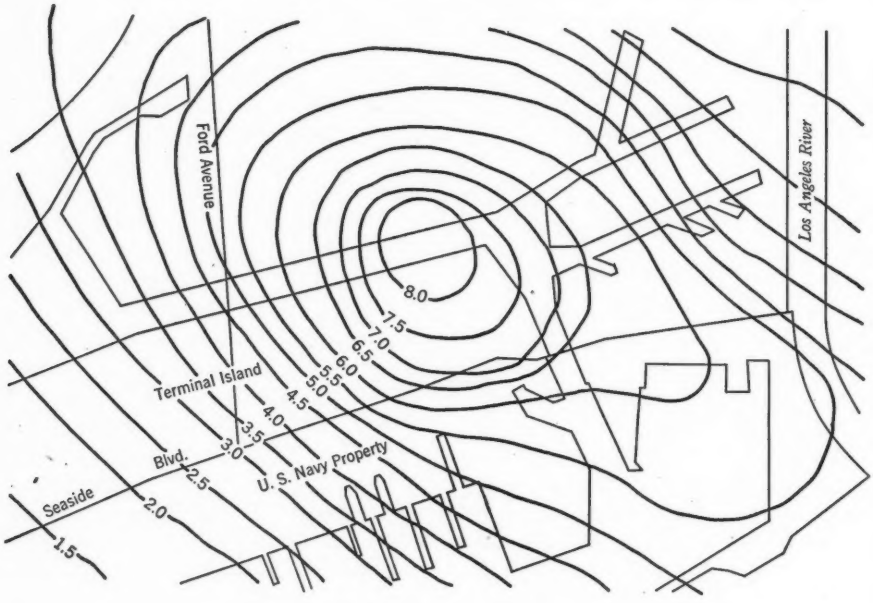

FIG. 12.—PROBABLE ULTIMATE SUBSIDENCE

to withstand such motion without excessive stresses, no particular damage will result.

Continued subsidence will necessitate a restudy of the elevations and grades of certain facilities. The design of gravity sewers should be re-examined in the light of probable future differential changes in grade. Lack of proper drainage may result in some places as the subsidence continues. The same problem applies to surface grades. Such sources of future difficulties can thus be anticipated to some extent, and provisions can be made to insure continued satisfactory operation.

In conclusion, this study indicates that this vicinity should continue to serve as the site for industrial development. Present structures will continue to function satisfactorily if suitable preventive measures are adopted to avoid known possibilities of trouble; future structures can be designed to allow for probable future subsidence, which will continue for many years at a slowly reducing rate.

ACKNOWLEDGMENT

This paper is based on a report prepared for the Bureau of Yards and Docks, United States Navy Department, by Frederic R. Harris, Incorporated, Consulting Engineers of New York, N. Y., dated December 18, 1945, with a supple-

ment dated February 25, 1946. Invaluable assistance was rendered by R. R. Desmond, and C. M. Duke, Juniors, ASCE, who, together with the junior author, assembled the basic data examined during the investigation. Gratitude is due many individuals and agencies for their assistance in making available the necessary data—Capt. H. E. Wilson, Public Works Officer at the Terminal Island Naval Base, and members of his staff; Lt.-Comdr. A. S. Porter and Frank F. Mead and Trent R. Dames, Members, ASCE; Messrs. R. Winterburn and Butterfield of the Union Pacific Railroad Company; and many others. To all these sincere appreciation is offered.

APPENDIX. BIBLIOGRAPHY ON LAND SUBSIDENCE

(1) **"Earth Movements in California Determined from Apparent Variations in Tidal Datum Planes,"** by H. Leypoldt, *Bulletin*, Seismological Soc. of America, January, 1934, p. 63.

(2) **"Periodicity of Earth Movements in Los Angeles Harbor,"** by H. Leypoldt, *ibid.*, January, 1938.

(3) **"Surveys Show Long Beach, California, Is Moving Up, Down and Sideways,"** by J. R. McHenry, *Engineering News-Record*, March 26, 1942, p. 477.

(4) **"Variations in Levels 1919 to 1927, in Los Angeles Harbor,"** by G. F. Nicholson, *Bulletin*, Seismological Soc. of America, December, 1929, p. 200.

(5) **"Subsidence and Elevation in the Los Angeles Region,"** by U. S. Grant, *Science in the University*, Univ. of California, Berkeley, Calif., 1944, p. 129.

(6) **"Wilmington Oil Field,"** by R. Winterburn, in **"Geological Formations and the Economic Development of the Oil and Gas Fields of California,"** *Bulletin No. 18*, State Div. of Mines, Pt. 3, San Francisco, Calif., March, 1943.

(7) **"Report to Southern California Edison Company on Soil Explorations and Studies as to Effect on Edison Plants from Navy Construction Operations,"** by R. Labarre, Los Angeles, Calif., 1941 (unpublished).

(8) **"Report to Navy on Soil Explorations and Foundation Studies for Graving Dock at Fleet Operating Base,"** by D. R. Warren and F. J. Converse, Los Angeles, Calif., 1941 (unpublished).

(9) **"Compressibility of Artesian Aquifers,"** by O. E. Meinzer, *Economic Geologist*, Vol. 23, 1928, pp. 263–291.

(10) **"Development of Underground Waters in the Central Coastal Plain Region of Southern California,"** by Walter C. Mendenhall, *Water-Supply Paper No. 138*, U.S.G.S., U. S. Govt. Printing Office, Washington, D. C., 1905.

(11) **"Description of Water Wells in the Coastal Zone of the Long Beach-Santa Ana Area, Calif.,"** by J. F. Poland and others, U.S.G.S. Rept., Los Angeles, Calif., December, 1942 (unpublished).

(12) **"Ground Water,"** by C. F. Tolman, McGraw-Hill Book Co., Inc., New York, N. Y., 1937.

(13) **"Some Recent Changes of Elevation in the Los Angeles Basin of California and Their Possible Significance,"** by U. S. Grant and W. E. Sheppard, *Bulletin*, Seismological Soc. of America, April, 1939, p. 299.

(14) *Engineering News-Record*, June 10, 1937, p. 858.

(15) **"Local Subsidence of the Goose Creek Oil Field,"** by W. E. Pratt and D. W. Johnson, *Journal of Geology*, Vol. 34, 1926, pp. 577–590.

(16) **"Wilmington Oil Field,"** by W. J. Crown, in **"Summary of Operations, California Oil Fields,"** 26th Annual Rept. of State Oil and Gas Supervisor, Dept. of Natural Resources, Div. of Oil and Gas, San Francisco, Calif., 1940–1941.

(17) **"Summary of Operations—California Oil Fields,"** Annual Repts., Dept. of Natural Resources, Div. of Oil and Gas, 1932–1945, inclusive.

(18) **"Electrical Coring,"** by C. Schlumberger, in **"The Science of Petroleum,"** Oxford Univ. Press, Oxford, England.

(19) **"The Compressibility of Minerals and Rocks at High Pressures,"** by L. H. Adams and E. D. Williamson, *Paper No. 484*, Carnegie Inst. Geophysics Laboratory, Pittsburgh, Pa. (reprinted from *Journal of the Franklin Institute*, April, 1923, pp. 475–529).

(20) **"Measurements of Compressibility of Consolidated Oil-Bearing Sandstones,"** by C. B. Carpenter and G. B. Spencer, *Report No. 3540*, U. S. Bureau of Mines, U. S. Govt. Printing Office, Washington, D. C., October, 1940.

(21) **"The Effect of Pressure on the Migration and Accumulation of Petroleum,"** by F. M. Van Tuyl and A. C. Beckstrom, *Bulletin*, Am. Assn. of Petroleum Geologists, October, 1926, pp. 917–930.

(22) **"Theoretical Soil Mechanics,"** by K. Terzaghi, John Wiley & Sons, Inc., New York, N. Y., 1943.

(23) **"Los Angeles Basin Earthquake of October 1941 and Its Effect on Certain Producing Wells in Dominguez Field,"** by K. Bravinder, *Bulletin*, Am. Assn. Petroleum Geologists, March, 1942, p. 387.

AMERICAN SOCIETY OF CIVIL ENGINEERS

Founded November 5, 1852

PAPERS

VARIATION OF COEFFICIENTS OF SIMULTANEOUS LINEAR EQUATIONS

By Bernard L. Weiner,[1] M. ASCE

Synopsis

Simultaneous equations are of great importance in modern structural engineering, and the purpose of going through a solution is, obviously, to obtain numerical results for a specific set of conditions. It is often of equal importance, however, to know the effect of a change in the geometric and elastic properties of the structure. Without such knowledge it is impossible to study the design with a view toward obtaining the most in economy and certain other desirable qualities. Such studies, except for the simplest structures, can be made only at the expense of re-solving the equations each time a change is made in the coefficients, and the labor involved is so great that studies cannot ordinarily be made except very roughly and sketchily. With the theory presented in this paper, the effect on the solution produced by a change in any number of the coefficients in any one equation, or in any number of coefficients of any one unknown, can be computed quickly and simply in one step.

Although the variation of coefficients is the primary purpose of the paper, other useful properties of the theory, such as the solution of equations and the rapid correction of errors, follow simply as corollaries. In the actual operation of the method, however, the procedure is the same whether coefficients are being varied in a set of equations that have already been solved, or whether the purpose is to solve the equations. It is, as a matter of fact, possible to vary the coefficients endlessly and any particular "solution" therefore becomes merely a stopping point in an endless series of variations—from which it follows that the method is very flexible.

Variation of coefficients as a method of solving simultaneous equations has several marked advantages over the classical methods and leads also to the derivation of several useful properties of such equations. The numerical

Note.—Written comments are invited for immediate publication; to insure publication the last discussion should be submitted by March 1, 1948.

[1] Associate Engr., D. B. Steinman, Cons. Engr., New York, N. Y.

work required for a solution by the method presented in this paper is very much less than that required by standard methods; and, what is perhaps more important, fewer significant digits are necessary in the intermediate computations to obtain any desired degree of accuracy in the final solution. In fact, with a little care and by using a few fairly obvious arithmetical manipulations, results sufficiently accurate for design purposes often may be obtained by slide rule for the bulk of the computations. The method is an exact one, however, and computations may be carried out to any degree of accuracy but with much less labor than that required by the classic methods.

In addition, the method of solution has another very important property. As will be shown, the solution falls into distinct steps, or partial solutions, each and every one of which is complete in itself. As a result, the computation may be checked completely and absolutely at the conclusion of each step or variation, so that it is not necessary to wait for the end of the solution to check for an arithmetical error. Should the computer, however, either neglect to check his work at intermediate points, or discover an error in the original setup of the equations, the basic theory of the solution is such that it offers a quick method for the correction of an error without the necessity of changing the entire computation from the point at which the error was made to the end of the solution. Furthermore, the method is self-checking in many different ways, so if it is found that the intermediate computations at some particular point in the solution have not been carried out to a sufficient number of significant digits, the defect may be remedied by using one of the checks to recompute the defective quantity.

Introduction

Structural analysis and many other engineering problems occasionally require the solution of simultaneous equations. Since classical methods of solution involve small differences resulting from the subtraction of large numbers, computations must be carried to many significant digits, thus making the work very laborious. Study of the effect of varying the characteristics of a structure (which involves, among other things, changing the coefficients of the unknowns) by these same methods is so time consuming as to make such studies prohibitive except in the simplest cases. The value of a direct and simple method for finding the effect of varying coefficients of simultaneous equations is therefore obvious.

Since an error in coefficients can be interpreted to mean that, in effect, a structure has been analyzed whose characteristics are expressed by the incorrect coefficients, the correction of such errors becomes a problem in "variation of coefficients." It was to meet just such a problem that the methods outlined in this paper were developed and later extended to other applications. An

obvious extension of the concept involved leads directly to a new method for solving this type of equations—for, as will be shown, a "solution" is merely a stopping point in an endless chain of variations.

The theory presented, as it applies to the solution of simultaneous equations, differs in one respect from the classical theories in that it is developed from a different point of view. The usual method of solution for this and other types of equations consists, essentially, of what might be termed a process of "breaking down"—that is, the complete equations are converted to such forms that the extraction of a root or the elimination of other unknowns will result in a simple equation with only one unknown or root. This method, on the contrary, consists of a process of "building up"—that is, the solution begins with simple, reduced equations that are easily solved or need no solution, and are then built up, step by step, to the required equations by converting the solutions to conform to the new equations at each step. In this process, it is necessary to vary the coefficients of the unknowns and to find the resulting effect on the values of the unknowns. This process is direct, and the theory for the variation of the coefficients makes the method of solution almost self-evident.

Derivation of Theory for Variation of Coefficients

Each one of a set of simultaneous equations takes the form:

$$a_{1n} X_1 + a_{2n} X_2 + a_{3n} X_3 + \cdots = c_n \quad \ldots\ldots\ldots\ldots\ldots\ldots (1)$$

in which the X_m's are unknowns; the a_{mn}'s are coefficients dependent only on the elastic and geometric properties of the structure; and the c_n's are constants determined by the position and magnitude of the loads in addition to the properties of the structure.

For any given structure the coefficients are, of course, constant, but c_n will have as many sets of values as there are loading conditions to be analyzed. It has often been erroneously stated that the equations must be solved for each one of these sets of constants—a statement that is only a half-truth. If the work is properly arranged and the equations are solved for one set of values of c_n, the solution for any other set requires comparatively little additional labor. In practice, the equations are solved in a routine manner for all sets of values of c_n at the same time and the computation of influence lines is therefore no great additional hardship. A simple illustration of such a procedure is presented in Table 1, which gives a solution for the simultaneous equations:

$$\left.\begin{array}{l} +4x + 6y = \left|\begin{array}{c|c} 42 & a \\ \hline 31 & 0 \end{array}\right| \left|\begin{array}{c|c} 0 & \\ \hline b & \end{array}\right| \\ +2x + 5y = \end{array}\right\} \quad \ldots\ldots\ldots\ldots\ldots\ldots (2)$$

Attention is called to Col. 7, from which it is easily seen that if a set of equations is solved for one set of values of c_n a solution for another set can be obtained simply by using the factors and performing on the new constants only the operations indicated in this column. However, if the number of sets of values for c_n is large, it is often advantageous to solve for sets of constants such as are shown in Cols. 5 and 6. The numerical solution $y = 5$, for example may then be obtained by setting $a = 42$ and $b = 31$, from which (line 5)

$y = -\frac{1}{4} \times 42 + \frac{1}{2} \times 31 = 5$. Similarly (line 8), $x = +0.625 \times 42 - 0.75 \times 31 = 3$.

Any number of solutions may therefore be found either by following the operations indicated in Col. 7 or by using the factors in Cols. 5 and 6. It

TABLE 1.—SOLUTION OF EQS. 2 BY THE PROCESS OF ELIMINATION

Line No.					Variation Coefficients		Remarks
(1)	(2)	(3)		(4)	(5)	(6)	(7)
1.....	$+4x$	$+6y$	=	42	a	0	
2.....	$+2x$	$+5y$	=	31	0	b	
3.....	$+2x$	$+3y$	=	21	$0.5a$	0	$\frac{1}{2}$ (line 1)
4.....		$+2y$	=	10	$-0.5a$	b	(line 2) − (line 3)
5.....		y	=	5	$-0.25a$	$0.5b$	$\frac{1}{2}$ (line 4)
6.....		$5y$	=	25	$-1.25a$	$2.5b$	5 (line 5)
7.....	$2x$		=	6	$+1.25a$	$-1.5b$	(line 2) − (line 6)
8.....	x		=	3	$+0.625a$	$-0.75b$	$\frac{1}{2}$ (line 7)

should be noted that these latter factors are actually solutions of Eqs. 2 for $c_n = a,0$ and $0,b$. However, if the coefficients of x and y were changed, it would give rise to a new set of equations. By the classical methods, solutions for the new set of equations can be found only by actually re-solving the equations. The factors in Cols. 5 and 6 can be used to avoid this difficulty and therefore are termed "variation coefficients."

Let it be supposed that it is desired to change the coefficient of x in line 1, Table 1, from 4 to 7. The new set of equations then becomes:

$$\left.\begin{aligned} 7x' + 6y' &= 42 \\ 2x' + 5y' &= 31 \end{aligned}\right\} \quad \ldots\ldots(3)$$

which may be rewritten as

$$\left.\begin{aligned} 4x' + 6y' &= (42 - 3x') \\ 2x' + 5y' &= 31 \end{aligned}\right\} \quad \ldots\ldots(4)$$

Now let $(42 - 3x'),31$ be treated as new values of c_n—that is, as additional constants of Eqs. 2 for which solutions are to be found. Substitution of $a = 42 - 3x'$, and $b = 31$, in line 8, Table 1, gives $x' = 0.625\,(42 - 3x') - 0.75 \times 31 = 3 - 1.875x'$; which gives

$$x' = \frac{3}{1 + 1.875} = \frac{24}{23} \quad \ldots\ldots(5)$$

From line 5, Table 1, $y' = -0.25\,(42 - 3x') + 0.5 \times 31 = 5 + 0.75x'$; from which

$$y' = 5 + 0.75 \times \frac{24}{23} = \frac{133}{23} \quad \ldots\ldots(6)$$

These values of x' and y' obviously satisfy Eqs. 3 and are therefore solutions of these equations. Furthermore, since the variation coefficients are also solutions of Eqs. 2, they too can be revised to satisfy Eqs. 3 for $c_n = a',0$ and

0,b'. Thus, by setting $a = a' - 3x'$, and $b = 0$,

$$x'_a = 0.625\,(a' - 3x'_a); \quad \text{or} \quad x'_a = \frac{0.625\,a'}{2.875} = \frac{5}{23}a' \ldots\ldots (7)$$

and

$$y'_a = -0.25\,(a' - 3x'_a); \quad \text{or} \quad y'_a = -\frac{a'}{4} + \frac{3}{4} \times \frac{5}{23}a' = -\frac{2}{23}a' \ldots (8)$$

Likewise, by setting $a = -3x'$, and $b = b'$,

$$x'_b = 0.625\,(-3x') - 0.75\,b'; \quad \text{or} \quad x'_b = -\frac{0.75\,b'}{2.875} = -\frac{6}{23}b' \ldots (9)$$

and

$$y'_b = -0.25\,(-3x') + 0.5\,b'; \quad \text{or} \quad y'_b = -\frac{3}{4} \times \frac{6}{23}b' + \frac{1}{2}b' = \frac{7}{23}b' \ldots (10)$$

The complete solution of Eqs. 3 for all values of c_n, as obtained by revision of Eqs. 2, is given in Table 2.

Eqs. 3 can be changed back to Eqs. 2—or may be "varied" to any other equations—by using the new variation coefficients, since it obviously does not matter whether one set of equations was solved by revising another set or was solved directly.

For simplicity, only one coefficient was varied in the previous problem. It will now be shown that any number of coefficients of the same unknown can be varied at the same time.

TABLE 2.—SUMMARY OF SOLUTION OF EQS. 3

Line No.					Variation Coefficients	
(1)	(2)	(3)		(4)	(5)	(6)
1.....	$+7x'$	$+6y'$	=	42	a'	0
2.....	$+2x'$	$+5y'$	=	31	0	b'
3.....	x'		=	$\frac{24}{23}$	$\frac{5}{23}a'$	$-\frac{6}{23}b'$
4.....		y'	=	$\frac{133}{23}$	$-\frac{2}{23}a'$	$\frac{7}{23}b'$

GENERAL FORMULAS FOR VARIATION OF COEFFICIENTS

Let it be assumed that the equations—

$$\left.\begin{array}{l} A_1x + B_1y + C_1z = \left|\begin{array}{c||c|c|c} K_1 & a & 0 & 0 \end{array}\right| \\ A_2x + B_2y + C_2z = \left|\begin{array}{c||c|c|c} K_2 & 0 & b & 0 \end{array}\right| \\ A_3x + B_3y + C_3z = \left|\begin{array}{c||c|c|c} K_3 & 0 & 0 & c \end{array}\right| \end{array}\right\} \ldots\ldots\ldots\ldots (11)$$

—have been solved by some method, no matter what, with results as shown in Table 3.

Also, suppose that the coefficients A_1, A_2, A_3 are increased by d_1, d_2, and d_3, respectively. Following the procedure used in varying Eqs. 2:

$$\left.\begin{array}{l} a = K_1 - d_1x' \\ b = K_2 - d_2x' \\ c = K_3 - d_3x' \end{array}\right\} \ldots\ldots\ldots\ldots\ldots\ldots (12)$$

Substituting in line 4, Table 3,

$$x' = a_1\,(K_1 - d_1x') + a_2\,(K_2 - d_2x') + a_3\,(K_3 - d_3x') \ldots\ldots (13a)$$

from which

$$x' + a_1 d_1 x' + a_2 d_2 x' + a_3 d_3 x' = a_1 K_1 + a_2 K_2 + a_3 K_3 \quad (13b)$$

and

$$x' = \frac{a_1 K_1 + a_2 K_2 + a_3 K_3}{1 + a_1 d_1 + a_2 d_2 + a_3 d_3} \quad (14)$$

As previously shown (Table 1), a solution for any set of constants, such as K_1, K_2, and K_3, may be found by setting $a = K_1$, $b = K_2$, and $c = K_3$. Therefore,

$$a_1 K_1 + a_2 K_2 + a_3 K_3 = S_1 \quad (15a)$$

Similarly, by substituting $a = d_1$, $b = d_2$, and $c = d_3$:

$$a_1 d_1 + a_2 d_2 + a_3 d_3 = x_d \quad (15b)$$

in which x_d is the solution for x, for a set of values of $c_n = d_1$, d_2, and d_3.

Substituting Eqs. 15*a* and 15*b* in Eq. 14,

$$x' = \frac{S_1}{1 + x_d} \quad (16)$$

However, since S_1 is any solution for x,

$$x' = \frac{x}{1 + x_d} \quad (17)$$

In a similar manner, substituting Eq. 12 in line 5, Table 3,

$$y' = b_1 (K_1 - d_1 x') + b_2 (K_2 - d_2 x') + b_3 (K_3 - d_3 x') \quad (18a)$$

$$y' = (b_1 K_1 + b_2 K_2 + b_3 K_3) - (b_1 d_1 + b_2 d_2 + b_3 d_3) x' \quad (18b)$$

$$y' = S_2 - x' \sum b_n d_n \quad (18c)$$

Since S_2 is any solution for y, and $\sum b_n d_n$ is a solution for y when $c_n = d_1$, d_2, and d_3,

$$y' = y - y_d x' \quad (19)$$

Similarly,

$$z' = z - z_d x' \quad (20)$$

TABLE 3.—SUMMARY OF SOLUTION OF EQS. 11

Line No.						Variation Coefficients		
(1)	(2)	(3)	(4)		(5)	(6)	(7)	(8)
1...	$+ A_1 x$	$+ B_1 y$	$+ C_1 z$	=	K_1	a	0	0
2...	$+ A_2 x$	$+ B_2 y$	$+ C_2 z$	=	K_2	0	b	0
3...	$+ A_3 x$	$+ B_3 y$	$+ C_3 z$	=	K_3	0	0	c
4...	x			=	S_1	$a_1 a$	$a_2 b$	$a_3 c$
5...		y		=	S_2	$b_1 a$	$b_2 b$	$b_3 c$
6...			z	=	S_3	$c_1 a$	$b_3 b$	$c_3 c$

Three equations with three unknowns were chosen for simplicity. The derivation would obviously be the same for any number of unknowns. Also, in this derivation the coefficients of x were varied; but this is evidently immaterial, as no restriction is involved. Revised solutions for the unknown whose coefficients are being varied are given by Eq. 17; revised values for the solutions of all other unknowns are given by Eqs. 19 and 20.

Generalizing:

$$u' = \frac{u}{1 + u_d} \quad \ldots\ldots\ldots\ldots\ldots\ldots\ldots\ldots (21a)$$

and

$$v' = v - v_d\, u' \quad \ldots\ldots\ldots\ldots\ldots\ldots\ldots\ldots (21b)$$

in which u and u' represent, in the original and revised equations, respectively, the unknown whose coefficients are being varied; v and v' represent any other unknown in the original and final equations, respectively; d_n is the amount by which A_n, any coefficient of u, is increased; and u_d and v_d are solutions for u and v, respectively, when $c_n = d_1, d_2, \cdots, d_n$.

Application of basic Eqs. 21 to the solution of the equations—

$$\left.\begin{array}{rl} 4x + 3y + 2z = & \left|\begin{array}{c||c|c|c} 28 & a & 0 & 0 \\ 26 & 0 & b & 0 \\ 49 & 0 & 0 & c \end{array}\right| \\ x + 4y + 3z = & \\ 5x + 2y + 6z = & \end{array}\right\} \quad \ldots\ldots\ldots\ldots\ldots\ldots (22)$$

—is illustrated in Table 4.

Explanation of Table 4

In Table 4, it is assumed that the set of simultaneous equations on lines 1, 2, and 3 (Eqs. 22) has been solved by some method, no matter what. The solutions corresponding to the four sets of constants are given on the next three lines. Let it be supposed that it is desired to reduce the coefficients of these equations by the amounts shown in brackets on the first three lines of the table. For example, on line 1 the coefficient of x, which totals 4, is to be reduced by 3 to a net value of 1; the coefficient of z, on the same line, is to be reduced by 2—that is, it is to be eliminated entirely. The order of variation is immaterial; by arbitrary choice the coefficients of z will be varied first.

From Eq. 21a, $u = z$, $u' = z'$, and $u_d = z_d$. Also, from Col. 4, lines 1, 2, and 3, $d_1 = -2$; $d_2 = -3$; and $d_3 = -5$. By definition, $u_d = z_d$ is a solution of the original equations for z corresponding to a set of constants $c_n = d_n$—that is, $c_1 = d_1 = -2$; $c_2 = d_2 = -3$; and $c_3 = d_3 = -5$.

To obtain this solution, z_d, it is necessary only to substitute the set of constants in line 6, setting $a = -2$, $b = -3$, and $c = -5$, as indicated in Col. 15, lines 7 to 9. Making this substitution, $u_d = z_d = \left(-\frac{2}{7}\right)(-2) + \frac{1}{9}(-3) + \frac{13}{63}(-5)$, from which $z_d = \frac{4}{7} - \frac{1}{3} - \frac{65}{63} = -\frac{50}{63}$, as shown on line 9, Cols. 9 to 12. Also, $1 + z_d = 1 - \frac{50}{63} = \frac{13}{63}$, and $\frac{1}{1 + z_d} = \frac{63}{13}$ as shown on line 9, Cols. 13 and 14.

Having computed the reciprocal of the denominator in Eq. 21a, the next step is to find the revised values of z. Thus, for $z = 5$, $z' = 5 \times \frac{63}{13} = \frac{315}{13}$; for $z = -\frac{2}{7}a$, $z' = \left(-\frac{2}{7}a\right) \times \frac{63}{13} = -\frac{18}{13}a$; that is, the original values on line 6 are multiplied by $\frac{1}{1 + z_d} = +\frac{63}{13}$ to obtain the revised values, z', on

TABLE 4.—WORK SHEET FOR THE APPLICATION OF EQS. 21*a* AND 21*b* TO VARIATION OF COEFFICIENTS OF EQS. 22

Line No.						Variation Coefficients			Conversion Factors						Substitution factors
									$a_n d_1$	$b_n d_2$	$c_n d_3$	u_d or v_d	$1 + u_d$	$\frac{1}{1+u_d}$	
(1)	(2)	(3)	(4)		(5)	(6)	(7)	(8)	(9)	(10)	(11)	(12)	(13)	(14)	(15)
1.....	$+x + [3x]$	$+ [3y]$	$+ [2z]$	=	28	a	0	0							
2.....	$+ [x]$	$+y + [3y]$	$+ [3z]$	=	26	0	b	0							
3.....	$+ [5x]$	$+ [2y]$	$+z + [5z]$	=	49	0	0	c							
4.....	x			=	$+3$	$+\frac{2}{7}a$	$-\frac{2}{9}b$	$+\frac{1}{63}c$							
5.....		y		=	$+2$	$+\frac{1}{7}a$	$+\frac{2}{9}b$	$-\frac{10}{63}c$							
6.....			z	=	$+5$	$-\frac{2}{7}a$	$+\frac{1}{9}b$	$+\frac{13}{63}c$							
7.....					$+\frac{5}{13}$	$-\frac{2}{91}a$	$+\frac{1}{117}b$	$+\frac{1}{63}c$	$-\frac{4}{7}$	$+\frac{2}{3}$	$-\frac{5}{63}$	$+\frac{1}{63}$			$a = d_1 = -2$
8.....					$-\frac{50}{13}$	$+\frac{20}{91}a$	$-\frac{10}{117}b$	$-\frac{10}{63}c$	$-\frac{2}{7}$	$-\frac{2}{3}$	$+\frac{50}{63}$	$-\frac{10}{63}$			$b = d_2 = -3$
9.....					$+\frac{315}{13}$	$-\frac{18}{13}a$	$+\frac{7}{13}b$	$+c$	$+\frac{4}{7}$	$-\frac{1}{3}$	$-\frac{65}{63}$	$-\frac{50}{63}$	$+\frac{13}{63}$	$+\frac{63}{13}$	$c = d_3 = -5$
10.....	x'			=	$+\frac{34}{13}$	$+\frac{4}{13}a$	$-\frac{3}{13}b$	0							
11.....		y'		=	$+\frac{76}{13}$	$-\frac{1}{13}a$	$+\frac{4}{13}b$	0							
12.....			(x')	=	$+\frac{315}{13}$	$-\frac{18}{13}a$	$+\frac{7}{13}b$	$+c$							

TABLE 4.—(*Continued*)

Line No.						Variation Coefficients			Conversion Factors						Substitution factors
									$a_n d_1$	$b_n d_2$	$c_n d_3$	u_d or v_d	$1 + u_d$	$\frac{1}{1+u_d}$	
(1)	(2)	(3)	(4)		(5)	(6)	(7)	(8)	(9)	(10)	(11)	(12)	(13)	(14)	(15)
13.....					$-\frac{57}{13}$	$+\frac{3}{52}a$	$-\frac{3}{13}b$	0	$-\frac{12}{13}$	$+\frac{9}{13}$	0	$-\frac{3}{13}$			$a = d_1 = -3$
14.....					$+19$	$-\frac{1}{4}a$	$+b$	0	$+\frac{3}{13}$	$-\frac{12}{13}$	0	$-\frac{9}{13}$	$+\frac{4}{13}$	$+\frac{13}{4}$	$b = d_2 = -3$
15.....					$+\frac{133}{13}$	$-\frac{7}{52}a$	$+\frac{7}{13}b$	0	$+\frac{54}{13}$	$-\frac{21}{13}$	-2	$+\frac{7}{13}$			$c = d_3 = -2$
16.....	x''			$=$	$+7$	$+\frac{1}{4}a$	0	0							
17.....		(y'')		$=$	$+19$	$-\frac{1}{4}a$	b	0							
18.....			z''	$=$	$+14$	$-\frac{5}{4}a$	0	c							
19.....					$+28$	$+a$	0	0	$-\frac{3}{4}$	0	0	$-\frac{3}{4}$	$+\frac{1}{4}$	$+4$	$a = d_1 = -3$
20.....					-7	$-\frac{1}{4}a$	0	0	$+\frac{3}{4}$	-1	0	$-\frac{1}{4}$			$b = d_2 = -1$
21.....					-35	$-\frac{5}{4}a$	0	0	$+\frac{15}{4}$	0	-5	$-\frac{5}{4}$			$c = d_3 = -5$
22.....	(x''')			$=$	$+28$	$+a$	0	0							
23.....		y'''		$=$	$+26$	0	b	0							
24.....			z'''	$=$	$+49$	0	0	c							

line 12. For reasons that will be obvious later, the values of z' are also shown on line 9, Cols. 5 to 8.

With z', the revised values of z determined, the revised values of the other unknowns can be computed. With $v = x$, and $v_d = x_d$, x_d is the only value on the right-hand side of Eq. 21*b* that has not already been computed. Again by definition, $v_d = x_d$ is a solution for x of the original equations corresponding to the same sets of constants $c_n = d_n$. Therefore, substituting in line 4 the values $a = -2$, $b = -3$, and $c = -5$, $v_d = x_d = +\frac{2}{7}(-2) + \left(-\frac{2}{9}\right)(-3) + \frac{1}{63}(-5)$ from which $x_d = -\frac{4}{7} + \frac{2}{3} - \frac{5}{63} = +\frac{1}{63}$, as shown on line 7, Cols. 9 to 12.

Having obtained $v_d = x_d$, the term $v_d u' = x_d z'$ may be computed. Thus, for $x = 3$ and $z' = +\frac{315}{13}$, $x_d z' = \frac{315}{13} \times \frac{1}{63} = +\frac{5}{13}$. Likewise, for $x = +\frac{2}{7}a$ and $z' = -\frac{18}{13}a$, $x_d z' = \left(-\frac{18}{13}a\right)\frac{1}{63} = -\frac{2}{91}a$; that is, the values of z' on line 9 are multiplied by $x_d = +\frac{1}{63}$ to obtain the term $x_d z'$ on line 7 corresponding to each value of x (in the original equations) on line 4. Since, by Eq. 21*b*, $x' = x - x_d z'$, values on line 7, Cols. 5 to 8, are subtracted algebraically from corresponding values on line 4 to give the revised values, x', on line 10. Thus, for $x = 3$, $x' = 3 - \frac{5}{13} = +\frac{34}{13}$. Likewise, for $x = \frac{2}{7}a$, $x' = +\frac{2}{7}a - \left(-\frac{2}{91}a\right) = +\frac{4}{13}a$.

Similarly, setting $v = y$, $v' = y'$, and $v_d = y_d$ in Eq. 21*b* and substituting $a = -2$, $b = -3$, and $c = -5$ in line 5, $y_d = +\frac{1}{7}(-2) + \frac{2}{9}(-3) + \left(-\frac{10}{63}\right)(-5)$, from which $y_d = -\frac{2}{7} - \frac{2}{3} + \frac{50}{63} = -\frac{10}{63}$, as shown on line 8, Cols. 9 to 12. Multiplying the values of z' on line 9 by $y_d = -\frac{10}{63}$, the values of the terms $y_d z'$ are obtained as shown on line 8, Cols. 5 to 8. Thus, for $y = 2$ and $z' = +\frac{315}{13}$, $y_d z' = +\frac{315}{13}\left(-\frac{10}{63}\right) = -\frac{50}{13}$. Also, for $y = \frac{1}{7}a$ and $z' = -\frac{18}{13}a$, $y_d z' = \left(-\frac{18}{13}a\right)\left(-\frac{10}{63}\right) = +\frac{20}{91}a$.

Since, by Eq. 21*b*, $y' = y - y_d z'$, values on line 8, Cols. 5 to 8, are subtracted algebraically from corresponding values on line 5 to give the revised values, y', on line 11. For example, for $y = 2$, $y' = 2 - \left(-\frac{50}{13}\right) = +\frac{76}{13}$; for $y = +\frac{1}{7}a$, $y' = \frac{1}{7}a - \frac{20}{91}a = -\frac{1}{13}a$.

The computation for the variation of the coefficients of z is now complete,

and lines 10, 11, and 12 are the solutions for the revised set equations—

$$\left.\begin{array}{rcl} 4\,x' + 3\,y' & = & \left|\begin{array}{c||c|c|c} 28 & a & 0 & 0 \\ 26 & 0 & b & 0 \\ 49 & 0 & 0 & c \end{array}\right| \\ x' + 4\,y' & = & \\ 5\,x' + 2\,y' + z' & = & \end{array}\right\} \quad \ldots\ldots\ldots\ldots\ldots\ldots (23)$$

In the next step of Table 4, Eqs. 23 are further revised by varying the coefficients of y' from 3, 4, and 2 to 0, 1, and 0, respectively. For this step, referring again to Eqs. 21, $u = y'$, and $v = x'$ or z' as the case may be. The computations follow, step by step, the procedure described in detail for varying the coefficients of z. Since the new set of equations are now being varied—that is, Eqs. 23—their solutions on lines 10, 11, and 12 are used to compute x'', y'', and z'' on lines 16, 17, and 18.

These solutions correspond to another new set of equations—

$$\left.\begin{array}{rcl} 4\,x'' & = & \left|\begin{array}{c||c|c|c} 28 & a & 0 & 0 \\ 26 & 0 & b & 0 \\ 49 & 0 & 0 & c \end{array}\right| \\ x'' + y'' & = & \\ 5\,x'' + z'' & = & \end{array}\right\} \quad \ldots\ldots\ldots\ldots\ldots\ldots (24)$$

In the last step of Table 4, Eqs. 24 are revised further by varying the coefficients of x'' from 4, 1, and 5 to 1, 0, and 0, respectively. For this variation, $u = x''$, and $v = y''$ or z''. The new solutions are given on lines 22, 23, and 24, corresponding to the new equations:

$$\left.\begin{array}{rcl} x''' & = & \left|\begin{array}{c||c|c|c} 28 & a & 0 & 0 \\ 26 & 0 & b & 0 \\ 49 & 0 & 0 & c \end{array}\right| \\ y''' & = & \\ z''' & = & \end{array}\right\} \quad \ldots\ldots\ldots\ldots\ldots\ldots (25)$$

Attention is called to the fact that each step in Table 4 is entirely independent and complete. Once the solution to a set of equations is known, it is immaterial whether it was obtained independently or by varying the coefficients of some other set of equations.

Solution of Simultaneous Equations by Variation of Coefficients

In Table 4, the coefficients have been varied in a more or less arbitrary manner. This numerical example illustrates clearly that, once the variation coefficients are known for any set of simultaneous equations, the coefficients can be varied at will and the order of the operations is almost entirely arbitrary. Also, the process is obviously reversible—which leads directly to another method for solving such equations.

In Table 4, it was assumed that Eqs. 22 were solved in some way, no matter how—the solutions being given on lines 4, 5, and 6. By a series of variation operations, all the coefficients in brackets in this original set of equations were removed, resulting in the corresponding revised solutions given on lines 22, 23, and 24. However, this last result obviously can be obtained directly by inspection. Since the process is reversible, the results shown on these last three lines can be varied back to the original set of equations—or to any other set of equations, for that matter. This reverse process is illustrated in Table 5, and thus another method for solving simultaneous linear equations is obtained.

TABLE 5.—WORK SHEET FOR SOLUTION OF EQS. 22 BY VARIATION OF COEFFICIENTS

Line No.						Variation Coefficients			Conversion Factors						Substitution factors
									$a_n\ d_1$	$b_n\ d_2$	$c_n\ d_3$	u_d or v_d	$1+u_d$	$\frac{1}{1+u_d}$	
(1)	(2)	(3)	(4)		(5)	(6)	(7)	(8)	(9)	(10)	(11)	(12)	(13)	(14)	(15)
1.....	$+x+[3\,x]$	$+[3\,y]$	$+[2\,z]$	=	28	a	0	0							
2.....	$+[x]$	$y+[3\,y]$	$+[3\,z]$	=	26	0	b	0							
3.....	$+[5\,x]$	$+[2\,y]$	$+z+[5\,z]$	=	49	0	0	c							
4.....	x			=	28	a	0	0							
5.....		y		=	26	0	b	0							
6.....			z	=	49	0	0	c							
7.....					+7	$+\frac{1}{4}a$	0	0	+3	0	0	+3	+4	$+\frac{1}{4}$	$a=d_1=+3$
8.....					+7	$+\frac{1}{4}a$	0	0	0	+1	0	+1			$b=d_2=+1$
9.....					+35	$+\frac{5}{4}a$	0	0	0	0	+5	+5			$c=d_3=+5$
10.....	(x)			=	+7	$+\frac{1}{4}a$	0	0							
11.....		y		=	+19	$-\frac{1}{4}a$	b	0							
12.....			z	=	+14	$-\frac{5}{4}a$	0	c							

TABLE 5.—(*Continued*)

TABLE 5.—(*Continued*)

Line No.						Variation Coefficients			Conversion Factors						Substitution factors
(1)	(2)	(3)	(4)		(5)	(6)	(7)	(8)	$a_n\,d_1$ (9)	$b_n\,d_2$ (10)	$c_n\,d_3$ (11)	u_d or v_d (12)	$1+u_d$ (13)	$\frac{1}{1+u_d}$ (14)	(15)
13.....					$+\frac{57}{13}$	$-\frac{3}{52}a$	$+\frac{3}{13}b$	0	$+\frac{3}{4}$	0	0	$+\frac{3}{4}$			$\left.\begin{array}{l}a=d_1=+3\\ b=d_2=+3\\ c=d_3=+2\end{array}\right)$
14.....					$+\frac{76}{13}$	$-\frac{1}{13}a$	$+\frac{4}{13}b$	0	$-\frac{3}{4}$	3	0	$+\frac{9}{4}$	$+\frac{13}{4}$	$+\frac{4}{13}$	
15.....					$-\frac{133}{13}$	$+\frac{7}{52}a$	$-\frac{7}{13}b$	0	$-\frac{15}{4}$	0	2	$-\frac{7}{4}$			
16.....	x			=	$+\frac{34}{13}$	$+\frac{4}{13}a$	$-\frac{3}{13}b$	0							
17.....		(y)		=	$+\frac{76}{13}$	$-\frac{1}{13}a$	$+\frac{4}{13}b$	0							
18.....			z	=	$+\frac{315}{13}$	$-\frac{18}{13}a$	$+\frac{7}{13}b$	c							
19.....					$-\frac{5}{13}$	$+\frac{2}{91}a$	$-\frac{1}{117}b$	$-\frac{1}{63}c$	$+\frac{8}{13}$	$-\frac{9}{13}$	0	$-\frac{1}{13}$			$\left.\begin{array}{l}a=d_1=+2\\ b=d_2=+3\\ c=d_3=+5\end{array}\right)$
20.....					$+\frac{50}{13}$	$-\frac{20}{91}a$	$+\frac{10}{117}b$	$+\frac{10}{63}c$	$-\frac{2}{13}$	$+\frac{12}{13}$	0	$+\frac{10}{13}$			
21.....					$+5$	$-\frac{2}{7}a$	$+\frac{1}{9}b$	$+\frac{13}{63}c$	$-\frac{36}{13}$	$+\frac{21}{13}$	$+5$	$+\frac{50}{13}$	$+\frac{63}{13}$	$+\frac{13}{63}$	
22.....	x			=	$+3$	$+\frac{2}{7}a$	$-\frac{2}{9}b$	$+\frac{1}{63}c$							
23.....		y		=	$+2$	$+\frac{1}{7}a$	$+\frac{2}{9}b$	$-\frac{10}{63}c$							
24.....			(z)	=	$+5$	$-\frac{2}{7}a$	$+\frac{1}{9}b$	$+\frac{13}{63}c$							

Furthermore, it is not necessary to begin with lines 22, 23, and 24 of Table 4, which are duplicated in lines 4, 5, and 6 of Table 5. If a solution of any set of equations is known—from some previous computation or in any other way—it can be varied to any other set of equations desired. "Knowing a solution" means that the "variation coefficients"—which result from solving the equations for a set of constants a, 0, 0; 0, b, 0; and 0, 0, c—are known. The process is the same for any number of unknowns.

Explanation of Table 5

Referring to Table 5, Eqs. 22 (lines 1, 2, and 3) are to be solved by a series of steps which is the reverse of that in Table 4. All the coefficients and parts of coefficients in brackets are considered removed, giving rise to the new set of equations:

$$\left.\begin{array}{rl} x = & \left|\begin{array}{c|c|c|c} 28 & a & 0 & 0 \end{array}\right| \\ y = & \left|\begin{array}{c|c|c|c} 26 & 0 & b & 0 \end{array}\right| \\ z = & \left|\begin{array}{c|c|c|c} 49 & 0 & 0 & c \end{array}\right| \end{array}\right\} \quad \ldots\ldots\ldots\ldots\ldots\ldots (26)$$

This new set of equations can obviously be solved by inspection; the solutions shown on lines 4, 5, and 6 are merely the repetition of Eqs. 26. To solve the original set of equations, it is necessary to vary the coefficients of this reduced set until all the coefficients and parts of coefficients which have been removed are replaced. By arbitrary choice and also to furnish a comparison between Table 5 and Table 4, the coefficients are varied in the order of x, y, and z.

To replace the coefficients of x, $d_1 = +3$, $d_2 = +1$, and $d_3 = +5$, since comparison of Eqs. 26 with lines 1, 2, and 3 in Col. 2 shows that these values are the coefficients and parts of coefficients which have been removed. Substitution in line 4 of $a = d_1 = +3$, $b = d_2 = +1$, and $c = d_3 = +5$ gives $x_d = +3$, since x has a value other than zero only when $c_n = a$.

From this point to the end of the computation the procedure is exactly similar to that used in Table 4 and needs no further explanation. The final solution is given on lines 22, 23, and 24.

Reciprocal Properties of Simultaneous Equations

For ready reference, and also to bring out certain relationships, the operations shown in Tables 4 and 5 have been summarized in Table 6. It is customary to consider x, y, and z as the unknowns and a, b, and c as the constants; that is, the equations would be set up on this basis in a practical problem. However, once the equations are solved—considering lines 1 to 6 of Table 6—it is equally correct, mathematically, to consider a, b, and c as the unknowns and x, y, and z as the constants.

From this point of view, considering a, b, and c as the unknowns, lines 1, 2, and 3 give the solutions for the equations on lines 4, 5, and 6. To illustrate: Substitution in line 4 of the values $a = 4x$, $b = x$, and $c = 5x$, for example, gives $\frac{2}{7}(4x) - \frac{2}{9}(x) + \frac{1}{63}(5x) = x$, which checks. Similarly, substitution at

random (in line 5, for example) of $a = 28$, $b = 26$, and $c = 49$ gives $\frac{1}{7} \times 28 + \frac{2}{9} \times 26 - \frac{10}{63} \times 49 = 2$, which checks again.

It should be remembered that, after a variation operation is completed, the set of resulting equations with their solutions are complete in themselves. The equations may not be those that are finally desired, but they are nevertheless complete. It therefore follows that any set of equations is merely a stopping point in an endless series of variations. Lines 7, 8, and 9, for example, are the solutions for a set of equations in which the coefficient of z is zero in the first two and equals unity in the third, but which is otherwise the same as the original set on lines 1, 2, and 3 (Eqs. 23). Either x, y, and z or a, b, and c may be considered as the unknowns and if the corresponding solutions are substituted the results will check in the new equations.

The reciprocity of the equations plus the fact that at each step in a variation process the results are complete makes the operations self-checking. Furthermore, there are so many methods of checking that some of the checks may be used to reduce the numerical work and still leave a sufficient number for actual verification.

A consideration of the fundamental theory of equations will bring to light other ways of checking not mentioned. For example, the fact that rows and columns of determinants may be interchanged leads to the conclusion that other sets of equations exist which may be obtained by "rotating" the coefficients to positions consistent with the corresponding "rotated" determinants.

Furthermore, in a practical problem in structural analysis, most coefficients occur in pairs as a consequence of the Maxwell theorem of reciprocal deflections. The final "variation coefficients" also occur in pairs and in the same order as the coefficients of the unknowns—furnishing an automatic check, which may also have other uses besides checking.

An examination of Table 6(*c*) will show that, on any line, terms above the heavy line are merely repetitions of the terms on the line immediately above. It will also be noted that the values of the solution on line 24 are not needed until the last step, those on line 20 are not needed until the next to last step, and so on, if there are more than three equations. Furthermore, once a value appears in the computation, it must be revised at every subsequent step. Hence, if there were a method of obtaining these values at the time they are actually required for the next step, they could be omitted from all the previous computations, thus saving part of the work of revising them. This abbreviation can be achieved by using one of the checks to obtain the omitted values.

The revised variation operations illustrated in Table 7 show that there is a considerable saving in work even though it is partly offset by the necessity of making a substitution computation at every step in the process.

Theory of Abbreviated Solution

The procedure followed in Table 5 for solving a set of simultaneous equations may be simplified by taking advantage of certain characteristics of this type of solution.

Reference to Eqs. 21*a* and 21*b* will show that u', the revised value of the unknown whose coefficients are being varied in the particular step or "variation" under consideration, is computed first and that it also enters in the

TABLE 6.—COMPARISON OF RESULTS OF TABLE 4 AND TABLE 5

Line No.	Equations in x, y, and z →				Constants		← Equations in a, b, and c		
(1)	(2)	(3)	(4)		(5)		(6)	(7)	(8)
	(*a*) Statement of Eqs. 22 with Solutions (from Table 4)								
1.....	$+4x$	$+3y$	$+2z$	=	28	=	a	0	0
2.....	$+x$	$+4y$	$+3z$	=	26	=	0	b	0
3.....	$+5x$	$+2y$	$+6z$	=	49	=	0	0	c
4.....	x	0	0	=	3	=	$+\frac{2}{7}a$	$-\frac{2}{9}b$	$+\frac{1}{63}c$
5.....	0	y	0	=	2	=	$+\frac{1}{7}a$	$+\frac{2}{9}b$	$-\frac{10}{63}c$
6.....	0	0	z	=	5	=	$-\frac{2}{7}a$	$+\frac{1}{9}b$	$+\frac{13}{63}c$
	(*b*) Variation of Coefficients of Eqs. 22 (from Table 4)								
7.....	x	0	0	=	$+\frac{34}{13}$	=	$+\frac{4}{13}a$	$-\frac{3}{13}b$	0
8.....	0	y	0	=	$+\frac{76}{13}$	=	$-\frac{1}{13}a$	$+\frac{4}{13}b$	0
9.....	0	0	(z)[a]	=	$+\frac{315}{13}$	=	$-\frac{18}{13}a$	$+\frac{7}{13}b$	c
10.....	x	0	0	=	+7	=	$+\frac{1}{4}a$	0	0
11.....	0	(y)	0	=	+19	=	$-\frac{1}{4}a$	b	0
12.....	0	0	$[z]$[b]	=	+14	=	$-\frac{5}{4}a$	0	c
13.....	(x)	0	0	=	+28	=	a	0	0
14.....	0	$[y]$	0	=	+26	=	0	b	0
15.....	0	0	$[z]$	=	+49	=	0	0	c

formula for the revised values of the other unknowns. The term u' may thus be considered the critical one for its step. It will be shown that, in a sense, a solution reduces to the computation of critical values only—that is, values of the unknowns that have not been critical in previous steps, and that are also not critical in the step under consideration or in the one immediately following, need not be computed.

In Table 5, for example, the solutions on lines 16, 17, and 18 correspond to Eqs. 23, in which the values of x and y are obviously determined by the first two equations and are independent of the third. Mathematically, this fact becomes evident in the computation for x_d and y_d on lines 7 and 8, respectively,

Table 5; that is, $c = d_3 = +5$ is substituted in lines 4 and 5, where it is multiplied by zero; d_3 is obviously the coefficient of x in the third of Eqs. 23. The corresponding result occurs in the computation for x_d and y_d in lines 13

TABLE 6.—(*Continued*)

Line No.	Equations in x, y, and z →				Constants		← Equations in a, b, and c		
(1)	(2)	(3)	(4)		(5)		(6)	(7)	(8)
	(*c*) Solution of Eqs. 22 by Variation of Coefficients (from Table 5)								
16.....	x	0	0	=	+28	=	a	0	0
17.....	0	y	0	=	+26	=	0	b	0
18.....	0	0	z	=	+49	=	0	0	c
19.....	$(x)^a$	0	0	=	+ 7	=	$+\frac{1}{4}a$	0	0
20.....	0	y	0	=	+19	=	$-\frac{1}{4}a$	b	0
21.....	0	0	z	=	+14	=	$-\frac{5}{4}a$	0	c
22.....	$[x]^b$	0	0	=	$+\frac{34}{13}$	=	$+\frac{4}{13}a$	$-\frac{3}{13}b$	0
23.....	0	(y)	0	=	$+\frac{76}{13}$	=	$-\frac{1}{13}a$	$+\frac{4}{13}b$	0
24.....	0	0	z	=	$+\frac{315}{13}$	=	$-\frac{18}{13}a$	$+\frac{7}{13}b$	c
25.....	$[x]$	0	0	=	+3	=	$+\frac{2}{7}a$	$-\frac{2}{9}b$	$+\frac{1}{63}c$
26.....	0	$[y]$	0	=	+2	=	$+\frac{1}{7}a$	$+\frac{2}{9}b$	$-\frac{10}{63}c$
27.....	0	0	(z)	=	+5	=	$-\frac{2}{7}a$	$+\frac{1}{9}b$	$+\frac{13}{63}c$

[a] (u) Unknown whose coefficients are being varied in step under consideration. [b] $[u]$ Unknown whose coefficients have been varied in previous steps.

and 14, wherein $c = d_3 = +2$ is multiplied by zero when substituted in lines 10 and 11; $d_3 = +2$ is obviously the coefficient of y in this same third equation.

Since the values of x and y are independent of the third of Eqs. 23, all the coefficients in this equation may be neglected in the computation up to this point. However, once x and y are known, the values of z can be computed from the third equation by direct substitution. It therefore follows that the values of z need not necessarily be computed in the previous steps. The values of z must be computed at this point, however, since the coefficients of z are varied in the next step of Table 5 and the critical value $u' = z'$ could not otherwise be computed.

Similarly, the solutions on lines 10, 11, and 12, Table 5, correspond to Eqs. 24, in which x is determined by the first equation and is independent of

TABLE 7.—WORK SHEET FOR ABBREVIATED SOLUTION OF EQS. 22 BY VARIATION OF COEFFICIENTS

Line No.						Variation Coefficients			Conversion Factors					Substitution factors
(1)	(2)	(3)	(4)		(5)	(6)	(7)	(8)	$a_n\, d_1$ (9)	$b_n\, d_2$ (10)	$c_n\, d_3$ (11)	u_d or v_d (12)	$\frac{1}{1+u_d}$ (13)	(14)
1.....	$+x+[3x]$	$+[3y]$	$+[2z]$	=	28	a	0	0						
2.....	$+[x]$	$+y+[3y]$	$+[3z]$	=	26	0	b	0						
3.....	$+[5x]$	$+[2y]$	$+z+[5z]$	=	49	0	0	c						
4.....	x			=	28	a	0	0						
5.....		y		=	26	0	b	0						
6.....			z	=	49	0	0	c						
7.....	(x)			=	$+7$	$+\frac{1}{4}a$	0		3			$+3$	$\frac{1}{4}$	$(a = d_1 = +3)$
8.....		y		=	$+19$	$-\frac{1}{4}a$	b							
9.....					$+\frac{57}{13}$	$-\frac{3}{52}a$	$+\frac{3}{13}b$		$+\frac{3}{4}$	0		$\frac{3}{4}$		$\left(\begin{matrix}a = d_1 = +3\\ b = d_2 = +3\end{matrix}\right)$
10.....					$+\frac{76}{13}$	$-\frac{1}{13}a$	$+\frac{4}{13}b$		$-\frac{3}{4}$	$+3$		$+\frac{9}{4}$	$\frac{4}{13}$	
11.....	$+5x$			=	$+\frac{170}{13}$	$+\frac{20}{13}a$	$-\frac{15}{13}b$	0						
12.....		$+2y$		=	$+\frac{152}{13}$	$-\frac{2}{13}a$	$+\frac{8}{13}b$	0						
13.....					$+\frac{322}{13}$	$+\frac{18}{13}a$	$-\frac{7}{13}b$	0						
14.....	x			=	$+\frac{34}{13}$	$+\frac{4}{13}a$	$-\frac{3}{13}b$	0						
15.....		(y)		=	$+\frac{76}{13}$	$-\frac{1}{13}a$	$+\frac{4}{13}b$	0						
16.....			z	=	$+\frac{315}{13}$	$-\frac{18}{13}a$	$+\frac{7}{13}b$	c						

TABLE 7.—(*Continued*)

Line No.						Variation Coefficients			Conversion Factors					Substitution factors
									$a_n\ d_1$	$b_n\ d_2$	$c_n\ d_2$	u_d or v_d	$\frac{1}{1+u_d}$	
(1)	(1)	(3)	(4)		(5)	(6)	(7)	(8)	(9)	(10)	(11)	(12)	(13)	(14)
17.....					$-\frac{5}{13}$	$+\frac{2}{91}a$	$-\frac{1}{117}b$	$-\frac{1}{63}c$	$+\frac{8}{13}$	$-\frac{9}{13}$	0	$-\frac{1}{13}$		$a = d_1 = +2$
18.....					$+\frac{50}{13}$	$-\frac{20}{91}a$	$+\frac{10}{117}b$	$+\frac{10}{63}c$	$-\frac{2}{13}$	$+\frac{12}{13}$	0	$+\frac{10}{13}$		$b = d_2 = +3$
19.....					$+5$	$-\frac{2}{7}a$	$+\frac{1}{9}b$	$+\frac{13}{63}c$	$-\frac{36}{13}$	$+\frac{21}{13}$	5	$+\frac{50}{13}$	$\frac{13}{63}$	$c = d_3 = +5$
20.....	x			=	$+3$	$+\frac{2}{7}a$	$-\frac{2}{9}b$	$+\frac{1}{63}c$						
21.....		y		=	$+2$	$+\frac{1}{7}a$	$+\frac{2}{9}b$	$-\frac{10}{63}c$						
22.....			(z)	=	$+5$	$-\frac{2}{7}a$	$+\frac{1}{9}b$	$+\frac{13}{63}c$						

the other two. Mathematically, this fact is again evident in the computation—the appropriate d_n-values are multiplied by zero in the computation for x_d. Hence, all the coefficients of the second and third equations may be neglected in the computation up to this point—that is, in the computation for $u' = x'$.

The values of both y' and z' may be computed by direct substitution, once x' is known. However, it is necessary to compute only the values of the unknown whose coefficients are to be varied in the next step—in this case y' is the next unknown to become critical. The revised values of z can be computed later, as already explained.

The abbreviated procedure may now be summarized. In Table 7, lines 1, 2, and 3, all the coefficients below the lower heavy line in each column may be neglected in each step or "variation." The values of u', which is critical, are computed by Eq. 21*a*; the values of v', corresponding to the unknowns whose coefficients have already been varied in previous steps, are computed by Eq. 21*b*; and the values of v', corresponding to the unknown whose coefficients are to be varied in the next step, are computed by direct substitution. The values of the remaining unknowns are neglected because they are not essential to the final solution, and are not computed until they are about to become critical in the step immediately following.

Explanation of Table 7

In Table 7, the order of variation of the coefficients is the same as in Table 5: x, y, and z.

In the first step, it is only necessary to use $d_1 = 3$, corresponding to $[3\,x]$ in line 1, Col. 2, as previously explained. With this exception, nothing new is presented by line 7, which gives the first revised value of x. The primes are omitted for simplicity—the x in line 7, for instance, is really x'. Since the solution in this step will correspond to Eqs. 24, the values of y, which is critical in the next step, may be computed from the second of these equations—$y = c_2 - x$.

Values of x on line 7, Cols. 5, 6, and 7 subtracted from the corresponding values on line 2 result in the revised values of y in line 8. As previously explained, it is not essential to compute the revised values of z at this point.

In the second step, variation of the coefficients of y, it is only necessary to use $d_1 = +3$ and $d_2 = +3$. With this exception, the computations on lines 9 and 10, and lines 14 and 15 present nothing new. Since the solution in this step will correspond to Eqs. 23, the values of z can be computed from the third of these equations—$z = c_3 - (+5\,x + 2\,y)$. The quantities in parentheses are computed on lines 11 and 12 and are summed up on line 13. Subtraction of the values on line 13 from the corresponding values on line 3, Cols. 5, 6, 7, and 8, gives the revised values of z on line 16.

The third and last step presents nothing new since d_1, d_2, and d_3 are used and there is no substitution to be made; the last variation in Table 7 is exactly the same as that in Table 5.

Multiple Variation

If the number of unknowns is large, the solution still requires considerable work—there will be as many steps or variation operations as there are unknowns. A further simplification is possible in such a case. If the coefficients of two or more unknowns are varied at the same time, an auxiliary set of simultaneous equations must be solved. If the coefficients of all the unknowns were varied simultaneously, for instance, the auxiliary equations would simply be a repetition of the original equations. However, since it is fairly easy to solve a set of two or even three equations, it does save considerable work to vary two or three unknowns at a time. The result of such a procedure is, in effect, that one large set of equations is broken up into several smaller sets. It is well known that, when a similar situation occurs in an analysis as the result of symmetry, the resulting equations are much easier to solve.

Referring to Eqs. 11, let it be supposed that the coefficients A_1, A_2, and A_3 are to be increased by d_1, d_2, and d_3, respectively, as before. In addition, however, the coefficients B_1, B_2, and B_3 also are to be increased by amounts e_1, e_2, and e_3, respectively. Following the same procedure used for varying the coefficients of only one unknown:

$$\left.\begin{aligned} a &= K_1 - d_1 x' - e_1 y' \\ b &= K_2 - d_2 x' - e_2 y' \\ c &= K_3 - d_3 x' - e_3 y' \end{aligned}\right\} \quad \ldots\ldots\ldots\ldots\ldots\ldots (27)$$

Substituting these values in line 4, Table 3, gives

$$\begin{aligned} x' = a_1(K_1 - d_1 x' - e_1 y') &+ a_2(K_2 - d_2 x' - e_2 y') \\ &+ a_3(K_3 - d_3 x' - e_3 y') \quad \ldots\ldots\ldots\ldots\ldots\ldots (28a) \end{aligned}$$

or

$$\begin{aligned} (1 + a_1 d_1 + a_2 d_2 + a_3 d_3)x' + (a_1 e_1 + a_2 e_2 + a_3 e_3)y' \\ = a_1 K_1 + a_2 K_2 + a_3 K_3 \quad \ldots\ldots\ldots\ldots\ldots\ldots (28b) \end{aligned}$$

Therefore,

$$(1 + x_d)x' + x_e y' = x \quad \ldots\ldots\ldots\ldots\ldots\ldots (29)$$

Similarly, substitution of the values for a, b, and c, in line 5, Table 3, gives

$$y_d x' + (1 + y_e)y' = y \quad \ldots\ldots\ldots\ldots\ldots\ldots (30)$$

and substitution in line 6 gives

$$z' = z - z_d x' - z_e y' \quad \ldots\ldots\ldots\ldots\ldots\ldots (31)$$

To obtain x' and y', Eqs. 29 and 30 must be solved simultaneously; the values of z' are then computed directly from Eq. 31.

If there were more than three unknowns, the equations for the remaining ones would take the same form as Eq. 31; for example:

$$r' = r - r_d x' - r_e y' \quad \ldots\ldots\ldots\ldots\ldots\ldots (32)$$

Generalizing,

$$(1 + u_d)u' + u_e w' = u \quad \ldots\ldots\ldots\ldots\ldots\ldots (33a)$$

$$w_d u' + (1 + w_e)w' = w \quad \ldots\ldots\ldots\ldots\ldots\ldots (33b)$$

$$y' = v - v_d u' - v_e w' \quad \ldots\ldots\ldots\ldots\ldots\ldots (34)$$

TABLE 8.—WORK SHEET FOR SOLUTION OF EQS. 35 BY MULTIPLE VARIATION OF COEFFICIENTS

Line No.							Variation Coefficients				Conversion Factors						Substitution factors
(1)	(2)	(3)	(4)	(5)		(6)	(7)	(8)	(9)	(10)	$a_n\,d_1$ (11)	$b_n\,d_2$ (12)	$c_n\,d_3$ (13)	$f_n\,d_4$ (14)	u_d (15)	$1+u_d$ (16)	(17)
1.....	$+10w$	$+9x$	$+8y$	$+7z$	=	$+114$	a	0	0	0							
2.....	$+9w$	$+6x$	$+5y$	$+4z$	=	$+76$	0	b	0	0							
3.....	$+8w$	$+5x$	$+3y$	$+2z$	=	$+53$	0	0	c	0							
4.....	$+7w$	$+4x$	$+2y$	$+z$	=	$+39$	0	0	0	f							
5.....	w				=	$+114$	a	0	0	0							
6.....		x			=	$+76$	0	b	0	0							
7.....			y		=	$+53$	0	0	c	0							
8.....				z	=	$+39$	0	0	0	f							
9.....	$+10w$	$+9x$			=	$+114$	a	0	0	0	$+9$	0			$+9$	$+10$	$d_1=+9$
10.....	$+9w$	$+6x$			=	$+76$	0	b	0	0	0	$+9$			$+9$		$d_2=+9$
11.....	w				=	0	$-\frac{2}{7}a$	$+\frac{3}{7}b$	0	0	$+9$	$+0$			$+9$		$e_1=+9$
12.....		x			=	$+\frac{266}{21}$	$+\frac{3}{7}a$	$-\frac{10}{21}b$	0	0	0	$+5$			$+5$	$+6$	$e_2=+5$
13.....	$+8w$				=	0	$-\frac{16}{7}a$	$+\frac{24}{7}b$	0	0							
14.....		$+5x$			=	$+\frac{1,330}{21}$	$+\frac{15}{7}a$	$-\frac{50}{21}b$	0	0							
15.....	$+7w$				=	0	$-2a$	$+3a$	0	0							
16.....		$+4x$			=	$+\frac{1,064}{21}$	$+\frac{12}{7}a$	$-\frac{40}{21}a$	0	0							
17.....	w				=	0	$-\frac{2}{7}a$	$+\frac{3}{7}b$	0	0							
18.....		x			=	$+\frac{266}{21}$	$+\frac{3}{7}a$	$-\frac{10}{21}b$	0	0							
19.....			y		=	$-\frac{217}{21}$	$+\frac{1}{7}a$	$-\frac{22}{21}b$	c	0							
20.....				z	=	$-\frac{245}{21}$	$+\frac{2}{7}a$	$-\frac{23}{21}b$	0	f							

TABLE 8.—*(Continued)*

TABLE 8.—(*Continued*)

Line No.							Variation Coefficients				Conversion Factors						Substitution factors
(1)	(2)	(3)	(4)	(5)		(6)	(7)	(8)	(9)	(10)	$a_n\,d_1$ (11)	$b_n\,d_2$ (12)	$c_n\,d_3$ (13)	$f_n\,d_4$ (14)	u_d (15)	$1+u_d$ (16)	(17)
21.....			$-23y$	$-25z$	=	-217	$+3a$	$-22b$	$+21c$	0	$-\frac{16}{7}$	$+\frac{15}{7}$	0	0	$-\frac{1}{7}$		$d_1=+8$
22.....			$-25y$	$-29z$	=	-245	$+6a$	$-23b$	0	$+21f$	$+\frac{24}{7}$	$-\frac{50}{21}$	0	0	$+\frac{22}{21}$		$d_2=+5$
23.....											$+\frac{8}{7}$	$-\frac{110}{21}$	2	0	$-\frac{44}{21}$	$-\frac{23}{21}$	$d_3=+2$
24.....			y		=	$+4$	$+\frac{3}{2}a$	$+\frac{3}{2}b$	$\left(-\frac{29c}{42}\right)21$	$\left(+\frac{25f}{42}\right)21$	$+\frac{16}{7}$	$-\frac{115}{21}$	0	2	$-\frac{25}{21}$		$d_4=+2$
25.....				z	=	$+5$	$-\frac{3}{2}a$	$-\frac{1}{2}b$	$\left(+\frac{25c}{42}\right)21$	$\left(-\frac{23f}{42}\right)21$							
26.....											-2	$+\frac{12}{7}$	0	0	$-\frac{2}{7}$		$e_1=+7$
27.....	$w_d\,y$				=	$-\frac{4}{7}$	$-\frac{3}{14}a$	$-\frac{3}{14}b$	$+\frac{29}{14}c$	$-\frac{25}{14}f$	$+3$	$-\frac{40}{21}$	0	0	$+\frac{23}{21}$		$e_2+=4$
28.....	$w_e\,z$				=	$-\frac{10}{7}$	$+\frac{3}{7}a$	$+\frac{1}{7}b$	$-\frac{25}{7}c$	$+\frac{23}{7}f$	$+1$	$-\frac{88}{21}$	2	0	$-\frac{25}{21}$		$e_3=+2$
29.....											$+2$	$-\frac{92}{21}$	0	0	$-\frac{50}{21}$	$-\frac{29}{21}$	$e_4=0$
30.....		$x_d\,y$			=	$+\frac{88}{21}$	$+\frac{11}{7}a$	$+\frac{11}{7}b$	$-\frac{319}{21}c$	$+\frac{275}{21}f$							
31.....		$x_e\,z$			=	$+\frac{115}{21}$	$-\frac{23}{14}a$	$-\frac{23}{42}b$	$+\frac{575}{42}c$	$-\frac{529}{42}f$							
32.....	w				=	$+2$	$-\frac{1}{2}a$	$+\frac{1}{2}b$	$+\frac{3}{2}c$	$-\frac{3}{2}f$							
33.....		x			=	$+3$	$+\frac{1}{2}a$	$-\frac{3}{2}b$	$+\frac{3}{2}c$	$-\frac{1}{2}f$							
34.....			y		=	$+4$	$+\frac{3}{2}a$	$+\frac{3}{2}b$	$-\frac{29}{2}c$	$+\frac{25}{2}f$							
35.....				z	=	$+5$	$-\frac{3}{2}a$	$-\frac{1}{2}b$	$+\frac{25}{2}c$	$-\frac{23}{2}f$							

in which both u and w represent the unknowns whose coefficients are being varied, and e_n is the amount by which each of the coefficients of w is being varied. The notation is otherwise the same as that of Eqs. 21*a* and 21*b*, and the primes have the same meaning.

Revised values of the unknowns whose coefficients are being varied simultaneously are computed by solving an auxiliary set of simultaneous equations such as Eqs. 33. The remaining unknowns are then computed by Eq. 34. Eqs. 33*a*, 33*b*, and 34 can obviously be extended to include the simultaneous variation of any number of unknowns and the solution of a large set of simultaneous equations can thus be broken up into the solution of several smaller sets. The optimum number of simultaneous variations is more or less a matter of individual preference. The procedure is illustrated in Table 8 for a set of four equations split into pairs of two each.

Explanation of Table 8

The procedure for the variation of the coefficients of more than one unknown at one time is similar, in general, to that illustrated in the previous tables for variation of the coefficients of only one unknown.

In Table 8, the set of four equations—

$$\left.\begin{array}{rl} +10w+9x+8y+7z= & \left|\begin{array}{c|c|c|c|c} 114 & a & 0 & 0 & 0 \\ 76 & 0 & b & 0 & 0 \\ 53 & 0 & 0 & c & 0 \\ 39 & 0 & 0 & 0 & f \end{array}\right| \\ +9w+6x+5y+4z= & \\ +8w+5x+3y+2z= & \\ +7w+4x+2y+z= & \end{array}\right\} \quad \cdots\cdots\cdots (35)$$

—is broken up into a pair of sets with two unknowns each, as indicated by the heavy lines in lines 1 to 4, Cols. 2 to 5. Since Table 8 illustrates a solution, the procedure and abbreviations of Table 7, suitably modified, are also used in Table 8.

Remembering that Eqs. 33*a*, 33*b*, and 34 are used instead of Eqs. 21*a* and 21*b*, reference to Table 7 will clarify the work in Table 8. Coefficients below the lower heavy line, for example, are omitted from the variation computations in both cases for reasons previously explained. However, since two sets of coefficients are being varied in the same step, the numerical equivalents of Eqs. 33 are shown in lines 9 and 10. These two auxiliary equations are solved simultaneously by inspection—as will be explained later—and the result is given in lines 11 and 12. Since the coefficients of both x and y are to be varied in the next step, their revised values are obtained at this point by direct substitution as shown in lines 13 to 16, and lines 19 and 20. It happens that there are no other unknowns, but if there were, their revised values would not have to be computed at this point; they can be computed later by direct substitution when needed. The complete solution for the first step is shown in lines 17 to 20.

The next step is similar: The auxiliary equations are shown in lines 21 and 22, their solution (by inspection) in lines 24 and 25, and part of the numerical equivalents of Eq. 34 in lines 30 and 31. The final solution for this step, which is the last of this computation, is shown in lines 32 to 35. Since this is the last

step and there are no other unknowns, there is no direct substitution to be made.

An over-all check of the entire computation may be made by adding the four equations on lines 1 to 4, Table 8, and substituting, in the resulting equation, the sum of the solutions on lines 32 to 35, Table 8, setting $a = b = c = f = 1$. For example, $w = 2 - \frac{1}{2} + \frac{1}{2} + \frac{3}{2} - \frac{3}{2} = 2$, as shown in line 1, Col. 8, Table 9. The result of this substitution (line 5, Col. 7, Table 9) should equal the sum of the constants in lines 1 to 4, Table 8 (again setting $a = b = c = f = 1$), all as shown on lines 1 to 5, Table 9.

TABLE 9.—CHECK FOR SOLUTION OF EQS. 35 BY MULTIPLE VARIATION

Line No. (1)	(2)	(3)	(4)	(5)		(6)	(7)	Substitution factors (8)
1.....	$34w$				=	+68	+115	$w = 2$
2.....		$24x$			=	+72	+77	$x = 3$
3.....			$18y$		=	+90	+54	$y = 5$
4.....				$14z$	=	+56	+40	$z = 4$
5.....						+286	+286	$a = b = c = f = 1$
6.....			c		=	+71	+3	$c = +71$
7.....				$-f$	=	−53	+4	$f = +53$
8.....						+18	+5	$w = x = y = z = 1$
9.....							+6	
10.....							+18	

The over-all check on lines 6 to 10, Table 9, is similarly made by considering a, b, c, and f as the unknowns and setting $w = x = y = z = 1$; that is, lines 32 to 35, Table 8, are considered as the simultaneous equations, with lines 1 to 4, Table 8, as the solutions.

As previously stated, the solutions of the auxiliary equations on lines 11 and 12, and on lines 24 and 25, Table 8, may be found practically by inspection. Considering a set of simultaneous equations such as is given in lines 1 to 4, Table 8, and its solutions on lines 32 to 35, it can be shown that the determinant formed from the coefficients of a, b, c, and f on lines 32 to 35 is the reciprocal of the determinant formed from the coefficients of w, x, y, and z on lines 1 to 4. Either determinant can be obtained from the other. An element a_{mn} of one determinant is equal to the cofactor of the element b_{nm} of the other determinant divided by the value of the latter determinant. The cofactors of a second order determinant are simply elements—in each case, simply the element not crossed out. It is also a simple matter to find the value of the determinant itself. The solution of the auxiliary equations can therefore be found practically by inspection.

As an illustrative example, reference is made to lines 9 and 10, Table 8, where the determinant formed by the coefficients of the auxiliary equations is: $\begin{vmatrix} 10 & 9 \\ 9 & 6 \end{vmatrix}$. The value of this determinant is $(10 \times 6) - (9 \times 9) = -21$.

The cofactor of the element 10 (which is a_{11}) is 6, and the element b_{11} of the reciprocal determinant is therefore $-\frac{6}{21} = -\frac{2}{7}$. The cofactor of a_{12}, or 9, is -9; the element b_{21} is $+\frac{3}{7}$; etc. The reciprocal determinant is, therefore, $\begin{vmatrix} -\frac{2}{7} & +\frac{3}{7} \\ +\frac{3}{7} & -\frac{10}{21} \end{vmatrix}$. The elements of this determinant are the variation coefficients on lines 11 and 12, Cols. 7 and 8.

The values shown in parentheses in lines 24 and 25, Cols. 9 and 10, are similarly obtained from the determinant formed from the coefficients on lines 21 and 22, Cols. 4 and 5.

In both cases, the other values are obtained by using the variation coefficients to obtain other solutions. For example, the set of constants from lines 21 and 22, Col. 8 (that is— $-22\,b$ and $-23\,b$), are substituted for c in line 24, Cols. 9 and 10. Thus, $y' = \left(-\frac{29}{42}\right)(-22\,b) + \frac{25}{42}(-23\,b) = +\frac{3}{2}\,b$, which is the value of y' in line 24, Col. 8. The primes are not indicated in Table 8 for simplicity.

Similarly, substitution of the constants -217 and -245 for c, line 25, gives $z' = +\frac{25}{42}(-217) + \left(-\frac{23}{42}\right)(-245) = +5$, which is the value of z' in line 25, Col. 6. The other values are computed in similar manner.

It will be noticed that the coefficients on lines 1 to 4, Table 8, occur in pairs, as they would in a practical design problem as a result of the Maxwell theorem of reciprocal deflections. The variation coefficients, lines 32 to 35, also occur in pairs and in the same order.

Accuracy of Computations

In practical design, the question of the number of significant digits to which the computations must be carried is a difficult one to determine. It is, however, a very important consideration from the point of view of time. The method of variation of coefficients makes the determination of the required accuracy a simple matter.

AMERICAN SOCIETY OF CIVIL ENGINEERS

Founded November 5, 1852

PAPERS

APPLICATION OF GEOLOGY TO TUNNELING PROBLEMS

BY ERNEST E. WAHLSTROM,[1] ESQ.

SYNOPSIS

Geological examination of tunnel sites prior to and during tunneling operations has become established procedure. The geologist should study and appraise carefully all surface and subsurface features having any bearing on the engineering problems associated with the drawing of the tunnel. Particular attention should be given to the following: (1) Internal structures, physical characteristics, and distribution of the rocks and overburden; (2) secondary structural features such as folds, faults, and joints; (3) chemical alteration of the rocks; and (4) the distribution and flow of ground water.

Suggestions for overcoming or minimizing difficulties presented by caving ground and other undesirable conditions in tunnels are given, and the causes and effects of caving in selected examples are discussed in detail.

INTRODUCTION

Geological investigations play an increasingly important part in the planning and completion of certain types of engineering projects. Geological examination of dam sites, bridge and building foundations, and tunnel sites prior to and during construction has become an established procedure that has yielded substantial or even spectacular returns in the form of safety and reduced costs of construction and maintenance.

The writer has spent considerable time as a consultant studying the geological features of several proposed water diversion tunnels, and in connection with this work has examined many existing tunnels and adits in an effort to discover and evaluate the various geological factors that are important in economical tunneling operations. Mine tunnels yield the most valuable data because, in general, these tunnels follow or cut across ore bodies formed where faulting, fracturing, and alteration are at a maximum. However, much pertinent in-

NOTE.—Written comments are invited for immediate publication; to insure publication the last discussion should be submitted by **March 1, 1948.**

[1] Dept. of Geology, Univ. of Colorado, Boulder, Colo.

formation has been obtained from railroad tunnels, drainage tunnels, and existing water diversion tunnels.

The Functions of the Geologist

The functions of the geologist in tunneling operations are manifold. Generally, he is called upon to examine the proposed site for a tunnel to determine if it is located to the best advantage. Such an investigation entails a geologic study of the portal areas and the surface over and adjacent to the line of the tunnel. The results of the study may lead to one of several conclusions:

(1) The tunnel is favorably situated and little or no difficulty should be experienced in driving it.

(2) There are geologic indications of the presence of sections of bad ground in the course of the tunnel. (It is the geologist's responsibility to indicate the probable location and nature of the bad ground in these sections.)

(3) The tunnel site is unfavorably situated, and the cost of driving the tunnel will be very high if not prohibitive.

If the location of the tunnel cannot be changed or if conditions demand that the tunnel be driven in spite of the unfavorable prognostication, then the geologist is faced with the responsibility of predicting to the best of his ability the extent and character of the various undesirable conditions that will be encountered.

Many tunnel sites are in areas partly or wholly covered by concealing alluvium or overburden. In covered areas the geologist must decide to what extent and by what methods the subsurface should be explored. Frequently, trenching or drilling is needed, which should be supervised by the geologist with attention to minute detail. Exploratory work of this type is expensive and the geologist generally must be satisfied with a bare minimum of information even though the facts he obtains do not begin to solve the host of unanswered problems that are associated with regions of thick or widespread blanketing deposits. Under certain conditions geophysical investigations yield pertinent information, and the geologist's duty is to determine which geophysical method or methods should be employed and to what extent.

Once the tunnel is started, the geologist should make periodic examinations of the completed sections and the face. He should maintain a detailed written account and a map showing the geological features of the tunnel as well as the day-by-day progress. The study of the rocks and structures encountered in the tunnel may lead to an increase in the accuracy with which the geologist may predict the changes in the rocks or structures beyond the tunnel face. The geologist may give advice as to the type and the amount of support needed in bad sections and as to the most effective manner of drilling and blasting at the face—giving due consideration to the relationship between the structure of the rock and the ease with which it is mined. In the event that unexpected difficulty is encountered because of extremely bad ground, he may offer counsel as to the best method of overcoming the difficulty.

The importance of a detailed geologic map of the tunnel cannot be overemphasized. This map not only should show the geologic structures and rocks encountered, but it also should serve as a lasting record to indicate the location

of bad sections, which may require attention many years after the tunnel is completed.

The geologist should act in an advisory capacity to the engineer in charge of the tunneling operation. Too often the geologist's advice does not carry the weight it should because either the engineer does not understand what the geologist is attempting to do or he feels that the geologist's predictions are too vague and indefinite. However, this situation is gradually becoming less serious and the engineer and the geologist are reaching an amicable understanding based on mutual respect and profitable cooperation. A geologist should not attempt to assert authority in any problems facing the engineer except those which bear directly upon, or are the outgrowth of, the geological study. On the other hand, the engineer generally is not qualified by training or experience to make a critical appraisal of the findings of a trained geologist and must accept the advice of the geologist as the best that can be offered.

Physical Characteristics of Consolidated Rocks

Consolidated rocks are those in which the constituent particles or fragments are bound together strongly enough to produce an aggregate with moderate to considerable strength. The rock or mineral components may be held together with a cementing material as in certain clastic sediments, or the contacts of the mineral grains may be interlocked or intermeshed as in igneous rocks and in most metamorphic rocks.

Certain rocks are massive or isotropic. The physical characteristics of these rocks, from the points of view of the geologist and the tunnel engineer, are the same in all directions within the rock. There is no preferred orientation of the mineral particles, and the ease of tunneling in such a rock is the same irrespective of the direction of the tunnel. In this category belong igneous rocks such as certain types of granite, sedimentary rocks such as certain limestones, and metamorphic rocks such as certain marbles and quartzites. Completely isotropic rocks are relatively rare.

Most rocks possess directional structures as a result of the parallel to subparallel orientation of many or most of the mineral particles. Such rocks are anisotropic and show distinct variations in physical properties in different directions. Consideration of the nature of the anisotropy of rocks is important to the tunnel engineer because it has a direct bearing on the cost of driving the tunnel.

In igneous rocks layered or linear structures are commonly present. If the rock contains "platy" minerals such as tabular feldspar or mica, there is a tendency for these minerals to rotate into parallel or subparallel positions during the intrusion and crystallization of the rock. The resulting formation is called "flow layering" or "platy structure." Rocks which show a well-developed platy structure have a gneissoid aspect and commonly contain flat, lenticular, dragged-out inclusions of foreign rocks called "schlieren." Generally, such rocks show a strong tendency to split or break along planes paralleling the flow layering, and they part or break with difficulty in directions at right angles to the layering.

Rocks containing minerals of prismatic or needle-like habit tend to develop

a unidirectional formation which is described as "linear structure" or "flow lineation." This formation results from the parallel to subparallel alinement of the prismatic minerals during the intrusion and crystallization of the rock. It is not uncommon to find both platy and linear structures in the same rock.

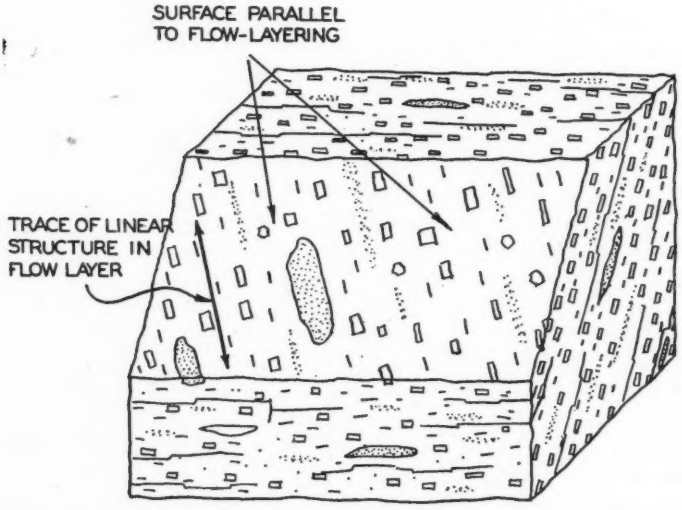

FIG. 1.—BLOCK DIAGRAM SHOWING FLOW LAYERING AND LINEAR STRUCTURE IN AN IGNEOUS ROCK; STIPPLED AREAS ARE INCLUSIONS OF FOREIGN ROCK

If both are present, the needles or prisms lie in the plane of the platy structure. Linear structure may be emphasized by the presence of elongated, spindle-shaped inclusions of foreign rocks. Igneous rocks in which linear structure is well-developed generally break easily parallel to the lineation and break with difficulty at right angles to the linear structure.

Fig. 1 is a block diagram of an igneous rock showing platy and linear structures. When the geologist describes these features, he generally gives the strike and dip of the platy structure and the direction of the trace of the linear structure on a horizontal plane. These data permit the easy calculation of the pitch angle of the flow lineation. Where flow lineation and flow layering are steeply inclined, lineation is of slight practical importance in the tunnel operation. However, the direction of the tunnel with respect to the flow layering merits careful consideration. A tunnel being driven across the flow layering probably will have the following characteristics: The face will advance relatively rapidly because in the blasting operation the rocks will break cleanly and easily away from the planes of weakness paralleling the flow layering. The walls, floor, and roof will tend to be rough and blocky. On the other hand, if the tunnel is parallel to the strike of steeply dipping flow layering, the forward progress of the tunnel will be slowed because the tunnel is parallel to a direction of maximum strength and toughness in the rock. The walls of the tunnel will probably be relatively smooth; the floor and roof, more or less irregular.

The irregularity of the walls increases with a decrease in the angle of dip of the layering.

In metamorphic rocks the layering is commonly called "foliation" and is well developed in gneisses and schists. A typical gneiss consists of alternating layers of granular rocks of differing mineral composition and physical properties. A schist, although foliated, is relatively homogeneous in its mineral composition. Slate is a fine-grained rock with a highly developed tendency to split into thin plates. Foliated metamorphic rocks generally tend to split most easily along planes parallel to the foliation.

The effect of foliated metamorphic rocks on the progress of the tunneling operation is even more pronounced than the effect of layering in igneous rocks—for the same reasons and with the same results. A tunnel at right angles to the strike of the foliation in general is constructed much more rapidly than is one following the foliation, although the tunnel is likely to be much more blocky and irregular. A tunnel following the strike of steeply dipping foliated rocks tends to cave in from the roof. The smoothness of the walls lessens and the tendency of the walls to cave increases as the dip of the foliation decreases, if the tunnel is following the strike of the foliation. Certain gneisses and schists are complexly folded and crumpled; and, where this is true, the difficulty of prediction of the relation between the ease of tunneling and the rock structure increases.

In one tunnel in Boulder County, Colorado, the cost of driving the tunnel was as much as 25% greater in the sections paralleling the foliation than in the sections cutting across the foliation. However, the overbreak in the latter was about 20% greater than in the first instance because of the irregularity of breakage along the walls and roof.

Typical conditions are illustrated in Fig. 2, which shows one tunnel cutting across steeply dipping, foliated rocks, and another following the foliation of steeply inclined layers. The latter condition should be avoided if possible.

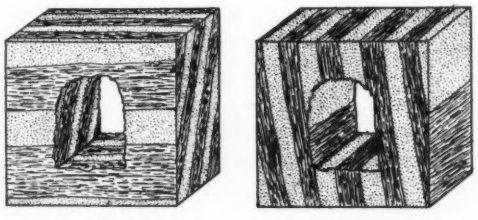

FIG. 2.—BLOCK DIAGRAMS SHOWING A TUNNEL IN STEEPLY DIPPING FOLIATED ROCKS
(a) Cutting Across Strike
(b) Parallel to Strike

In sedimentary rocks bedding or stratification may be conspicuous, but the strength of an individual layer parallel to the bedding is not much different from the strength across the bedding. However, if the rock is thinly stratified or consists of alternating thin layers of different composition (for example, thin-bedded alternating sandstones and shales), it acts in much the same manner as a foliated metamorphic rock. In sedimentary sections where shale is abundant, there is a pronounced tendency toward caving and slumping, and considerable supporting timber may be required as the tunnel is driven.

If a tunnel is driven through inclined layered rocks at right angles to their strike, an additional factor should be considered—that is, the direction in which

the tunnel is being driven relative to the dip of the layers. Preferably, the tunnel should be driven so that the layers will dip away from the heading. If this is done, drilling and blasting operations will be expedited because the cleavage in the rocks tends to produce an overhanging face rather than one which is sloping back toward the already completed section of the tunnel. This suggestion applies equally well to tunnels being driven in faulted or strongly jointed rocks. In general, the tunnel should be headed in the down dip direction of the planes of weakness in the rock.

These conclusions purposely are generalized. No attention is paid to the modifying effects of fracturing, alteration, and other features because these are considered separately. It is not claimed that the generalizations noted are without exception because various conditions have modifying effects.

Folds, Joints, and Faults

Folding in layered rocks requires consideration by the geologist because, if folded structures are present, a correct interpretation permits prediction of the attitudes of the layers in different sections of the tunnel. In foliated metamorphic rocks, particularly, the prediction of variation of the attitudes of the layers at the tunnel level may call for detailed surface studies and all the ingenuity, skill, and experience at the command of the geologist.

Actual or incipient fractures are present in all rocks. Fractures along which there has been little or no movement are called "joints." "Faults" are fractures along which there has been appreciable to considerable movement. Joints result from various causes, most important of which are expansion or contraction of the rock due to thermal, chemical, or mechanical causes, or fracturing of the rock in response to deformation by stresses accompanying movements in the outer part of the earth's crust. Faults show relative displacement of the rocks on either side of the fault plane. Fault displacements range from a few inches to several miles. A fault may be very narrow and sharply defined or may involve rocks in a zone hundreds of feet wide.

Joints and faults are a major cause of bad, caving ground in tunnels and deserve careful consideration. Joint surfaces commonly are rough and irregular in coarsely granular rocks, particularly if the joints developed as a result of shrinkage or decompression. Blocks bounded by such joints rarely cause trouble because friction along the rough surfaces prevents disengagement of blocks from the walls or roof of the tunnel. However, if the irregularities of the joint surfaces have been smoothed by slight movements between adjacent blocks or if the joints are smooth for other reasons, the tendency to cave is increased. Moreover, if water has permeated closely jointed rocks and has resulted in alteration and formation of clay minerals along the joints, a particularly bad, "running" or raveling type of ground is produced.

A careful study of a rock mass may show that several joint systems are present and, moreover, that certain of the joint systems are better developed than others. If possible, the tunnel should be located so that its direction is at right angles to the most prominent, most steeply inclined joint system. This course should be chosen because in drilling and blasting the ease of breaking the rock in the heading away from joints or "slips," is advantageous. Moreover, if a

tunnel follows a major joint system, the danger of overhead caving is constantly present. In igneous rocks showing flow layering it has been observed that a very prominent joint system commonly parallels the flow layering.

Engineers and geologists have developed a real fear of faults in tunnels, and justly so. Of course, a tunnel should not be driven through or along an active fault; but, fortunately, most faults are not active. The fear of encountering a fault in a tunnel should be justified or tempered by a detailed study of the faults in the region where it is proposed to drive the tunnel. Some faults offer no difficulty, others present distressing problems.

Among the faults which cause little or no trouble are those which show a sharp, clean offset of the rocks and are not accompanied by decaying alteration of the wall rocks. Certain faults or fault zones have served to localize the circulation of mineralizing solutions and examples are known where the substances deposited from the solutions have produced a tight, well-cemented rock stronger than the original rock. However, mineralizing solutions may produce the opposite effect, and a broad zone within and on either side of the fault may be converted into rotten, swelling, or squeezing ground. Alteration of feldspars to clay minerals or micaceous minerals often produces a weak, slippery rock which will cause considerable trouble.

Fault movements commonly develop selvages of weak, pulverized rock flour or "gouge." In wide fault zones where the gouge is present in weaving, criss-crossed, or braided fractures, extensive caving is likely to result. In some faults the rock are brecciated into loose, porous aggregates. Additional movements may cause the rounding of the angular fragments. Generally, such faults are filled with water and the combination of loose rock and water under hydrostatic pressure has caused more than one tunnel to be rerouted or even abandoned. Such fault zones were encountered in the Elton tunnel under the

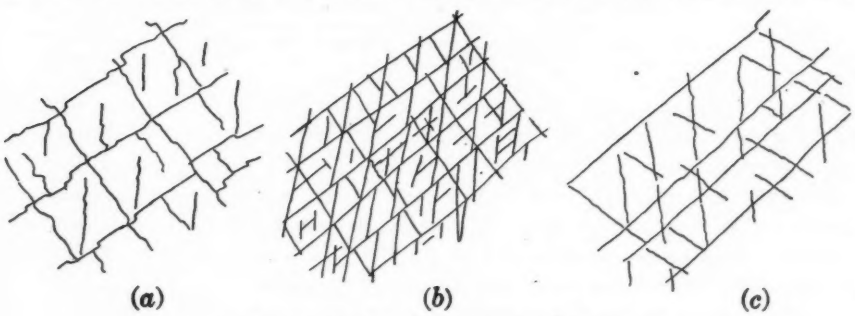

FIG. 3.—TYPICAL JOINT PATTERNS; JOINT SURFACES
(*a*) Rough and Irregular, Minimum Caving
(*b*) Smooth Surfaced, Maximum Caving
(*c*) Smooth and Rough, Considerable Caving

Oquirrh Range in Utah and in the Leadville drainage tunnel in Colorado. Fig. 3 shows typical joints and Fig. 4 shows several common types of faults.

In summary, it may be stated that a study of the joint systems and faults in an area where it is proposed to drive a tunnel should be included in the geological investigations over the line of the tunnel and in the area adjacent to it.

Altered Rocks and Swelling Ground

In the preceding section brief reference was made to altered rocks in the vicinity of joints and faults. It was suggested that alteration might produce effects of a serious nature in tunneling operations.

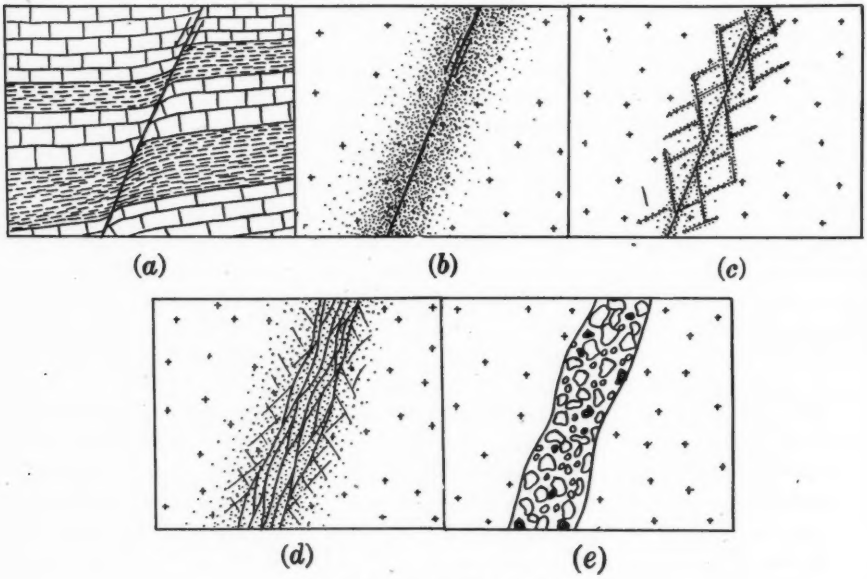

Fig. 4.—Types of Faults
(*a*) Clean Sharp Break, No Alteration of Wall Rocks
(*b*) Sharply Defined, No Subsidiary Fractures, Pervasive Alteration
(*c*) Sharply Defined, with Subsidiary Fractures, Localized Alteration
(*d*) Braided, with Subsidiary Fractures, General Alteration
(*e*) Open, Porous, Filled with Breccia

One of the minerals most susceptible to alteration in rocks is feldspar. Attack on feldspar by reactive solutions of surface origin or of deep-seated derivation may cause feldspar to be converted from a fresh, physically strong substance to a weak, pulverulent aggregate of clay minerals or micaceous minerals, and of fine-grained silica. This change, essentially a chemical one, generally is most pronounced in and near zones of intensive jointing or faulting, where altering solutions move with maximum freedom.

Grain size controls the amount of alteration to a certain extent. Fine-grained feldspathic rocks in general alter more readily than coarse-grained rocks, probably in part because fine-grained rocks may be more closely jointed than coarse-grained rocks and in part because the small size of each grain promotes more rapid, pervasive alteration. Fault movement may pulverize the rocks along the fault and cause the development of a multitude of tiny fractures in the rocks in the vicinity of the fault, thus producing ideal conditions for rock alteration. Moreover, faulting causes the minerals in the rock along the fault to be strained and, in general, strained minerals decompose more readily than do unstrained ones.

If the altering solutions are of deep-seated origin, alteration may not change the strength of the rock. For example, hydrothermal solutions commonly deposit condiderable silica in the wall rocks of fissures, and the silicified rock will stand in the tunnel as well or even better than the original rock. Sulfides deposited in fractures or in the wall rocks along fractures tend to oxidize on exposure so that mineralized areas containing abundant sulfides have a tendency to swell slowly and to slough after exposure to air.

Swelling or squeezing ground in tunnels is much to be feared. In squeezing rock the tunnel cross section is reduced by the plastic flow of very weak rocks in response to the pressure of the overlying rocks. Rocks that act in this manner generally are highly altered, are rich in clay minerals, and contain considerable water. The plasticity increases with the water content.

In swelling ground there is an actual increase in the volume of the rock resulting from hydration or chemical reaction or from a combination of these processes. Certain clay minerals and anhydrite have a remarkable affinity for water. If rocks containing these minerals are encountered in the tunnel, water from the atmosphere and other sources tends to be absorbed and swelling results. Tunnel sections have been studied where the rock when first encountered appeared to be reasonably fresh and unaltered; but, after being exposed for a short time, it began to swell and eventually was converted into a sticky, plastic mass of clay minerals. This same material broke down on the dump into an almost impalpable powder. Probably, the rock was partly altered at depth by hydrothermal solutions, but the confining pressure of the overlying rocks did not permit complete hydration and expansion. When the pressure was released by the tunnel, the rock, in a metastable state, rapidly reached a state of chemical equilibrium in response to the release of the confining pressure. Pressures as high as 20 tons per sq ft have been encountered in swelling ground.

The most spectacular example that has come to the writer's attention was the swelling of a dike of fine-grained porphyry cut by a tunnel in a gold mining operation. Within a few days after exposure, the originally fresh looking rock had almost completely filled the tunnel with sticky, relatively cohesive mud. In the Moffat tunnel water bore (in Colorado), a deceptively fresh looking granite irresistibly splintered Oregon fir timbers, 12 in. by 18 in. Many similar examples may be cited.

Rocks in a metastable condition may swell by chemical reaction as well as by simple hydration. It is an established principle that the release of pressure on a rock tends to produce a new mineral assemblage which is in equilibrium with the new environment. Fortunately, however, chemical changes in response to pressure changes in most rocks are so slow that they are of no importance in tunneling operations.

Unconsolidated Rocks

The range of composition, texture, and structure in unconsolidated rocks is extreme. Texturally these rocks grade from the finest muds to coarse aggregates such as are found in rock slides and bouldery glacial deposits. Unconsolidated rocks are characterized by the lack of interlocking contacts between adjacent grains or by the lack of a strong, binding cement or matrix. Some rocks,

as, for example, certain sandstones, have been converted into loose aggregates of mineral grains through the removal of the cement by dissolution.

In tunnel operations unconsolidated rocks generally are encountered at the portals, where the bedrock is blanketed with rock waste or alluvium. Loose sand and gravel, wet or dry, present a considerable obstacle as does loose material consisting of large, round, or angular boulders with no cementing material. The difficulty of tunneling through unconsolidated rocks consisting partly or largely of very fine-grained or clayey materials increases in direct proportion to the amount of water present. Dry or slightly moist clayey aggregates stand fairly well in portal areas; and, despite a slumping tendency, the walls and roof generally will stand long enough to permit support and lining to be set before caving starts. As the water content increases, however, the plasticity and mobility of the clay mineral aggregate increase, and considerable difficulty may be experienced in excavating and supporting such ground.

One of the most vexing situations arises when a tunnel is driven through water-saturated volcanic ash beds. In wet ash beds a mobile, gelatinous slurry is generally present which is held with only the greatest of difficulty. On the other hand, if the material is compact and dry, it offers little trouble except that it may swell on exposure to water.

A railroad tunnel near Leadville, Colo., was driven through dry, bouldery glacial till without mishap. The clayey matrix of the till was dry enough to have considerable strength and to serve as a reasonably strong binding medium. On the other hand, a near-by drainage tunnel driven through water-saturated glacial deposits encountered so many difficulties that part of the tunnel had to be abandoned and the cost of the tunnel greatly exceeded the most pessimistic cost estimates.

Ground Water

Prediction of ground-water conditions in tunnels is one of the most baffling problems confronting the geologist. Any prediction must be based on a consideration of the porosity and permeability of the rocks and the availability of ground water. Rapid movement of water in rocks generally is determined by the presence of connected open joints, fissures, or faults. It is a common experience of the tunnel engineer to drive through a fault containing little or no water and then to encounter a narrow crack or a section of jointed ground from which water issues in great volume and with destructive velocity. This phenomenon is explained in terms of relative permeability. Many faults, but not all of them, contain abundant clayey gouge which effectively prevents the rapid movement of water. Joints and small fractures, however, generally are not clogged with impermeable material and will permit the easy flow of water.

Faults characterized by abundant breccia and open spaces generally are permeable and contain ample water. Tunnels driven in limestone are likely to encounter underground caverns filled with water. The location of these caverns commonly is determined by the presence of fractures which have permitted the easy circulation of water with a consequent dissolution of the limestone.

A knowledge of the configuration of the ground-water table is useful; but, in general, the accurate determination of the depths of the upper surface of the saturated zone is obtained only by extensive drilling or geophysical study. In

compact, consolidated, relatively impermeable rocks, the configuration of the ground-water table is of no great significance, because impermeable rocks do not permit the circulation of water. In alluvium or any permeable or unconsolidated rock, however, the story is quite different.

The Tunnel Cross Section

Too little attention has been paid to the relationship between the tunnel cross section and the ease or difficulty with which rocks of the wall and roof cave. In certain tunnels, much time and expense can be saved if careful consideration is given to details of rock composition and structure and to methods of preventing or reducing the hazard of caving ground. It is the purpose of this section briefly to describe the nature of the caving and to suggest a remedy in certain selected examples. The generalizations do not apply to tunnel sections in squeezing or swelling ground.

The caving tendency is present in all tunnels, but the extent of caving depends on the strength and structure of the rocks. It is well known that in average caving ground the caving tendency does not extend for a great distance above the tunnel unless the ground is almost completely without strength and is of the free running type. Observations in hundreds of caved sections of rock tunnels indicate that the caved area commonly extends to a height above the roof nearly equal to the width of the tunnel. If the rock is highly fractured or altered, the caved section may involve a mass of rock above the tunnel roof with a height equal to as much as twice the width of the tunnel. As the caving proceeds, the tunnel tends to assume a cross section similar to that of a Gothic arch. When the arch is finally developed, it acts to support the walls and roof of the tunnel and to prevent further collapse. Except in shallow tunnels or in tunnels in free running ground the caving effects almost never extend to the earth's surface. In supporting the average tunnel roof, then, the maximum strength of the supporting structure, even in the worst kind of caving ground, in general need not exceed that necessary to support an arch-shaped block of ground above the tunnel roof having a maximum height equal to twice the width of the tunnel. For average rock the potential dead weight on the roof of the tunnel is considerably less than in very bad ground. However, this dead weight needs support only when the rock has small strength. In massive, unaltered rocks, the potential dead weight of the roof rocks is more than compensated for by the inherent strength of the rock, the rock load is reduced to zero, and little or no support is necessary. Also, if the caving is not allowed to begin, even in bad ground, the ground may be held by a relatively weak supporting structure because the caved arch can develop only by progressive slumping starting at or near the roof of the tunnel and extending upward.

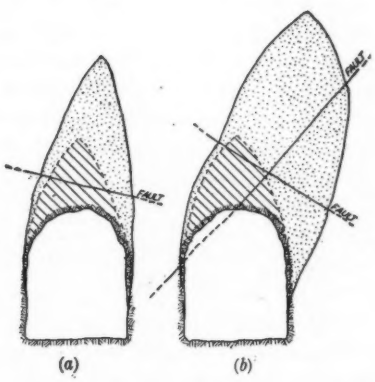

Fig. 5.—Tunnel Sections Showing How Faults May Affect the Caving Tendency

The shape assumed by the arch resulting from caving is to a certain extent a function of the geologic structures in the roof rocks. In general, the height of the caved area is greater in faulted and highly fractured or altered rocks than in rocks in which these features are absent or poorly defined. Fig. 5 shows the effects of faults on the upward extension of caving ground in two selected examples from tungsten mines in Boulder County, Colorado.

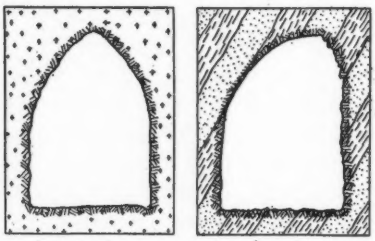

FIG. 6.—SUGGESTED TUNNEL SECTIONS FOR CAVING GROUND IN
(*a*) Relatively Homogeneous Unlayered Rock
(*b*) Inclined Layered Rocks

In driving tunnels through caving ground special attention should be paid to the tunnel cross section. Much time and effort can be saved by arching the roof in such a manner as to utilize what strength there is in the caving rock until supporting structures can be set in place. Obviously, it is not generally feasible to drive a tunnel in which the height is twice or three times the width; but, nevertheless, it is profitable to arch the roof somewhat and, if possible, to make the arch resemble in shape the Gothic-like arch that will result from caving. In nonlayered rocks the tunnel cross section is made as symmetrical as possible; but, in layered or foliated rocks, an asymmetrical arch may serve the purpose to better advantage.

Fig. 6 shows two suggested tunnel cross sections for caving ground. Of course, in spite of all precautions and in spite of the maintenance of an arched cross section, some ground will continue to cave. However, if this caving tendency is offset to even a slight degree, the precautions suggested will pay off in the more rapid forward advance of the tunnel and in the need for less temporary or permanent supporting structure. Of course, if the rock in the tunnel is strong, a cross section is preserved which will be most economical considering the purpose of the tunnel and the immediate requirements of the engineers driving it.

It may be argued that altering the cross section of the tunnel in response to changes in the rocks and rock structures might in the long run cost more than attempting to preserve a standard section and taking a chance on caving ground. However, even a slight concession in the direction of tailoring the tunnel cross section to the rocks will pay dividends. Thus, from a practical point of view, the actual cross section employed necessarily must be a compromise between what is wanted by the geologist and what is desired by the engineer.

In squeezing or swelling ground a circular cross section with closely spaced circular supporting ribs appears to overcome the difficulty to best advantage.

ACKNOWLEDGMENT

The writer wishes to express his appreciation to Prof. W. O. Thompson, Department of Geology, University of Colorado, in Boulder, who read the manuscript and offered several helpful suggestions.

AMERICAN SOCIETY OF CIVIL ENGINEERS

Founded November 5, 1852

PAPERS

THE GENERAL PRINCIPLES OF HIGHWAY TRANSITION CURVE DESIGN

BY JOHN JOSEPH LEEMING,[1] ESQ.

SYNOPSIS

The theoretical and experimental background of the published theory of highway transition curve design is explored in this paper. The writer shows (1) that the theory is fallacious in its disregard of the superelevation, and (2) that the experimental evidence produced for it is questionable.

A modified theory, called "the lateral force theory," is outlined. Experimental evidence is produced to show that the length of the transition curve is not a matter of great importance, and the proposal is made that it should be made a fixed proportion of the total length of the curve. It is also shown that the transition need not necessarily be spiral in form.

Simplified equations for the solution of the compound curve are given, based on the radius of the arc as parameter, together with a table of spiral functions. There is also a brief description of the proposed method of curve design, illustrated by a worked example.

1. INTRODUCTION

In designing transition curves the fundamental principle of the method described by John Oran Eichler, Assoc. M. ASCE, and Howard W. Eves[2,3] is, in the words of the authors,[4]

> "* * * that the rational way to achieve this transition [from tangent to curve] is to make the rate of gain of the 'centrifugal ratio,' P/W, constant throughout the curve. This is equivalent to the demand that the driver sharpen his curve by turning his steering wheel at a constant rate."

The symbol P in this context denotes the centrifugal force. In this theory it is also postulated that the rate of change of centrifugal force, for which W. H. Shortt's[5] symbol C will be used, should be the same for all curves. Mr.

NOTE.—Written comments are invited for immediate publication; to insure publication the last discussion should be submitted by **March 1, 1948.**

[1] County Surveyor, Dorsetshire, England.

[2] "Mathematical Examination of the Highway Transition Spiral," by John Oran Eichler and Howard W. Eves, *Transactions*, ASCE, Vol. 111, 1946, p. 959.

[3] *Ibid.*, p. 972.

[4] *Ibid.*, p. 960.

[5] "A Practical Method for the Improvement of Existing Railway-Curves," by W. H. Shortt, *Proceedings*, Inst. C. E., Vol. 176, 1909, p. 97.

Shortt, in England, suggested that this rate for C should be 1 ft per sec^3, claiming that this is the maximum rate that will pass unnoticed. The value has been accepted by others, although in the United States values of 2 ft per sec^3 and 3 ft per sec^3 have been proposed.

This theory gives the same length for a transition curve whether superelevation is present or not, although it is obvious that this factor must have some effect on a car.

Consideration of the foregoing from the viewpoint of first principles at once raises the question as to whether the rate of change of centrifugal force is the important effect for transition curve design. To find an answer it is necessary to consider the forces acting on a car traveling on a canted road.

2. The Lateral Force

Fig. 1 represents a car traveling on a curve of radius R, at a speed v, on a road canted at an angle α. The angle, and all forces, are considered to be positive as drawn. The centrifugal force is F_c. The reactions of the road on the car, parallel and normal to the surface, are designated by $j\,W$ and $n\,W$, respectively, and are called the lateral and normal forces. Then, resolving forces and eliminating W, the weight of the car,

$$j = \frac{v^2}{g\,R}\cos\alpha - \sin\alpha \qquad (1)$$

and

$$n = \frac{v^2}{g\,R}\sin\alpha + \cos\alpha \qquad (2)$$

in which g is the acceleration due to gravity. The two quantities, j and n, are called the lateral and normal ratios, respectively. They are pure numbers, provided the units used are mutually consistent.

The normal force, $n\,W$, is very little greater than W under road conditions. Its increase due to curvature is a very small increase in an already existing force, acting in a direction that cannot affect the stability of the car or the comfort of the passengers. Therefore, it may be neglected.

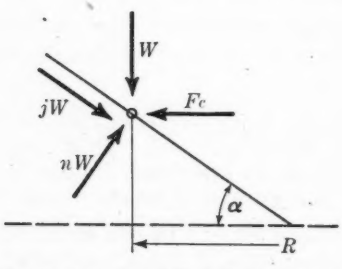

Fig. 1.—Forces on Car Traveling on a Superelevated Curve

The lateral force, $j\,W$, is the key to the situation. It is the sum of the components of the centrifugal force, and of the weight of the car, along the surface of the road and is the force which tends to cause the car to skid or to overturn, or which causes the passengers discomfort by urging them sideways in their seats. It is also the force that must be applied by the driver through the steering wheel, as it is the force he must overcome in turning his wheel to make the car travel around a curve.

The full implications of the lateral force as a factor in road design were dealt with at some length in a previous paper,[6] but the most important must

[6] "Road Curvature and Superelevation," by J. J. Leeming, *Road Paper No. 7*, Inst. C. E., October, 1942.

be mentioned in passing—namely, that a change in cant is equivalent to a change in curvature and that one change should never occur without the other.

At a certain speed, called the "hands-off speed," the lateral ratio j is equal to zero. At this speed the car steers itself around the curve, provided the steering is properly adjusted, and the driver need not touch the wheel at all. The centripetal force is acting still, but it is applied to the car by the superelevation. If the curvature and cant are changing together in due proportion (on a well-designed transition curve, for example), the wheel can be seen to turn itself if the proper speed is held. Alternatively, if the driver reaches the hands-off speed on a superelevated circular arc, he may then steer the car in a zigzag course by varying the speed without touching the wheel, which again will turn itself.

At any speed different from the hands-off, the driver must exert some force to follow the curve, but the direction as well as the magnitude of this force will be decided by whether the speed is more or less than the hands-off. If it is less he must steer away, if more he must steer toward, the center of curvature. Thus, the presence of the superelevation does make a very vital difference to the driver, and also to the passengers, who are affected similarly. Therefore, it is the rate of change of lateral force that is the important result and should be kept constant on a transition curve.

A significant effect follows from this consideration. In Eq. 1, cos α approximates to unity. Then, at any constant speed, the requirement for maintaining a constant hands-off speed is that

$$\frac{k}{R} = \sin \alpha \qquad (3)$$

in which k equals v^2/g. For this condition a circular arc is not essential. Any curve for which it is possible to keep the curvature and superelevation proportional will do, including the conventional transition spiral.

Similarly, the condition for maintaining a constant rate of change of latera force, Q, at constant speed is

$$Q = \frac{dj}{dt} = \frac{d}{dt}\left(\frac{k}{R} - \sin \alpha\right) \qquad (4)$$

A spiral, if correctly superelevated, will provide this condition, but its use is not essential and other types of curves can be used. Before discussing this matter, however, it is necessary to decide whether the rate of change of force is important in itself.

The principle of this section may be summarized in another manner. Assume the car to be traveling at a constant speed on a well-designed transition curve of spiral form. Then the rate of change of direction in plan will be proportional to C, the rate of change of centrifugal force, but the change will be made by two agencies. The first is by the rate of change of the superelevation. This is solely a function of road design, the driver has nothing whatsoever to do with it, and in most cases will be unaware of it. The second agency is the application of force by the driver at the steering wheel, and this is pro-

portional to Q, the rate of change of lateral force. In his turn, the road engineer has nothing to do with this.

The whole essence of the theory put forward in this paper is that this latter effect must be studied and allowed for in design, because it may cause variation between theory and practice. However well designed a curve may be according to spiral principles, if the driver does not follow a constant Q proportional to the value of C on which the spiral has been designed, he is not following the design curve. It is surely logical that the curve should be laid out to conform to the driver's practice; and, if he prefers, and habitually uses, some method of turning his wheel other than the constant rate expressed by constant Q, then the type of transition should be chosen to conform with his habits—even if this curve is not of spiral form.

3. The Rate of Turning the Steering Wheel

If the rate of application of force by the driver at the steering wheel is defined as "the rate of turning the wheel," the foregoing principle raises two further questions of fact, namely:

1. Does the driver turn his wheel at a constant rate on any given transition curve?
2. Does he turn it at the same rate on all transition curves?

These two questions are not the same, although they have not hitherto been separated. The first decides the shape of the transition curve, but does not involve any condition as to its length. The assumption that this question can be answered affirmatively has formed the case for the spiral curve, although it is seen that other curves can also satisfy the condition. The second part, if answered similarly, means that all transition curves must be designed to provide the same rate of change of force, at some chosen speed. The assumption that both questions can be answered affirmatively forms the basis of the previous theory.

Examination of the literature setting forth the case for this affirmative answer to the two questions shows that it rests entirely on Mr. Shortt. All other writers have merely repeated his conclusions; but his experiments were made on uncanted railway tracks, and some doubts may be felt at once on examining the original paper. Mr. Shortt stated that he had found that a rate of change of centrifugal force of 1 ft per sec^3 was the maximum which would pass unnoticed. This statement must involve the idea of comfort, and it has been so read in the past by most people. However, it is impossible for an observer to analyze his feelings so delicately and accurately as to be able to decide beyond doubt that the rate of change of force affected his comfort, and not the force itself. Nevertheless, there must be some value of the force that will cause discomfort, and the possibility that some lower value might cause some lesser degree of discomfort obviously is present. Mr. Shortt did not even discuss this possibility, nor did he state how he arrived at his conclusions so that the reader could judge for himself.

F. G. Royal-Dawson[7] applied Mr. Shortt's principle to roads, without ex-

[7] "Curve Design," by F. G. Royal-Dawson, E. & F. N. Spon, Ltd., London, 1932.

perimental proof of the validity of the transfer, and called the rate of $C = 1$ a "natural rate of turning." In this case the difficulty of the limit to the value of the force itself, previously referred to, was avoided by the expedient of stipulating a maximum value for the centrifugal ratio, usually 0.25. The superelevation was specified as some fraction of the centrifugal ratio, and it was then stated that the natural rate of turning should be adhered to, provided that the centrifugal ratio did not exceed this amount at some "design speed."

This argument is not very convincing, quite apart from the fact that it contains the fundamental fallacy of using C and the centrifugal ratio, ignoring the superelevation. The theory gives the same length for a transition curve, no matter what the value of the superelevation. However, Mr. Shortt himself stated, in his original paper,[5] that "* * * a curve which cannot be given superelevation is more in need of easing at the ends than one which can be superelevated," thus implying that superelevation does affect the problem, although, mathematically, he and his followers ignored this principle.

There has also been a large school among British engineers, both railway and highway, that has not accepted the principles of Messrs. Shortt and Royal-Dawson on practical grounds. Finally, H. A. Warren[8] carried out some experiments which threw doubt on the validity of the rate of change of force as the criterion for transition curve design. These experiments were on a small scale, and there was some question as to the accuracy of the work, by which C was derived from the plotted path of the car.

Thus, it was thought that there was need for experimental work on the rate of turning the wheel. The writer, therefore, undertook this work, in collaboration with A. N. Black. A preliminary report on the results has been published,[9] but a summary is given herein, which includes later work.

4. Reasons for the Experimental Procedure

The experimental technique had to be based on the previous theory, because, despite its shortcomings, this held the field, and because it had found some measure of acceptance. Therefore, the experiments were designed to answer the two questions:

(1) How do drivers actually take curves?
(2) What is the criterion of comfort on curves?

The two questions of Section 3 are included in the first of these latter two.

Since the force the driver applies at the wheel is proportional to j, the best method of investigating these questions is to measure j as directly as possible. That part of the centripetal force applied through the superelevation (that is, $W \sin \alpha$), being independent of the driver and imposed on him by the road designer, is irrelevant to the purpose. To make the conclusions general, it is also essential that the tests be carried out under the most natural conditions possible, to avoid distractions to the driver that would tend to influence his method

[8] "Experimental Transition Curves," by H. A. Warren and E. R. Hazeldine, *Journal*, Inst. Municipal & County Engrs., London, March, 1939, p. 1021.

[9] "Road Curvature and Superelevation: Experiments on Comfort and Driving Practice," by J. J. Leeming and A. N. Black, *ibid.*, December, 1944, p. 137.

of driving, and also that the tests should include as many cars and drivers as possible.

The method used by Mr. Warren was to trace out and survey the path of the car. This procedure, however, is open to a number of objections. In the first place it is inaccurate, because it involves some process of double differentiation of the path, to determine the centrifugal ratio, from which the superelevation must be deducted to find j. It is laborious in every way, and involves considerable apparatus as well as a technique which must infallibly distract the driver. Finally, the method can only be useful on a limited number of curves because of the labor involved—resulting from the fact that a detailed survey of the curve is necessary, since the superelevation must be known. Thus, the answer obtained would be limited to some extent, and would therefore be of less general application.

5. Experimental Procedure

From the considerations mentioned, it was decided that the ideal method would be to use a recording accelerometer. This instrument measures j directly, and Q can be determined by simply measuring the slope of the line on the record. Accordingly, such a device was designed and built, which, although simple to make with the materials available in wartime England, could fit into most cars.

The accelerometer consists of a 10-lb weight hung on springs from the baseboard of a strong wooden case. When the instrument is placed athwart the car, under the influence of the lateral force the weight shifts over against the springs, moving a stylus on the end of a long magnifying lever. This records the movement of the weight on a strip of metallic paper traveling over a drum driven by a phonograph motor. A fixed stylus provides a datum line.

This instrument was carried in cars traveling on ordinary journeys. Before starting, it was emphasized that the driver should not vary his usual driving methods in any way. When the car approached any curve thought suitable, the operator started the motor; and, for each curve, recorded its direction of curvature, the average speed of the car, and the comfort sensations of himself and the driver.

In the subsequent analysis, the individual curves were identified, and smoothed off to average straight lines if this could reasonably be done. For more than 90% of the curves it was found that the rate of change of force could be represented by sloping straight lines, and the curve as a whole by two such lines, with or without a length of straight line parallel to the datum—that is, of constant j—between them. Thus, the assumption that the driver turns his wheel at a constant rate on any given transition seems justified.

It soon appeared that there was considerable variability in a driver's practice. Records made on the same curve with the same car and driver at different times showed very marked differences even at the same speed, and Q varied between such wide limits as to make it quite obvious that there can be no natural rate of turning. In other words, the answer to question 2, Section 3, is that drivers do not always turn their wheels at the same rate. The variability also made it essential to use statistical methods, so that an

extensive statistical analysis was started and a large number of records were taken in a variety of vehicles.

No conclusive evidence could be found of wide differences in practice between drivers, considering the general variability and the inevitable differences in speeds. Most of the records were taken, perforce, in the British type of light car, but a fair range of commercial vehicles was also included. Among these latter was one of the largest and heaviest rigid wheel base vehicles made—an eight wheeler—loaded with 15 tons of bricks. In England its speed is limited by law to 20 miles per hr, but allowing for this it did not seem to show any marked difference from the smaller cars, nor did the one American car it was possible to include. It was not possible to take records in an articulated vehicle, nor in a fast, heavy, passenger vehicle.

A marked tendency was found for Q to vary with the value of j reached on any curve. This tendency can be expressed by the regression equation:

$$\bar{Q} = 1.3\, e^{3.5j} \ldots\ldots\ldots\ldots\ldots\ldots\ldots\ldots\ldots (5)$$

in which e is the base of natural logarithms, and $\bar{Q}$ is the mean value of Q observed, in feet per second^3. This expression refers to entrance transitions, and is independent of speed. The scatter was moderately wide, and the equation represents only a trend. Another way of expressing this principle is that the driver turns his wheel faster on entering a sharp curve than on entering a flat one. Values of Q as low as 1 ft per sec^3 were comparatively rarely observed, and then only on curves in the lower ranges of j.

Another fairly marked tendency was for the driver to use a definite proportion of the curve as transition, with an over-all mean of two thirds. The use of the all-transitional curve was comparatively rare. There was also a marked tendency for the exit transition to be slightly shorter than the entrance one, although the difference is not great enough to be of practical importance. This latter effect is probably related to the caster action of the steering, which helps the driver on the exit, and opposes him on the entrance. The proportion of transition tended to vary with the value of j reached, and with the speed of the car and the length of the curve, according to the regression equation:

$$\bar{p} = 0.34 + 6.3\, j - 25.5\, j^2 + 33.0\, j^3 - 0.002\, v + 0.007\, L/v \ldots\ldots (6)$$

In this expression, $\bar{p}$ is the mean proportion of transition observed (that is, the length of the two transitions combined, divided by the total length of the curve); v is the speed, in miles per hour; and L is the total length of the curve, in feet. For $j \geqq 0.1$, Eq. 6 gives values of p ranging from two thirds to one half. It should, however, be viewed with caution. Because of wartime restrictions in England, the data from which Eq. 6 was calculated do not include very large samples of curves taken at speeds higher than 50 miles per hr, although, since the completion of the regression analysis, more records at higher speeds have been made, and it appears unlikely that the conclusions will be materially altered.

The curves were also analyzed by class of road, including right-angle junctions and rotary intersections. This procedure gave a rough classification by the deviation angle of the curve, which appears to have little effect. This

analysis cannot be made with any confidence by measuring the deviation angle of the curves themselves, because it is not possible to decide on the driver's angle of approach to the curve, and the records gave reason to believe that this varies fairly widely.

In recording comfort, no attempt was made to separate the sensations due to the force or to its rate of change. The observer was merely asked if a sensation of curvature was felt or not, according to the groups: (*a*) Easy, when no sensation of curvature was felt at all; (*b*) comfortable, when a sensation of curvature was felt, but not thought uncomfortable; (*c*) slightly uncomfortable; and (*d*) uncomfortable. The effects of the force and of its rate of change were separated in the statistical analysis.

As was to be expected, there was considerable variation in the assessment of comfort, but the application of statistical methods showed that comfort depends mainly on j, although high rates of Q tended to reduce the tolerable values of j slightly. Speed does not appear to affect the assessment of comfort. No uncomfortable or noticeable value of Q could be detected at low values of j.

6. Conclusions from the Experiments

The main conclusions from the experiments are:

(1) The driver does appear to turn his wheel at a constant rate on any given transition.

(2) There is no such thing as a constant rate of turning applicable to all transitions. The driver tends to turn his wheel faster when entering a sharp curve than when entering a flat one. This conclusion is in accordance with general observation, but is in contradiction to the previous theory.

(3) There is some marked tendency for drivers to use about two thirds to one half of the curve as the transition.

(4) As far as comfort is concerned, j is the important effect; and Q is unimportant.

From these conclusions it appears that there is no sound reason for using the rate of change of force as the criterion of transition curve design, and it is suggested that this theory should be abandoned. On the other hand, it may be urged that some value of C or Q in the range of 1, 2, or 3 ft per sec^3 according to opinion, is a value which is safe or comfortable, and that its use is convenient. To counter this argument it is necessary to consider the mathematics of the compound curve.

7. The Compound Curve

Mathematics.—Although the condition for constant Q can be satisfied by curves of other types than the usual spiral, this curve is not unsatisfactory provided the superelevation is properly designed to comply with the conditions of Eq. 3. It is so simple and easy to use, and so familiar, that there is little to be gained by abandoning it. At the same time, the lemniscate has its advocates, and, if preferred, there is no reason whatever against its use. Nevertheless, the spiral will be used herein. Its mathematics have been dealt with elsewhere[2] at some length and need not be repeated. However, since it has

been shown that the rate of change of force is not important, it also follows that the length of the curve is relatively unimportant, and may be eliminated from the equations for the main dimensions of the curve, basing these on the

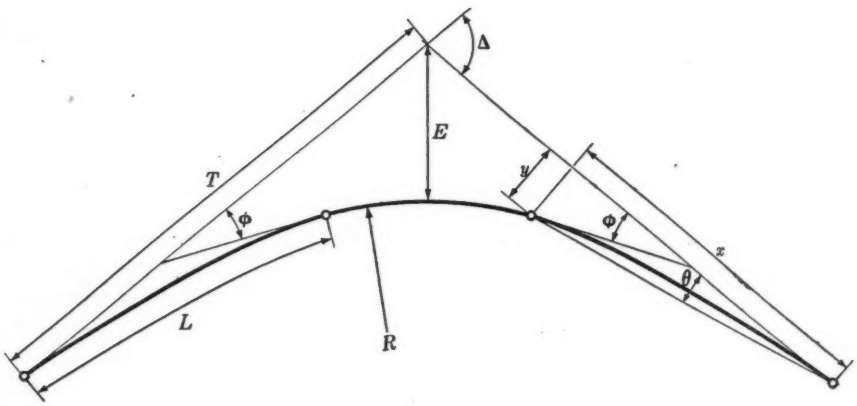

FIG. 2.—BASIC DIMENSIONS OF SYMMETRICAL CIRCULAR CURVE WITH TRANSITION SPIRAL AT BOTH ENDS

radius. These modifications were first published by I. Kursbatt[10] in a slightly different form.

Referring to Fig. 2,

$$x = N\,R \qquad (7a)$$

$$y = P\,R \qquad (7b)$$

$$T = R\left(M \tan\frac{\Delta}{2} + S\right) \qquad (8a)$$

$$E = R\left(M \sec\frac{\Delta}{2} - 1\right) = R\left[(M-1) + \left(\sec\frac{\Delta}{2} - 1\right) + (M-1)\left(\sec\frac{\Delta}{2} - 1\right)\right] \qquad (8b)$$

$$L = 2\,\phi\,R \qquad (8c)$$

$$\theta = \phi/3\text{—small correction} \qquad (8d)$$

and

$$\phi = \frac{p}{2\,(2-p)}\,\Delta \qquad (8e)$$

in which T is the total tangent distance from the point of intersection to the starting point of transition; E is the external distance from the intersection point to the nearest point of the curve; R is the radius at the point on the transition defined by the angle ϕ; x and y are the coordinates of the same point

[10] "Calculations for a Circular Curve with Transitions," by I. Kursbatt, *Highways, Bridges and Aerodromes*, London, February, 14, 1945, p. 226.

from the starting point of transition as origin:

$$N = 2\phi\left(1 - \frac{\phi^2}{5\,(2!)} + \frac{\phi^4}{9\,(4!)} - \frac{\phi^6}{13\,(6!)} \cdots\right) \quad \ldots\ldots\ldots (9a)$$

$$P = 2\phi\left(\frac{\phi}{3} - \frac{\phi^3}{7\,(3!)} + \frac{\phi^5}{11\,(5!)} - \frac{\phi^7}{15\,(7!)} \cdots\right) \quad \ldots\ldots\ldots (9b)$$

$$M = P + \cos\phi = 1 + \frac{\phi^2}{6} - \frac{\phi^4}{168} + \frac{\phi^6}{7{,}920} \cdots \quad \ldots\ldots\ldots\ldots (9c)$$

and

$$S = N - \sin\phi = \phi - \frac{\phi^3}{30} + \frac{\phi^5}{1{,}080} - \frac{\phi^7}{65{,}520} \cdots \quad \ldots\ldots\ldots (9d)$$

In these expressions, which apply whether or not a circular central arc is present, ϕ is in radians.

TABLE 1.—VALUES OF SPIRAL FUNCTIONS IN EQS. 8*d*, 8*e*, 9*a*, 9*b*, 9*c*, AND 9*d*

ϕ °	ϕ ′	N	P	M	S	$\left(\frac{\phi}{3}-\theta\right)$ (sec)
0	30...	0.017453	0.000051	1.000013	0.008727	....
1	0...	0.034905	0.000203	1.000051	0.017453	....
1	30...	0.052356	0.000457	1.000114	0.026178	....
2	0...	0.069805	0.000812	1.000203	0.034905	....
2	30...	0.087250	0.001269	1.000317	0.043630	....
3	0...	0.104691	0.001827	1.000457	0.052355	....
3	30...	0.122127	0.002487	1.000622	0.061079	....
4	0...	0.139558	0.003248	1.000812	0.069802	....
4	30...	0.156983	0.004110	1.001028	0.078524	....
5	0...	0.174400	0.005074	1.001269	0.087244	....
5	30...	0.191809	0.006139	1.001535	0.095964	....
6	0...	0.209210	0.007305	1.001827	0.104682	....
6	30...	0.226601	0.008572	1.002144	0.113398	1
7	0...	0.243982	0.009940	1.002486	0.122112	1
7	30...	0.261351	0.011409	1.002854	0.130825	1
8	0...	0.278709	0.012979	1.003247	0.139537	2
8	30...	0.296054	0.014649	1.003665	0.148244	2
9	0...	0.313385	0.016420	1.004109	0.156950	2
9	30...	0.330702	0.018292	1.004577	0.165654	3
10	0...	0.348004	0.020264	1.005071	0.174356	3
10	30...	0.365290	0.022336	1.005591	0.183054	4
11	0...	0.382560	0.024508	1.006135	0.191751	4
11	30...	0.399812	0.026780	1.006705	0.200444	5
12	0...	0.417045	0.029152	1.007299	0.209134	5
12	30...	0.434260	0.031623	1.007919	0.217821	6
13	0...	0.451455	0.034194	1.008564	0.226504	7
13	30...	0.468629	0.036865	1.009234	0.235184	8
14	0...	0.485783	0.039634	1.009930	0.243861	8
14	30...	0.502913	0.042502	1.010650	0.252533	9
15	0...	0.520022	0.045469	1.011395	0.261203	10
15	30...	0.537106	0.048535	1.012166	0.269867	11
16	0...	0.554166	0.051699	1.012961	0.278528	13
16	30...	0.571200	0.054961	1.013781	0.287185	14
17	0...	0.588209	0.058322	1.014626	0.295837	15
17	30...	0.605191	0.061780	1.015497	0.304485	17
18	0...	0.622146	0.065335	1.016392	0.313129	18
18	30...	0.639072	0.068988	1.017311	0.321767	20
19	0...	0.655969	0.072738	1.018256	0.330401	21
19	30...	0.672836	0.076584	1.019226	0.339029	23
20	0...	0.689673	0.080527	1.020220	0.347653	25
20	30...	0.706479	0.084566	1.021240	0.356271	27
21	0...	0.723252	0.088702	1.022282	0.364884	29
21	30...	0.739993	0.092933	1.023351	0.373492	31
22	0...	0.756700	0.097260	1.024444	0.382093	33
22	30...	0.773373	0.101682	1.025561	0.390689	35
23	0...	0.790010	0.106198	1.026703	0.399279	38
23	30...	0.806612	0.110810	1.027870	0.407863	40
24	0...	0.823178	0.115515	1.029061	0.416441	43
24	30...	0.839706	0.120315	1.030276	0.425013	46
25	0...	0.856196	0.125208	1.031516	0.433578	48

Table 1 gives these spiral functions to six decimal places, for angles to 25° at half degree intervals. Corrections for the polar deflection angle in Eq. 8*d* are also given, although this is usually negligible for small values of ϕ.

The second form of Eq. 8*b* will be found rather simpler for calculation purposes, in spite of its more complicated appearance.

In Eq. 8*e*, if $p = \frac{2}{3}$, $\phi = \Delta/4$, and if $p = \frac{1}{2}$, $\phi = \Delta/6$.

The Practical Problem.—Under practical road conditions the engineer will have two tangents, meeting at an angle Δ, which will have been measured on the ground. If there is unlimited room available, no complications are involved; the curve can be made as flat as desired. Frequently, however, some obstacle or other restricts either the exterior distance E (Fig. 2), or the tangent distance T. The problem is to make the best use of the room available.

Whichever of these distances is limited can be substituted in Eq. 8*a* or Eq. 8*b* to find R, provided the value of ϕ is known so that the values of the appropriate functions may be determined from Table 1. When $\phi/\Delta = \frac{1}{2}$ the curve will be all-transitional; and, as ϕ/Δ decreases, R increases, with a corre-

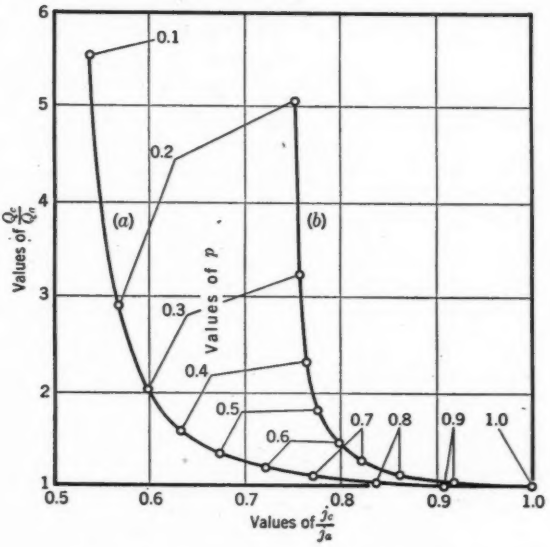

FIG. 3.—PLOT OF $\frac{Q_c}{Q_a}$ VERSUS $\frac{j_c}{j_a}$ FOR $\Delta = 60°$ AND
(*a*) Fixed T
(*b*) Fixed E

sponding reduction in j, but the length of the transition decreases, thus increasing Q. Finally, when $\phi/\Delta = 0$, the curve is a circular arc without transitions and R is a minimum for the conditions, but Q will be infinite.

If the superelevation is assumed to be proportional to the centrifugal ratio, a quite usual practice, and if the value of j on any compound curve is denoted as j_c and that for the corresponding all-transitional curve as j_a, with the corresponding values of Q denoted as Q_c and Q_a, the following expressions can be written for the ratios between these quantities: For fixed E,

$$\frac{j_c}{j_a} = \frac{M_\phi \sec \Delta/2 - 1}{M_{\Delta/2} \sec \Delta/2 - 1} \quad \ldots\ldots (10a)$$

and, for fixed T,

$$\frac{j_c}{j_a} = \frac{M_\phi \tan \Delta/2 + S_\phi}{M_{\Delta/2} \tan + S_{\Delta/2}} \quad \ldots\ldots (10b)$$

For either condition,

$$\frac{Q_c}{Q_a} = \left(\frac{j_c}{j_a}\right)^2 \frac{\Delta}{2\phi} \quad \ldots\ldots (11)$$

The symbols M_ϕ and S_ϕ represent the values of M and S for the value of ϕ used, and $M_{\Delta/2}$ and $S_{\Delta/2}$, those for $\Delta/2$. These expressions depend only on the relative values of the angles, and express the ratio of the value of j or Q on any

compound curve on which E or T is fixed to that on the all-transitional curve for the same conditions. Fig. 3 gives curves for Q versus j for $\Delta = 60°$, although the effect of Δ is so small that they may be considered approximately general. In effect, these curves show the effects on j and Q caused by the various values of ϕ/Δ chosen by the engineer, although the latter has been expressed as a proportion of transition.

TABLE 2.—SUGGESTED RATES OF SUPERELEVATION

Radius, in feet	Superelevation	
	1 on:	Feet per foot
1,200[a]...	14½	0.069
1,400....	17	0.059
1,600....	19	0.053
1,800....	22	0.045
2,000....	24	0.042
2,500....	30	0.033
3,000....	36	0.028
3,500....	37	0.027
4,000....	38	0.026
4,500....	39	0.026
5,000....	40	0.025
7,500[b]...	48[b]	0.021[b]
>7,500....	....[c]	....[c]

[a] 1,200 ft or less. [b] 5,000 to 7,500 ft, superelevation for 1 on 40 to 1 on 48, or 0.025 ft per ft to 0.021 ft per ft, according to the nature of the material. [c] Normal camber or crossfall retained.

From Fig. 3 it is evident that the higher proportions of transition greatly increase j without reducing Q to any appreciable extent. The difference in Q between the all-transitional curve and one with 0.9 of transition is negligible, in the ratio of 1.00 to 1.03, although the difference in j is more important, in the ratio of 1.00 to 0.92. Thus, there is no justification whatever for the all-transitional curve. It merely increases j unnecessarily.

Thus, the case against a fixed rate of C or Q is clinched. No matter what rate is chosen, for a fixed E or T, and fixed speed, long transitions and eventually all-transitional curves are demanded as the room available decreases. As it decreases further, the ridiculous demand may be made that the transition be longer than the whole curve, even at low values of j. This argument is usually countered by ruling that in such cases the "design speed" must be reduced—making nonsense of the whole matter, because this theory completely ignores the driver, who cannot be expected to observe the "design speed," as he is, of course, completely unaware of its existence. It appears, in fact, that the driver slows down to reduce j and not to reduce Q and that, if a design speed is specified, it should be on the basis of j and not of Q. It is therefore suggested that the rate of change of force should be abandoned as a method of transition curve design.

8. ALTERNATIVE METHOD OF TRANSITION CURVE DESIGN

Although this paper only purports to deal with general principles, some new procedure must be suggested, since the effect of the argument is that the previous theory should be abandoned.

For the moment, the "proportion rule" first proposed elsewhere[9] is favored. This rule states that curves should be designed to have about two thirds of their length transitional, although the writer now inclines to the belief that one half is a better proportion. The exact length of the transition is not, however, a matter of extreme importance, so that ϕ may be taken to the nearest half degree.

The proposed procedure is illustrated by the following example, which is, however, only intended to demonstrate the method. The values used are not

put forward as recommendations, nor is the example intended to show that the rule is sound. The required information includes:

a. The maximum speed for which the road is intended, say (for purpose of example only), 80 miles per hr;

b. The maximum value of j considered safe at that speed, say, 0.15;

c. The rates of superelevation[11] to be used, say, as shown in Table 2; and

d. The proportion of transition, say, two thirds, so that $\phi = \Delta/4$, taken to the nearest half degree.

By substituting the foregoing known values in Eq. 1, the minimum permissible radius of curve will be found, in this example, to be 2,300 ft.

Next, the deviation angle, Δ, and the greatest lengths of T and E allowed by the topography are measured on the site. For the example, let $\Delta = 22° 38'$, and let the maximum possible $E = 55$ ft. Then $\phi = 5° 30'$; and, from Eq. 8*b*, using Table 1 to obtain the values of the spiral functions, $R = \dfrac{55.00}{0.001535 + 0.019828 + 0.000030} = 2{,}570.93$ ft. This value is permissible, resulting in $j = 0.13$, and a superelevation rate of 0.04 ft per ft. If not permissible, some reconsideration of the alinement is necessary.

From Eq. 8*a*, $T = 2{,}570.93\ (1.001535 \times 0.200122 + 0.095964) = 762.01$ ft, and $L = 2{,}570.93 \times 0.191986 = 493.58$ ft. The spirals may be set out in any convenient manner, the ten-chord method being especially suitable. The method has the merit of extreme simplicity.

9. Conclusion

The whole argument of this paper runs counter to established practice. It is submitted, nevertheless, that the rejection of the current theory is based on sound reasoning supported by experimental analysis, and that the new concept is far more in accord with common sense and with everyday observation. The objection will no doubt be raised that it takes the whole problem back to rule-of-thumb days, and that it is vague and unscientific. However, it does appear that vagueness is inherent to the subject, and that past theoretical and mathematical treatment is not justified by facts.

Far from the length of a transition curve being "a theoretically determinable quantity," as one of the enthusiasts for the previous theory has claimed, it varies widely at the driver's whim. Therefore, there seems to be little object in going to great lengths to find it. The principal aim is to arrive at some reasonable compromise. This, it is claimed, the proportion rule accomplishes.

10. Acknowledgments

The author's most grateful thanks are due to Mr. Black and to Mr. Kursbatt.

[11] "Memorandum on the Layout and Construction of Roads," *Memorandum No. 575*, Ministry of Transport, London, 1943, p. 7.

AMERICAN SOCIETY OF CIVIL ENGINEERS

Founded November 5, 1852

PAPERS

ANALYSIS OF STEPPED-COLUMN MILL BENTS

BY DANIEL S. LIN,[1] M. ASCE

SYNOPSIS

The "moment-distribution" technique is applied to the analysis of stepped-column mill bents, in this paper. Curves for obtaining the necessary distribution coefficients and the fixed-end moments are included. The method permits evaluating the relative resistance, to horizontal forces, of columns having different stiffnesses due to length, size, or other factors. Several examples of two-column and three-column bents are included to describe the method fully.

Although this method will require more time than that of obtaining moments from an assumed point of contraflexure, the additional time would seem to be justified, because of the difficulty in estimating the location of such a point of contraflexure accurately for stepped columns.

I. INTRODUCTION

In the design of mill buildings, especially where the crane clearances require considerable height, the horizontal forces from wind and crane thrust are important factors. In short buildings, it is simple enough to transmit these forces to the ground through a bracing system to the braced end bents of the building. However, with the trend toward larger and larger industrial buildings, the length increases so that one or more expansion joints are required; and horizontal forces must be resisted by each individual bent. Often, as a result, the bending stresses in the columns become greater than the direct stresses, and the "column" essentially becomes more of a vertical beam than a column from the standpoint of stress analysis.

The simple and more familiar method of analysis for such "columns" is to determine the bending moments from an assumed point of contraflexure. With a column of constant section from top to bottom, the location of this point can be assumed with reasonable accuracy under any set of assumptions regarding the base and top fixations. However, for a column supporting a crane runway, a "stepped section" is considerably more economical, in most cases. Immedi-

NOTE.—Written comments are invited for immediate publication; to insure publication the last discussion should be submitted by March 1, 1948.

[1] Associate of Paul S. Calkins, Cons. Engr., Detroit, Mich.

ately, the question arises as to the location of the point of contraflexure; inaccuracy as to this assumption may cause considerable error in the final result.

It is hoped that this paper will present a more satisfactory method for the analysis of stepped-column mill bents. The loadings given in the examples are used as illustrations of the method, and not as recommendations. Admittedly, these loadings are not the nearest approach to the probable applied conditions, but they do illustrate the various types of design loads as used by designers.

The method of successive approximations, or so-called "moment distribution," is used without explanation, to determine the true end moments, since this method is probably familiar to most engineers and can be found in various textbooks and reference books.

In particular, the writer has used a set of unpublished mimeographed notes, by L. C. Maugh, Assoc. M. ASCE, entitled "The Analysis of Continuous Framed Structures," as a reference in preparing this material. The discussion of the basic theory is given briefly herein as Example 1. For a more detailed discussion of the theory, reference can be made to "Statically Indeterminate Structures,"[2] also by Professor Maugh.

II. General Conditions and Design Assumptions

With the increasing necessity for the greatest economy in the use of steel and the resultant use of higher working stresses, it has been more than ever important to eliminate as many uncertainties as possible in structural design. Since these columns are essentially beams, they should be treated as such. The analysis of a beam of variable moment of inertia is generally understood; it is not difficult, although the work involved does require considerable time and is somewhat tedious. The writer used this general method, with good results, on several industrial buildings erected during World War II. To save time in the analysis of beams of variable moment of inertia, a series of curves is presented which reduces the work to that required for a continuous beam of two spans with the translation of one joint. By the well-known method of successive approximations introduced by Hardy Cross, M. ASCE,[3] the analysis is not a lengthy problem.

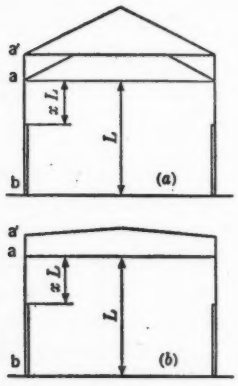

Fig. 1

As with any design problem, certain assumptions must be made to simplify the problem and to save time. Some of these assumptions are known to be erroneous. However, the error involved is so small as to be safely ignored. In this method of analysis the following assumptions were made (see Fig. 1):

a. Hooke's law applies.

b. The principle of superposition applies.

[2] "Statically Indeterminate Structures," by L. C. Maugh, John Wiley & Sons, Inc., New York, N. Y., 1946.

[3] *Transactions*, ASCE, Vol. 96, 1932, p. 1.

c. In the deflection of a bent, point a and point a′ move the same amount—that is, point a′ is always directly above point a. (Unless the truss is subject to considerable deflection, this is a safe assumption.)

d. The column is simply supported at points a and a′—that is, the truss or knee brace connections create no effective fixity at these individual points. Since the column is usually quite rigid in relation to the truss or knee brace members, this is a safe assumption.

e. Both columns deflect the same amount—that is, any change in length of roof trusses caused by horizontal forces is too small to be significant.

f. The relation between the moments of inertia of the upper and lower parts of the column is known. (This relation can be approximated readily and quite closely after some experience; but if the preliminary design indicates too large an error the analysis can be corrected quickly with a new ratio of moments.)

(It can be argued that, in effect, the column is fixed at the top. If points a and a′ are close together, it is true that there can be little deflection between these points; but, if this distance is larger, the deflection may be considerable. Assumption *d* is more general and therefore safer than the assumption of full fixity at point a.)

The explanation of such a design method is shown more readily by examples, and this device will be used in this paper. For greater ease in illustrating the principles of the method, the following loading conditions were used in the examples although it is realized that this procedure does not represent true wind action:

(1) Beam bending in a column, from wind, occurs entirely in the windward column;
(2) Wind force is assumed uniformly distributed over the entire length of a column; and
(3) Horizontal force from a crane is applied entirely to one column of a bent.

Symbols and Notation.—The letter symbols in this paper are defined where they first appear, in the text or by illustration, and are assembled for convenience of reference in Appendix I.

III. Illustrative Example

Example 1.—Consider a column of a symmetrical bent similar to those in Fig. 1 and fixed at the base. If I is the moment of inertia of the main section of the column and I_o is that of the smaller (reference) section above the step, let $I/I_o = 8$ and $x = 0.3$. The general slope-deflection equations, for moments in a beam (ab, Fig. 1) with a variable moment of inertia, are:

$$M_{ab} = \frac{E I_o}{L}\left[C_1 \theta_a + C_2 \theta_b - (C_1 + C_2)\frac{\Delta}{L}\right] + M_{f,ab} \quad \ldots\ldots (1a)$$

and

$$M_{ba} = \frac{E I_o}{L}\left[C_2 \theta_a + C_3 \theta_b - (C_2 + C_3)\frac{\Delta}{L}\right] + M_{f,ba} \quad \ldots\ldots (1b)$$

In Eqs. 1, E is the modulus of elasticity; C is the slope-deflection coefficient; θ is the angular rotation, with subscripts a or b denoting point of rotation; Δ is the relative displacement of one end of the beam to the other end; M_f is the fixed-end moment; M_{ab} equals moment in joint a of member ab; and M_{ba} equals moment at joint b of member ab. If the beam is hinged at point a, moment M_{ab} is zero. Solving for θ_a in Eq. 1a and substituting in Eq. 1b:

$$M_{ba} = \frac{E\,I_o}{L}\left(C_3 - \frac{C^2_2}{C_1}\right)\left(\theta_b - \frac{\Delta}{L}\right) + M_{f,ba} - \frac{C_2}{C_1}M_{f,ab} \ldots\ldots (2a)$$

Similarly, if the beam is hinged at point b:

$$M_{ab} = \frac{E\,I_o}{L}\left(C_1 - \frac{C^2_2}{C_3}\right)\left(\theta_a - \frac{\Delta}{L}\right) + M_{f,ab} - \frac{C_2}{C_3}M_{f,ba} \ldots\ldots (2b)$$

The relation between the end rotations and the end moments can be determined by obtaining B_{aa} and B_{ba}, the angles of rotation at joints a and b, respectively, caused in each case by a unit moment at joint a; and B_{ab} and B_{bb}, the angles of rotation at joints a and b, respectively, caused by a unit moment at joint b (Fig. 2). For any end moments M_{ab} and M_{ba}, then:

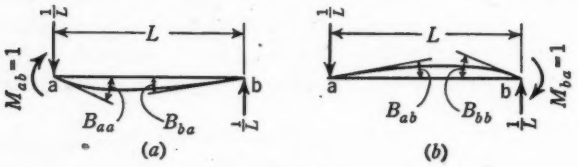

FIG. 2

$$M_{ab} = \frac{B_{bb}}{\beta}\theta_a + \frac{B_{ba}}{\beta}\theta_b \ldots\ldots (3a)$$

and

$$M_{ba} = \frac{B_{ba}}{\beta}\theta_a + \frac{B_{aa}}{\beta}\theta_b \ldots\ldots (3b)$$

in which

$$\beta = B_{aa}\,B_{bb} - B^2_{ba} \ldots\ldots (4)$$

Comparing Eqs. 3 with Eqs. 1, with $\frac{E\,I_o}{L} = K_o$:

$$C_1\,K_o = \frac{B_{bb}}{\beta} \ldots\ldots (5a)$$

$$C_2\,K_o = \frac{B_{ba}}{\beta} \ldots\ldots (5b)$$

and

$$C_3\,K_o = \frac{B_{aa}}{\beta} \ldots\ldots (5c)$$

In Eqs. 5, $\Delta = 0$ and fixed-end moments are temporarily ignored. Having determined the coefficients, the fixed-end moments can be determined for any applied loads by computing the angular rotations α_a and α_b of the end tangents of the beam considered simply supported. The fixed-end moment must pre-

vent any rotation of the end tangents; therefore,

$$M_{f,ab} = C_1 K_o (-\alpha_a) + C_2 K_o (-\alpha_b) \ldots\ldots\ldots\ldots\ldots (6a)$$

and

$$M_{f,ba} = C_2 K_o (-\alpha_a) + C_3 K_o (-\alpha_b) \ldots\ldots\ldots\ldots\ldots (6b)$$

The angles in Eqs. 5 can readily be determined by the conjugate beam method, by determining the reactions of a beam loaded with the $\frac{M}{I}$-diagram (since E is constant). Figs. 3(a) and 3(b) illustrate the use of that method for this example. An end moment of ten units is applied at end a and the length L is divided into ten units. For the $\frac{M}{I}$-diagram applied as a load the reaction at end a is $23.329/I_o$, and at end b it is $5.233/I_o$. Since these values are for an

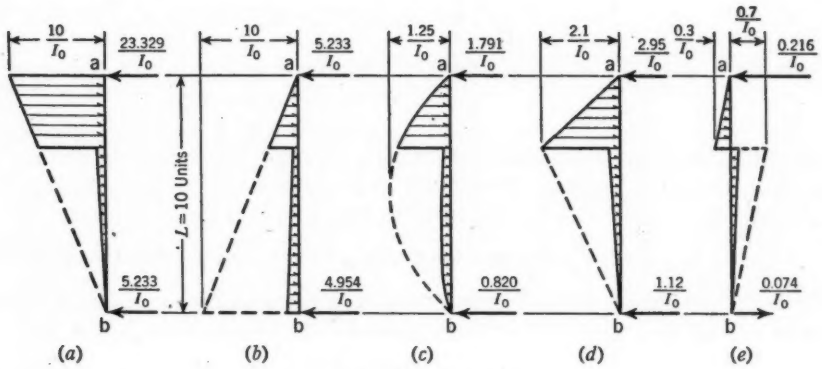

FIG. 3

end moment of ten units and a length of ten units, the end rotation B_{aa} at end a is $\frac{23.329}{100} \times \frac{L}{I_o}$ or $0.23329 \frac{L}{I_o}$; and the rotation B_{ba} at end b is $0.05233 \frac{L}{I_o}$. In the same way, by applying an end moment of ten units at end b it is found that $B_{ab} = 0.05233 \frac{L}{I_o}$ and $B_{bb} = 0.04954 \frac{L}{I_o}$. Substituting these values in Eq. 4: $\beta = \frac{0.23329}{K_o} \times \frac{0.04954}{K_o} - \left(\frac{0.05233}{K_o}\right)^2 = \frac{0.00881}{(K_o)^2}$. Then (see Eq. 5$a$) $C_1 K_o = \frac{0.04954}{K_o} \times \frac{(K_o)^2}{0.00881}$. The stiffness ratio K_o cancels and $C_1 = 5.63$. Likewise $C_2 = \frac{0.05233}{0.00881} = 5.95$; and $C_3 = \frac{0.23329}{0.00881} = 26.50$. The carry-over factor from end a to end b is $\frac{C_2}{C_1} = \frac{5.95}{5.63} = 1.06$; and from end b to end a the carry-over factor $\frac{C_2}{C_3} = \frac{5.95}{26.50} = 0.22$. Substituting these values in Eqs. 6:

$$M_{f,ab} = K_o (-5.63 \alpha_a - 5.95 \alpha_b) \ldots\ldots\ldots\ldots\ldots (7a)$$

and

$$M_{f,ba} = K_o\,(-\,5.95\,\alpha_a - 26.50\,\alpha_b) \ldots\ldots\ldots\ldots\ldots\ldots (7b)$$

As shown in Fig. 4, the loadings on this column which produce bending are of three types—a uniform load of 0.5 kips per ft, a concentrated load (at the change in section) of 8 kips, and an eccentric load of 120 kips. The upper load of 32 kips will also produce some bending, particularly in the upper section; however, this will not be especially severe, since it is near the center line of the lower section. In this example, clockwise resisting moments are designated "plus (+)" and counter-clockwise resisting moments, "minus (−)"; the number within a box indicates the ratio of the moment distributed to that side of joint; the number at an arrow between joints indicates the "carry-over" to the adjacent joint in the direction of the arrow; and, at the completion of single distribution at a joint, a single line is drawn under the numbers and after the final distribution (unbalanced factor of negligible size) a double line is drawn under the numbers and a summation is made.

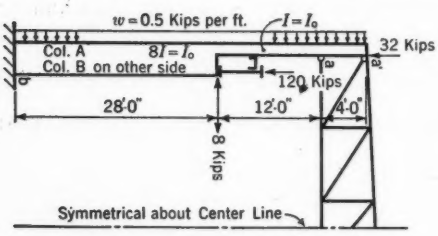

FIG. 4

Fig. 3(*c*) shows the $\frac{M}{I}$-diagram for a unit uniform load applied to a beam of length L. As before, the end reactions give the end rotations or, in this case, angles α_a and α_b. Substituting the values of the end reactions in Eqs. 7:

$$M_{f,ab} = 0.0516\,W\,L \ldots\ldots\ldots\ldots\ldots\ldots (8a)$$

For $W = 20$ kips and $L = 40$ ft, Eq. 8*a* yields $M_{f,ab} = 0.0516 \times 20 \times 40 = 41.3$ ft-kips; and $M_{f,ba} = 0.1126\,W\,L = 0.1126 \times 20 \times 40 = 90.1$ ft-kips.

Fig. 3(*d*) shows the $\frac{M}{I}$-diagram for a unit load applied 0.3 L from end a; thus:

$$M_{f,ab} = 0.0994\,P\,L \ldots\ldots\ldots\ldots\ldots\ldots (8b)$$

For $P = 8$ kips and $L = 40$ ft, Eq. 8*b* yields $M_{f,ab} = 0.0994 \times 8 \times 40 = 31.8$ ft-kips and $M_{f,ba} = -\,0.1210\,P\,L = -\,0.1210 \times 8 \times 40 = -\,38.7$ ft-kips.

For a unit moment applied 0.3 L from end a, Fig. 3(*e*) shows the $\frac{M}{I}$-diagram. Again substituting in Eq. 7:

$$M_{f,ab} = +\,0.166\,M_x \ldots\ldots\ldots\ldots\ldots\ldots (8c)$$

For $M_x = 120$ ft-kips Eq. 8*c* yields $M_{f,ab} = 0.166 \times 120 = +\,19.9$ ft-kips and $M_{f,ba} = +\,0.325\,M_x = +\,39.0$ ft-kips.

For the column under consideration—with $C_1 = 5.63$; $C_2 = 5.95$; and $C_3 = 26.50$—the carry-over ratios from points a to b and from points b to a, respectively, are: $\frac{C_2}{C_3} = \frac{5.95}{26.50} = 0.22$; and $\frac{C_2}{C_1} = \frac{5.95}{5.63} = 1.06$. Computations

for the distribution factors r at point b, Fig. 4, are shown in Table 1; and fixed-end moments for the several types of load are shown in Table 2. The unbalanced moments at end a are distributed as shown in Fig. 5(*a*), assuming full

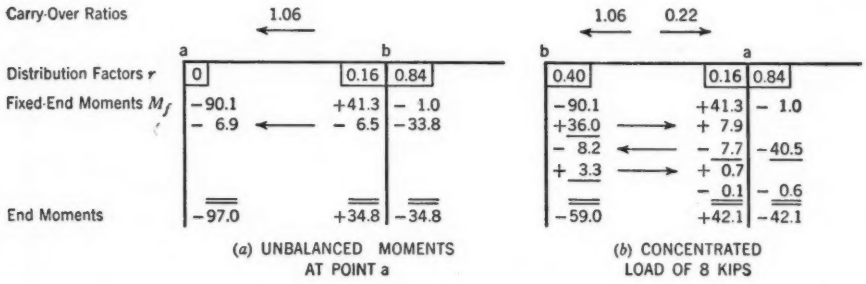

FIG. 5.—DISTRIBUTION OF MOMENTS, EXAMPLE 1

fixity at the base; and the shear H_b is computed as $\frac{0.5 \times 40}{2} + \frac{97.0 - 34.8}{40}$ $= 11.56 \leftarrow$ kips.

In a like manner distributing the fixed-end moments (in ft-kips) for the 8-kip concentrated load produces: $M_{ba} = -44.1$, $M_{ab} = +26.7$, $M_{aa'} = 26.7$ and (in kips) $H_b = 2.84$. For the 120-kip eccentric load: $M_{ba} = +35.6$, $M_{ab} = +16.7$, and $M_{aa'} = -16.7$. If only 60% fixity is assumed at point b the procedure is similar (see Fig. 5); and H_b becomes $10.0 + \frac{59.0 - 42.1}{40}$ $= 10.42 \leftarrow$ kips.

TABLE 1.—DISTRIBUTION FACTORS, r, AT POINT b, FIG. 4

Member	C	K	CK	r
ab.....	5.63	$I_c/40$	$0.141\ I_c$	0.16
bc.....	3.00	$I_c/4$	$0.750\ I_c$	0.84
Σ.....	....	....	$0.891\ I_c$	....

The horizontal forces, of course, cause a translation of the top of the column in relation to the base or, conversely (since by assumption *c*—points a and a′ move the same amount), point b moves some distance Δ in relation to points a and a′. This translation, naturally, causes additional end moments in the column. These moments are not readily determined directly but can be obtained easily as follows:

TABLE 2.—FIXED-END MOMENTS, EXAMPLE 1, IN FOOT-KIPS

Loading	$M_{f,aa'}$	$M_{f,ab}$	$M_{f,ba}$
Uniformly Distributed:			
0.5 kips per ft.....	$0.5 \times 4^2/8 = 1.0$	41.3	−90.1
Point Loads:			
8 kips concentrated...	....	31.8	−38.7
120 kips eccentric.....	....	19.9	39.0

Assume a value of $E\Delta$; in this case, assume $E\Delta = 40$ units. From Eqs. 1 the end moments for this translation, only, are:

$$M_{f,ab} = K\left[(C_1 + C_2)\frac{E\Delta}{L}\right] = (5.63 + 5.95)\frac{40}{40} = 11.58 \text{ ft-kips } (K = 1)$$

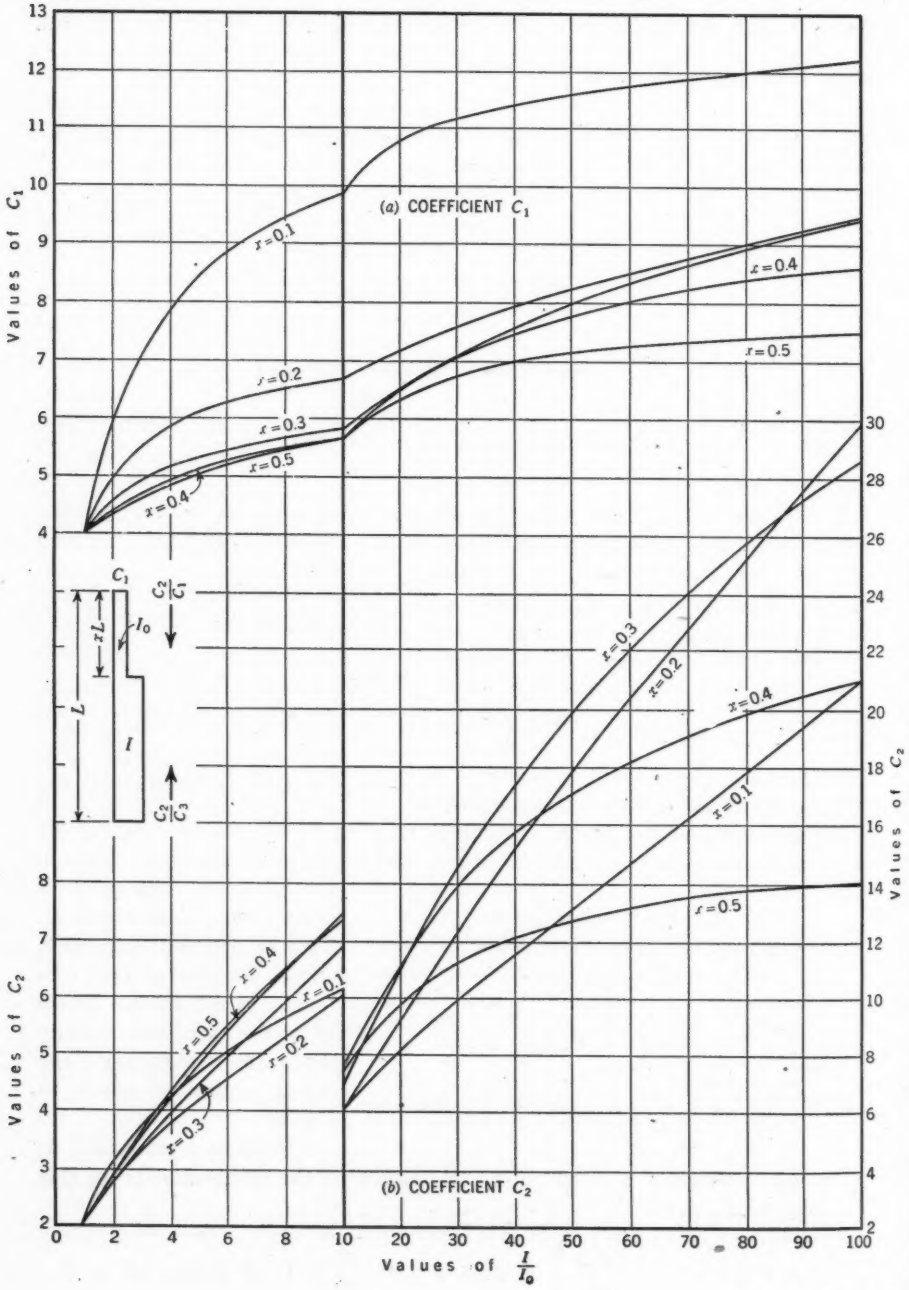

FIG. 6.—CURVES OF

and

$$M_{f,ba} = K\left[(C_2 + C_3)\frac{E\,\Delta}{L}\right] = (5.95 + 26.50)\frac{40}{40} = 32.45 \text{ ft-kips.}$$

By distribution, as before, the final moments, in foot-kips, become:

$$M_{ab} = -11.58 + 0.16 \times 11.58 = -9.73$$
$$M_{ba} = -32.45 + 1.06 \times 0.16 \times 11.58 = -30.49$$

and, in kips:

$$H_b = \frac{30.49 + 9.73}{40} = 1.01$$

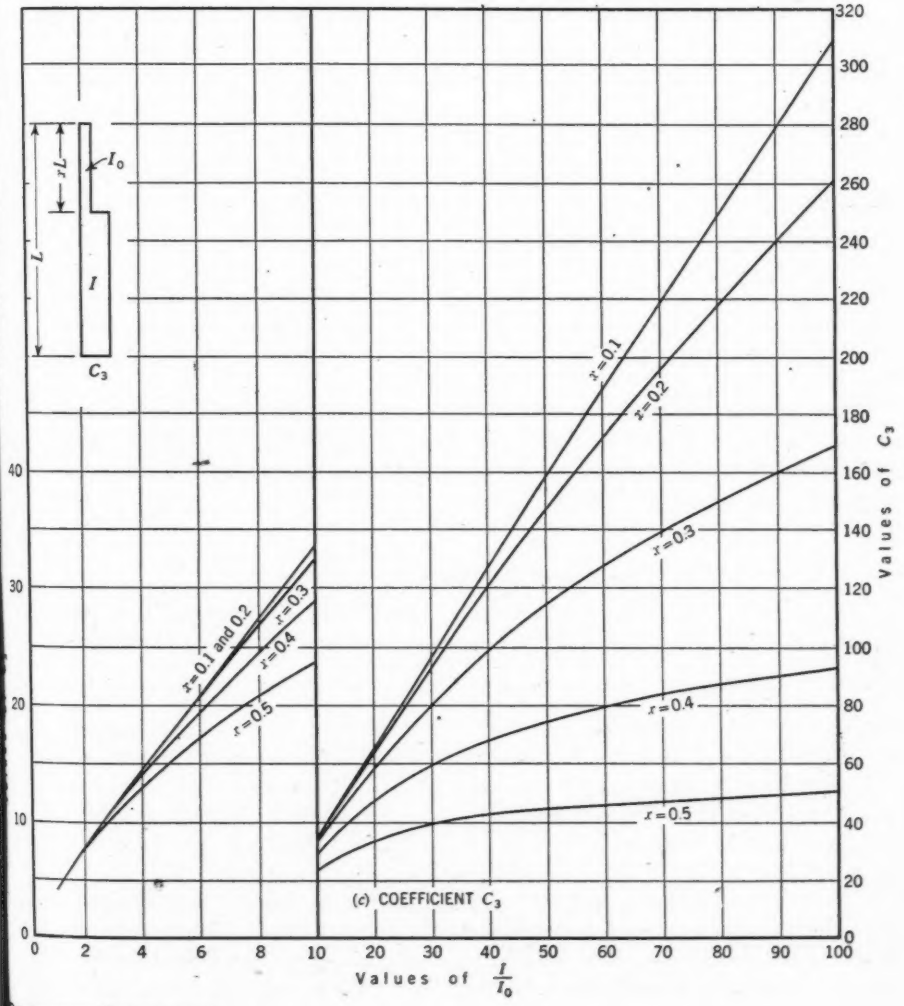

DISTRIBUTION COEFFICIENTS

For the uniform horizontal load on the column, and with no translation considered, it was shown that the shear at point b on the windward column was 11.56 kips. Since the total force assumed acting on the column was 22 kips a force of 22 − 11.56 = 10.44 kips is the force creating deflection in the bent. Assuming that both columns resist this deflection equally, the force resisted by each column is 5.22 kips. Then the end moment M_{ab} for this 5.22 kips is $\frac{5.22}{1.01} \times -9.73 = -50.5$ ft-kips and M_{ba} is $\frac{5.22}{1.01} \times -30.49 = -157.6$ ft-kips.

For the 8-kip concentrated load the force causing bent deflection is 8 − 2.84 = 5.16 kips. Since the crane thrust is spread to adjacent bents by the roof bracing, it is logical to assume that three bents resist this force or $\frac{5.16}{3} = 1.72$ kips. This is 0.86 kips per column; and $M_{ab} = \frac{0.86}{1.01} \times -9.73 = -8.2$ ft-kips; and $M_{ba} = \frac{0.86}{1.01} \times 30.49 = 25.7$ ft-kips.

For design purposes, of course, it is now only necessary to total the moments from logical loading conditions which produce the most severe effect.

As stated previously, Example 1 is given only to illustrate the method of determining the moments in a column from any set of loads under the conditions assumed, and it is not intended as a criterion of loading conditions. For instance, most codes require a percentage of the wind applied as acting outward on the lee side of the building. The method shown here would apply equally to this condition.

The general principles involved in this example—such as the determination of constants and fixed-end moments for beams of variable moments of inertia, the distribution of moments, and the computation of moments from translation—are no doubt familiar to most engineers and are to be found in various textbooks and reference books.

IV. Curves for Constants and Moments

In general, this method of analysis is relatively simple; but the determination of the constants and the fixed-end moments by the construction of $\frac{M}{I}$-diagrams is somewhat laborious and time consuming; thus it may have deterred others from such an analysis. Figs. 6 to 9, inclusive, illustrate a series of curves that will give the coefficients and fixed-end moments directly, thus reducing the work to a simple distribution of moments, as described in Example 1. These curves are drawn in groups of five, each being for a different location of the change in section and ranging from the top, by tenths, from $x = 0.1$ to $x = 0.5$.

The location of the crane girder is not likely to be below the midheight of the column, so no curves were determined for lower points. The curves are all drawn with the varying values of I/I_o as abscissas and the coefficients or fixed-end moments as the ordinates. Intermediate values of x ($x\,L$ being the distance from the top of column section to the change in section) can readily be

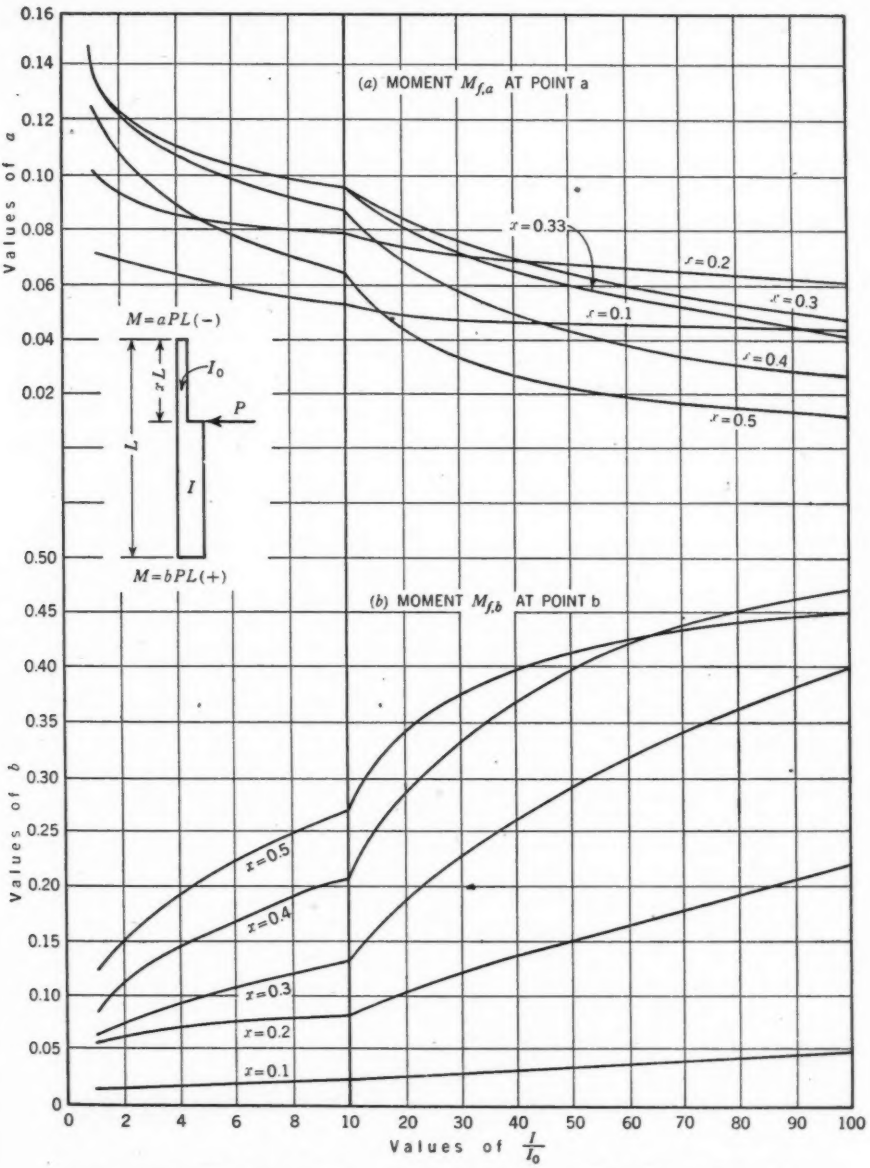

FIG. 7.—FIXED-END MOMENTS FOR A FORCE APPLIED AT THE CHANGE OF SECTION

interpolated. In two of the series of curves (Figs. 7(*a*) and 9(*a*)) it was found desirable to add a curve for $x = 0.33$.

Example 2. Use of Curves.—For the known values of $I/I_o = 8$ and $x = 0.3$, Fig. 6 reveals that $C_1 = 5.65$, $C_2 = 5.95$, and $C_3 = 26.5$. Thus, the "carry-over" from point a to point b $= \dfrac{5.95}{5.65} = 1.05$. Similarly, for the horizontal

load of 8 kips, Fig. 7(*a*) yields $M_{f,ab} = 0.99\ P\ L = 0.099 \times 8 \times 40 = 31.7$ ft-kips and Fig. 7(*b*) yields $M_{f,ba} = 0.122\ P\ L = 0.122 \times 8 \times 40 = 39.0$ ft-kips. For the uniform load of 20 kips, from Fig. 8, $M_{f,ab} = 0.0514\ W\ L = 0.0514$

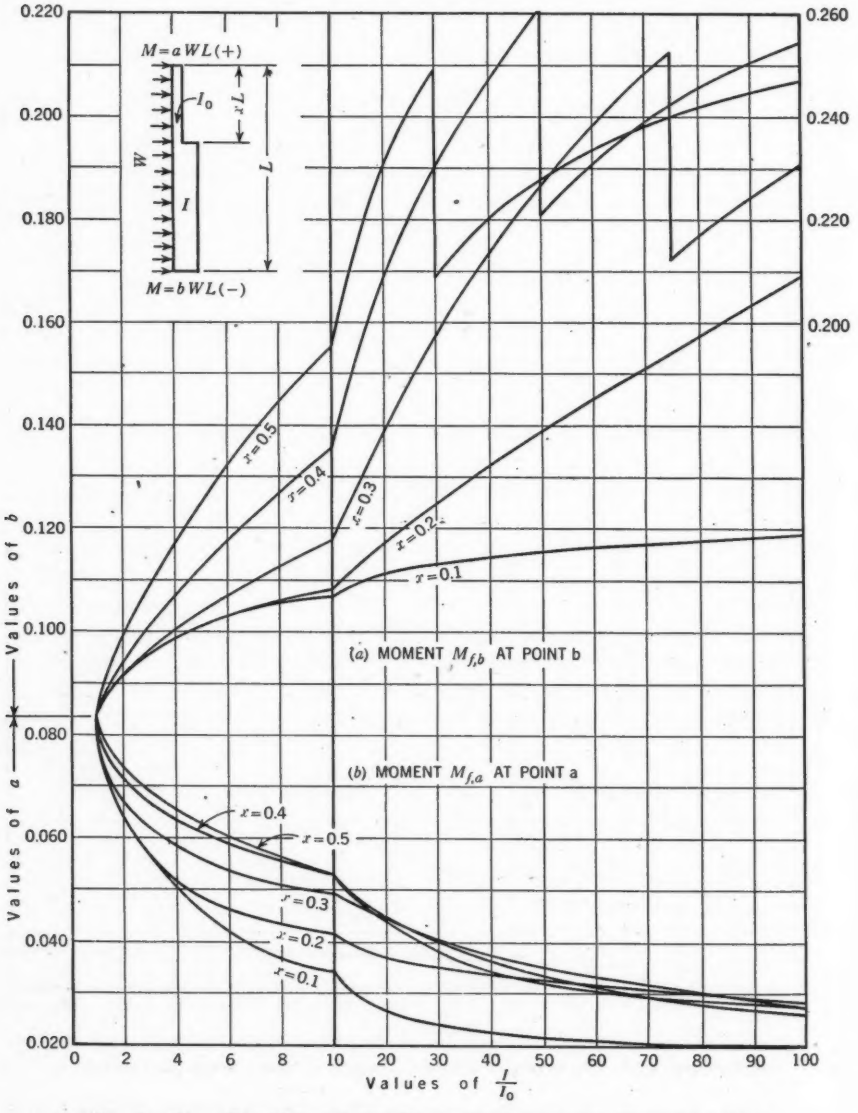

FIG. 8.—FIXED-END MOMENTS FOR UNIFORMLY DISTRIBUTED HORIZONTAL LOAD

$\times 20 \times 40 = 41.1$ ft-kips and $M_{f,ba} = 0.1125\ W\ L = 0.1125 \times 20 \times 40 = 90.0$ ft-kips. For the applied moment of 120 ft-kips from Fig. 9, $M_{f,ab} = 0.167\ M_1 = 0.167 \times 120 = 20.0$ ft-kips and $M_{f,ba} = 0.323\ M_1 = 0.323 \times 120 = 38.8$

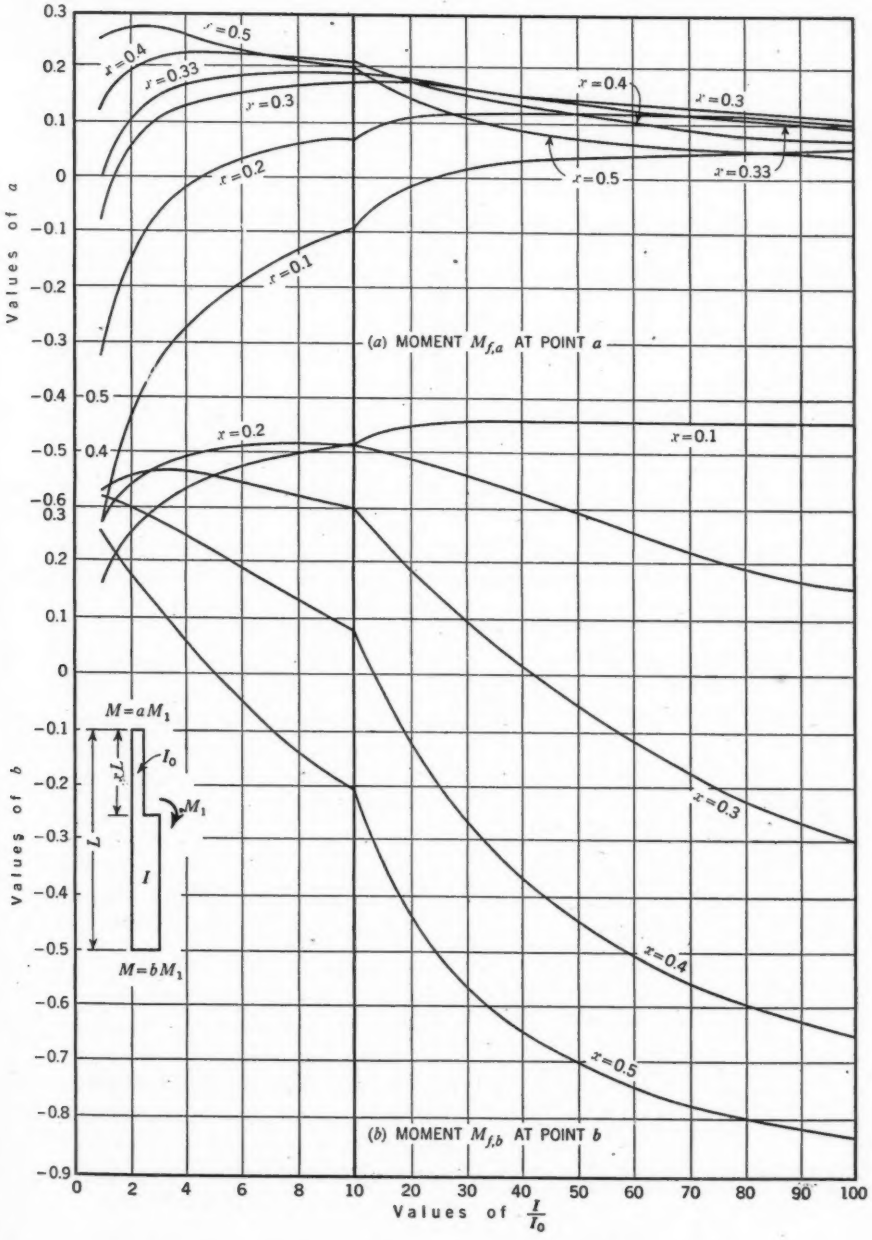

FIG. 9.—FIXED-END MOMENTS FOR A MOMENT COUPLE (AN ECCENTRIC LOAD) APPLIED AT THE CHANGE OF SECTION

ft-kips. It will be noted that these values are all very close to those obtained in Example 2.

Thus, the use of the graphs eliminates the need of constructing the several $\frac{M}{I}$-diagrams and determining the constants and the fixed-end moments from

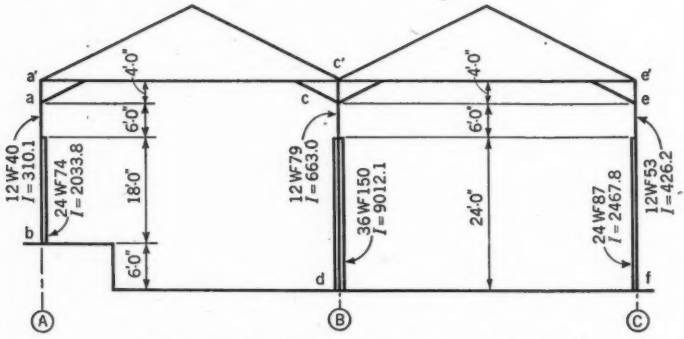

FIG. 10.—THREE-COLUMN UNSYMMETRICAL BENT

them. The time element is thus reduced to the point where this method of analysis becomes entirely practicable and lends itself to a logical and accurate result within the limits of the original assumption.

Finally, it presents a method of approach by which columns in adjacent bents or opposite columns in the bent are of varying stiffness due to mezzanine levels of framing, heavier column section, or other factors.

TABLE 3.—COMPUTATION OF DISTRIBUTION FACTORS r, IN FIG. 10

Member	C	K	CK	r
(*a*) JOINT a IN SECTION A				
aa'	3	77.5	232.5	0.75
ab	5.9	12.9	76.1	0.25
Σ	....	....	308.6	1.00
(*b*) JOINT c IN SECTION B				
cc'	3	165.75	497.2	0.765
cd	6.9	22.1	152.5	0.235
Σ	....	....	649.7	1.000
(*c*) JOINT e IN SECTION C				
ee'	3	106.55	319.6	0.78
ef	6.2	14.2	88.0	0.22
Σ	....	....	407.6	1.00

V. APPLICATIONS SHOWING THE USE OF THE CURVES AND DESIGN METHOD TO SPECIFIC PROBLEMS

Example 3.—Fig. 10 illustrates a three-column unsymmetrical bent. The solution of this relatively simple problem varies but little from the symmetrical bent. Since the distribution of the moments on an individual column has already been illustrated (Example 1), only the effect of translation of the upper joints of the bent will be shown.

For line A: $\frac{I}{I_o} = \frac{2{,}033.8}{310.1} = 6.55$; $x = \frac{6.0}{24.0} = 0.25$; $C_1 = 5.9$; $C_2 = 5.0$; and $C_3 = 22.0$ (from Fig. 6). Carry-over ratios are: $\frac{5}{22.0} = 0.23$ and $\frac{5}{5.9} = 0.85$.

Also, $K_{aa'} = \frac{310}{4} = 77.5$; $K_{ab} = \frac{310}{24} = 12.9$; and the distribution factors are computed as in Table 3(*a*). For $E\,\Delta = 10$:

$$M_{f,ab} = \frac{(5.9 + 5.0) \times 12.9 \times 10}{24} = 58.5 \text{ ft-kips}$$

and

$$M_{f,ba} = \frac{(5.0 + 22.0) \times 12.9 \times 10}{24} = 145.0 \text{ ft-kips}$$

Carry-Over Ratios	← 0.85			← 1.04			← 0.71		
	b		a	d		c	f		e
r	0		0.25 | 0.75	0		0.235 | 0.765	0		0.22 | 0.78
M_f	+145.0		+58.5 | −43.9	+381.0		+103.8 | −79.4	+115.2		+50.2 | −39.2
	− 12.4	←	−14.6 |	− 24.9	←	− 24.4 |	− 7.8	←	−11.0 |
M	+132.6		+43.9 | −43.9	+356.1		+ 79.4 | −79.4	+107.4		+39.2 | −39.2
	(*a*) SECTION A			(*b*) SECTION B			(*c*) SECTION C		

FIG. 11.—DISTRIBUTION OF MOMENTS, EXAMPLE 3, FIG. 10

These values of fixed-end moment are distributed as in Fig. 11(*a*), with the result that the shear at point b is computed as $\frac{132.6 + 43.9}{24} = 7.35$ kips.

For line B: $\frac{I}{I_o} = \frac{9{,}012.1}{6{,}630} = 13.6$; $x = \frac{6.0}{30.0} = 0.2$; $C_1 = 6.9$; $C_2 = 7.2$; and $C_3 = 44.5$. Carry-over ratios are: $\frac{7.2}{44.5} = 0.16$ and $\frac{7.2}{6.9} = 1.04$. Also, $K_{cc'} = \frac{663}{4} = 165.75$; $K_{cd} = \frac{663}{30} = 22.1$; and the distribution factors are computed as in Table 3(*b*). For $E\,\Delta = 10$:

$$M_{f,cd} = \frac{(6.9 + 7.2) \times 22.1 \times 10}{30} = 103.8 \text{ ft-kips}$$

and

$$M_{f,dc} = \frac{(7.2 + 44.5) \times 22.1 \times 10}{30} = 381.0 \text{ ft-kips}$$

As for line A, these values of fixed-end moment are distributed in Fig. 11(*b*), the resulting shear at point d being $\frac{356.1 + 79.4}{30} = 14.53$ kips.

For line C: $\frac{I}{I_o} = \frac{2{,}467.8}{426.2} = 5.8$; $x = 0.2$; $C_1 = 6.2$; $C_2 = 4.4$; and $C_3 = 20.0$. Carry-over ratios are: $\frac{4.4}{20.0} = 0.22$ and $\frac{4.4}{6.2} = 0.71$. Also, $K_{ee'} = \frac{426.2}{4} = 106.55$; $K_{ef} = \frac{426.2}{30} = 14.2$; and the distribution factors are computed as in Table 3(*c*).

For $E\,\Delta = 10$:

$$M_{f,cf} = \frac{(6.2 + 4.4) \times 14.2 \times 10}{30} = 50.2 \text{ ft-kips}$$

and

$$M_{f,fe} = \frac{(4.4 + 20.0) \times 14.2 \times 10}{30} = 115.4 \text{ ft-kips}$$

These values of fixed-end moment are distributed as in Fig. 11(*c*), the shear at point f being $\frac{107.4 + 39.2}{30} = 4.89$ kips.

From the foregoing it is then evident that column line A takes $\frac{7.35}{7.35 + 14.53 + 4.89} = 27.5\%$ of the thrust from bent sidesway; line B takes $\frac{14.53}{7.35 + 14.53 + 4.89} = 54.3\%$; and line C takes $\frac{4.89}{7.35 + 14.53 + 4.89} = 18.3\%$.

Example 4.—Fig. 12(*a*) shows a simple bent with a shed roof lean-to on one side. The lean-to columns are relatively small and, assuming hinged bases, they provide no horizontal stiffness to the bent. However, since joint e can

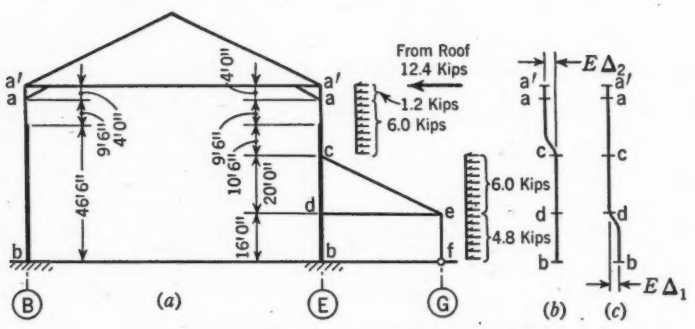

FIG. 12.—SIMPLE BENT WITH LEAN-TO

move only horizontally (the column prevents vertical translation) the stiffness of the lean-to roof truss insures that although joints c and d can deflect horizontally, they deflect the same distance. Thus, the column translation (E-line) in this case, will be a combination of two types as shown in Figs. 12(*b*) and 12(*c*), and the total stiffness of these columns is much increased.

A somewhat different method is required to analyze this bent. First, assuming that $E\,\Delta_2 = 0$, assign an arbitrary value to $E\,\Delta_1$ and distribute the moments produced. Then express the shears in terms of $E\,\Delta_1$, or since E is a constant, it can be dropped. Next, with $E\,\Delta_1 = 0$, assign a value to $E\,\Delta_2$, distribute the moments, and express the shears in terms of Δ_2. The total shear in the column between any two joints is the sum of these two shear terms. Thus knowing the force system which produces translation, equations can be set up for the solution of Δ_1 and Δ_2. However, since column B also offers resistance to this force system, the method used in Example 1 must be applied. For horizontal forces acting only on column B, the shears in column E produced by

translation are the same between points a and c and between points d and b. Assume any value for this shear, and solve for Δ_1 and Δ_2. Then the total deflection at point a is the sum of these for this particular shear. Since the tops of columns B and E move the same amount (assumption *e*), determine the shear in the B columns for the same Δ-value and the relative stiffness of the two lines of columns is proportionate to these shears.

TABLE 4.—COMPUTATION OF DISTRIBUTION FACTORS *r* FOR COLUMN B, FIG. 12

Member	*C*	*K*	*CK*	*r*
aa'.....	3	107.5	322.5	0.85
ab.....	7.3	7.7	56.2	0.15
Σ.....	....	....	787.7	1.00

To apply the foregoing to a numerical example, first consider column B, Fig. 2, with: $I_o = 430$; $I = 3{,}130$; $\frac{I}{I_o} = 7.3$; and $x = \frac{9.5}{56} = 0.17$. From Fig. 6:

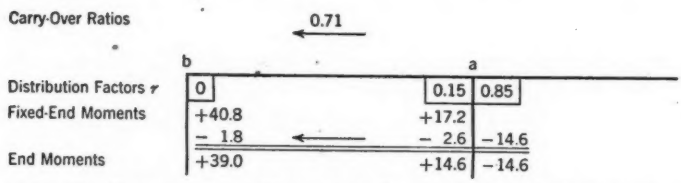

FIG. 13.—DISTRIBUTION OF MOMENTS IN COLUMN B, FIG. 12 (EXAMPLE 4)

TABLE 5.—COMPUTATION OF DISTRIBUTION FACTORS *r* FOR COLUMN E, FIG. 12

Member	*C*	*K*	*CK*	*r*
(*a*) JOINT a				
aa'.....	3	107.5	322.5	0.74
ac.....	5.3	21.5	114.0	0.26
Σ.....	....	....	436.5	1.00
(*b*) JOINT c				
ca.....	20	21.5	430.0	0.41
cd.....	4	156.5	626.0	0.59
Σ.....	....	....	1,056	1.00
(*c*) JOINT d				
dc.....	4	156.5	626.0	0.445
db.....	4	195.6	782.4	0.655
Σ.....	....	....	1,408.4	1.00

$C_1 = 7.3$; $C_2 = 5.2$; $C_3 = 24.5$; and the carry-over factor is $\frac{5.2}{7.3} = 0.71$. Also, $K_{aa'} = \frac{430}{4} = 107.5$; $K_{ab} = \frac{430}{56} = 7.7$; and the distribution factors are computed as in Table 4. For $E\Delta = 10$:

$$M_{f,ab} = \frac{10\,K_o\,(C_1 + C_2)}{L}$$

$$= \frac{10 \times 7.7\,(7.3 + 5.2)}{56} = 17.2 \text{ ft-kips}$$

and

$$M_{f,ba} = \frac{10\,K_o\,(C_2 + C_3)}{L}$$

$$= \frac{10 \times 7.7\,(5.2 + 24.5)}{56} = 40.8 \text{ ft-kips}$$

These values of fixed-end moment are distributed as in Fig. 13, the shear at point b, Fig. 12, being $\frac{39.0 + 14.6}{56} = 0.96$ kips.

For E line: Assume I_o and I the same as for column B, with $I/I_o = 7.3$. Furthermore: $x = \frac{9.5}{20} = 0.475$; and (see Fig. 6) $C_1 = 5.3$; $C_2 = 6.1$; and

$C_3 = 20.0$. Carry-over ratios are: $\frac{6.1}{5.3} = 1.15$; and $\frac{6.1}{20} = 0.305$. Finally: $K_{aa'} = 107.5$; $K_{ac} = \frac{430}{20} = 21.5$; $K_{cd} = \frac{3{,}130}{20} = 156.5$; and $K_{db} = \frac{3{,}130}{16} = 195.6$. Distribution factors are computed as in Table 5.

For $E\,\Delta_1 = 1$:

$$M_{f,bd} = M_{f,db} = \frac{6\,K\,E\,\Delta}{L} = \frac{6 \times 195.6 \times 1}{16} = 73.4 \text{ ft-kips}$$

and, for $E\,\Delta_2 = 1$:

$$M_{f,ac} = \frac{(C_1 + C_2)\,K\,E\,\Delta}{L} = \frac{(5.3 + 6.1) \times 21.5 \times 1}{20} = 12.3 \text{ ft-kips}$$

and

$$M_{f,ca} = \frac{(C_2 + C_3)\,K\,E\,\Delta}{L} = \frac{(6.1 + 20.0) \times 21.5 \times 1}{20} = 28.0 \text{ ft-kips}$$

These values of fixed-end moment are distributed as in Fig. 14.

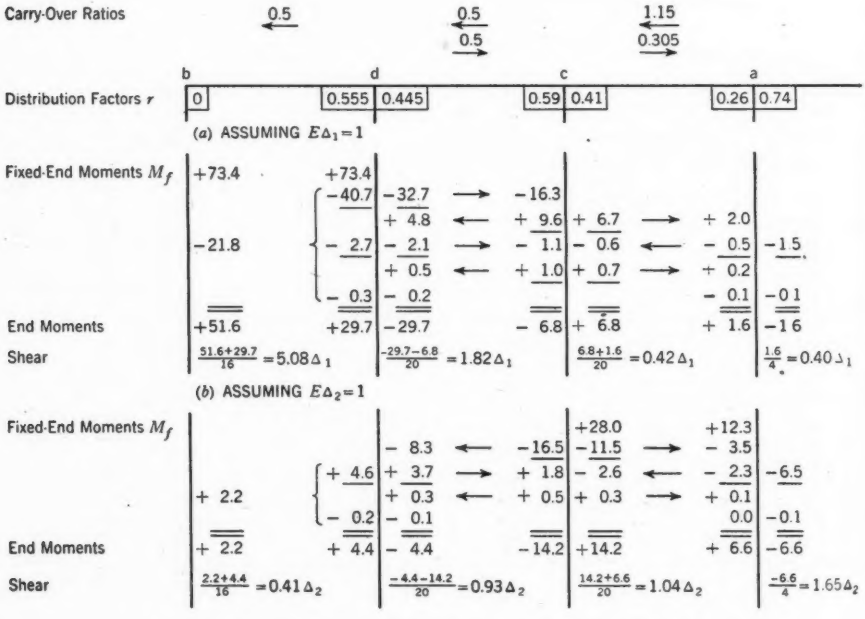

FIG. 14.—DISTRIBUTION OF MOMENTS IN COLUMN E, FIG. 12 (EXAMPLE 4)

Assume that $E\,\Delta_1 + E\,\Delta_2$ is caused by forces which produce shears in lengths ac and db each equal to 1 kip (forces at points a and a′ total 1 kip and reaction at point b equals 1 kip) then:

$$5.08\,\Delta_1 + 0.41\,\Delta_2 = 1 \ldots\ldots\ldots\ldots\ldots\ldots (9a)$$

and

$$0.42\,\Delta_1 + 1.04\,\Delta_2 = 1 \quad \ldots\ldots\ldots\ldots\ldots\ldots\ldots\ldots (9b)$$

Multiplying Eq. 9*b* by $\frac{5.08}{0.42}$, it becomes:

$$5.08\,\Delta_1 + 12.58\,\Delta_2 = 12.1 \quad \ldots\ldots\ldots\ldots\ldots\ldots\ldots\ldots (9c)$$

Solving Eqs. 9*a* and 9*c* simultaneously: $\Delta_2 = 0.913$; and $\Delta_1 = 0.124$. Consequently, $\Delta_1 + \Delta_2 = 1.037$.

Since both columns are assumed to deflect the same amount at the top, Δ for column B would be 1.037 to correspond to the foregoing values. The total shear is distributed in the bent as follows:

Deflection	Computation	Shear	
Column B	$\frac{0.96}{10} \times 1.037$		0.100
Column E:			
$\Delta_1 = 0.124$	5.08×0.124	0.63	
$\Delta_2 = 0.913$	0.41×0.913	0.37	
$\Delta_1 + \Delta_2 = 1.037$	....		1.00
Total shear in bent	....		1.10

Column E then resists $\frac{1.00}{1.10}$ or 91% of the horizontal thrust and column B resists $\frac{0.10}{1.10}$ or 9%.

Carry-Over Ratios		0.5 ←		0.5 ←		1.15 ←	
				0.5 →		0.305 →	
	b		d		c		a	a′
Distribution Factors *r*	0		0.555	0.445	0.59	0.41	0.26	0.74	
Fixed-End Moments *M*						+16.3	−7.0	+0.6	
						+ 1.9 ←	+1.7	+4.7	
				−5.4 ←	−10.7	− 7.5 →	−2.3		
			+3.0	+2.4 →	+ 1.2	+ 0.7 ←	+0.6	+1.7	
				−0.6	− 1.1	− 0.8 →	−0.2		
			+0.3	+0.3			+0.1	+0.1	
End Moments	+1.6 ←		+3.3	−3.3	−10.6	+10.6	−7.1	+7.1	
Simple Beam Shear	0		0	0	0	3.0 ↓	↓ 3.0	0.6 ↓	0.6↓
Correction	0.37↓		↑0.37	0.70↑	↓0.70	0.18↓	↑ 0.18	1.77↓	↑1.77
H	0.37↓		↑0.37	0.70↑	↓0.70	3.18↓	↓2.82	2.37↓	↑1.17
Reactions	0.37↓		↑1.07		↓3.88		↓5.19		↑1.17

FIG. 15.—MOMENTS IN COLUMN E WHEN HORIZONTAL FORCES ACT ON COLUMNS E AND G

When the horizontal forces act on columns E and G, however, the shear between points a and c and between points d and b is no longer equal, and the relative values of Δ_1 and Δ_2 change. The first step, as in previous examples, is the distribution of the moments from forces acting between joints, with all joints held against translation (see Fig. 15).

As a first step in the solution of the auxiliary force system, assume that all resistance to translation is taken by the E-line columns. The force system on the E-line columns then consists of forces at joints a, a′, c, and d equal and opposite to the reactions determined in Fig. 15 plus forces applied directly to the joints such as wind forces on the roof. Since the base of column G is hinged, half the uniform load of 4.8 kips, shown acting on it, is assumed to go to base f and half to the top point e. This half at point e plus the 6 kips acting on the lean-to roof are distributed between points c and d on column E, Fig. 12. Without another set of calculations (translating points c and d, distributing the moments produced, and determining the shears) the exact distribution between these two joints is not known, but such distribution is not needed for the present problem; only the shear is needed between points d and b, and between points a and c. The shear between points a and c is $5.19 - 1.17 = 4.02$ kips plus 12.4 kips from the roof, or a total of 16.42 kips. The shear between points d and b is increased by $3.88 - 1.07 + 6.0 + \frac{4.8}{2}$, or 27.63 kips. Since there is no relative translation between joints c and d the shear is not needed.

To determine the relative values of Δ_1 and Δ_2, set up formulas similar to Eqs. 9, except that the shear values are different:

$$5.08\,\Delta_1 + 0.41\,\Delta_2 = 27.63 \quad \ldots\ldots\ldots\ldots\ldots\ldots (10a)$$

and

$$0.42\,\Delta_1 + 1.04\,\Delta_2 = 16.42 \quad \ldots\ldots\ldots\ldots\ldots\ldots (10b)$$

Multiplying Eq. 10*b* by $\frac{5.08}{0.42}$, it becomes:

$$5.08\,\Delta_1 + 12.59\,\Delta_2 = 198.8 \quad \ldots\ldots\ldots\ldots\ldots\ldots (10c)$$

As in Eqs. 9, solve Eqs. 10*a* and 10*c* simultaneously, and determine: $\Delta_2 = 14.05$; and $\Delta_1 = 4.30$. Consequently, $\Delta_1 + \Delta_2 = 18.35$.

For a Δ-value on the B-line columns of 18.35 units, the shear would be $\frac{18.35}{10} \times 0.96$ or 1.76 kips. The E-line columns thus would take $\frac{27.63}{27.63 + 1.76} = 94.2\%$ of the thrust and the B-line columns only 5.8%.

VI. Conclusion

Although most of the examples in this paper are not complete they show the general procedure for the various cases. As with any method of design for indeterminate structures, the ability to make a relative close initial estimate of the members required is very helpful and saves repeated computations. This ability, of course, comes largely with experience and observation.

Although the types of problems described in this paper by no means exhausts the variations that are likely to occur in practice, it is felt that a practical approach to other forms of bents should not be found difficult.

The method of analysis probably is not original, although not commonly used. However, without the use of the curves presented herein, the solution would be quite time consuming. Although this method of solution with the

curves will require more time than that of assuming a point of contraflexure and solving as a statically determinate structure, the greater assurance of a reasonably accurate analysis should justify this extra time.

Acknowledgment

Figs. 6 to 9 were prepared by the writer for his own use in structural design and were original in form and development. L. T. Evans, Assoc. M. ASCE, in the revised edition of "Rigid Frames,"[4] has similar curves for all but the uniform load condition. His curves do not, however, cover the range of those presented. It appears that the curves by Mr. Evans were developed somewhat earlier than those presented herein.

The paper is based on data assembled and presented as a thesis[5] to the University of Michigan, Ann Arbor, Mich., in 1943, in partial fulfilment of the requirements for the professional degree of Civil Engineer.

APPENDIX I. NOTATION

The following letter symbols, used in the paper and in its discussion, conform essentially to American Standard Letter Symbols for Mechanics, Structural Engineering and Testing Materials (ASA—Z10a—1932), prepared by a Committee of the American Standards Association, with Society representation, and approved by the Association in 1932:

- a = a nondimensional coefficient of end moment at the top of a stepped column (see Fig. 7);
- B = angle of rotation caused by a unit torque; thus—B_{ab} = rotation at joint a caused by a unit torque applied at joint b;
- b = a nondimensional coefficient of end moment at the bottom of a stepped column (see Fig. 7);
- C = a coefficient, with suitable subscript, used in slope-deflection equations; thus:
  - C_1 = the distribution coefficient for point a for given values of I/I_o and x in Fig. 6(a);
  - C_2 = the coefficient (see Fig. 6(b)) which, with C_1 or C_3, gives the carry-over ratio (the carry-over ratio from point a to point b is C_2/C_1 and from point b to point a, is C_2/C_3);
  - C_3 = the distribution coefficient for point b, the bottom of the column, for given values of I/I_o and x in Fig. 6(c);
- E = modulus of elasticity;
- I = moment of inertia of a column section, the moment of inertia for the reference section (the upper and smaller section of a stepped column) being designated I_o;

[4] "Rigid Frames," by L. T. Evans, Edwards Bros., Ann Arbor, Mich., 1938.

[5] "Analysis of Mill Bents with Stepped Columns by the Method of Successive Approximations," by Daniel S. Ling, thesis presented to the Univ. of Michigan, Ann Arbor, in 1943, in partial fulfilment of the requirements for the professional degree of Civil Engineer.

K = stiffness ratio $E\,I/L$ used in moment distribution, the stiffness ratio of the upper and smaller section of a stepped column being designated $K_o = E\,I_o/L$:
L = length of member;
M = bending moment; the subscript f denotes "fixed end"; other subscripts refer to a designated joint and span—that is, in general, $M_{f,ba}$ equals fixed-end moment at joint b in member ab;
P = a point load or concentrated load;
r = distribution factor;
W = total weight, force, or pressure;
w = weight, force, or pressure per linear foot;
x = a ratio of length;
α = angular rotation of the end tangents of a deformed beam, considered simply supported;
β = a substitution constant, function of the unit rotation B;
Δ = linear displacement of one end of a beam with respect to the other end; and
θ = angular rotation of a beam.

AMERICAN SOCIETY OF CIVIL ENGINEERS

Founded November 5, 1852

DISCUSSIONS

THEORY OF INELASTIC BENDING WITH REFERENCE TO LIMIT DESIGN

Discussion

BY MICHAEL R. HORNE

BY MICHAEL R. HORNE,[9] ESQ.—

Methods of Stress Analysis Beyond the Elastic Limit.—Professor Hrennikoff's method for dealing with inelastic beams is ingenious, and has the advantage that, once the necessary tables have been compiled, it can be applied to any members of uniform section symmetrical about the plane of bending. However, it suffers from the very serious disadvantage that for complicated problems the application of Eqs. 12 and 21 becomes very involved. Many problems concerned with the elastic bending of beams may be solved quite simply by means of the three-moment theorem, and a similar method may be applied when the bending ceases to be elastic. In effect, it is possible to replace Eqs. 12 and 21 by a single relationship between the bending moments and deflections at three successive points in a beam.

Consider a beam ABC (Fig. 30) in which the bending moments at points A, B, and C are M_A, M_B, and M_C, respectively. It is assumed that between points A and B and between points B and C the bending moment diagram consists of straight lines. Let the length, depth, and web area of span AB be l_1, h_1, and A_{w1}, respectively, and let the corresponding values for span BC be l_2, h_2, and A_{w2}. If m_{AB}, and m_{BA} are the values of the function m at points A and B for the length AB, then, from Eq. 5,

$$m_{AB} = \frac{2\,M_A}{h_1\,A_{w1}}\,; \quad \text{and} \quad m_{BA} = \frac{2\,M_B}{h_1\,A_{w1}} \ldots\ldots\ldots\ldots (48a)$$

Similarly, m_{BC} and m_{CB}, the values of the function m at points B and C for the length BC, are

$$m_{BC} = \frac{2\,M_B}{h_2\,A_{w2}}\,; \quad \text{and} \quad m_{CB} = \frac{2\,M_C}{h_2\,A_{w2}} \ldots\ldots\ldots\ldots (48b)$$

NOTE.—This paper by Alexander Hrennikoff was published in March, 1947, *Proceedings*. Discussion on this paper has appeared in *Proceedings*, as follows: June, 1947, by George Winter, and D. C. Drucker.

[9] Research Asst., Dept. of Eng., Univ. of Cambridge, Cambridge, England.

Let n_{AB}, u_{AB}, etc., be the values of the functions n and u corresponding to these values of m. Considering the center line of the beam, let δ_1 be the deflection at point B relative to point A, and δ_2, the deflection at point C relative to point B; δ_1 and δ_2 are both measured positive downward. Referring to

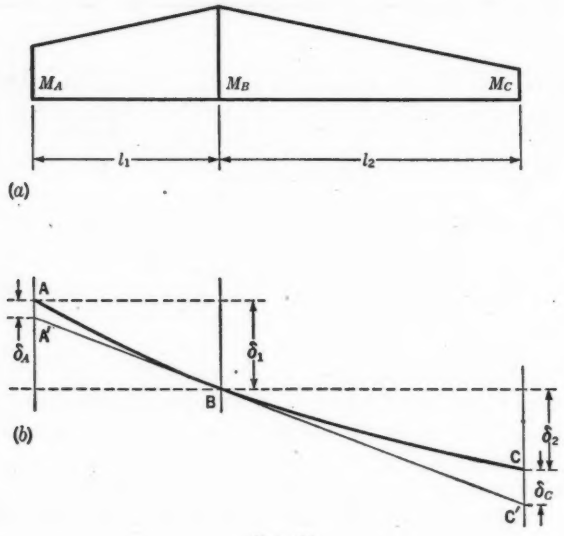

FIG. 30

Fig. 30, A′ BC′ is a straight line tangential to the center line at point B and, from the geometry of the figure,

$$\frac{\delta_1 - \delta_A}{l_1} = \frac{\delta_2 + \delta_C}{l_2} \quad \ldots\ldots\ldots\ldots\ldots\ldots\ldots\ldots (49)$$

Considering span AB, Fig. 30, it is readily proved that

$$\delta_A = \frac{2\,l^2_1}{h_1} \frac{[u_{BA} - u_{AB} - m_{AB}\,(n_{BA} - n_{AB})]}{(m_{BA} - m_{AB})^2} \quad \ldots\ldots\ldots\ldots (50a)$$

Similarly, for span BC,

$$\delta_C = \frac{2\,l^2_2}{h_2} \frac{[u_{BC} - u_{CB} - m_{CB}\,(n_{BC} - n_{CB})]}{(m_{BC} - m_{CB})^2} \quad \ldots\ldots\ldots\ldots (50b)$$

Substituting Eqs. 50*a* and 50*b* in Eq. 49:

$$\frac{l_1}{h_1} \frac{[u_{BA} - u_{AB} - m_{AB}\,(n_{BA} - n_{AB})]}{(m_{BA} - m_{AB})^2} + \frac{l_2}{h_2} \times \frac{[u_{BC} - u_{CB} - m_{CB}\,(n_{BC} - n_{CB})]}{(m_{BC} - m_{CB})^2} = \tfrac{1}{2}\left(\frac{\delta_1}{l_1} - \frac{\delta_2}{l_2}\right) \quad \ldots (51a)$$

If the beam ABC is uniform throughout, $h_1 = h_2$ and $m_{BA} = m_{BC}$. Hence,

there is no longer any need for the double suffixes, and Eq. 51*a* becomes

$$\frac{l_1\,[u_B - u_A - m_A\,(n_B - n_A)]}{(m_B - m_A)^2} + \frac{l_2\,[u_B - u_C - m_C\,(n_B - n_C)]}{(m_B - m_C)^2} = \frac{h}{2}\left(\frac{\delta_1}{l_1} - \frac{\delta_2}{l_2}\right) \ldots (51b)$$

Eqs. 51*a* and 51*b* are valid for negative as well as positive values of M_A, M_B, and M_C, as long as the following convention is applied: The functions m and u are given the same sign as the corresponding bending moment, and the function n is always to be regarded as positive, regardless of the sign of the bending moment. That this is satisfactory is readily proved in the derivation of Eqs. 50*a* and 50*b*.

Two simple examples will demonstrate the application of Eq. 51.

Example 1.—Consider the portal frame ABDE (Fig. 31(*a*)) of uniform sec-

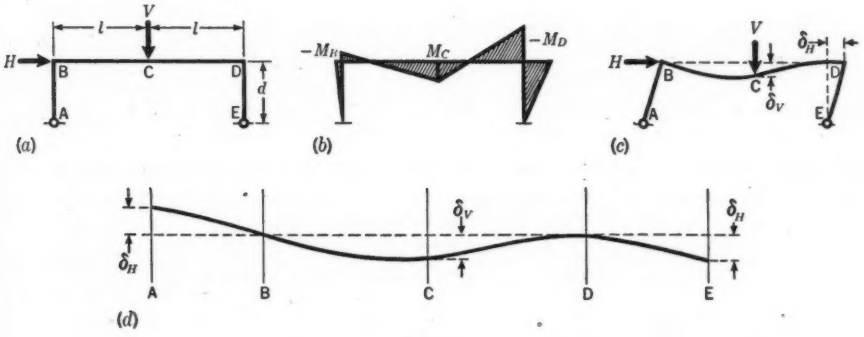

FIG. 31

tion throughout, supported on pins at points A and E. Let its height be d and its span $2\,l$, and let it carry a vertical load V at point C, the midpoint of span BD, and a horizontal load H applied at beam level. Let M_B, M_C, and M_D be the bending moments at points B, C, and D, respectively (Fig. 31 (*b*)), and let m_B, m_C, m_D be the corresponding values of the function m. Moments are accounted positive when they produce tension in the inner fibers of the frame. It follows from statical considerations that

$$2\,M_C - M_B - M_D = V\,l \ldots (52a)$$

and

$$M_B - M_D = H\,d \ldots (52b)$$

If h is the depth of the section, and A_w the web area, then, from Eq. 50*b*,

$$2\,m_C - m_B - m_D = \frac{2\,V\,l}{h\,A_w} \ldots (53a)$$

and

$$m_B - m_D = \frac{2\,H\,d}{h\,A_w} \ldots (53b)$$

For convenience, m_B and m_C can be expressed in terms of the one unknown m_D, and, hence

$$m_B = m_D + \frac{2\,H\,d}{h\,A_w} \quad \ldots\ldots\ldots\ldots\ldots\ldots\ldots\ldots (53c)$$

and

$$m_C = 2\,m_D + \frac{2}{h\,A_w}(H\,d + V\,l) \quad \ldots\ldots\ldots\ldots\ldots\ldots (53d)$$

It will be assumed that all bending that results from axial loads may be neglected, so that Eq. 51*b* is applicable. The vertical deflection at point C will be denoted by δ_V and the sidesway of the frame, by δ_H. Treating the entire frame as a continuous beam (Fig. 31(*d*)), Eq. 51*b* may be applied first to the part ABC, then to the part BCD, and finally to the part CDE, thus obtaining three equations:

$$\frac{u_B\,d}{m^2_B} + l\,\frac{[u_B - u_C - m_C\,(n_B - n_C)]}{(m_B - m_C)^2} = \frac{h}{2}\left(\frac{\delta_H}{d} - \frac{\delta_V}{l}\right) \quad \ldots\ldots (53e)$$

$$l\,\frac{[u_C - u_B - m_B\,(n_C - n_B)]}{(m_C - m_B)^2} + l\,\frac{[u_C - u_D - m_D\,(n_C - n_D)]}{(m_C - m_D)^2} = \frac{h\,\delta_V}{l} \quad \ldots (53f)$$

$$l\,\frac{[u_D - u_C - m_C\,(n_D - n_C)]}{(m_D - m_C)^2} + \frac{u_D\,d}{m^2_D} = -\frac{h}{2}\left(\frac{\delta_H}{d} + \frac{\delta_V}{l}\right) \quad \ldots\ldots (53g)$$

If δ_H and δ_V are eliminated from Eqs. 53*e* to 53*g*, a further relationship is obtained between m_B, m_C, and m_D:

$$d\left(\frac{u_B}{m^2_B} + \frac{u_D}{m^2_D}\right) + l\left(\frac{n_B - n_C}{m_B - m_C} + \frac{n_C - n_D}{m_C - m_D}\right) = 0 \quad \ldots\ldots (53h)$$

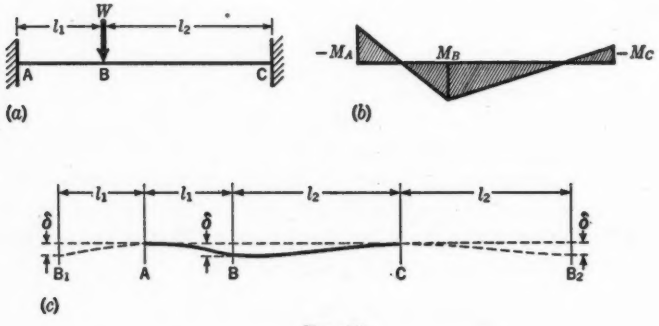

FIG. 32

In obtaining a solution for any given values of V and H it is necessary to assume a value of m_D. Deduce the values of m_B and m_C from Eqs. 53*c* and 53*d*, and then test whether Eq. 53*h* is satisfied. When the correct values of m_B, m_C, and m_D have been obtained, the values of δ_V and δ_H may be found from Eqs. 53*e* and 53*f*.

Example 2.—In Fig. 32, consider beam AC, fixed at points A and C, and subjected to a concentrated load W at a distance of l_1 from point A and l_2 from point C. If the bending moments at points A, B, and C are M_A, M_B, and

M_C, respectively, it follows from simple statics that

$$(l_1 + l_2)\, M_B - l_2\, M_A - l_1\, M_C = l_1\, l_2\, W \ldots\ldots\ldots\ldots (54a)$$

If m_A, m_B, and m_C are the corresponding values of the function m, then,

$$(l_1 + l_2)\, m_B - l_2\, m_A - l_1\, m_C = \frac{2\, l_1\, l_2}{h\, A_w}\, W \ldots\ldots\ldots\ldots (54b)$$

If δ is the deflection at point B relative to points A and C, then in applying Eq. 51*b* it is necessary that $\delta_1 = -\delta_2 = \delta$. Hence, two equations are available to determine the four unknowns, m_A, m_B, m_C, and δ, and it is necessary to find two more. If span AB is imagined to be reflected about end A into the position AB_1 in Fig. 32(*c*), then Eq. 51*b* may be applied to the length B_1AB, giving

$$\frac{[u_A - u_B - m_B\,(n_A - n_B)]}{(m_A - m_B)^2} = -\frac{h\,\delta}{2\,l^2_1} \ldots\ldots\ldots\ldots (55a)$$

Similarly, span BC may be reflected into the position CB_2, and the application of Eq. 51*b* to the length BCB_2 gives

$$\frac{[u_C - u_B - m_B\,(n_C - n_B)]}{(m_C - m_B)^2} = -\frac{h\,\delta}{2\,l^2_2} \ldots\ldots\ldots\ldots (55b)$$

For any given value of W it is necessary to solve Eqs. 51*b*, 54*b*, 55*a*, and 55*b* by trial and error until suitable values of m_A, m_B, and m_C are found.

The Stress-Strain Relationship of Steel in Bending.—This subject has been treated in a paper by F. G. Eric Peterson,[10] Assoc. M. ASCE, and in the subsequent discussions. As stated by J. F. Baker, Assoc. M. ASCE, and J. W. Roderick in their discussion,[11] the generally accepted theory in England is that the stress distribution is similar to that given by the tensile test when made in an autographic testing machine, care being taken to insure that the applied load is truly axial, but ignoring the effect of strain hardening, as shown in Fig. 33. Under such circumstances mild steel gives a stress-strain relationship in which the upper yield stress f_u may be between 25% and 45% in excess of the lower yield stress f_L. Professors Baker and Roderick also show that the assumption of such a stress distribution accounts very well for the behavior of rectangular mild steel beams in bending. Further work by these writers, at the Engineering Laboratory of Cambridge University at Cambridge, England, in collaboration with the British Welding Research Association, has confirmed these results. The stress-strain relationship assumed by Professor Hrennikoff differs from that assumed by Professors Baker and Roderick in two respects: Professor Hrennikoff ignores the upper yield stress and takes strain hardening into account, assuming that strain hardening occurs in bending in precisely the same way as in a tension test. Most of the work done by Professors Baker

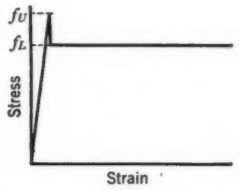

FIG. 33

[10] *Transactions*, ASCE, Vol. 112, 1947, p. 1201.
[11] *Ibid.*, p. 1238.

and Roderick has been on beams of rectangular cross section, whereas, the paper of Professor Hrennikoff refers also to rolled beams in which local yield due to rolling stresses is certain to occur. Under these circumstances to neglect the upper yield stress is reasonable. However, the assumptions made with respect to strain hardening cannot be justified so readily. The strains at the end of the plastic range are considerable, and under such circumstances it should not be assumed too readily that the strain-hardening effect is the same in bending as in tension. It is interesting to note that the work done at Cambridge indicates that the behavior of both simply supported and continuous beams up to the loads causing large deflections may be explained satisfactorily without reference to strain hardening.

The Importance of Strain Hardening in Limit Design.—Strain hardening, obviously, has an important bearing on attempts to arrive at a design method based on the ultimate capacity of steel structures, but its importance should not be overestimated. In designing ordinary building frames by the usual elastic methods, emphasis is always placed on stresses rather than on deflections. This is because within the elastic range the strains are small. However, when an ultimate load method of design is used, the deflections become as important as the stresses, because of the greatly increased strains within the plastic range. The structure will only be useful up to that load at which the deflections become excessive. The limit method of design justifies itself because the ultimate load calculated according to the principle of equalization of moments must coincide approximately with the load at which excessive deflections first occur. This is because both the equalization of moments and the appearance of large deflections result from the same property of mild steel—its capacity to undergo plastic deformation without increase in stress. The author has now shown that the plastic yield that occurs before strain hardening begins is insufficient to cause a complete equalization of moments. Since the deflections are becoming large, at this stage, however, the ultimate capacity has been reached, so that it becomes pointless to follow the behavior of the structure further. The limit method of design achieves its purpose if it leads to a reasonable estimate of the load at which deflections begin to increase rapidly. Professor Hrennikoff's work is of particular interest since it affords a means of checking the assumption that this is actually the case. The results obtainable in this way may best be illustrated by taking a numerical example.

Example 3.—Consider a portal frame of the type shown in Fig. 31(*a*), in which $d = l$. Let the cross section of the member be uniform throughout, the web and flange areas being equal so that $k = 1$. Let a vertical load V first be applied so that yield stress in the extreme fibers is just reached in the center of the beam, horizontal load only being applied thereafter. With steel having the properties assumed by Professor Hrennikoff, the value of V just sufficient to produce yield stress at point C is found to be $\frac{2\,V\,l}{h\,A_w} = 140.8$ kips per sq in. The entire frame remains elastic until H has reached a value given by $\frac{2\,H\,l}{h\,A_w} = 35.2$ kips per sq in. when yield stress is just reached in the extreme fibers at point D in Fig. 31(*a*). Thereafter it is necessary to obtain solutions by the

use of Eqs. 53*c* to 53*h*. The results are presented in Table 9(*a*). Cols. 2 to 7, Table 9(*a*), give the bending moments at points B, C, and D, and the corresponding extreme fiber strains, and Cols. 8 and 9 give, respectively, the vertical deflection δ_V and the horizontal deflection δ_H at the center of the beam. The

TABLE 9.—EFFECTS OF STRAIN HARDENING

Horizontal load $H\frac{2l}{h A_w}$ (kips per sq in.)	Bending Moments, $M\frac{2l}{h A_w}$ (Kips per Sq. In.)			Extreme Strains			Vertical Deflection, $10^3\frac{\delta h}{l^2}$ (In.)	
				1,000 ϵ_B	1,000 ϵ_C	1.000 ϵ_D		
	M_B	M_C	M_D				δ_V	δ_H
(1)	(2)	(3)	(4)	(5)	(6)	(7)	(8)	(9)
(*a*) Strain Hardening Considered								
0	−26.40	44.00	−26.40	−0.66	1.10	−0.66	0.513	0
35.20	−8.80	44.00	−44.00	−0.22	1.10	−1.10	0.513	0.586
40.00	−6.27	44.13	−46.27	−0.16	1.11	−1.44	0.515	0.677
45.00	−3.22	44.68	−48.22	−0.08	1.18	−2.41	0.531	0.796
50.00	0.56	45.96	−49.44	0.01	1.37	−11.00	0.568	0.970
50.43	0.95	46.14	−49.48	0.02	1.41	−18.00	0.574	0.990
51.03	1.51	46.40	−49.52	0.04	1.47	−18.06	0.583	1.022
55.00	5.20	48.10	−49.80	0.13	2.28	−18.49	0.660	1.236
57.20	7.20	49.00	−50.00	0.18	3.75	−18.80	0.727	1.379
58.60	8.38	49.48	−50.22	0.21	18.00	−19.13	0.816	1.517
60.00	9.38	49.78	−50.62	0.23	18.46	−19.80	1.010	1.742
65.00	12.94	50.84	−52.06	0.32	20.08	−22.00	1.597	3.824
(*b*) Strain Hardening Ignored								
0	−26.40	44.00	−26.40	−0.66	1.10	−0.66	0.513	0
50.43	0.95	46.14	−49.48	0.02	1.41	−18.00	0.574	0.990
51.03	1.53	46.42	−49.50	0.04	1.47	$-\infty$	0.584	1.022
55.00	5.50	48.40	−49.50	0.14	2.61	$-\infty$	0.679	1.267
57.20	7.70	49.50	−49.50	0.19	∞	$-\infty$	0.840	1.515

bending moment at which strain hardening begins occurs first at point D at a value of $\frac{2Hl}{hA_w} = 50.43$ kips per sq in., and subsequently at point C at a value of 58.60 kips per sq in. For the sake of comparison, results are given in Table

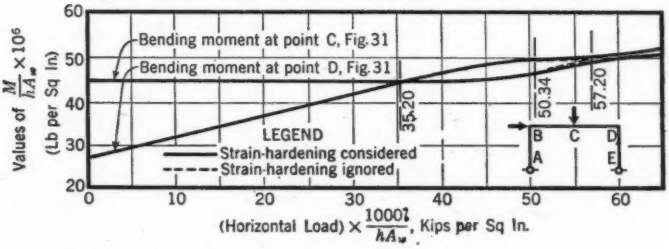

FIG. 34.—EFFECT OF STRAIN HARDENING ON BENDING MOMENTS

9(*b*), based on the assumption that the steel is capable of undergoing indefinite strain without change in stress after the attainment of yield. Where no data are given, the results are the same as in Table 9(*a*). This is equivalent to ig-

noring the effects of overstrain entirely, and complete failure occurs when equal moments sufficient to produce yield stress over the entire section have been reached at points C and D. This occurs when $\frac{2 M_C}{h A_w} = -\frac{2 M_D}{h A_w} = 49.50$ kips per sq in. and $\frac{2 H l}{h A_w} = 57.20$ kips per sq in. Fig. 34 shows the bending moments at points C and D plotted against the horizontal load; and Fig. 35 shows

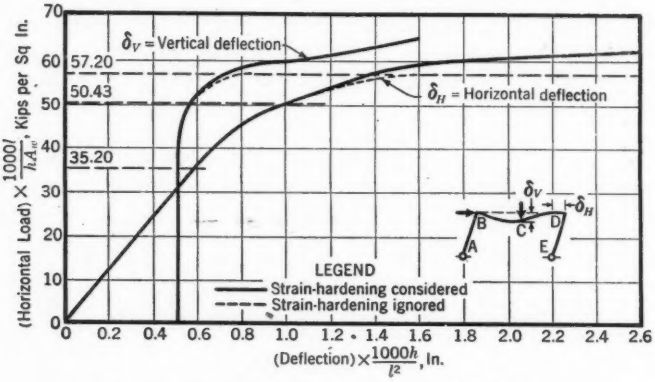

FIG. 35.—EFFECT OF STRAIN HARDENING ON DEFLECTION

the horizontal load plotted against the horizontal and vertical deflections at the center of the beam. In all cases the full lines refer to the solution taking account of the effect of strain hardening, the dotted lines indicating what happens when this is ignored. When strain hardening is taken into account the deflections begin to increase rapidly very soon after the value of $\frac{2 H l}{h A_w}$ exceeds 57.2 kips per sq in. This represents very nearly the collapse load of the frame. Hence, the collapse load obtained by ignoring strain hardening is very nearly the same as that obtained when it is considered. The percentage differences in the various calculated quantities at $\frac{2 H l}{h A_w} = 57.2$ kips per sq in. are as follows:

Description	Difference (%)
Bending moment at:	
Point C, Fig. 31	1.02
Point D, Fig. 31	−1.00
Deflection at Point C (Fig. 31):	
Vertical	15.56
Horizontal	9.83

The percentage errors in calculating bending moments resulting from the neglect of strain-hardening effects are negligible. The errors in the calculated deflections are large but by no means unreasonably so. This is an interesting result in view of the considerable simplification which results when overstrain is ignored. It is particularly so in the case of a highly redundant framework,

the analysis of which would involve the simultaneous solution of a number of formulas of the type of Eq. 51*b*. When overstrain is taken into account, these must all be solved by trial and error, and, obviously, with more than three such equations a solution would be virtually impossible. If overstrain is ignored, however, and if it is desired only to derive the deflections at the point of collapse, the bending moments become statically determinate everywhere, and the equations may be solved directly.

The general complexity of the behavior of rigid structures makes it difficult to draw any conclusions as to the importance of strain hardening in limit design. Three conclusions have been established, however, and are as follows:

(1) Tests at the Engineering Laboratory at Cambridge University indicate that the behavior of steel structures up to the point of collapse may satisfactorily be accounted for without any reference to strain hardening.

(2) Theoretical analysis indicates that, if the collapse load is calculated according to the limit design method, the error in the deduced values of the bending moments is very small. The deflections so deduced are somewhat in excess of the values obtained when strain hardening is considered.

(3) The neglect of strain hardening simplifies, very considerably, the stress analysis of structures beyond the elastic limit, particularly as the theoretical collapse load is approached.

It must be emphasized, however, that these conclusions are tentative. In particular, as Professor Hrennikoff indicates, the presence of semirigid joints may do much to prevent the equalization of moments, and, under such circumstances, the behavior of members in the strain-hardening range may be of considerable importance.

AMERICAN SOCIETY OF CIVIL ENGINEERS

Founded November 5, 1852

DISCUSSIONS

STABILITY OF THIN CYLINDRICAL SHELLS IN TORSION

Discussion

BY S. B. BATDORF AND MANUEL STEIN

S. B. BATDORF,[21] ESQ., and MANUEL STEIN,[22] ESQ.—An interesting addition to the literature on buckling of cylinders in torsion is presented by Professor Sturm. As far as the writers are aware, no one else has given a solution to the problem of determination of the critical torque in cylinders of finite length by the differential equation approach, in which equations other than the simplified ones of L. H. Donnell[5] are employed. The results for very long cylinders that buckle into an elliptical cross section (two circumferential waves) are in all probability more accurate than those of Mr. Donnell, since the approximations in the Donnell differential equation were based on the assumption that the square of the number of circumferential waves is large compared to 1. This discussion is primarily for the purpose of calling attention to the situation in the limiting case of very short cylinders, and to discuss certain features of the derivation used.

Physically, if the radius of the cylinder under torsion approaches infinity while the length and thickness remain fixed, there is obtained an infinitely long flat plate of width L subjected to shear. In this case, the critical stress is given by

$$\frac{\tau_c}{E} = k_s \frac{\pi^2 t^2}{12 (1 - \mu^2) L^2} \quad \ldots\ldots\ldots\ldots\ldots\ldots\ldots\ldots\ldots\ldots (35)$$

in which $k_s = 5.34$.[23,24] This agrees with the form used by Professor Sturm

NOTE.—This paper by R. G. Sturm was published in April, 1947, *Proceedings*.

[21] Physicist, Langley Memorial Aeronautical Laboratory, National Advisory Committee for Aeronautics, Langley Field, Va.

[22] Aeronautical Engr., Langley Memorial Aeronautical Laboratory, National Advisory Committee for Aeronautics, Langley Field, Va.

[5] "Stability of Thin-Walled Tubes Under Torsion," by L. H. Donnell, *Technical Report No. 479*, National Advisory Committee for Aeronautics, Washington, D. C., 1933.

[23] "Critical Shear Stress of an Infinitely Long Flat Plate with Equal Elastic Restraints Against Rotation Along the Parallel Edges," by Elbridge Z. Stowell, *Advance Restricted Report No. 3K12* (Wartime Report L476), National Advisory Committee for Aeronautics, Washington, D. C., 1943

[24] "On the Stability Under Shearing Forces of a Flat Elastic Strip," by R. V. Southwell and Silvia W. Skan, *Proceedings*, Royal Soc. of London, Series A, May 1, 1924, pp. 582–607.

(Eq. 25*b*), if

$$K_D = \frac{5.34\,\pi^2}{12\,(1-\mu^2)}\,\frac{D^2}{L^2} \cong 5\,\frac{D^2}{L^2} \qquad (36)$$

This value of K_D can be plotted in Fig. 5 as a straight line whose slope is -2. Since the critical stress of a curved sheet can never be below that of the corresponding flat sheet, Fig. 5 is unduly conservative when it predicts stresses below this value—that is, no curve should pass to the left of this straight line. That each of the curves of Fig. 5 should be faired into this line, rather than join it abruptly, is apparent from other studies of this problem.[5,25]

The problem of buckling of a finite cylinder in torsion defied solution for many years because of the difficulty of satisfying simultaneously the differential equation and the boundary conditions. Professor Sturm's solution does indeed satisfy the differential equations, but not the condition of simple support. That it satisfies the differential equation and one of the simple support conditions, $z = 0$ when $y = \pm\frac{L}{2}$, has been shown in the paper. That it does not, however, satisfy the other simple support condition, $\frac{\partial^2 z}{\partial y^2} = 0$ at $y = \pm\frac{L}{2}$ can be seen by differentiation of the buckle form assumed (Eq. 31*a*).

Some interesting light is thrown on this deflection function and the Sturm method of solution by solving the simple problem of an infinitely long flat plate in shear by this method, and comparing the results with those obtained by the energy method using the same deflection function, as well as with results obtained by exact methods for simply supported and clamped edges. These results [23, 24, 26] are summarized in Table 1.

TABLE 1.—COMPARISON OF RESULTS OF DIFFERENT COMPUTATION METHODS

Method of Computation	k_s	Wave length, λ/L	Wave angle, $\tan\alpha$
(1)	(2)	(3)	(4)
Simple support (exact)	5.34	1.26	....
Energy method	5.7	1.224	0.707
Sturm method	6.7	0.95	1.1
Clamped edges (exact)	8.98	0.84	....

Nodal angles are not given for the exact solutions because these solutions give curved rather than straight nodal lines. It appears that Professor Sturm's method is an exact solution for a type of restraint intermediate between simple support and clamped edges, but in which the moment applied to the edge is out of phase with the slope by a quarter wave length.

For other than very short cylinders the difference in buckling load for clamped and simply supported edges is quite small, so that it is not anticipated that any considerable error in critical stresses will result from the peculiar

[25] "Critical Stress of Thin-Walled Cylinders in Torsion," by S. B. Batdorf, Manuel Stein, and Murry Schildcrout, *Technical Note No. 1344*, National Advisory Committee for Aeronautics, Washington, D. C., 1947.

[26] "Theory of Elastic Stability," by S. Timoshenko, McGraw-Hill Book Co., Inc., New York, N. Y., 1936, p. 361.

boundary conditions implied. However, from the comparison in Table 1 it appears that there may be considerable error in the buckling configuration.

An ingenious suggestion is made by Professor Sturm on how to use results for complete cylinders to obtain approximate values for the shear buckling stress of the curved panels between adjacent stiffeners in stiffened cylinders. It may be of interest that calculations have been recently published for the critical shear stresses of simply supported and clamped curved panels.[27]

[27] "Critical Shear Stress of Curved Rectangular Panels," by S. B. Batdorf, Manuel Stein, and Murry Schildcrout, *Technical Note No. 1348*, National Advisory Committee for Aeronautics, Washington, D. C., 1947.

AMERICAN SOCIETY OF CIVIL ENGINEERS

Founded November 5, 1852

DISCUSSIONS

FORECASTING PRODUCTIVITY OF IRRIGABLE LANDS

Discussion

BY M. R. LEWIS

M. R. LEWIS,[13] M. ASCE.—A very interesting method of forecasting the productivity of an area has been presented. However, it is based on climatic conditions; and, because climate is only one of a number of important factors in crop production, it is obvious that any forecast which does not include other factors, particularly soil characteristics, must be subject to wide variation when applied to a single project.

The author suggests that the crop census data secured by the United States Bureau of Reclamation would furnish a basis for a very interesting extension of his study. In the limited time available the writer has attempted to do this for the projects in Region 1 of the Bureau, which is essentially the Columbia River drainage area. Figs. 2(*a*), 2(*b*), and 2(*c*) show the relation between the yield of alfalfa, potatoes, and sugar beets, respectively, to the total heat units on those projects in the region where sufficient acreage of the given crops is grown to make the results significant. In each figure has been indicated, in addition, the comparable data for two Bureau projects outside Region 1. These two projects have been chosen to indicate the wide variation which is found when projects scattered over a wide area are used for this comparison. The yield data are the 5-year averages, 1941 to 1945.

It will be noted that the sugar beet and potato yields for Region 1 projects conform to a linear relationship. Alfalfa yields do not follow this relationship so closely. As a general proposition, it seems doubtful if any one crop can be used to indicate the productivity over the extremely wide range suggested by the author. It is well known that, in practice, alfalfa in such areas as the Imperial and Salt River valleys grows very little during the extremely hot months. Potatoes have such a short growing season that they can use only a part of the total heat in most sections of the West. It is possible to grow two crops of potatoes, one after the other, in a single season in areas where

NOTE.—This paper by the late W. C. Muldrow was published in February, 1947, *Proceedings*. Discussion on this paper has appeared in *Proceedings*, as follows: May, 1947, by Arthur F. Johnson, H. W. Van Loo, and Will H. Noble; and June, 1947, by Charles Kirby Fox.

[13] With Region 1, U. S. Bureau of Reclamation, Boise, Idaho.

the total heat units amount to 10,000 day degrees or more. This is not a usual practice and it is therefore impossible to tell what the total production of potatoes might be if the whole of the long growing season were used in the hotter sections; nor do sugar beets require all the growing season in the more

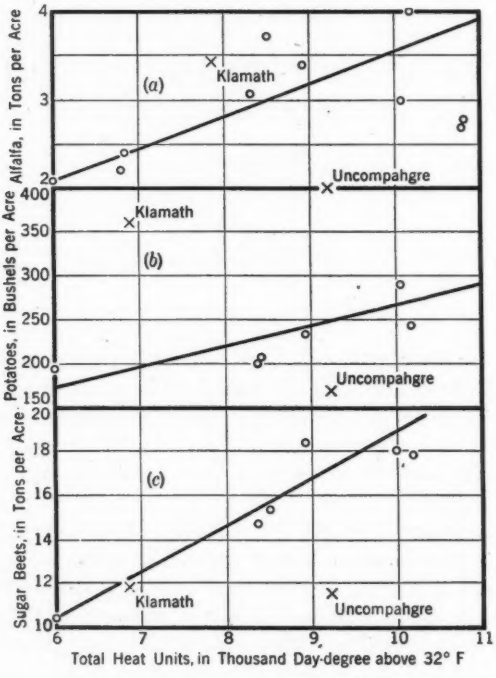

FIG. 2

southern valleys. It, therefore, appears that no crop is available which could be used to show the productivity over a very wide range—although it seems probable that in the hotter climates sugar cane might be used for this purpose.

AMERICAN SOCIETY OF CIVIL ENGINEERS

Founded November 5, 1852

DISCUSSIONS

FRICTION COEFFICIENTS IN A LARGE TUNNEL

Discussion

BY G. S. TAPLEY

G. S. TAPLEY,[40] Assoc. M. ASCE.—The authors are to be commended on their success in determining values of roughness coefficients under complicated conditions for the various types of surface of the structure examined; the values of coefficients obtained confirm, for very large-sized structures, the existing ideas as to the magnitude of such coefficients. The application of Eq. 6 to determine the measure of wall roughness, as shown in Table 9, is interesting.

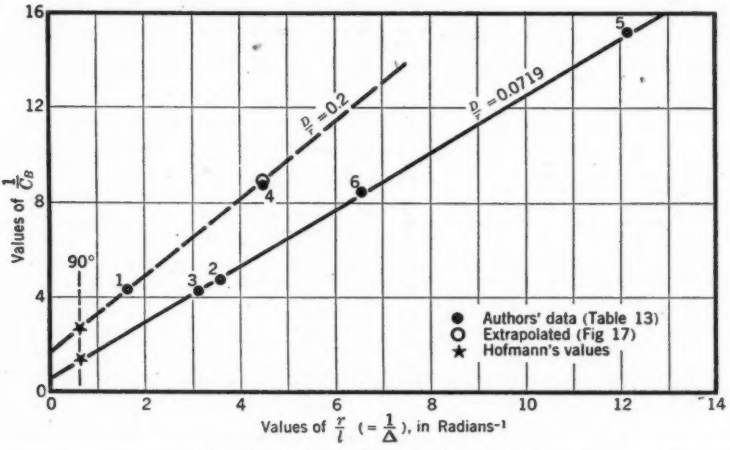

FIG. 16.—VALUES OF $1/C_B$ VERSUS $1/\Delta$

Of particular interest are the values of bend-loss coefficient, C_B, in Table 5. In deriving these values, certain assumptions were made in the preliminary calculations. Perhaps the effect of these assumptions is mirrored to some extent in the final results; for example, the authors' application of Fig. 67 of

NOTE.—This paper by G. H. Hickox, A. J. Peterka, and R. A. Elder was published in April, 1947, *Proceedings*. Discussion on this paper has appeared in *Proceedings*, as follows: June, 1947, by Weston Gavett; and September, 1947, by W. R. Barrows, Hunter Rouse, Karl R. Kennison, E. J. K. Chapman, Julian Hinds, and William P. Creager and Stephen H. Haybrook.

[40] Associate Civ. Engr., Bureau of Eng., Los Angeles, Calif.

W. Creager and J. Justin,[5] Members, ASCE, tacitly assumes that the minimum value of C_B corresponds to $r/D = 5$, and their application of Fig. 68 from the same reference may predetermine the manner of variation of C_B with the central angle. In so far as the authors' final results on bend loss may be considered independent of the assumptions, they furnish a basis for developing data to cover a considerable range of design conditions as shown hereinafter. Data, so developed, can be applied in design practice with less risk of error, perhaps, than can existing data.

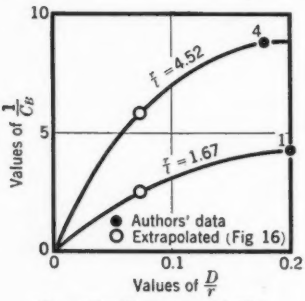

FIG. 17.—VALUES OF $1/C_B$ VERSUS D/r

With reference to Fig. 16, it may be noted that points representing bends 2, 3, 5, and 6 fall along a straight line representing $r/D = 13.9$. For $r/D = 5$, only one point (bend 1) was available. Bend 4, however, has a value of $r/D = 5.63$, and by extrapolating a short distance in Fig. 17, another point representing $r/D = 5$ and $1/\Delta = 4.52$ was obtained—thus furnishing two points through which the locus representing $r/D = 5$ was drawn. Here, $1/\Delta$, of course, equals r/L, where L is the length of curve and Δ is in radians. Calculations are shown in Table 13.

By passing curves through the origin and points representing the data in Fig. 16, Fig. 17 was constructed with maximum points at $D/r = 0.2$ ($r/D = 5$). Passing the curves through the origin in Fig. 17 is equivalent to the assumption that C_B is infinite when Δ is constant and r is infinite while D is finite; L, also, is then infinite.

TABLE 13.—COMPUTATION OF BEND-LOSS ELEMENTS

Bend No. (1)	Deflection angle, Δ, (degrees) (2)	r/D (3)	C_B (4)	$\Delta = L/r$ (radians) (5)	$\frac{1}{\Delta} = \frac{r}{L}$ (6)	D/r (7)	$1/C_B$ (8)
1	34.26	5.00	0.236	0.598	1.67	0.200	4.24
2	15.72	13.9	0.207	0.274	3.65	0.0719	4.83
3	18.32	13.9	0.239	0.320	3.13	0.0719	4.18
4	12.68	5.63	0.114	0.221	4.52	0.178	8.78
5	4.70	13.9	0.066	0.082	12.2	0.0719	15.2
6	8.72	13.9	0.119	0.152	6.58	0.0719	8.41
....[a]	90.0	5.0	0.40	1.57	0.637	....	2.50
....[a]	90.0	13.9	0.86	1.57	0.637	....	1.16

[a] "Der Verlust in 90°—Rohrkrümmern mit gleichbleibendem Kreisquerschnitt," by Albert Hofmann, *Mitteilungen des Hydraulischen*, Instituts der Technischen Hochschule, München, Heft 3, 1929, Fig. 1.

On the other hand, it may be noted in Fig. 16 that, when L is very great, although r/D is finite, C_B is not infinite; in fact, the intercepts on the axis of ordinates are $1/C_B = 0.5$ and $1/C_B = 1.5$, from which $C_B = 2$ and 0.667, respectively (for $r/D = 13.9$ and 5, respectively). In this case C_B has a maxi-

[5] "Hydro-electric Handbook," by William P. Creager and Joel D. Justin, John Wiley & Sons, Inc., New York, N. Y., 1927, pp. 119–120.

mum value depending on the value of r/D. The implication is that for a very long curve of very long radius (but finite pipe diameter) C_B is infinite; whereas, for a very long curve of finite radius and finite pipe diameter (such as in a coil of many loops) the coefficient has a finite value depending on r/D. This seems to suggest that the velocity distribution becomes adjusted to the curvature in the latter case, but continues to be disturbed in the former.

Since the authors' data covered central angles up to only a little less than 35°, it was desired to obtain confirmation of the data in Fig. 16 in the region of larger central angles. A. Hofmann's plotting[41] of the Williams, Hubbell, and Fenkell data referring to a 30-in.-diameter pipe curve with a 90° central angle ($r/L = 0.637$) was used by the writer to calculate values of $1/C_B$ for $r/D = 5$ and $r/D = 13.9$. The calculated values plotted exactly on the loci in Fig. 16 as previously derived from the authors' data. It was found, however, that other experimental data such as that of Balch, Davis, Brightmore, and others, differed from the authors' data considerably.

Pending further confirmation of the data in Fig. 16, it might be worth noting that the loci may be represented

$$\frac{1}{C_B} = c_1 + c_2 \frac{1}{\Delta} \qquad (12)$$

in which c_1 and c_2 are functions of r/D, and represent, respectively, the intercepts on the axis of ordinates and the slopes of the loci.

The straight-line equation (Eq. 12) can also be represented by the locus of an equilateral hyperbola whose coordinates are Δ and C_B and which has asymptotes at $C_B = 1/c_1$ and $\Delta = \frac{-c_2}{c_1}$. Only that section of the locus for which coordinates are positive is, of course, real. The data are plotted in hyperbolic form in Fig. 18. That the curves pass through the origin in Fig. 18 follows from the fact that the head loss due to the bend (and, therefore, C_B) must be zero when L is zero.

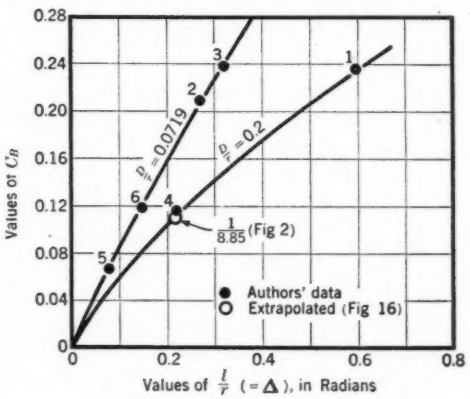

FIG. 18.—VALUES OF C_B VERSUS Δ

Although the authors' development of data on loss of head in bends was auxiliary to the main purpose of their paper, it is believed that the data have some merit as a basis for design material, in a form such as Fig. 16, to which additional lines can be added by the process already described. Needless to say, further confirmation by other experimental data is indicated.

[41] "Der Verlust in 90°—Rohrkrümmern mit gleichbleibendem Kreisquerschnitt," by Albert Hofmann, *Mitteilungen des Hydraulischen*, Instituts der Technischen Hochschule, München, Heft 3, 1929.

AMERICAN SOCIETY OF CIVIL ENGINEERS

Founded November 5, 1852

DISCUSSIONS

CLASSIFICATION AND IDENTIFICATION OF SOILS

Discussion

BY JAMES H. STRATTON, AND DONALD J. BELCHER

JAMES H. STRATTON,[4] M. ASCE.—The very nature of military operations in active theaters of war precludes other than "rule of thumb" methods in the design of airfields and roads, and the fluidity of the military situation generally requires that their construction and improvement be undertaken by stages. Improvements in bearing capacities must generally be accomplished in the face of enemy activity and increasing severity of use by the engineer's own forces. The military engineer must know, at all times, the capacities of his roads and airfields in terms of both traffic volume and loading intensities. This calls for rapid interpretations or analyses, and therefore some standardization of the "rule of thumb" design method is required to insure against faulty designs or interpretations of the strengths of roads and airfields which would adversely affect the plans of the military commander.

In the spring of 1942, the Corps of Engineers, United States Army, adopted the California highway method of evaluating the bearing values of road subgrades and extended the design curves developed by O. J. Porter, M. ASCE (25),[4a] to the higher loadings later required for airfields (see Fig. 7). An attempt was made to correlate the Public Roads Administration soils classification with the bearing-value curves in order to provide a design method for military road and airfield construction in the zone of operations through simple soil classification tests. As a result of the inability of the Corps of Engineers satisfactorily to correlate the Public Roads Administration soils classification with design procedures, Professor Casagrande was requested to study methods of soils classification. The material for the paper was taken from the resulting study.

Prior to adopting the Casagrande classification, a canvass was made of all district and division engineers with the interesting result that, of the forty-four

NOTE.—This paper by Arthur Casagrande appeared in June, 1947, *Proceedings*. Discussion on this paper has appeared in *Proceedings*, as follows: September, 1947, by Ralph E. Fadum.

[4] Col., U. S. Army, Superv. Engr., The Panama Canal, Diablo Heights, Canal Zone.

[4a] Numerals in parentheses, thus: (25), refer to corresponding items in the Bibliography (see Appendix of the paper), and at the end of discussion in this issue.

offices canvassed, thirty nine were in favor of the adoption and only five raised objections. The objections were largely concerned with the confusion that would result in the adoption of revised soils classification when construction was at a peak. However, in the light of the favoring majority opinion, it ap-

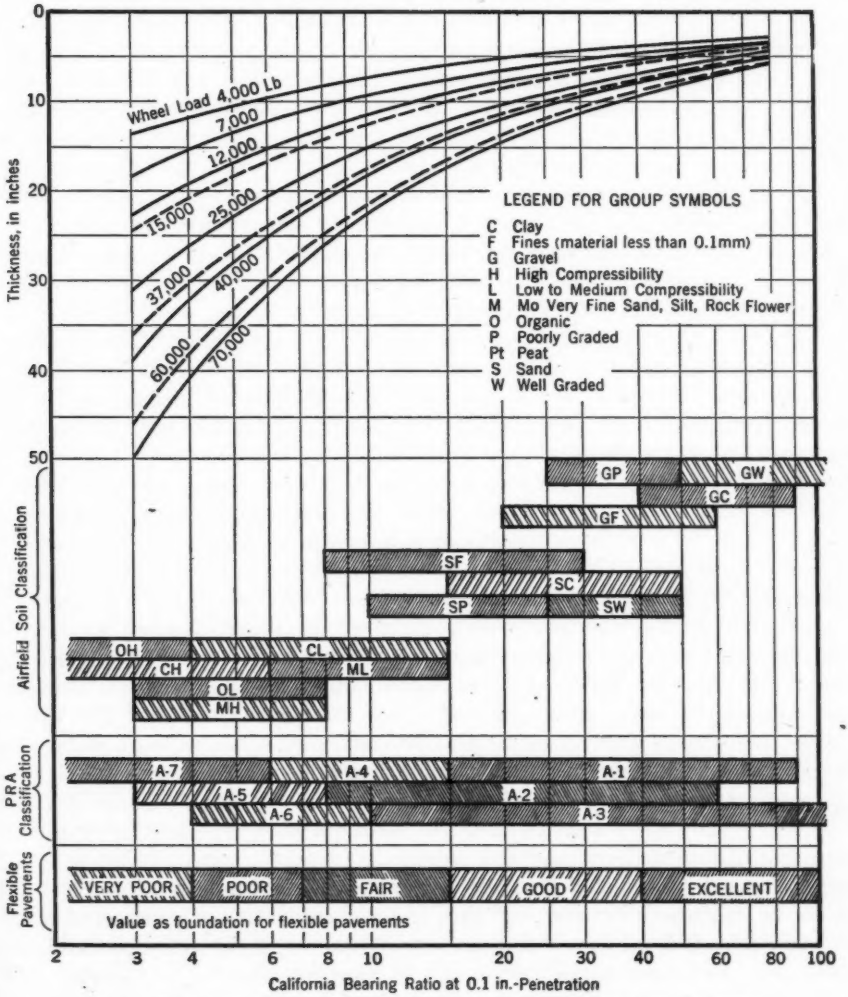

FIG. 7.—TENTATIVE RECOMMENDATIONS FOR COMBINED THICKNESS OF PAVEMENT AND BASE HAVING SATISFACTORY BEARING RATIO

peared that a change at that time would actually facilitate the transition by giving a wide opportunity for correlation with the Public Roads Administration system of classification that would aid in later revisions and improvements of the Casagrande classification. Accordingly, the Casagrande classification was adopted as standard for the Corps of Engineers.

Objections to the soil classification method were interposed by some of the most experienced soil technicians, who condemn all soils classification methods on the ground that their use encourages casual design conclusions whereas exhaustive investigations and study are required. In weighing this objection it must be noted that "symbols" identified with soils classification are a form of "engineering shorthand" which will always be popular in the profession despite the concern of those who recognize the complexity of soils and the difficulties in predicting their behavior. The Corps of Engineers does not propose to substitute a soil classification method for needed investigations and tests and orderly design procedures except where circumstances preclude other than rough or rudimentary methods of design.

It was the conclusion of the Corps of Engineers that the correlation of the soil classification methods proposed by Professor Casagrande with the bearing values of subgrades and base courses would be helpful in developing a "rule of thumb" method of design that could be employed where extensive investigations, tests, and deliberate design methods were infeasible.

The virtues ascribed by districts and divisions of the United States Engineer Department (U.S.E.D.) to the Casagrande method of classification may be summarized by stating that the improved classification is in consonance with general progress in soils engineering. One division of the U.S.E.D. commented favorably on the method because of its mnemonic characteristics.

The Lower Mississippi Valley Division, U.S.E.D., noted that a soil derivative of loess, frequently encountered in the Mississippi Valley, consisted of from 40% to 60% of silt and partakes of the nature of both an A-4 and an A-5 soil, and thus is not classifiable by the Public Roads Administration method. This division found that this soil also was not classifiable by the Casagrande method and that further study with a view to cataloging this soil is required. The same division also pointed out that soils classification correlation with the California Bearing Ratio (CBR) values must be predicated on standard methods of soil compaction and testing for the bearing values. The United States Waterways Experiment Station at Vicksburg, Miss., investigated a wide variety of soils and reported that the bearing values correlated very well with its interpretation of the Casagrande classification with one exception, which fell 3% outside the estimated range of CBR values as specified by Professor Casagrande for the particular soil type.

One district suggested that the percentage of soil binder and its plasticity index be indicated by numerical values in the classification of gravels and sands; for example, GW-3,1 would indicate a well-graded gravel with approximately 30% soil binder and a plasticity index of approximately 10%; likewise, SP-0 would indicate a poorly graded sand with no fines. If this plan were adopted, the GC, GF, SC, and SF groups would be eliminated. For the fine-graded soils, this district proposed correlating the plasticity index and moisture condition with the classification letters. For example, C5-3 would represent a "fat" clay with a plasticity index of 50% and a moisture content of 30%. There are certain virtues in this suggestion which may be realized indirectly by adopting the suggestion of the Upper Mississippi Valley Division, U.S.E.D., that the CBR number be added after the letter symbols; thus, for example, SF-25 would in-

dicate a soil to be a sand with an excess of fines and would give a picture of its internal structure. This suggestion is of value since the CBR is indicative of behavior under load. It is probable that this form of identification will be used when bearing tests have been made.

The North Atlantic Division, U.S.E.D., stated that the suggested soil groups are satisfactory with the exception of the gravels and sands in the fine groups—that is, GF and SF, respectively. These could be subdivided advantageously into additional groups reducing the wide latitude now covered by them. It was suggested by this division that an additional gravel and sand group, designated GL and SL, respectively, be added to the Casagrande classification, to include gravels and sands with excess of fines.

The Casagrande classification is not expected to supplant local names entirely for special soils, such as loess, buckshot, gumbo, etc. These names have special meaning in the localities of occurrence and it is expected that they will be used to supplement the Casagrande classification.

The foregoing discussion was prepared for delivery at the Annual Meeting of the Society in January, 1943. Subsequently, the discusser's duties deprived him of opportunity to participate in engineering activities where he might have noted the results of use of the Casagrande soils classification system. It would be of interest to learn if the method of classification found favor and if it assisted military engineers in the construction of roads and airfields in the theater of operations.

DONALD J. BELCHER,[5] ASSOC., M. ASCE.—Professor Casagrande's review of the present status of soil classification and identification provides a well-organized framework that is necessary to a perspective of the current situation in this field. The trial and error process, plus native ingenuity, has produced a "system" for each large organization dealing with soil in the engineering sense. This review organizes soil classifications and identification and places them in juxtaposition so that they may be evaluated and their relationships noted. All too often various methods are treated with an intolerance that indicates a lack of scientific maturity or perspective. Much of this intolerance appears when something "fails"—that is, the system is wrong. The same people throw golf clubs and tennis rackets because their game is poor.

Perhaps there have been many instances where each system has been applied too broadly—used beyond the limitations originally perscribed. Professor Casagrande points this out with respect to the Public Roads (PR) system. It is true of other systems as well and cannot be considered as a fundamental fault. In this respect a highly desirable development of Fig. 1 would be to introduce a vertical distribution based on grain size. The author indicates this particularly under the heading, "3. Textural Soil Classifications," where it is to be noted that such a method is inadequate for fine-grained soils. Similar limitations can be placed on several of the others, particularly those in Fig. 1 under the division dealing with "Properties of Soil in its Undisturbed Condition."

In the detailed discussions of the various classifications, especially those under the heading, "4. Agricultural Soil Classification," and "5. Geologic Soil

[5] Associate Prof., Civ. Eng., Cornell Univ., Ithaca, N. Y.

Classification," some additional attention will add to the perspective that can be gained from the over-all treatment of the subject. Primarily, it is erroneous to describe the first method as an "Agricultural Soil Classification." Engineers are in fact unintentionally perpetuating a careless description of a science; this is the proper place to correct this concept in the minds of civil engineers. To tell an engineer that this is an agricultural method (as has been done for so long) is to send him elsewhere looking for an engineering method. Unfortunately, to describe it as a pedological soil classification is a dubious improvement. It is, more simply, the science of soil formation; the classification is based on all the properties of the soils. Therein lies an advantage not found in other methods.

First, and for the record as it stands in the original paper, it would be more complete to state that it is a classification for the purpose of describing a soil and the conditions under which that soil exists. On that basis there is no fundamental leaning toward any one field of application, but any field of interest may interpret the data for its own particular use. If there is a technical predilection toward agriculture on the part of some pedologists, it is attributable to the fact that agriculture supports their programs by the allotment of funds.

It is to be regretted that an influential paper such as this should label the pedological system as a complicated one. On the contrary, its principles are simple and logical, particularly when the method is interpreted for engineering use. It also possesses simplicity of another order: With this system a soil is classified in three dimensions, length, width, and depth. With one well chosen auger boring a soil area can be classified, whereas in other methods the area shrinks to the size of the auger hole and a sample has little significance beyond the hole from which it was obtained.

It has been commonplace to find the pedological classification described in the literature as a classification of surface soils for agricultural purposes. Although Professor Casagrande described it in this way, he also states that the underlying parent materials are included. The term "surface soils" is a relative one. When it is used in conjunction with "agricultural purposes," "surface soil" is immediately interpreted as meaning 6, 8, or at most 10 in. of depth below the surface. For the sake of clarification this point should be examined in some detail and emphasis added to Professor Casagrande's inclusion of the parent material, which may extend to considerable depths. Actually, there is no arbitrary boundary or basement beyond which lies the realm of the geologist, and there is no particular need for such a limitation.

No one will advocate this method for material existing at depths common to deep foundations. Therefore, at depths of from 80 ft to 100 ft it will never be of value. Depths of from 60 ft to 80 ft are still much too great for any general use of this method, but sand dunes of that depth are found in some areas that are or can be classified on the pedological basis. Also, there are extensive areas of deep wind-blown silt that reach these and even greater depths (from 100 ft to 200 ft). These may be called Aeolian (geologic classification) or loess deposits but they also coincide with pedologic units. Along the Lower Mississippi Valley these are classified as the Memphis soil; to the north, especially in Iowa, Illinois, and Missouri, they are described as Clinton soils; and in the State of Washington as Palouse.

As the surface is approached, in the 40-ft to 60-ft depth range, the application of pedology becomes somewhat greater although only geologic deposits that form the parent materials are as yet under consideration. In this range are included much rock and drift in the glaciated areas. In those soils weathered from rock there are valid relationships in many areas between the soil mantle and the character of the rock at such depths. In the drift areas the character of the mass of of material below the surface is sufficiently well described, so that general compaction and several other requirements (26) can be anticipated on the basis of the series name of a soil (a unit of pedological classification).

Each 10-ft increment, as the surface is approached, emphasizes two trends: First, that the application of the pedological principles increases to its greatest value in the 10-ft zone immediately below the surface; and, secondly, that the dollar volume of highway and airport construction increases to its greatest volume within the same general zone.

This somewhat brief illustration is intended to show that, on a national basis, a sliding scale of applicability is necessary. In smaller units, such as within a state or district, the scale becomes more fixed. It will be found that the significance of the pedological method, as it applies to soils in the depth, is a function of the type of deposit or formation. In areas where bare rock is exposed, or, where very shallow soils exist on rough terrain, the value of the method vanishes.

Climate is also important. Within the United States climatic differences are sufficiently great that they strongly influence soil development. In the humid regions much water percolates downward through the soil, constantly leaching the soil and rock, and in general building up accumulations of clay at depths of several feet below the surface. In this process soluble materials are removed. In the west, however, the situation is often reversed. There, rainfall and melting snows in the mountains are a contrast to the desert climate prevailing in the intervening valleys a few thousand feet below. Much of the water proceeds as ground water to the valley area, where it is largely dissipated by evaporation from the surface. This reversed process precipitates salts near the surface to form the alkali and caliche soils. These are also areas where the clays may easily become saturated with exchangeable ions and thus take on characteristics of abnormally high volume change and plasticity. Such soils occur as far east as western Minnesota, where small areas of alkaline soil are associated with the Fargo (clay) series.

At present relatively little correlation has been accomplished in this way, but it is known that pavement performance, base thickness requirements, and many construction details are related to the individual soil series. The alkali attack on concrete slabs, head walls, culverts, and steel pipe is a severe action in many of these areas (27).

If this method is adaptable to engineering use, then who is using it, where is it being used, and how? An examination of this field reveals the following:

The Portland Cement Association in its work on soil-cement stabilization uses and recommends the use of the pedological method as a basis for obtaining soil data (28).

> "Missouri [(26)] uses the pedological system as used by the U. S. Bureau of Chemistry and Soils, in making soil surveys for highway purposes. Mis-

souri takes an attitude similar to that of Michigan, in that, of the three best known methods of classifying soils, the pedological system seems best to suit their needs. The other two methods seem to be limited in their scope because the classification by texture, as in the triaxial chart takes into account no other soil properties and the classification as developed by the Public Roads Administration is more an index of the behavior of disturbed soils and so does not take into account field conditions. The pedological system is essentially a reflection of drainage, topography, parent material, weathering agencies, as well as textural class. Missouri, however, does require that samples of each horizon of each soil type be taken and submitted to the testing laboratory for analysis. Field density tests are also made of each horizon in order that the theoretical soil shrinkage can be calculated for each horizon.

"The Michigan State Highway Department [(26)] has found that the pedological scheme of soil classification provides an excellent means of studying soils for general highway purposes, and that it serves as a foundation for all other soil studies in the department. The soil type, in addition to serving as a unit in mapping, also serves as a unit to which laboratory test results, road behavior observations, construction problems, and maintenance experiences are related. In other words, the soil type serves as a means for classifying and coordinating the accumulated soil experience of the entire highway department personnel."

The Nebraska Department of Roads and Irrigation (29) states:

"The pedological system of soil classification which has international recognition, was selected.

"By adopting this method of classifying and indentifying soils, it was possible to make use of a wealth of available scientific information on soils, including the published county soil maps and reports, and to supplement such knowledge with the test data and information obtained by observation on this survey as well as that which may be obtained through future investigations."

Tennessee and Nebraska have established (30)(31) a correlation between the soil series name and the texture of the material, as well as a further correlation between these and pavement performance.

The writer has observed a distinct positive correlation between the pumping of rigid pavements and the occurrence of the Superior clay series near Superior, Wis.; the Sharkey clay series near New Orleans, La.; and the Susquehanna clay series in Texas (partially reported in (32)).

There is a fair but incomplete correlation between the California Bearing Ratio (CBR) value and the soil series. This is indicated in the results of United States Engineer Department tests on the Clermont and Brookston soil series in Indiana; and by inference in the reported CBR experiments at Stockton, Calif. (33).

The North Carolina Department of Highways reports (32) "Pumping was not encountered on soils of the Norfolk or Ruston series. Pumping occurred on the Portsmouth and Plummer series * * *." It occurred also on the Lufkin, Elkton, and Coxville series.

In 1935, H. F. Janda (34) reported that excessive longitudinal cracks in a particular concrete pavement were confined to an area of Colby silt loam. W. S. Housel, M. ASCE (35), and F. V. Reagel (36) have related soil-cement con-

struction to the soil series and L. D. Hicks (37) has established the relationship between the principal horizons of several soil series and the cement required for proper stabilization. Public Roads Administration (PRA) studies (38) show results of typical soils of the coastal plain (Norfolk, Portsmouth, and Ruston) and their relationship to base course performance in North Carolina.

Professor Casagrande's description of "5. Geologic Soil Classifications" is significant. It would be of considerable value if the method could be evaluated in greater detail, or perhaps less subtly; for truly "it is damned by faint praise."

The weakness of the method seems to be lodged in the broad basis of the classification and in the recognition of age and general origin as the most important factors. For those reasons it can seldom be used in engineering without considerable modification. An evaluation of this situation was concisely expressed by Karl Terzaghi, M. ASCE (39), in summing up the results of an investigation in this field:

> "There are no definite relations [between geologic classifications and engineering properties], because for a given geologic origin and petrographic character of a stratum the strength of the material, rock, or soil depends on conditions that are not, and cannot be, recognized by a purely geological investigation. For almost every geologically well-defined stratum the possible scattering of its physical properties from the statistical average is so important, that one cannot even make an acceptable guess based on precedent."

Essentially the pedological classification includes a refined geological classification and the parent material of a soil is directly related to materials that are mapped and described by geologists. F. R. Olmstead (40) and others have shown this in various sections of the United States.

Bibliography.—

(25) "**The Preparation of Subgrade,**" by O. J. Porter, *Proceedings*, Highway Research Board, National Research Council, Washington, D. C., Vol. 18, 1938.

(26) "**Soil Survey Practice in the United States,**" by Levi Muir and William F. Hughes, *Proceedings*, Highway Research Board, National Research Council, Washington, D. C., Vol. 19, 1939, p. 467.

(27) "**Engineering Significance of National Bureau of Standards Soil Corrosion Data,**" by K. H. Logan, *Paper No. RP 1171*, National Bureau of Standards, Washington, D. C., January, 1939.

(28) "**Soil-Cement Mixtures, Laboratory Handbook,**" Portland Cement Assn., Chicago, Ill., 1939–1942.

(29) "**State-Wide Highway Planning Survey Soil Study,**" *Bulletin No. 6*, Nebraska Dept. of Roads and Irrig., Lincoln, Nebr., 1939.

(30) "**Special Papers on the Pumping Action of Concrete Pavements,**" *Research Reports No. 1–D*, Highway Research Board, National Research Council, Washington, D. C., Vol. 25, 1945.

(31) "**Characteristics and Uses of Loess in Highway Construction,**" by R. E. Bollen, *American Journal of Science*, May, 1945, p. 283.

(32) "**Special Papers on the Pumping Action of Concrete Pavements,**" *ibid.*, 1946.

(33) **"Flexible Pavement Test Section For 300,000 lb. Airplanes, Stockton, California,"** by R. A. Freeman and O. J. Porter, *Proceedings*, Highway Research Board, National Research Council, Washington, D. C., Vol. 25, 1945, p. 23.

(34) **"Longitudinal Cracking of Concrete Pavements on State Highway 13 in Clark and Taylor Counties, Wisconsin,"** by H. F. Janda, *ibid.*, Vol. 15, 1935, p. 157.

(35) **"Experimental Soil-Cement Stabilization at Cheboygan, Michigan,"** by W. S. Housel, *ibid.*, Pt. II, Vol. 17, 1937, p. 46.

(36) **"Soil-Cement Stabilization in Missouri,"** by F. V. Reagel, *ibid.*, p. 66.

(37) **"Sampling, Soil Classification and Cement Requirement—North Carolina,"** by L. D. Hicks, *ibid.*, Vol. 19, 1939, p. 521.

(38) **"Experimental Sand-Clay Base Course in North Carolina,"** by James A. Kelley, *Public Roads*, April–May–June, 1947, p. 299.

(39) *Transactions*, ASCE, Vol. 110, 1945, p. 324.

(40) **"Application of Geologic and Soils Principles to Highway Research,"** by F. R. Olmstead, paper presented at the seminar on engineering geology, Section on Eng. Geology, U. S. G. S., Denver, Colo., November, 1946.

AMERICAN SOCIETY OF CIVIL ENGINEERS

Founded November 5, 1852

DISCUSSIONS

MISSISSIPPI RIVER BRIDGE AT DUBUQUE, IOWA

Discussion

BY A. FLORIS, AND T. H. RUST

A. FLORIS,[6] ESQ.—It is not quite clear why the builders of this bridge made the bottom chord of the end spans straight and level with the suspended floor of the arched center span. Additional navigation clearance could be gained, without increase in cost, by making the top chord of the end spans straight, while arching their bottom chord. This arrangement permits the lowering of the midpiers, if the suspended floor of the center span is also raised to the level of the top chord of the end spans. A perusal of the literature on the subject shows that designers of this type of steel bridges prefer this arrangement.

In the stress analysis of the truss of the present bridge, the authors use the customary procedure of removing first the quantities not obtainable by statics. By subsequently applying the principle of virtual displacements to the base system thus formed, the necessary elastic equations are established. However, the choice of this base system and the method of obtaining the elastic equations are open to criticism. The base system is cumbersome and the derivation and solution of the elastic equations laborious. The coefficients of Eqs. 17*a*, 17*b*, and 17*c* are such that for their solution great accuracy is needed to obtain useful results.

Substantial savings in labor could have been achieved, if the authors had used more advanced methods of stress analysis. These methods, although of long standing,[7, 8, 9] have found, with one exception,[10] little favor among authors and stress analysts in the United States.

It is always possible to select the hyperstatic quantities, their direction, and point of application in such a way as to obtain as many independent elastic

NOTE.—This paper by R. N. Bergendoff and Josef Sorkin was published in June, 1947, *Proceedings*. Discussion on this paper has appeared in *Proceedings*, as follows: September, 1947, by Jonathan Jones.

[6] Asst. to Structural Engr., Pacific Elec. Ry. Co., Los Angeles, Calif.

[7] "Zur Berechnung mehrfach statisch unbestimmter Tragwerke," by Siegmund Müller, *Zentralblatt der Bauverwaltung*, 1907, p. 23.

[8] "Die graphische Statik der Baukonstruktionen," by Heinrich Müller-Breslau, Alfred Kröner, Stuttgart, 1907, Vol. II, Pt. I, p. 162.

[9] "Elastizitätsgleichungen gegenseitiger Unabhängigkeit," by Martin Grüning, *Der Eisenbau*, 1921, p. 305.

[10] "An Application of Orthogonal Moments to Problems in Statically Indeterminate Structures," by W. M. Kincaid and V. Morkovin, *Quarterly of Applied Mathematics*, 1944, p. 334.

equations as are needed. The procedure is somewhat analogous to the method used for fixed arches and two-legged frames. In this case, by choosing the elastic center of the structure as the point of application of the hyperstatic quantities, the elastic equations containing one hyperstatic quantity only are obtained. In the solution of equations of this type, containing one unknown each, slide-rule accuracy is ample.

A complete analysis of a truss similar to that of the bridge under discussion and employing the methods previously explained is given elsewhere.[11] The base system is obtained by inserting three hinges in the structure; one at the crown of the arch, and one each at the second panel of the end spans counted from the midpiers. The influence lines of this base system are determined by statics and utilized subsequently to calculate those of the hyperstatic structure.

T. H. RUST,[12] Assoc. M. ASCE.—A statically indeterminate bridge as important as the new highway bridge at Dubuque, Iowa, with piers resting on pile foundations, arouses interest about the amount and kind of settlement and movement that may occur in the piers. All foundations that depend on piles for support are subject to settlement. Appreciable settlement or rotation of the piers of this bridge will introduce stresses in the continuous trusses which may become critical, depending on the amount and the nature of the pier movements. Piles that can be driven into the stream bed to a depth of 95 ft penetrate material which could be vulnerable to settlement. More detailed information about the nature of the material in the stream bed at the pier sites would be welcome: The soil's capacity to sustain the pile loads, the method of driving, the results of pile tests, the probability of scour at these locations, facts about the soil support on vertical planes at the sides and ends of the piers, the pile plans with spacing, and the actual sizes and pile loads—all would be welcome information in the paper about the Dubuque bridge.

Structural engineers have believed that a statically indeterminate bridge, especially one of the size and the importance of this one, should be supported on piers resting on rock or some other substance closely approaching rock in its capacity to sustain the loads without appreciable settlement. Although a statically determinate simple span of steel cannot be specified with economy, under accepted working stresses, for a length much more than 650 ft, a cantilever span or perhaps some other type can be specified to obviate much of the redundant effects from pier settlement.

In a simple span of two trusses, four supports are provided, one of which is redundant, because of the portal and lateral bracing. The bracing between the trusses can be designed to lessen the effect that could result from unequal settlement of the ends of a supporting pier. Settlements of one pier with respect to the others do not affect simple and cantilever spans, as such settlements affect continuous spans. If it is planned to observe in the future the settlements of the four piers which support the continuous trusses, it may be that the necessity for such observations will be disregarded after some years of small, inconsequential settlements.

[11] "Die Statik des ebenen Tragwerkes," by Martin Grüning, Julius Springer, Berlin, 1925, p. 370.
[12] Structural Engr., Chicago, Ill.

The writer has seen deterioration in 50-ft statically indeterminate concrete arch spans due to settlement of their pile foundations, and has known of the deterioration of continuous steel structures from the nonrigidity of their supports. Allowable pile loads, due to different specifications and the methods of figuring the load sustaining capacity of piles, have varied so greatly that publication of the research and field knowledge available from the Dubuque bridge piles would be welcome. Those who have had direct charge of the driving of the piles must possess much practical knowledge of the driving, which if published would be of lasting value to the engineering profession. The transfer of the pier loads of this bridge into the stream bed composed of the implied material constitutes an unknown discontinuity in load transfer, which results from the imperfect and incomplete knowledge of soil mechanics.

The precedent has been set for a number of years of sustaining continuous bridges on pile foundations, and the precedent is followed in this bridge. It seems that the capacity of the piles to sustain their loads without critical settlement should be supported by factual evidence as well as by a geologist's advice, in an endeavor to justify these foundations.

AMERICAN SOCIETY OF CIVIL ENGINEERS

Founded November 5, 1852

DISCUSSIONS

A RATIONAL EXPLANATION OF COLUMN BEHAVIOR

Discussion

BY ERNEST L. ROBINSON

ERNEST L. ROBINSON,[25] Assoc. M. ASCE.—As any devotee of the sport of archery knows very well, there is nothing uncertain or mysterious about the behavior of an elastic column beyond the Euler length. In 1915, and in 1916, the writer published two analyses of the curve whose ordinate is everywhere proportional to the curvature. The first gave[26] equations for a deflecting column connecting load and deflection both with the original length and the deflected length, and presented graphic solutions of these equations, as well as charts for the required elliptic integrals. The second paper presented charts[27] for the hydraulic catenary connecting the middle depth with the tension, area, wetted perimeter, and mean hydraulic radius as well as a fairly large diagram showing the actual shape of the curve.

NOTE.—This paper by Frederick L. Ryder was published in March, 1947, *Proceedings*. Discussion on this paper has appeared in *Proceedings*, as follows: May, 1947, by R. Robinson Rowe, and George Winter; and June, 1947, by Robert M. Mains, and Chi-Teh Wang.

[25] Structural Engr., Turbine Generator Eng. Div., Gen. Elec. Co., Schenectady, N. Y.

[26] "Curves for Strength and Deflection of Very Long Columns," *Engineering News*, June 10, 1915, pp. 1108–1109.

[27] "Design Charts for Open Flumes with Catenary Section," by Ernest L. Robinson, *ibid.*, March 23, 1916, pp. 566–567.

AMERICAN SOCIETY OF CIVIL ENGINEERS

Founded November 5, 1852

DISCUSSIONS

TESTS OF TIMBER STRUCTURES FROM GOLDEN GATE INTERNATIONAL EXPOSITION

Discussion

BY JAMES H. CARR, JR., HOWARD J. HANSEN, AND E. G. STERN

JAMES H. CARR, JR.,[7] Assoc. M. ASCE.—Much has been added to the knowledge of timber design and construction by this interesting study, which has already resulted in further studies being made by those who had advance information on the results. The Timber Engineering Company, one of the sponsors of the San Francisco (Calif.) study, for three years has been carrying on a series of tests on full-scale trusses, has completed a series of tests on eccentric joints, and has developed, therefrom, an empirical formula. In addition, it has sponsored research at the Massachusetts Institute of Technology at Cambridge on the distribution of stress around timber connectors.

There are three treatments in the paper with which the writer did not agree at the time of preparation. The first of these is that in many places in the paper the factors relating test load to design load are given when the failure was not directly connected to the design load used. In such cases, the factor given represents only the minimum amount of test load to which the section of the truss was submitted and does not indicate the maximum load it might sustain. The factor therefore is meaningless.

The second is that the comparisons in regard to allowable connector values are based on data published in 1939, although the original designs were not prepared on the basis of these data, but on data published in 1935. It is believed that it would have been more correct to compare either with the 1935 data or with the recommendations published in 1943, which were in effect, and current practice, at the time the report was in preparation, and which continue to be recommended and used in 1947.

The third is that much of the paper centers around a so-called factor of "tension perpendicular to grain," occurring particularly in eccentric joints. The writer disagreed with this theory at the time the report was in process

NOTE.—This paper by a Committee of the San Francisco (Calif.) Section, ASCE, on Timber Test Program was published in May, 1947, *Proceedings*.

[7] Secy., Timber Eng. Co., Washington, D. C.

TABLE 26.—COMPARISON BETWEEN RATIO OF TEST LOAD STRESS AND DESIGN CAPACITY AS BASED ON 1939 DATA AND ON 1943 RECOMMENDATIONS

Truss (1)	Joint (2)	R_{ca} 1939	R_{ca} 1943
(*a*) BRAZIL BUILDING TRUSSES			
TB–1	....	2.95	3.86
TB–2	....	2.48	3.28
(*b*) FRENCH BUILDING TRUSS			
TF	....	1.7	4.45[a]
(*c*) MERRY-GO-ROUND BUILDING TRUSSES			
TM–1	L2	3.25	4.5
	L1	3.30	4.6
	L4	2.53	3.1
TM–1	....	3.3	4.6
TM–2	....	3.6	4.9
(*d*) NORTH SQUARE COURT BUILDING TRUSS			
TNS	L3	2.07	3.15
	U2	1.78	2.99
	U6	1.83	3.06
TNS	....	1.78	2.99
(*e*) JOINT TESTS (STEEL GUSSETS)			
....	J2	4.56	5.61
....	J3	3.53	4.30
....	J4	3.48	4.17
....	J5	4.84	6.44
....	J6	4.81	6.40
....	J7	5.04	6.70
....	J8	4.77	5.78
....	J9	4.79	6.38
....	J10	4.54	5.73
....	J11	3.12	5.70
....	J12	4.08	4.55
....	J13	5.06	....[b]
....	J14	2.5	3.33
....	J15	2.91	3.87
....	J16	2.93	3.96
....	J17	1.83	....[b]
(*f*) JOINT TESTS (ECCENTRIC)			
....	J1	2.16	3.56
(*g*) JOINT TESTS (SPLIT RINGS)			
....	J23	1.55[c]	1.82
....	J24	3.00[c]	3.69
....	J25	2.6[d]	3.55
....	J26	2.55[d]	3.48
....	J27	2.55[d]	3.48
....	J28	2.75[d]	3.75

[a] Based on shear formula. [b] Connectors did not fail. [c] Not true factors, as grooves sheared and test setup failed. [d] Tests not carried to failure of connector joints.

and stated that he felt the tests indicated and closely followed another theory, advanced by Everett Lank, that the shear theory for notched beams more closely fitted the data. The authors, while stressing the "tension perpendicular to grain" theory, offer no design approach. Mr. Lank has subsequently been proved correct by a series of tests[8] substantiating the shear theory, and an empirical formula for design application based on this theory has been developed, as follows:

$$\frac{3}{2}\frac{V}{b\,d_e} = 1.5\,H \quad \ldots\ldots\ldots\ldots (3)$$

in which V is the total vertical shear; b is the width of the section; and d_e is the effective depth of the section, or the distance from the inside edge of the connector (nearest the unloaded edge of the member) to the loaded edge of the member.

Application of these three comments to the data presented brings forth the results given hereafter. In order to simplify the presentation, all values of R_{ca} as developed in the paper for the 1939 data and those based on the 1943 data, published by the National Lumber Manufacturers' Association,[9] are given in Table 26.

The report states the first failure for truss TB–1 is at joints U1 and L10. It is not clear as to just what the initial failure was. However, a comparison on current data gives the result shown in Table 26(*a*).

The writer cannot reconcile Fig. 25 with Fig. 26, or the description of the French Building truss at failure. Assuming Fig. 26 and the description to be correct, and applying the shear formula, the 1943 factor becomes 4.45 (Table 26(*b*)) as against the 1939 factor reported, based on connector values (which did not fail) of 1.7, an appreciable increase.

In the Merry-Go-Round Building trusses the lumber failed and not the connector joint, hence the *R*-values are not true results. However,

[8] "Tests of Eccentric Split-Ring Joints Yield Rational Design Formula," by R. H. Glass, *Engineering News-Record*, May 29, 1947, pp. 69–70.

[9] "National Design Specification for Stress-Grade Lumber and its Fastenings," National Lumber Manufacturers' Assn., Washington, D. C., 1944.

based on current recommendations the factors of Table 5 become those shown in Table 26(*c*).

As to the discussion of theoretical stress around a connector (under the heading, "Merry-Go-Round Building (M) Trusses"), a paper to be presented at the 1947 Fall Meeting of the Society on tests conducted at the Massachusetts Institute of Technology, under the direction of Prof. Albert Dietz, Assoc. M. ASCE, discusses data developed by use of stress coats and electrical strain gages. Current recommendations include factors developed in these tests; connectors of improved design have also been developed and are now available.

In the North Square Court truss tests the failure was due to eccentric joints and hence the shear formula applies. Factors secured by this method show that for joint L3 the 1943 factor is 2.98. Although they do not reflect the true failure, the factors on the 1943 data would correct the factors in Table 6 to those given in Table 26(*d*).

Also, in Table 8, the changes in factors, where applicable, based on the 1943 data would be as shown in Tables 26 (*a*), (*b*), (*c*), and (*d*). The writer disagrees entirely with conclusion 6 (see heading, "Comments on Tests of Trusses") as it is believed that eccentric joints may be properly and capably handled with the shear formula.

On the basis of the 1943 data, the factors in Table 9 should be corrected as shown in Table 26(*e*). Based on the shear formula application, the 1943 factor for test joint J1 becomes 3.3. However, if connector factors must be considered, the factors are changed as shown in Table 26(*f*). As regards the tests of joints with ring connectors, the factors given in Tables 13 and 14 should be corrected to the 1943 values, as shown in Table 26(*g*).

After eleven years' experience, the writer feels that the comments or conclusions on the tests of joints with steel gusset plates are broader than the data available.

However, in view of the results of this program, it is this writer's opinion that the designer who uses the 1943 recommendations, including the shear formula, is assured of factors which are more than safe when based on these tests inasmuch as the smallest corrected true factor is 2.98, whereas a factor in the neighborhood of 2 would be considered sufficient by experienced timber designers and research men.

HOWARD J. HANSEN,[10] ASSOC. M. ASCE.—The descriptions of the equipment used and the methods of testing are quite complete, and will be valuable guides in future tests of full-scale trusses and joints involving eccentricity and loads at an angle to the grain. In most cases, the tests of any one type were too few in number and the variables too involved to provide an exact design procedure for similar types. The writer is, however, much pleased that this extensive test program has been published and is particularly interested to note that the complete report including test data, curves, field notes, photographs, and calculations is filed at several strategic points throughout the United States.

The sudden failure under test loads of the Cavalcade cantilever truss (TC) and the detailed examination of joints in other trusses again emphasizes the

[10] Prof. of Mechanics and Acting Head, Industrial Eng. Dept., Univ. of Florida, Gainesville, Fla.

need for competent engineering supervision of timber structures if the factor of safety expected in design is to be provided in actual construction. This same fact was brought out during World War II when timber structures were built with little or no competent engineering inspection and investigations of several failures showed that failure was due to improper construction.

The R_{ca}-values calculated for the Brazil Building (TB) trusses did not include the bending effects of the chords. This fact was noted in the report. However, since the stresses due to bending could be rather high, they should have been included in the computations of the R_{ca}-values. The fact that the nature of the failures in the joints of these and other trusses emphasizes the importance of secondary stresses is significant. It is believed that many typical designs of shallow timber trusses have not been checked for secondary stresses in the past. The authors mention the need for additional tests on joints in which a combination of shearing stress, direct stress, and bending stress is involved. This is one of the greatest needs in the field of timber engineering and additional experimental data on combined stresses will aid materially in the development of more efficient and economical design in timber.

TABLE 27.—COMPARISON OF R_{ca}-VALUES FOR JOINTS AS BASED ON 1939 AND 1943 ALLOWABLE LOADS

Joint	R_{ca}		Col. 2—Col. 3[a]
	1943	1939	
(1)	(2)	(3)	(4)
1.....	2.5	2.16	+0.34
2.....	4.62	4.56	+0.06
3.....	3.44	3.53	−0.09
4.....	3.33	3.48	−0.15
5.....	5.1	4.84	+0.26
6.....	5.08	4.81	+0.27
7.....	5.32	5.04	+0.28
8.....	3.37	4.77	−1.40
9.....	5.06	4.79	+0.27
10.....	4.52	4.54	−0.02
11.....	2.82	3.12	−0.20
12.....	3.68	4.08	−0.40
13.....	4.91	5.06	−0.15
14.....	2.3	2.5	−0.20
15.....	3.05	2.91	+0.14
16.....	3.12	2.93	+0.19
17.....	1.94	1.83	+0.11

[a] Excess or deficiency of 1943 values over 1939 values.

Although the data on the lateral strength of nails in plywood are worthwhile and may be used as a guide for further experimental investigations, considerably more data on nailed construction are definitely needed. The tests covered in the report do not include a wide enough range in nail sizes, spacing, and end and edge distances to predict the behavior of nailed joints other than those tested.

As noted in the report, the buckling tests of plywood panels were not exhaustive enough to provide design details. The conclusion that stud spacing may be increased beyond the customary 16 in. or 24 in. seems feasible, but additional tests on Douglas fir structural plywood should be conducted along the lines investigated by the United States Forest Products Laboratory at Madison, Wis., on aircraft plywoods.

In the joint tests the factor of safety of each joint was calculated on the basis of recommended allowable loads from the TECO manual.[1] A comparison of the R_{ca}-values based on a later TECO manual[11] are given in Table 27.

There are several questions that have arisen from the study of this report and it is believed that the value of the report will be enhanced if the answers to these questions are given. The questions are:

[1] "Timber Connector Construction," Manual of the Timber Eng. Co., Inc., Washington, D. C., 1939.

[11] "Design Manual for Teco Timber Connector Construction," Manual of the Timber Eng. Co., Inc., Washington, D. C., 1943.

1. What approximate method was used in computing the stresses in the members of an eccentric joint?

2. How was the lower chord splice of truss TM-2 reinforced before testing?

3. Why were blocks added to joint J1 under test loads? Would this give a true picture of the type of failure for this joint?

4. Cannot some explanation for the large difference in movement of the gusset plates in joint J2 be given?

5. Is the statement under the heading, "II. Joint Tests: Comments on Tests of Joints with Steel Gusset Plates: (10)," that "* * * in these tests the load was always parallel to grain" correct?

The values of R based on the ultimate shear loads for various thicknesses of Douglas fir plywood, as obtained by the test results given in the report and the allowable stresses for various grades of Douglas fir plywood, are given in Table 28. The report does not mention the grade of plywood used and the values in Table 28 may prove valuable as a comparison of the R-values for the different grades.

In conclusion, the report is a valuable contribution to the literature and design data pertaining to timber structures, as well as an indication of the need for more full-scale tests of timber trusses, joints with combined stresses, nail tests, and structural plywood tests of all types. It is true that no two identical timber trusses or joints will behave exactly the same under load; but, as more tests of this nature are conducted, the results can be correlated with those contained in this report.

TABLE 28.—VALUES OF R FOR SHEAR TESTS OF DOUGLAS FIR PLYWOOD

Grade[a]	Stress (Lb per Sq In.)		R
	Ultimate	Allowable	
(1)	(2)	(3)	(4)
(*a*) Three Ply, $\frac{1}{4}$ In. Thick			
G-2-S....	575	480	1.22
G-1-S....	575	456	1.28
So-2-S...	575	420	1.39
So-1-S...	575	384	1.52
Sheathing	575	360	1.62
(*b*) Three Ply, $\frac{1}{16}$ In. Thick			
G-2-S....	775	480	1.61
G-1-S....	775	456	1.70
So-2-S...	775	420	1.84
So-1-S...	775	384	2.02
Sheathing	775	360	2.15
(*c*) Five Ply, $\frac{1}{16}$ In. Thick			
G-2-S....	1,090	480	2.27
G-1-S....	1,090	456	2.39
So-2-S...	1,090	420	2.60
So-1-S...	1,090	384	2.84
Sheathing	1,090	360	3.03

[a] "G" denotes "Good"; "S" denotes "Side"; and "So" denotes "Sound."

E. G. STERN,[12] Assoc. M. ASCE.—The report of the committee contains much valuable information for timber designers and fabricators of timber structures. It is of interest to learn what comments designers and fabricators of the tested timber structures may make; whether their assumptions, theories, and computations were verified by the test data, and which theories were contradicted. It is believed that additional valuable information could be obtained from the designers and fabricators if a review of their designs and construction logs could be made available on the basis of the test data obtained.

The fabricators probably can give the answer to this question: Were split rings and shear plates, respectively, omitted purposely in joints L7, L8, and L9 of truss TB-1, and in joint J8 because they were considered unnecessary?

[12] Associate Prof. and Head, Wood Constr., Virginia Polytechnic Inst., Blacksburg, Va.

Several of the findings seem to confirm the previously made assumption that, during initial loading and failures of a minor nature, adjustments take place in the local and secondary stresses—often anticipated but not included in detailed computations—which result in reduction and more uniform distribution of such internal stresses and, thus, make the structure safer than it was before adjustments took place. Although such adjustments may increase the load-carrying capacity of the structure, the deformation and total deflection may also be increased beyond those computed. Rolling shear of the core within split rings may often be accounted for as a result of such adjustments.

It is hoped that the appropriate industry will sponsor performance of some of the recommended, additional tests in order to secure the needed information. It cannot be expected that engineers or architects will employ timber structures as long as some of the basic design data are lacking and not available to them. Industry may be reminded that several United States technical institutions and universities are willing to assist industry in obtaining such vital data by assigning specific problems to graduate students interested in timber structures or by assigning their experienced staff to industry-sponsored projects.

The statement is made that member L5–U5 in truss TF was replaced before test performance. According to Fig. 25, a member of such designation does not exist.